Reappraising Schmidpeter's Bis(iminophosphoranyl)phosphides: Coordination to Transition Metals and Bonding Analysis

Adrien T. Normand,* E. Daiann Sosa Carrizo,* Corentin Magnoux, Esteban Lobato, Hélène Cattey, Philippe Richard, Stéphane Brandès, Charles H. Devillers, Anthony Romieu, Pierre Le Gendre and Paul Fleurat-lessard

Supporting Information

TABLE OF CONTENTS

V. CRYSTALLOGRAPHIC STUDIES S102

I. General procedures

1. Reagents and conditions

All reactions were carried out under Ar using conventional Schlenk techniques or in an Ar glovebox. Toluene, CH_2Cl_2, Et_2O, pentane and THF were dried using an MBraun MB SPS-800 solvent purification system. Bromobenzene was distilled over CaH_2 and stored over activated 3Å molecular sieves in the glovebox. 1,4-Dioxane was distilled over sodium benzophenone ketyl and stored similarly. Deuterated solvents were dried by passage through a short column of activated neutral alumina (Brockman grade II) and stored over activated 3Å molecular sieves in the glovebox, either at room temperature (C_6D_6, C_6D_5Br...) or at -18°C (d_8-THF, CD_2Cl_2...). Alumina and molecular sieves were activated by heating for at least 6 hours above 230°C under vacuum. Diatomaceous earth (dicalite) was dried in an oven at 110 °C. The following compounds were prepared according to literature procedures: aminophosphines,[1] $[TiCl_3(THF)]_3$,[2] $[(C_5H_5)_2Fe][B(C_6H_5)_4]$,[3] $[TiCl_2(N^tBu)(Py)_3]$,[4] [Au(THT)Cl)].[5] Copper(I) bromide was purified and dried according to the literature.[6] Sodium 2,6-dimethylphenate was prepared by reaction of 2,6-dimethylphenol with NaH in Et_2O. Lithium phosphinoamides were prepared by the reaction of the corresponding aminophosphines with n-BuLi in Et_2O (**1a**) and pentane (**1b**). All other reagents were commercially available and used as received.

2. Analyses

The identity and purity of the compounds were established using elemental analysis, high-resolution mass spectrometry (ESI-MS), X-ray diffraction analysis, cyclic voltammetry, NMR, EPR, IR and UV-vis spectroscopies.

Elemental analyses were performed by Mr Marcel Soustelle using analytical equipement of the Plateforme d'Analyse de l'Institut de Chimie Moléculaire de l'Université de Bourgogne.

IR and UV-Vis spectra were obtained on an Agilent Cary 630 FTIR and an Agilent Cary 60 UV-Vis spectrometer respectively in an Ar glovebox.

NMR spectra (^1H, ^{11}B, ^{13}C, ^{19}F, ^{31}P) were recorded on Bruker AV500 and AV600 spectrometers. NMR spectroscopy chemical shifts are quoted in parts per million (δ) relative to TMS (for ^1H and ^{13}C), $BF_3{\cdot}Et_2O$ (for ^{11}B and ^{19}F) or H_3PO_4 (for ^{31}P). For ^1H and ^{13}C spectra, values were determined

---

[1] a) R. F. Hudson, R. J. G. Searle and F. H. Devitt, *J. Chem. Soc. C: Organic* **1966**, 1001-1004; b) C. Jiang and D. W. Stephan, *Dalton Trans.* **2013**, *42*, 3318-3325.

[2] N. A. Jones, S. T. Liddle, C. Wilson and P. L. Arnold, *Organometallics* **2007**, *26*, 755-757.

[3] I. M. Piglosiewicz, R. Beckhaus, G. Wittstock, W. Saak, D. Haase and *Inorg. Chem.* **2007**, *46*, 7610-7620.

[4] A. J. Blake, P. E. Collier, S. C. Dunn, W.-S. Li, P. Mountford and O. V. Shishkin, *J. Chem. Soc. Dalton Trans.* **1997**, 1549-1558.

[5] R. Uson, A. Laguna and J. Vicente, *J. Organomet. Chem.* **1977**, *131*, 471-475.

[6] W. L. F. Armarego and C. L. L. Chai, *Chapter 5 - Purification of Inorganic and Metal-Organic Chemicals: (Including Organic compounds of B, Bi, P, Se, Si, and ammonium and metal salts of organic acids)*, in Purification of Laboratory Chemicals (Sixth Edition), Eds.: W. L. F. Armarego and C. L. L. Chai, Butterworth-Heinemann, Oxford, **2009**, pp. 445-576.

by using solvent residual signals (*e.g.* $CDHCl_2$ in CD_2Cl_2) as internal standards.[7] The ^{31}P, ^{19}F and ^{11}B NMR spectra were referenced according to IUPAC recommendations (Absolute referencing).

EPR spectra were obtained on a Bruker ELEXSYS 500 spectrometer. The instrument was equipped with a 4122SHQE/0405 X-band resonant cavity operating at 9.43GHz, and an X-band high-power dual-gun-oscillator bridge.

Electrochemical manipulations were performed in an Ar glovebox at room temperature, using 0.1M $NaBPh_4$ in THF as a supporting electrolyte. The following electrolyte volumes were used fo voltammetric analyses: working electrode compartment: $V = 5$ mL; reference electrode compartment: $V = 5$ mL. Voltammetric analyses were carried out in a standard three-electrode cell, with Biologic SP-300 potentiostat, connected to an interfaced computer that employed EC-Lab (v. 11.25) software. The reference electrode was a silver wire separated from the analyzed solution by a sintered glass disk filled with the background solution. The auxiliary electrode was a platinum foil. For all voltammetric measurements, the working electrode was a glassy carbon (GC) electrode ($\emptyset = 3$ mm). Before each voltammetric analysis, the GC electrode was polished with a diamond suspension. In these conditions, when operating in THF $NaBPh_4$ 0.1M, the formal potential for the ferrocene (+/0) couple was +0.57 V *vs.* Ag^+/Ag.

Luminescence measurements of compound **9b** in solution were performed on a SAFAS Flx-Xenius XC spectrofluorimeter using quartz cells (SAFAS, Quartz Suprasil for SAFAS flx Xenius, 45 × 12.5 × 12.5 mm, pathlength: 10 mm, chamber volume: 3.5 mL), at 298 K (using a temperature control system combined with water circulation). The following set of parameters was used: Ex./Em. bandwidth = 5 nm, integration time = 0.1 s, 1 nm step and tunable PMT voltage (actual: 1200 V). All emission spectra were corrected. Solid state measurements were also achieved with the same spectrofluorimeter equipped with a $BaSO_4$ integrating sphere and using the following set of parameters: Ex./Em. bandwidth = 5 nm, integration time = 0.1 s, 1 nm step, full filtering both in Ex. and Em.)

X-ray diffraction analyses: crystals of all compound were selected and mounted on a mylar loop with oil on a 'Bruker APEX-II CCD' or a ‘Bruker D8 venture Photon 100’ diffractometer. Crystal were kept at 115 K or 100 K during data collection. Using Olex2,[8] the structures were solved with the ShelXT[9] structure solution program using Direct Methods and refined with the XL[10] refinement package using Least Squares minimization. More details can be found in section V and in the Crystallographic Information Files in which are included .res and .hkl files.

---

[7] G. R. Fulmer, A. J. M. Miller, N. H. Sherden, H. E. Gottlieb, A. Nudelman, B. M. Stoltz, J. E. Bercaw and K. I. Goldberg, *Organometallics* 2010, **29**, 2176-2179.

[8] O. V. Dolomanov, L. J. Bourhis, R. J. Gildea, J. A. K. Howard and H. Puschmann, *J. Appl. Crystallogr.* 2009, **42**, 339-341.

[9] G. Sheldrick, *Acta Crystallogr. Sect. A* 2015, **71**, 3-8.

[10] G. Sheldrick, *Acta Crystallogr. Sect. C* 2015, **71**, 3-8.

II. Synthesis of compounds

Synthesis of P_4 (white phosphorus)

Hazards and risks analysis:

Mechanical hazards:

The allotropic conversion of phosphorus originally developed by H. Brereton Baker involves the thermolysis of red phosphorus under vacuum in a sulphur vapour bath (444 °C).[11] Maintaining the physical integrity of the glassware throughout this procedure is of paramount importance due to the combination of vacuum, heat, and the presence of toxic and pyrophoric materials.

Recently, Baker's procedure was adapted to modern day chemistry techniques by Arnold, Hu and Tsai.[12] However, these authors used normal borosilicate glassware. Due to the superior heat resistance of fused silica glass over that of borosilicate, the former is an intrinsically safer alternative. Indeed, we have observed cracks in the borosilicate Schlenk flasks used to perform the thermolysis — 2000 W heatgun at maximum power, ~650 °C — of red phosphorus on several occasions, whilst this problem was never encountered with the fused silica glass Schlenk tube depicted below (Steps 2, 3, 7 and 8). Therefore, **we warn against the use of borosilicate glass for the thermolysis of red phosphorus**.

Chemical hazards:

Red phosphorus is a flammable solid and it is sensitive to friction. It should also be considered toxic by inhalation and ingestion, but it is not a cause for special concern in an academic chemistry lab, especially when stored in a glovebox.

White phosphorus, on the other hand, is considerably more hazardous due to its well-documented toxicity (by inhalation/ingestion and, indirectly, through exposure to pyrophosphoric acid, ultimately causing the occupational disease known as "phossy jaw"[13]) and pyrophoric properties. Obviously, the risk level associated with these hazards correlates with the manipulated quantities, the presence of flammable material (*e.g.* organic solvents, paper wipes…) in the vicinity of white phosphorus, and compliance of the operator with health and safety regulations, including the obligation to wear personal protective equipment.

Upon exposition to moist air, white phosphorus becomes covered with a protective layer of sticky dust. This is due to the oxidation by atmospheric oxygen, generating P_4O_{10} fumes, which react with moisture to give a complex mixture containing ortho- and pyrophosphoric acid. As a result, white phosphorus particles become passivated and hence, can be difficult to quench completely: **passivated white phosphorus is stable in air and can be reactivated by washing with water. This phenomenon is a serious hazard, especially if the glassware is to be cleaned with a flammable**

---

[11] H. B. Baker, *Phil. Trans. A* **1888**, *179*, 571-559.

[12] C. W. Hsu, Y. C. Tsai, B. M. Cossairt, C. Camp, J. Arnold, B. M. Cossairt, B. M. Cossairt, C. C. Cummins and Y. C. Tsai *Synthetic route to white phosphorus (P4) and arsenic triphosphide (AsP3)*, *in* Inorganic Syntheses, (Ed. P. P. Power), **2019**, pp. 123-134.

[13] W. B. Hinshaw and L. D. Quin, *Phosphorus, Sulfur, Silicon Relat. Elem.* **2015**, *190*, 2082-2093.

solvent (such as acetone) subsequently. We have found that it is preferable to burn small quantities of white phosphorus residues under a vigorous stream of air (*vide infra*, Step 7) in order to eliminate most of the pyrophoric material before washing the glassware. This step should be performed under a well ventilated fumehood with the sash lowered to a minimum. Oxidation of white phosphorus may also be achieved with concentrated nitric acid, but this procedure is tedious, generates large amounts of corrosive waste, and it can be dangerous when performed with finely divided white phosphorus (due to the risk of ignition).

Procedure:

In an Ar glovebox, red phosphorus (12.4 g, 0.400 mol) was placed in a fused silica glass Schlenk tube (General Electric, semiconductor grade) greased with Apiezon H grease. The vessel was removed from the glovebox and evacuated at a vacuum line for 5 min. The vessel was positioned almost horizontally with a very slight twist, in order to force the flow of liquid P_4 towards the stopper (*vide infra*, Step 1). A 2000 W heatgun at full power was placed underneath the pile of red phosphorus and moved progressively (ca. 30 min) towards the bottom end of the vessel. After cooling, the vessel was taken into the glovebox and scraped with a spatula. The gathered solids were extracted during the night with 500 mL of CH_2Cl_2 in a normal borosilicate Schlenk flask. The suspension was filtered over a grade 4 sintered glass frit, the red solid was dried on the frit; this residue (5.7 g) can be reused to make white phosphorus, although ideally it should be mixed with fresh red phosphorus. The solution was evaporated to dryness, and finely divided P_4 was obtained and stored away from light in the glovebox freezer (4.5 g, yield 82%).

White phosphorus residues were burned under a vigorous stream of air; after cooling, water was used to remove the acidic residue, and the glassware was cleaned using water and cleaning powder. Borosilicate glassware was cleaned in a base bath followed by an acid bath, whilst the fused silica glass Schlenk tube was cleaned with water, acetone and CH_2Cl_2 (to remove the grease) only.

$^{31}P\{^1H\}$ NMR (202 MHz, C_6D_6, 298 K): $\delta = -521.1$

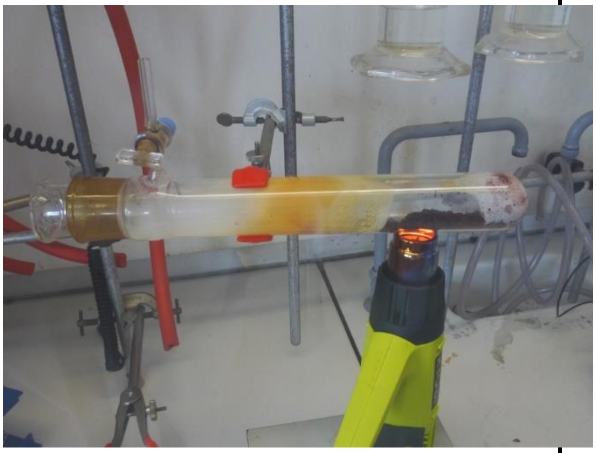

Step 1: *beginning of thermolysis. The heatgun is placed underneath the pile of red phosphorus. Note that the Schlenk tube is placed under static vacuum and lubricated with Apiezon H grease.*	***Step 2:*** *after a few minutes, white phosphorus condenses on the cooler parts of the Schlenk tube. The heatgun is progressively moved towards the bottom end of the tube (right).*
	
Step 3: *after cooling and transfer in the glovebox, the Schlenk tube is scraped and the solids are extracted with CH_2Cl_2 in an ordinary Schlenk flask lubricated with Dow Corning Si grease.*	***Step 4:*** *after overnight extraction, the solids are filtered over a grade 4 glass frit in the glovebox. Note that for this batch, residual lumps of P_4 can be observed. A second extraction was necessary in order to completely separate P_4 from red phosphorus.*
	
Step 5: *the CH_2Cl_2 solution is evaporated to dryness with a vacuum line.*	***Step 6:*** *finely divided P_4 is obtained after collection in the glovebox.*

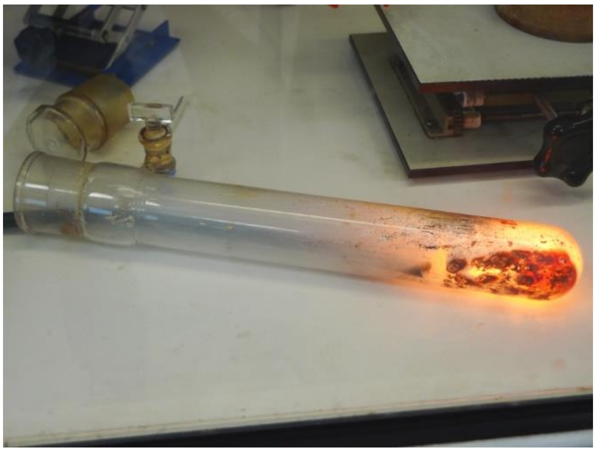	
Step 7: *residues of P_4 are burned under a flow of air. Note that this step is performed with the sash of the fumehood completely lowered, in order to protect the operator from toxic P_xO_y fumes. A larger metal pan may also be used as a protection from airborne burning P_4 particles if required. The glassware may then be cleaned with water and cleaning powder.*	***Step 8:*** *the Schlenk tube can now be cleaned safely.*

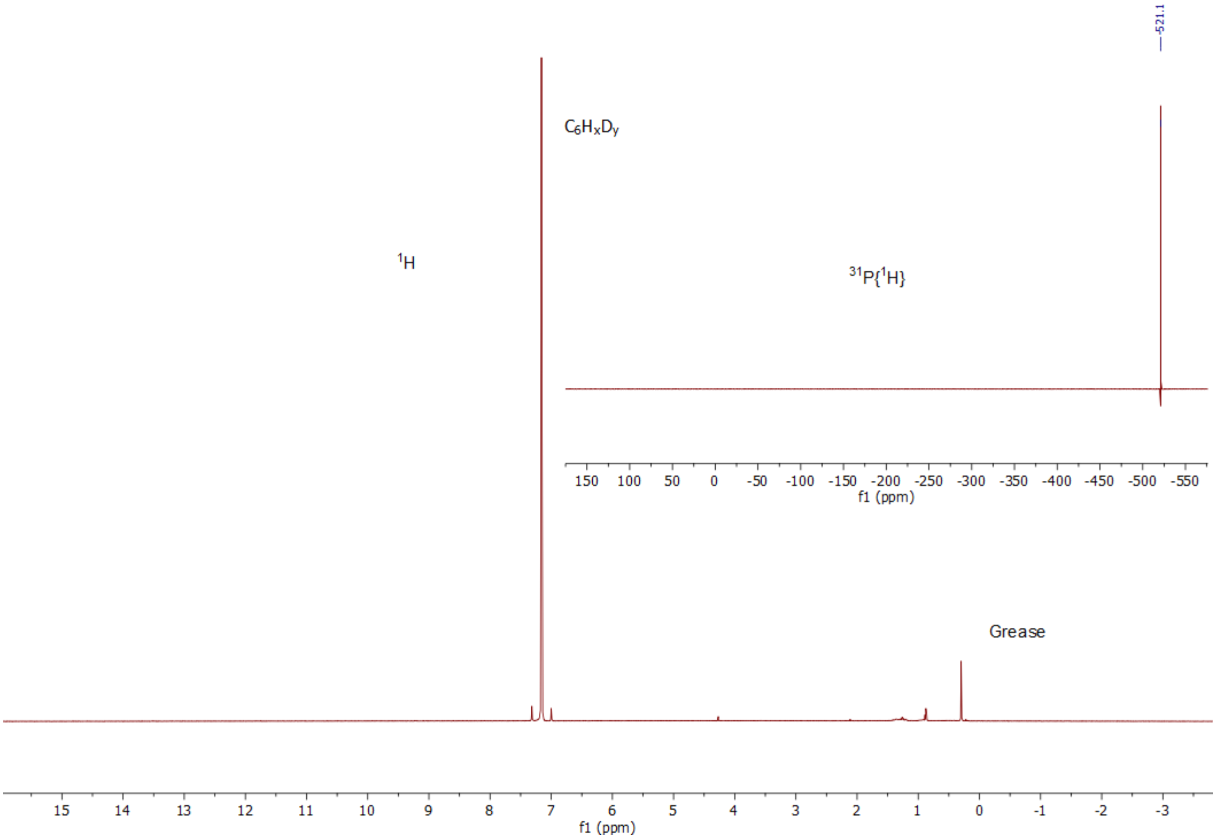

Figure S1: ^1H (500MHz, C_6D_6, 298 K) and $^{31}P\{^1H\}$ NMR (202 MHz, C_6D_6, 298 K)

Synthesis of pro proligand ***2a***

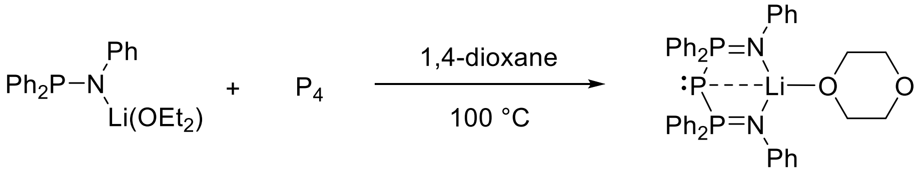

1a

2a *(3.20 g, 81%)*

In an Ar glovebox, lithium phosphinoamide **1a** (4.29 g, 12.0 mmol) and white phosphorus (2.97 g, 24.0 mmol) were suspended in 1,4-dioxane (30 mL) in a Schlenk flask. The vessel was transferred into a sand bath at 100 °C, stirred for a couple of minutes under Ar, then closed under slight static vacuum (quick 180 ° rotation of the stopcock). The heterogeneous reaction mixture quickly turned dark brown and was heated to 100 °C for 66 h, after which it was allowed to cool to room temperature, and filtered over a sintered glass frit in the glovebox. The black cake was rinsed with 1,4-dioxane, and the filtrate was evaporated to dryness outside of the glovebox. Upon returning to the glovebox, the solid residue was triturated in 50 mL of pentane and stirred until a fine powder was obtained. The powder was filtered over a sintered glass frit and rinsed with pentane (4 x 10 mL), then dried on the frit. Compound **2a** was obtained as a pale yellow powder (3.20 g, yield 81%).

[†] Cautionary note: Extreme care must be taken when disposing of reaction by-products, since even minute amounts of residual P_4 may ignite upon exposure to air. This is especially critical when using an isopropanol base bath to clean glassware. In this particular instance it is essential that the LixPy black cake be rinsed with solvent and not be allowed to become too warm upon removal from the glovebox, otherwise it may ignite spontaneously. The cake can be quenched in a dish by slow oxidation by atmospheric O_2; cooling by periodic additions of small amounts of liquid N_2 was found to be both convenient and safe. Refer to local chemical waste disposal policies to dispose of the oxidized residue.

Elemental Analysis: calculated for $C_{40}H_{38}LiN_2O_2P_3$: C, 70.80; H, 5.64; N, 4.13. Found: C, 70.53; H, 5.47; N, 4.06.

UV-vis (0.1 mm cell): λ_1 = 298 nm (shoulder, ε = 27000 $M^{-1}.cm^{-1}$).

IR (ATR): 1586 (m), 1478 (s), 1432 (m), 1292 (s), 1261 (s), 1255 (s), 1175 (m), 1117 (m), 1095 (m), 1074 (m), 1029 (m), 996 (s), 980 (m), 971 (m), 871 (m), 768 (m), (767 (m), 750 (s), 741 (s), 715 (m), 690 (vs), 631 (b, s), 609 (s), 539 (s), 516 (m), 491 (s) cm^{-1}.

^{1}H NMR (500 MHz, d_8-THF, 298 K): δ = 7.60 (m, 8H, *o* of PPh_2), 7.19 (m, 4H, *p* of PPh_2), 7.09 (m, 8H, *m* of PPh_2), 6.74 (m, 4H, *m* of NPh), 6.52 (m, 4H, *o* of NPh), 6.39 (m, 2H, *p* of NPh), 3.56 (s, 8H, CH_2O).

^{1}H-^{1}H COSY (500 MHz, d_8-THF, 298 K)[selected cross-peaks]: 7.60 / 7.09 (*o* of PPh_2 / *m* of PPh_2), 7.19 / 7.09 (*p* of PPh_2 / *m* of PPh_2), 7.09 / 7.60 (*m* of PPh_2 / *o* of PPh_2), 7.09 / 7.49 (*m* of PPh_2 / *p* of PPh_2), 6.74 / 6.52 (*m* of NPh / *o* of NPh), 6.74 / 6.39 (*m* of NPh / *p* of NPh), 6.52 / 6.74 (*o* of NPh / *m* of NPh), 6.39 / 6.74 (*p* of NPh / *m* of NPh).

^{1}H-^{13}C HMBC (500 MHz / 126 MHz, d$_8$-THF, 298 K)[selected cross-peaks]: 7.60 / 136.0 (*o* of PPh$_2$ / *i* of PPh$_2$), 7.60 / 132.7 (*o* of PPh$_2$ / *m* of PPh$_2$), 7.19 / 132.7 (*p* of PPh$_2$ / *m* of PPh$_2$), 7.09 / 136.0 (*m* of PPh$_2$ / *i* of PPh$_2$), 7.09 / 132.7 (*m* of PPh$_2$ / *m* of PPh$_2$), 7.09 / 128.1 (*m* of PPh$_2$ / *o* of PPh$_2$), 6.74 / 153.7 (*m* of NPh / *i* of NPh), 6.74 / 128.3 (*m* of NPh / *m* of NPh), 6.52 / 123.6 (*o* of NPh / *o* of NPh), 6.52 / 117.1 (*o* of NPh / *o* of NPh), 6.39 / 123.6 (*p* of NPh / *o* of NPh).

^{13}C{^{1}H} NMR (126 MHz, d$_8$-THF, 298 K): δ = 153.7 (m, *i* of NPh), 136.0 (m, *i* of PPh$_2$), 132.7 (m, *m* of PPh$_2$), 130.3 (s, *p* of PPh$_2$), 128.3 (s, *m* of NPh), 128.1 (m, *o* of PPh$_2$), 123.6 (m, *o* of NPh), 117.1 (s, *p* of NPh), 67.7 (s, *C*H$_2$O overlapping with solvent signal).

^{31}P{^{1}H} NMR (202 MHz, d$_8$-THF, 298 K): δ = 31.8 (d, $^1J_{PP}$ = 411 Hz, *P*Ph$_2$), -118.7 (t, $^1J_{PP}$ = 411 Hz, central *P*).

^{7}Li NMR (194 MHz, d$_8$-THF, 298 K): δ = 1.2 ($\nu \approx$ 23 Hz).

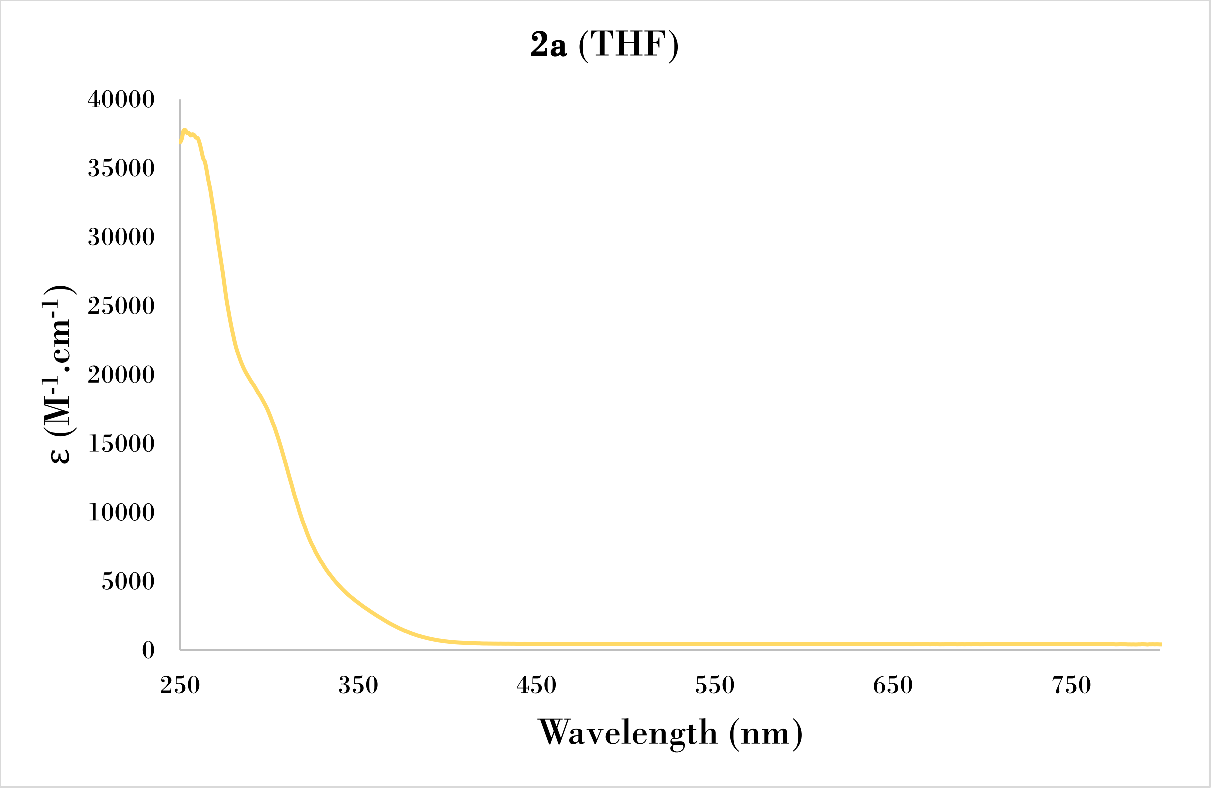

Figure S2: UV-vis (0.1 mm cell)

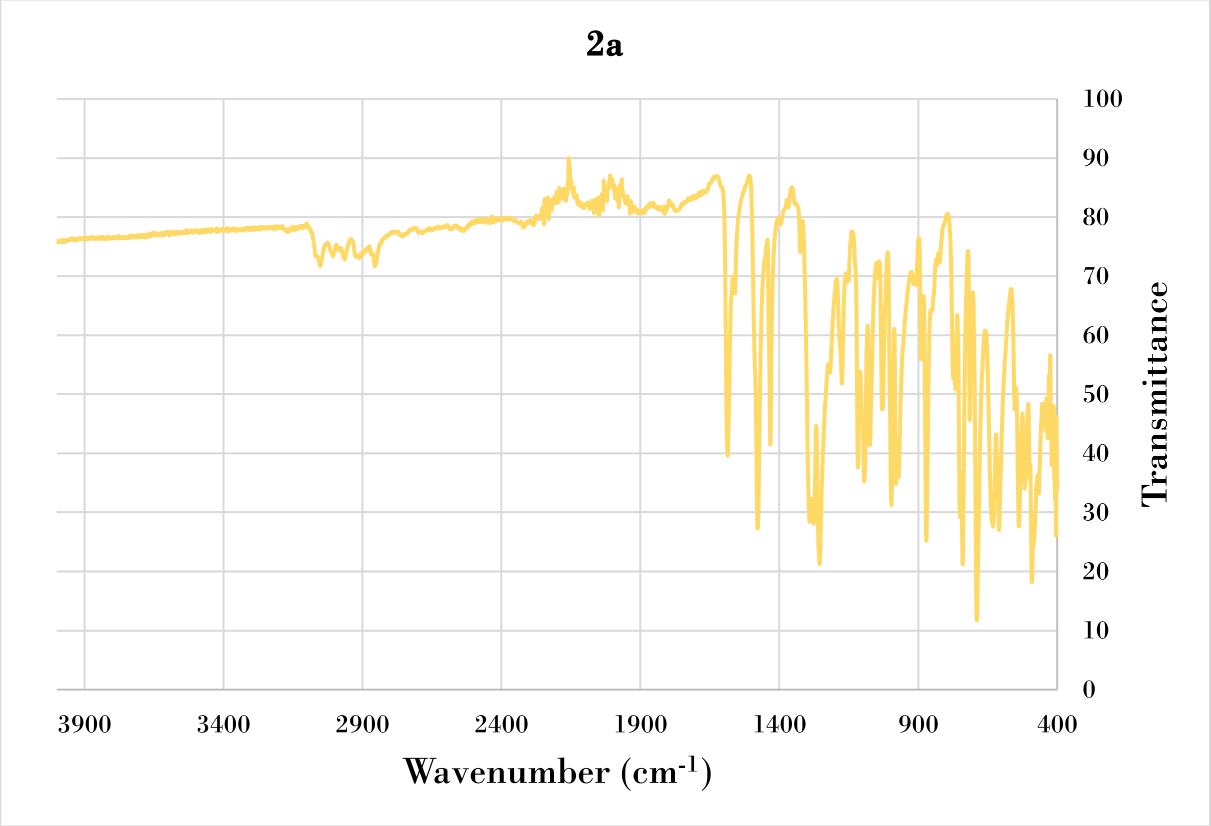

Figure S3: IR (ATR)

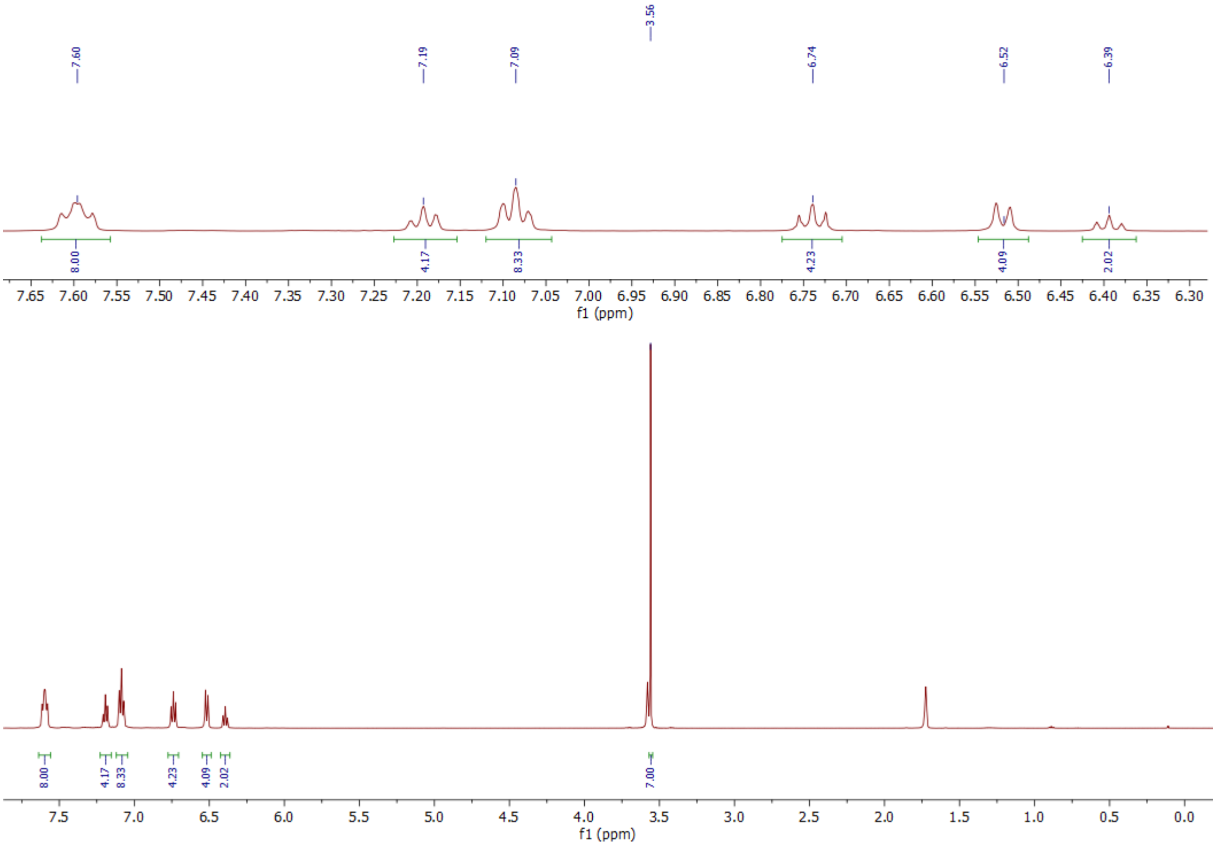

Figure S4: ^{1}H NMR (500 MHz, d_8-THF, 298 K)

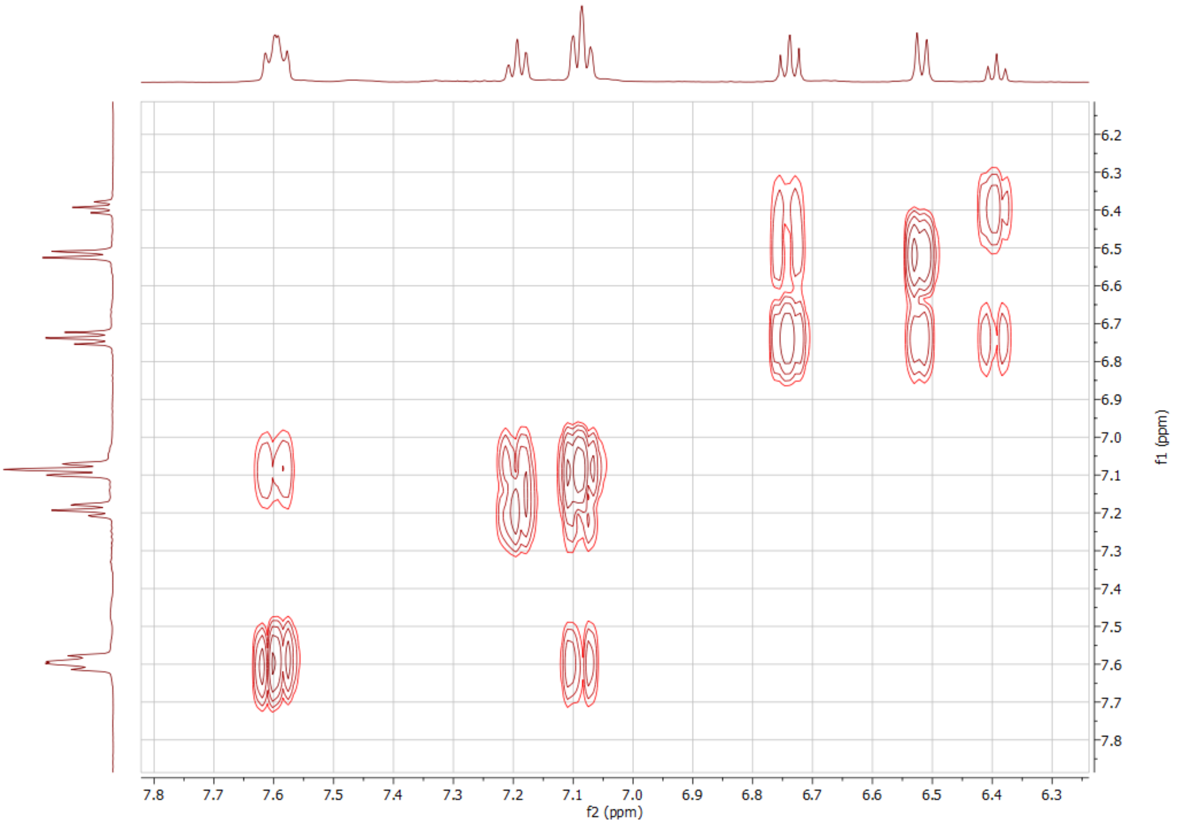

Figure S5: ^{1}H-^{1}H COSY (500 MHz, d_8-THF, 298 K)

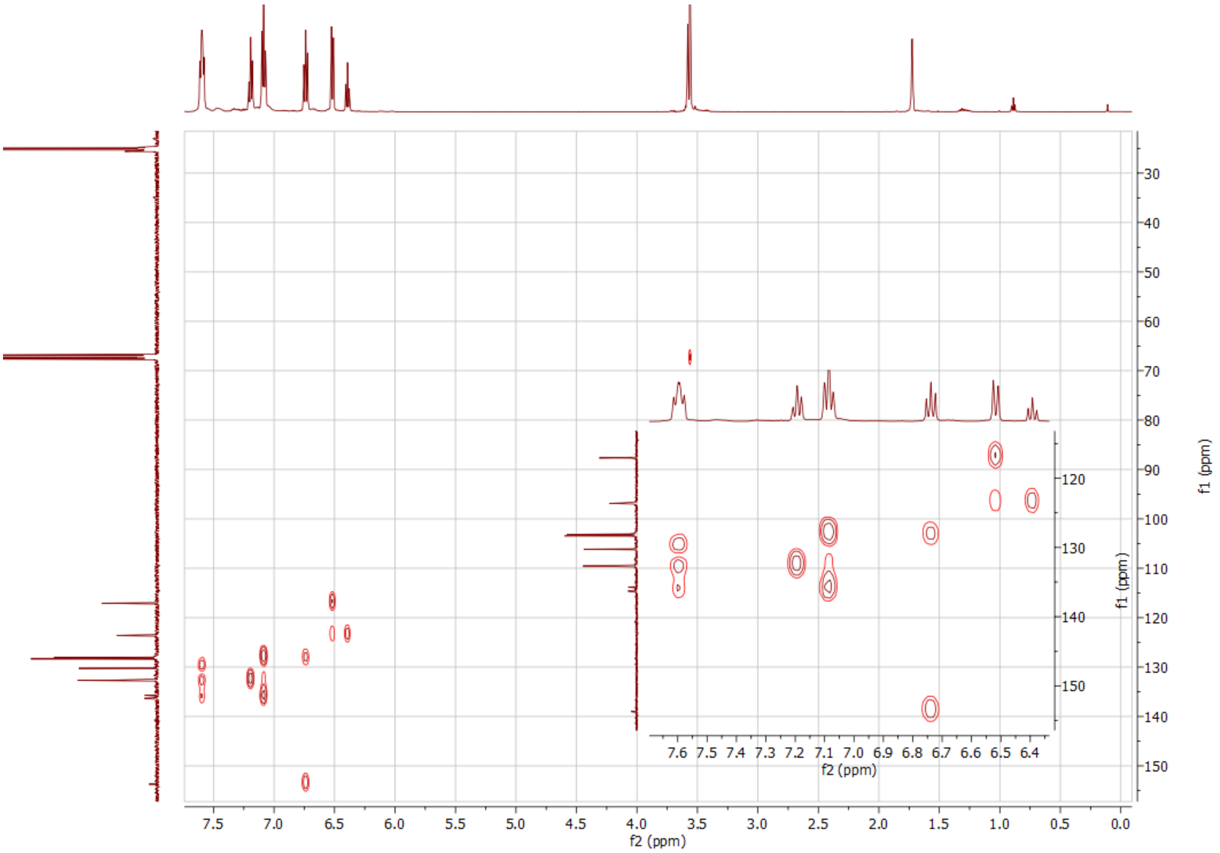

Figure S6: ^{1}H-^{13}C HMBC (500 MHz / 126 MHz, d_8-THF, 298 K)

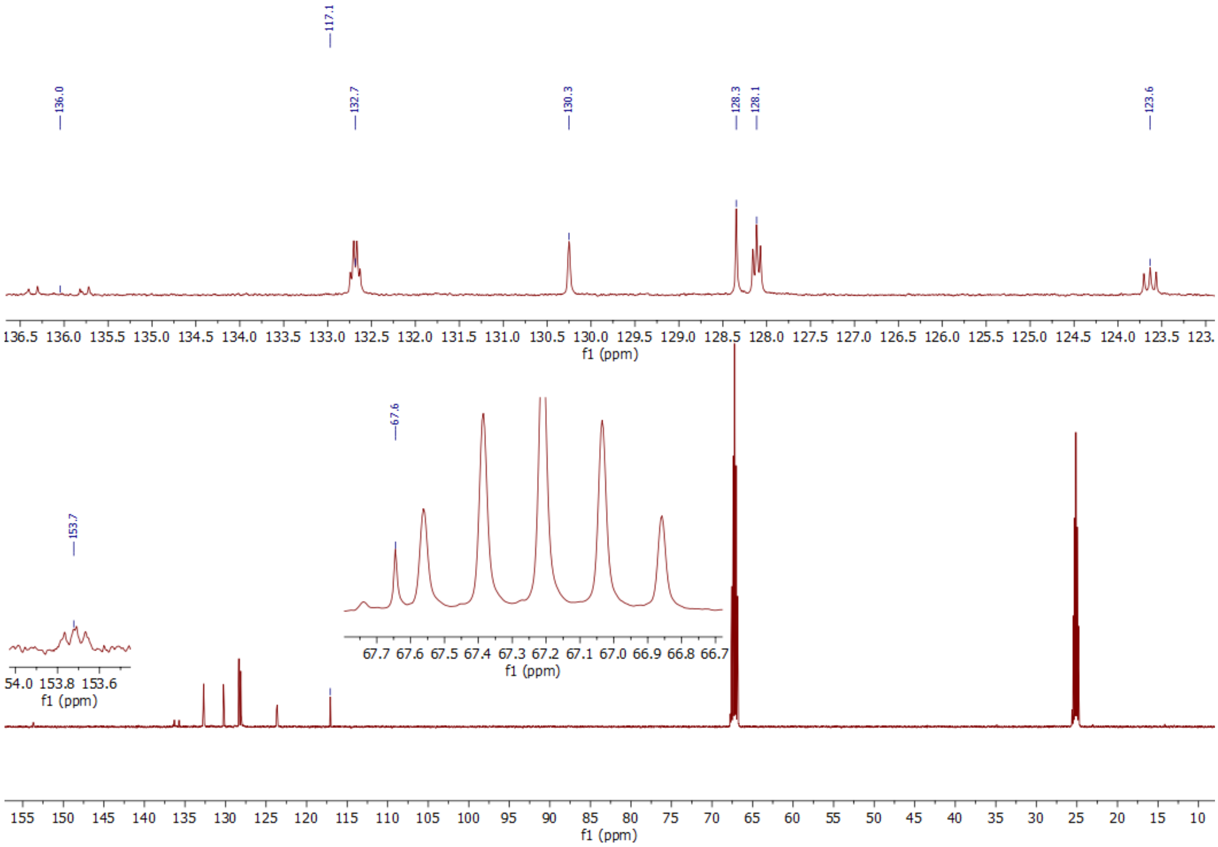

Figure S7: $^{13}C\{^{1}H\}$ **NMR (126 MHz, d₈-THF, 298 K)**

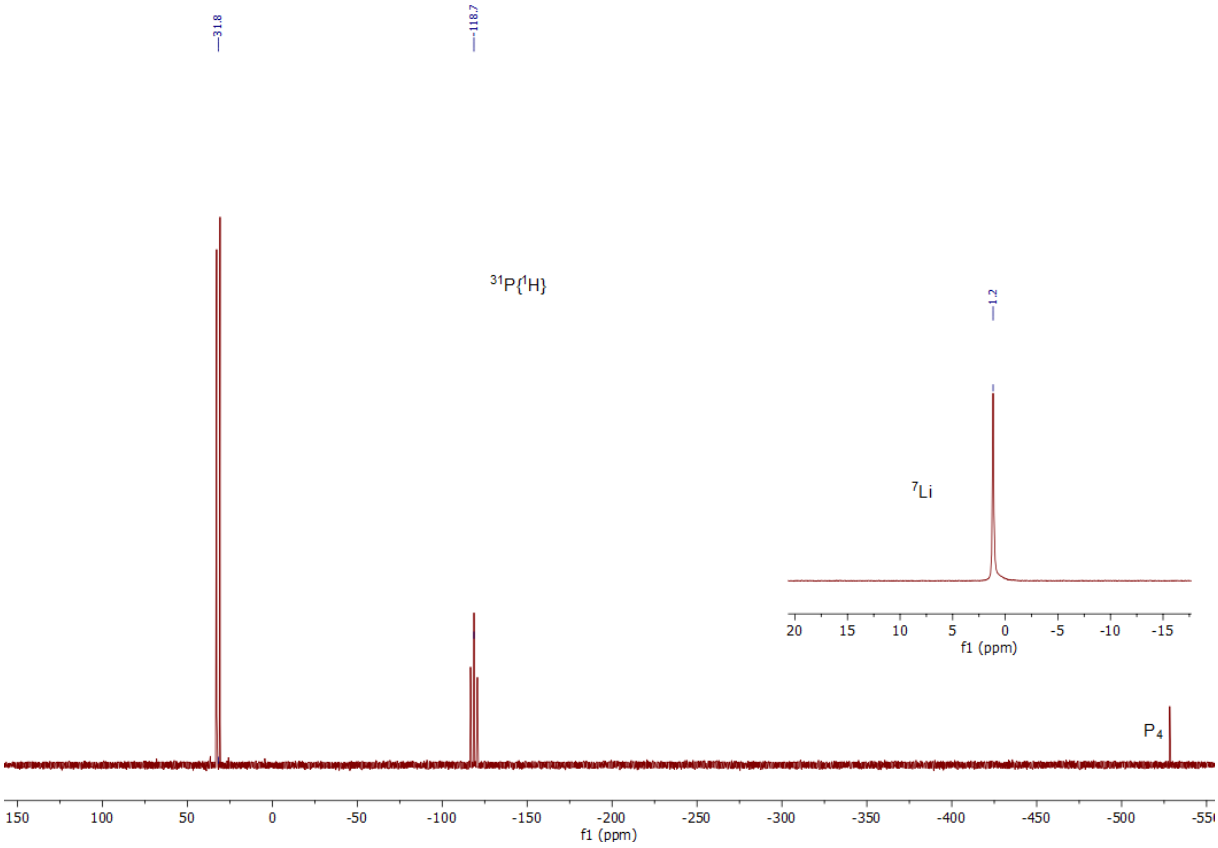

Figure S8: $^{31}P\{^{1}H\}$ **NMR (202 MHz, d₈-THF, 298 K);** ^{7}Li **NMR (194 MHz, d₈-THF, 298 K)**

*Synthesis of pro proligand **2b***

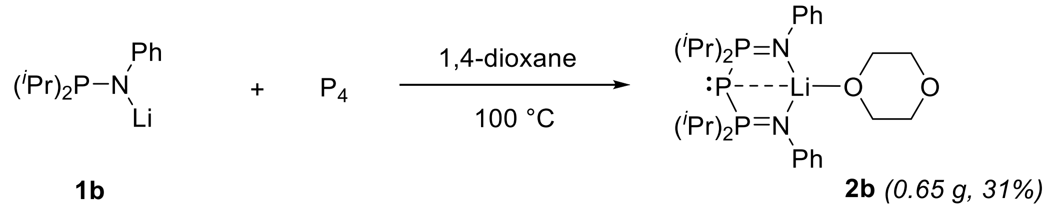

In an Ar glovebox, lithium phosphinoamide **1b** (1.78 g, 8.3 mmol) and white phosphorus (2.06 g, 16.6 mmol) were suspended in 1,4-dioxane (20 mL) in a Schlenk flask. A vivid pink color was observed immediately. The vessel was transferred into a sand bath at 100 °C, stirred for a couple of minutes under Ar, then closed under slight static vacuum (quick 180 ° rotation of the stopcock). The heterogeneous reaction mixture quickly turned dark brown and was heated to 100 °C for 13 h, after which it was allowed to cool to room temperature, and filtered over a sintered glass frit in the glovebox. The black cake was rinsed with pentane, and the filtrate was evaporated to dryness outside of the glovebox. Upon returning to the glovebox, the solid residue was dissolved in 15 mL of pentane stored in the glovebox freezer at -20 °C. Yellow crystals **2b** were collected and dried on a frit (0.65 g, yield 31%).

[†] Cautionary note: Extreme care must be taken when disposing of reaction by-products, since even minute amounts of residual P_4 may ignite upon exposure to air. This is especially critical when using an isopropanol base bath to clean glassware. In this particular instance it is essential that the LixPy black cake be rinsed with solvent and not be allowed to become too warm upon removal from the glovebox, otherwise it may ignite spontaneously. The cake can be quenched in a dish by slow oxidation by atmospheric O_2; cooling by periodic additions of small amounts of liquid N_2 was found to be both convenient and safe. Refer to local chemical waste disposal policies to dispose of the oxidized residue.

Elemental Analysis: calculated for $C_{28}H_{46}LiN_2O_2P_3$: C, 61.99; H, 8.55; N, 5.16. Found: C, 62.13; H, 9.22; N, 5.29.

UV-vis (THF, 0.1 mm cell): λ_1 = 270 nm (global maximum, ε = 27000 $M^{-1}.cm^{-1}$).

IR (ATR): 2958 (w), 2860 (m), 1582 (s), 1472 (s), 1448 (m), 1383 (w), 1360 (w), 1293 (m), 1243 (vs), 1228 (vs), 1166 (m), 1123 (s), 1107 (m), 1079 (m), 1029 (m), 995 (s), 969 (s), 949 (s), 892 (m), 877 (vs), 869 (vs), 775 (vs), 750 (s), 702 (vs), 680 (m), 655 (s), 613 (vs), 574 (vs), 548 (s), 525 (s), 503 (vs), 464 (s) cm^{-1}.

^{1}H NMR (500 MHz, C_6D_6, 293 K): δ = 7.18 (m, 4H, *m* of NPh), 7.04 (m, 4H, *o* of NPh), 6.80 (m, 2H, *p* of NPh), 3.18 (s, 8H, CH_2O), 2.51 (m, 4H, C*H* of ^{i}Pr), 1.30 (m, 24H, CH_3 of ^{i}Pr).

^{1}H-^{1}H COSY (500 MHz, C_6D_6, 293 K)[selected cross-peaks]: 7.60 / 7.09 (*o* of PPh_2 / *m* of PPh_2), 7.19 / 7.09 (*p* of PPh_2 / *m* of PPh_2), 7.09 / 7.60 (*m* of PPh_2 / *o* of PPh_2), 7.09 / 7.49 (*m* of PPh_2 / *p* of PPh_2), 6.74 / 6.52 (*m* of NPh / *o* of NPh), 6.74 / 6.39 (*m* of NPh / *p* of NPh), 6.52 / 6.74 (*o* of NPh / *m* of NPh), 6.39 / 6.74 (*p* of NPh / *m* of NPh).

^{1}H-^{13}C HMBC (500 MHz / 126 MHz, C_6D_6, 293 K)[selected cross-peaks]: 7.60 / 136.0 (*o* of PPh_2 / *i* of PPh_2), 7.60 / 132.7 (*o* of PPh_2 / *m* of PPh_2), 7.19 / 132.7 (*p* of PPh_2 / *m* of PPh_2), 7.09 / 136.0

(*m* of PPh_2 / *i* of PPh_2), 7.09 / 132.7 (*m* of PPh_2 / *m* of PPh_2), 7.09 / 128.1 (*m* of PPh_2 / *o* of PPh_2), 6.74 / 153.7 (*m* of NPh / *i* of NPh), 6.74 / 128.3 (*m* of NPh / *m* of NPh), 6.52 / 123.6 (*o* of NPh / *o* of NPh), 6.52 / 117.1 (*o* of NPh / *o* of NPh), 6.39 / 123.6 (*p* of NPh / *o* of NPh).

$^{13}C\{^1H\}$ NMR (151 MHz, C_6D_6, 293 K): δ = 153.7 (m, *i* of NPh), 129.4 (s, *m* of NPh), 124.1 (m, *o* of NPh), 118.3 (s, *p* of NPh), 67.0 (s, CH_2O), 32.0 (m, *C*H of ^{i}Pr), 18.9 (m, CH_3 of ^{i}Pr), 18.7 (m, CH_3 of ^{i}Pr).

$^{31}P\{^1H\}$ NMR (202 MHz, C_6D_6, 293 K): δ = 62.2 (d, $^1J_{PP}$ = 462 Hz, P^iPr_2), -201.6 (t, $^1J_{PP}$ = 462 Hz, central *P*).

^{7}Li NMR (194 MHz, C_6D_6, 293 K): δ = 1.0 (ν ≈ 12 Hz).

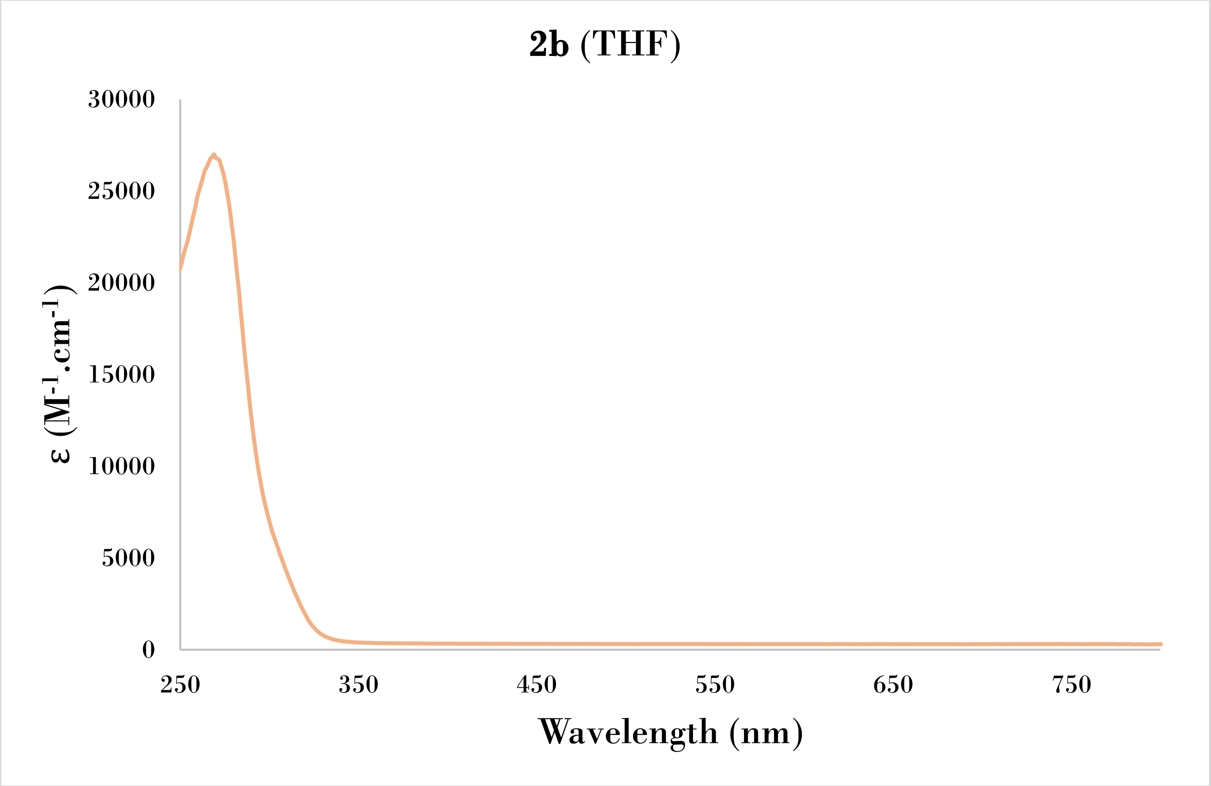

Figure S9: UV-vis (THF, 0.1 mm cell)

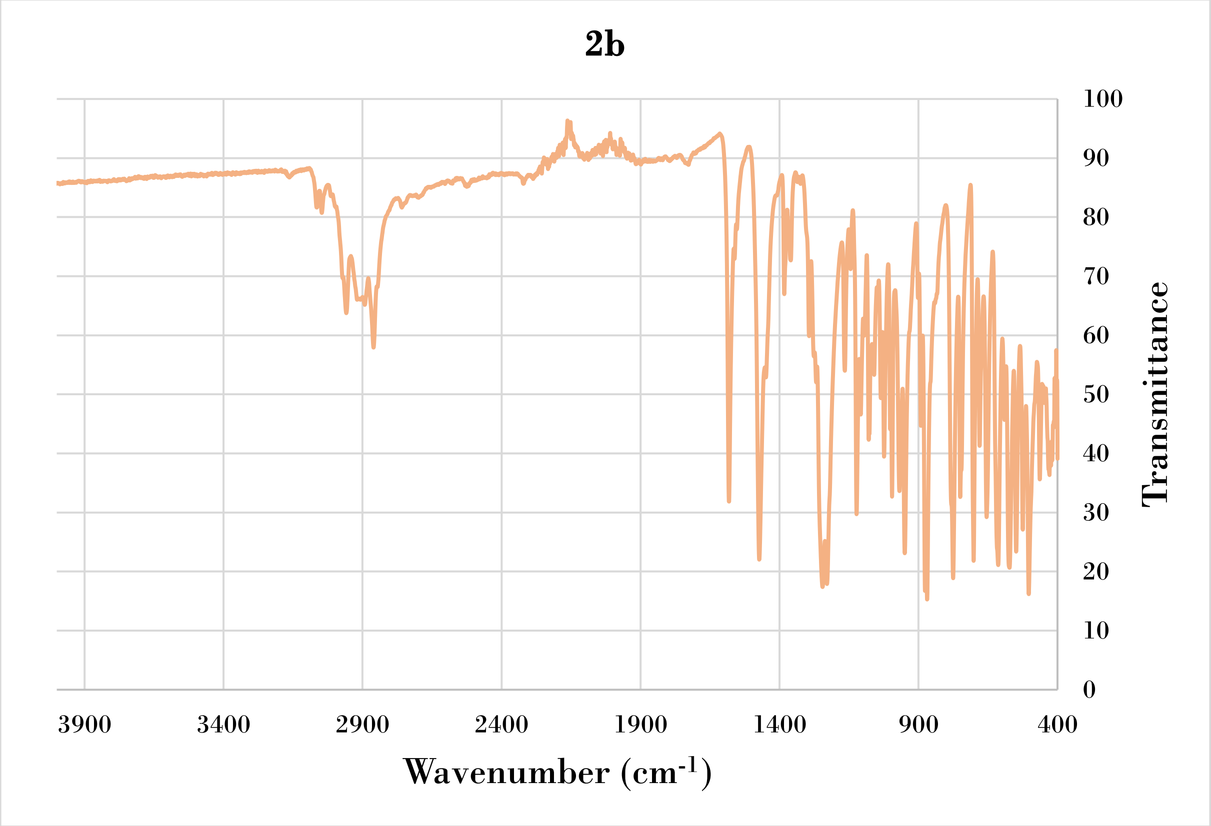

Figure S10: IR (ATR)

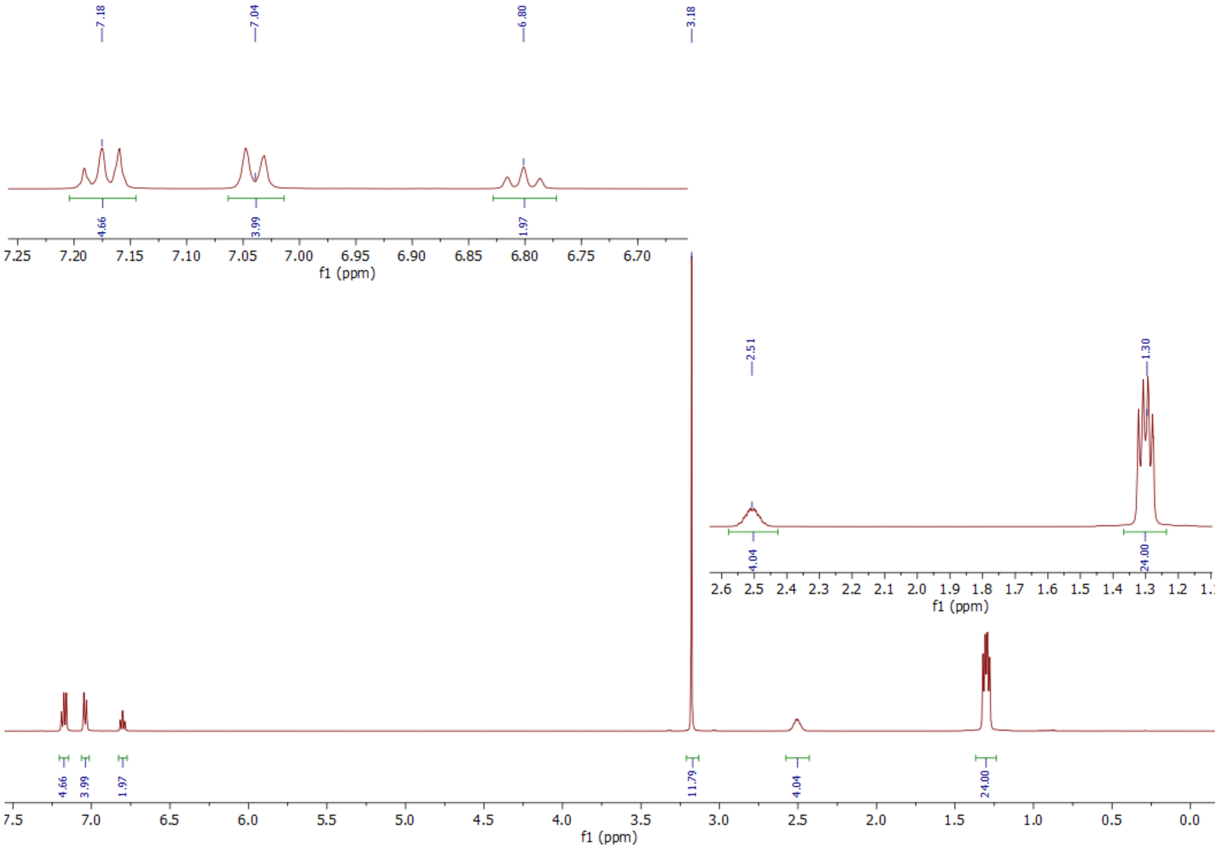

Figure S11: ^{1}H NMR (500 MHz, C_6D_6, 293 K)

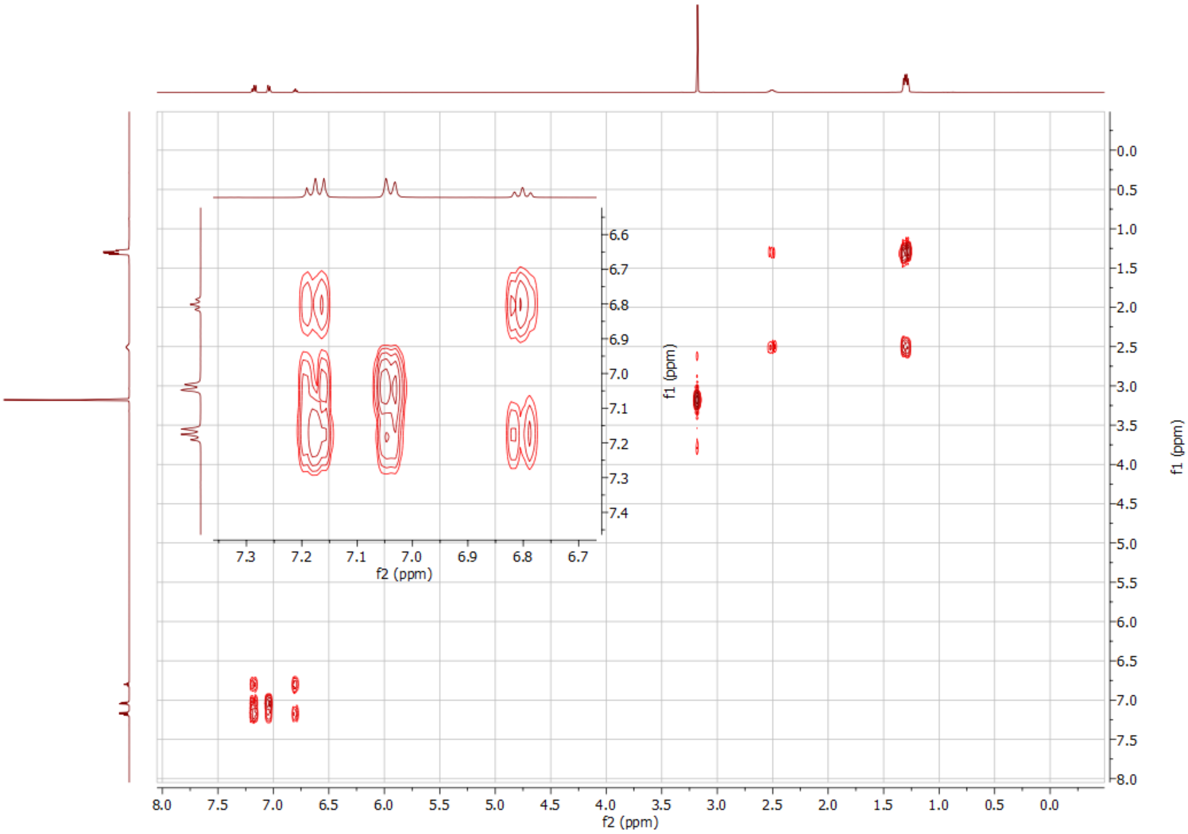

Figure S12: ^{1}H-^{1}H COSY (500 MHz, C_6D_6, 293 K)

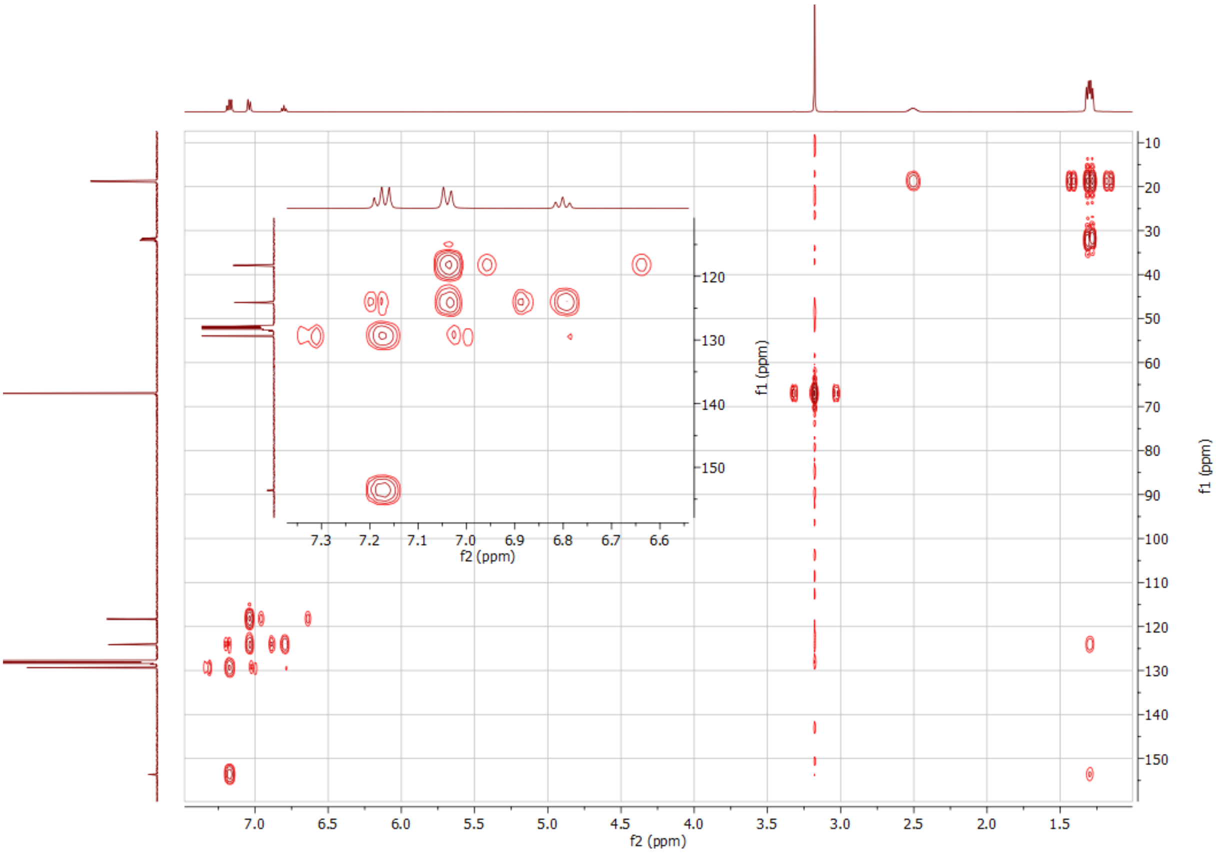

Figure S13: ^{1}H-^{13}C HMBC (500 MHz / 126 MHz, C_6D_6, 293 K)

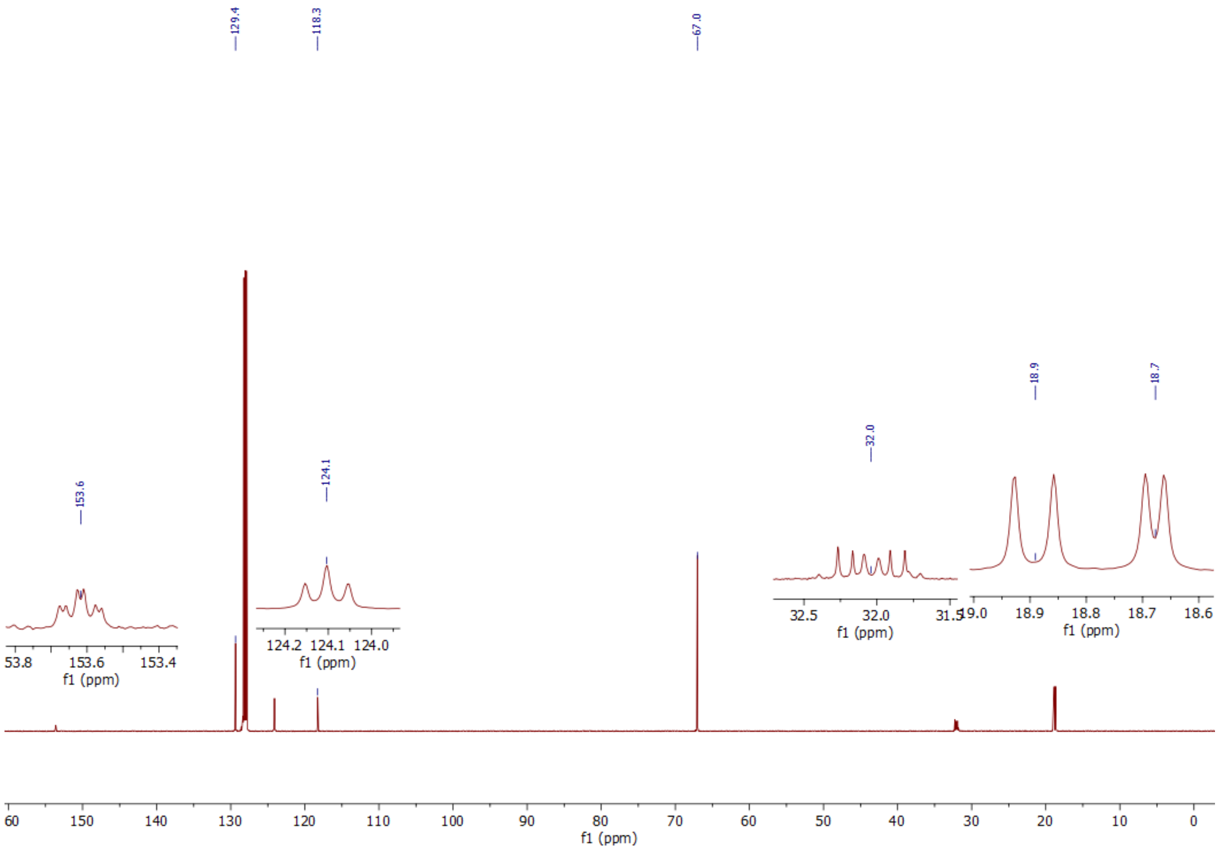

Figure S14: $^{13}C\{^{1}H\}$ NMR (126 MHz, C_6D_6, 293 K)

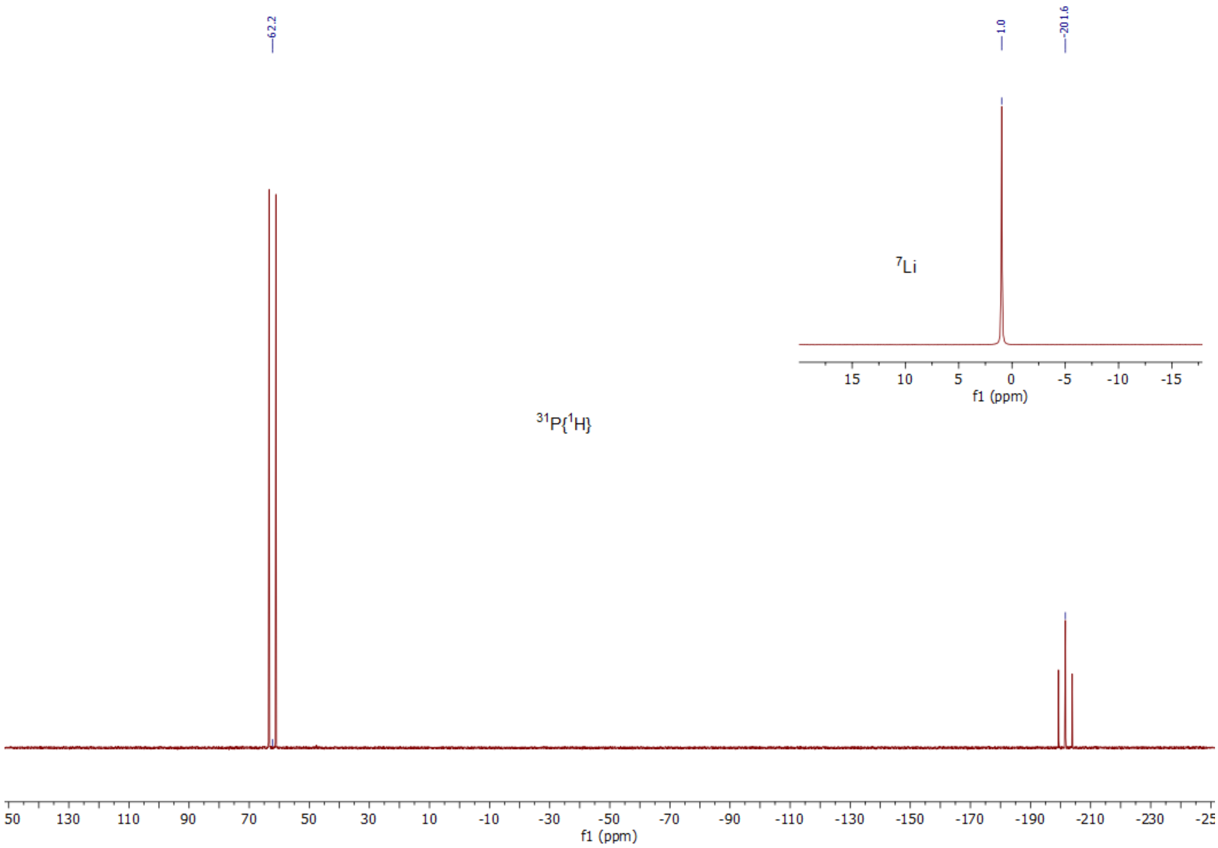

Figure S15: $^{31}P\{^{1}H\}$ NMR (202 MHz, C_6D_6, 293 K); ^{7}Li NMR (194 MHz, C_6D_6, 293 K)

*Synthesis of pro proligand **2b’***

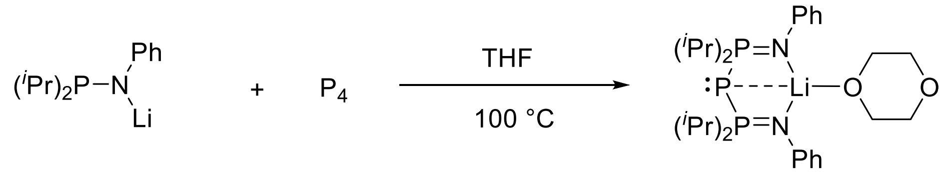

1b **2b'** *(1.25 g, 26%)*

In an Ar glovebox, lithium phosphinoamide **1b** (4.00 g, 18.2 mmol) and white phosphorus (1.13 g, 9.10 mmol) were suspended in THF (70 mL) in a Schlenk flask. A vivid pink color was observed immediately. The vessel was transferred into an oil bath at 65 °C, stirred for a couple of minutes under Ar, then closed under slight static vacuum (quick 180 ° rotation of the stopcock). The heterogeneous reaction mixture quickly turned dark brown and was heated to 65 °C for 40 min, after which it was allowed to cool to room temperature, and another portion of P_4 (1.13 g, 9.10 mmol) was added. The mixture was heated again for 45 min and this procedure was repeated twice, (overall amount of P_4: 4.50 g, 36.3 mmol). Analysis of the reaction mixture revealed that the reaction was not complete, therefore it was heated again at 65 °C for 2 h. After cooling, the mixture was filtered over a sintered glass frit in the glovebox. The black cake was rinsed with pentane, and the filtrate was evaporated to dryness outside of the glovebox. Upon returning to the glovebox, the solid residue was dissolved in 100 mL of pentane and evaporated again. Addition of 30 mL of pentane followed by agitation then storage in the glovebox freezer at –20 °C for two days afforded orange crystals. The crystals were collected, crushed and dried on a frit, yielding **2b’** as an orange powder (1.25 g, yield 26%). Single crystals suitable for X-ray diffraction analysis were grown by cooling a saturated solution of **2b’** in pentane at -20 °C.

[†] Cautionary note: Extreme care must be taken when disposing of reaction by-products, since even minute amounts of residual P_4 may ignite upon exposure to air. This is especially critical when using an isopropanol base bath to clean glassware. In this particular instance it is essential that the LixPy black cake be rinsed with solvent and not be allowed to become too warm upon removal from the glovebox, otherwise it may ignite spontaneously. The cake can be quenched in a dish by slow oxidation by atmospheric O_2; cooling by periodic additions of small amounts of liquid N_2 was found to be both convenient and safe. Refer to local chemical waste disposal policies to dispose of the oxidized residue.

Elemental Analysis: calculated for $C_{28}H_{46}LiN_2OP_3$: C, 63.87; H, 8.81; N, 5.32. Found: C, 63.15; H, 9.00; N, 5.34.

UV-vis (10 mm cell): λ_1 = 249 nm (global maximum, ε = 25000 $M^{-1}.cm^{-1}$); λ_1 = 270 nm (shoulder, ε = 17000 $M^{-1}.cm^{-1}$).

IR (ATR): 2955 (m), 2864 (m), 1586 (m), 1476 (s), 1381 (w), 1358 (w), 1284 (m), 1246 (m), 1228 (m), 1169 (m), 1123 (s), 1034 (m), 1027 (m), 1003 (m), 996 (m), 970 (m), 696 (m), 894 (m), 877 (m), 784 (m), 769 (m), 756 (m), 746 (m), 702 (s), 656 (m), 611 (s), 577 (s), 551 (m), 511 (b, m), 465 (m) cm^{-1}.

^{1}H NMR (500 MHz, d$_8$-THF, 298 K): δ = 7.00 (m, 4H, *m* of NPh), 6.97 (m, 4H, *o* of NPh), 6.56 (m, 2H, *p* of NPh), 3.62 (m, 4H, C*H*$_2$O), 2.57 (m, 4H, C*H* of ^{i}Pr), 1.77 (m, 4H, C*H*$_2$CH$_2$O), 1.27 (m, 24H, C*H*$_3$ of ^{i}Pr).

^{13}C{^{1}H} NMR (151 MHz, d$_8$-THF, 298 K): δ = 155.0 (m, *i* of NPh), 128.8 (s, *m* of NPh), 125.0 (m, *o* of NPh), 117.8 (s, *p* of NPh), 68.0 (s, *C*H$_2$O), 32.2 (m, *C*H of ^{i}Pr), 26.2 (s, *C*H$_2$CH$_2$O), 18.8 (m, *C*H$_3$ of ^{i}Pr), 18.7 (m, *C*H$_3$ of ^{i}Pr).

^{31}P{^{1}H} NMR (202 MHz, d$_8$-THF, 298 K): δ = 61.0 (d, $^1J_{PP}$ = 450 Hz, *P*^{i}Pr$_2$), -190.8 (t, $^1J_{PP}$ = 450 Hz, central *P*).

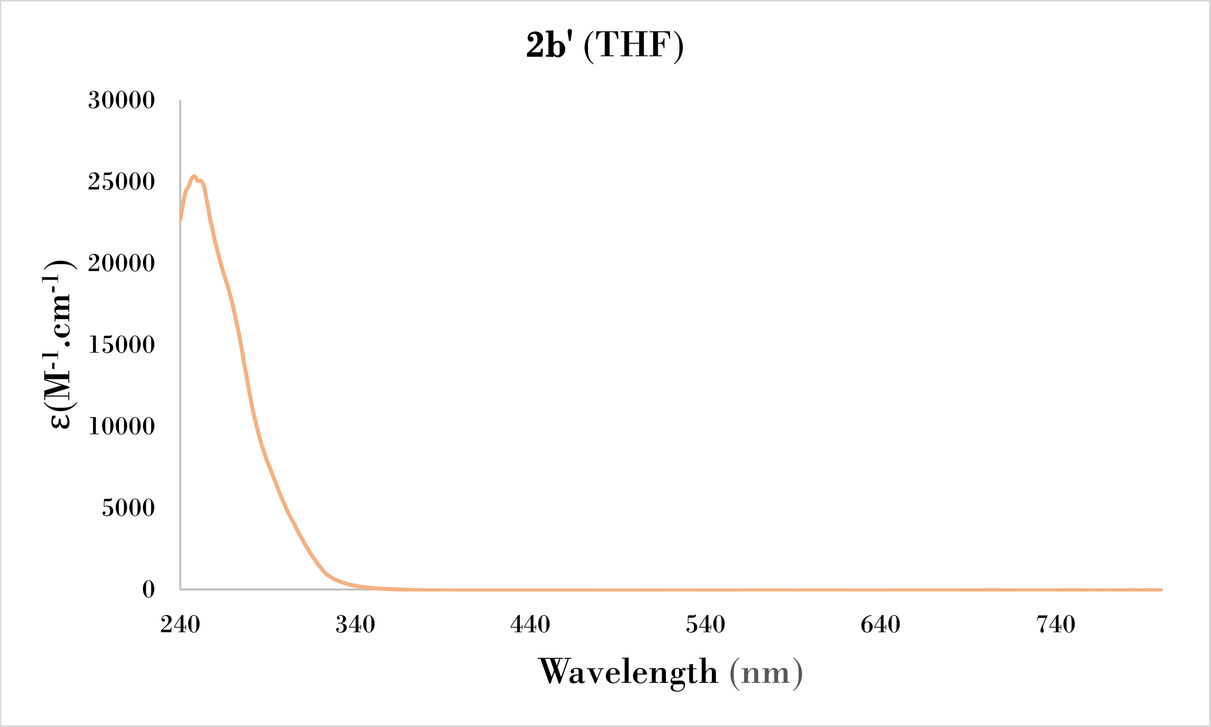

Figure S16: UV-vis (THF, 10 mm cell)

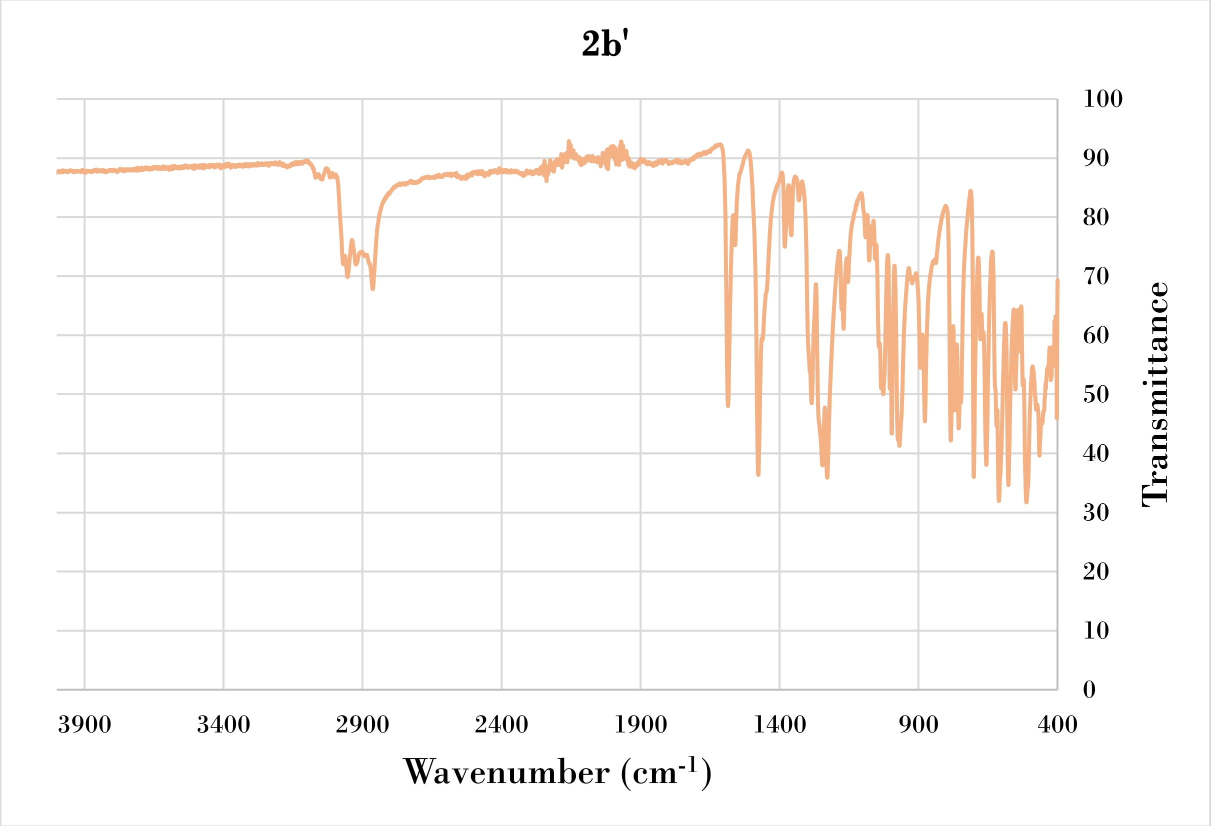

Figure S17: IR (ATR)

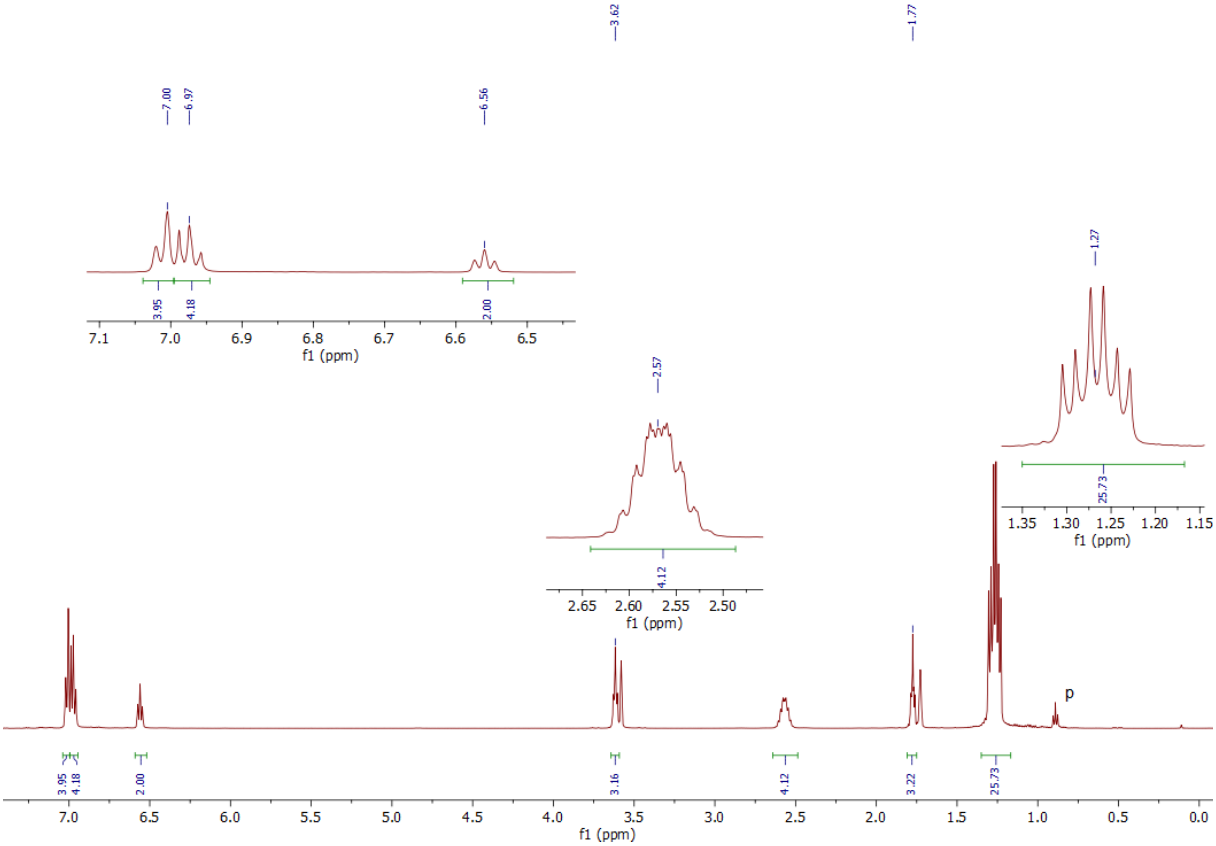

Figure S18: ^{1}H NMR (500 MHz, d$_8$-THF, 298 K)(p: pentane)

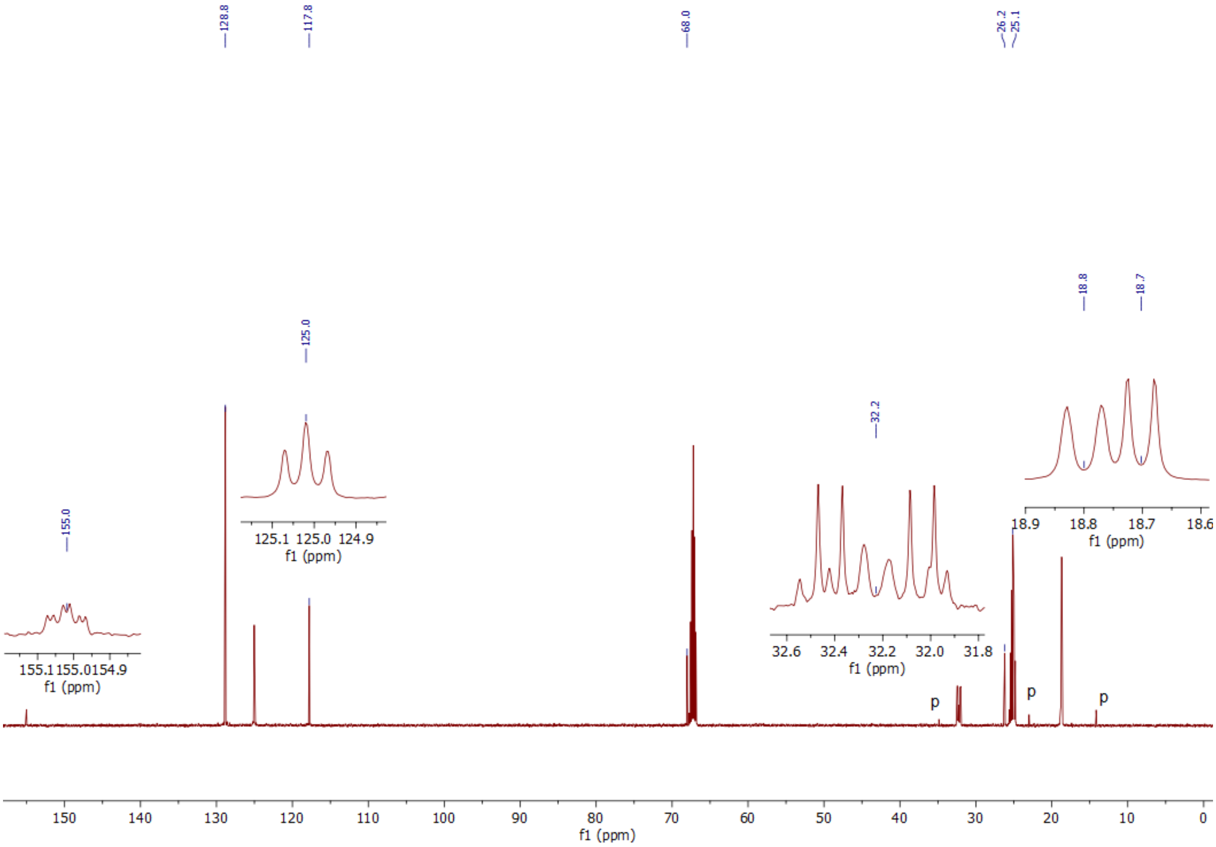

Figure S19: $^{13}C\{^{1}H\}$ **NMR (126 MHz, d_8-THF, 298 K)(p: pentane)**

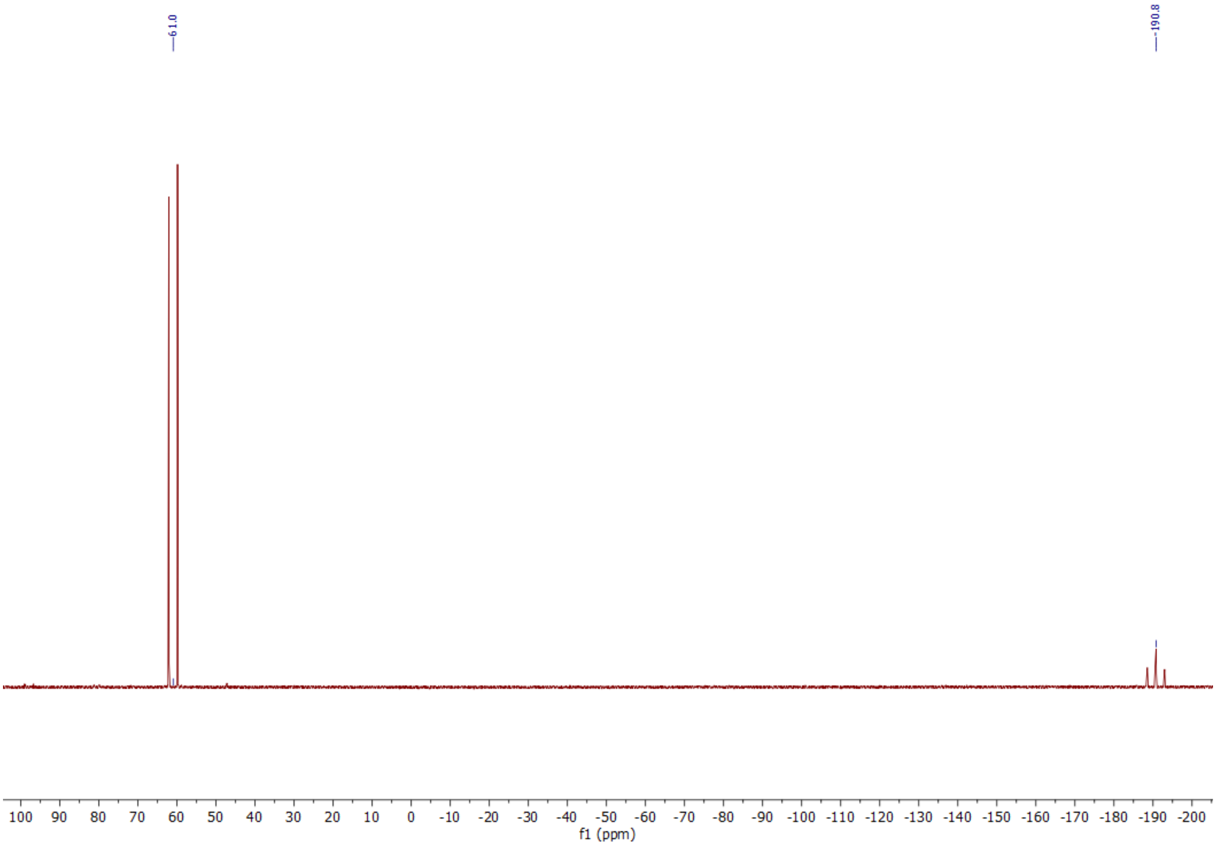

Figure S20: $^{31}P\{^{1}H\}$ **NMR (202 MHz, d_8-THF, 298 K)**

*Synthesis of complex **3a***

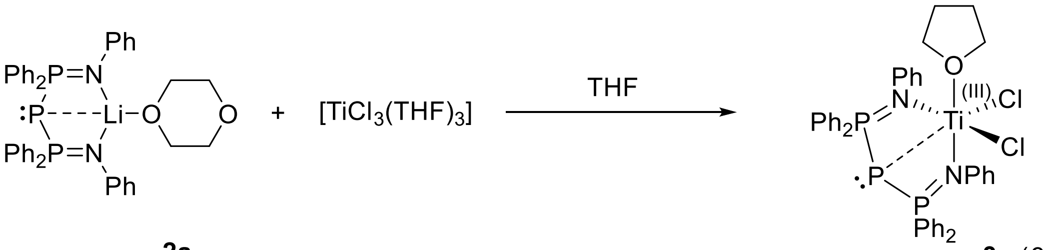

2a

3a *(2.28 g, 74%)*

In an Ar glovebox, proligand **2a** (2.63 g, 3.86 mmol) and [TiCl$_3$(THF)$_3$] (1.48 g, 4.00 mmol) were suspended in THF (20 mL). The reaction mixture was stirred for 14 h, during which a pale green precipitate appeared. The suspension was filtered over a sintered glass frit (porosity grade 4), the solid was rinsed with THF (3 x 10 mL) and dried on the frit, yielding **3a** as a blue-green powder (2.28 g, yield 74%). Single crystals suitable for X-ray diffraction were grown by cooling a saturated THF solution of **3a** at -20 °C.

Elemental Analysis: calculated for $C_{40}H_{38}Cl_2N_2OP_3Ti$: C, 62.04; H, 4.95; N, 3.62. Found: C, 61.69; H, 5.15; N, 3.61.

UV-vis (0,1 mm cell): λ = 300 nm (shoulder). (Note: due to the poor solubility of **3a** in organic solvents, the UV spectrum was recorded in a saturated, filtered solution in THF, hence the practical impossibility to determine an ε value)

IR (ATR): 3050 (w), 2873 (w), 1591 (m), 1483 (m), 1433 (m), 1335 (w), 1316 (w), 1278 (w), 1223 (s), 1189 (w), 1175 (w), 1160 (w), 1155 (w), 1097 (s), 1075 (w), 1034 (w), 1019 (w), 1018 (w), 999 (w), 973 (m), 957 (m), 903 (w), 886 (b, w), 801 (m), 787 (s), 752 (s), 737 (s), 718 (m), 686 (s), 635 (m), 632 (m), 611 (m), 611 (m), 561 (m), 540 (s), 532 (m), 525 (m), 512 (s), 503 (s), 482 (s), 439 (m) cm^{-1}.

EPR (THF, 295 K): g = 1.9524, ($A^{47/49Ti}$) = 15.7 x 10^{-4} cm^{-1}.

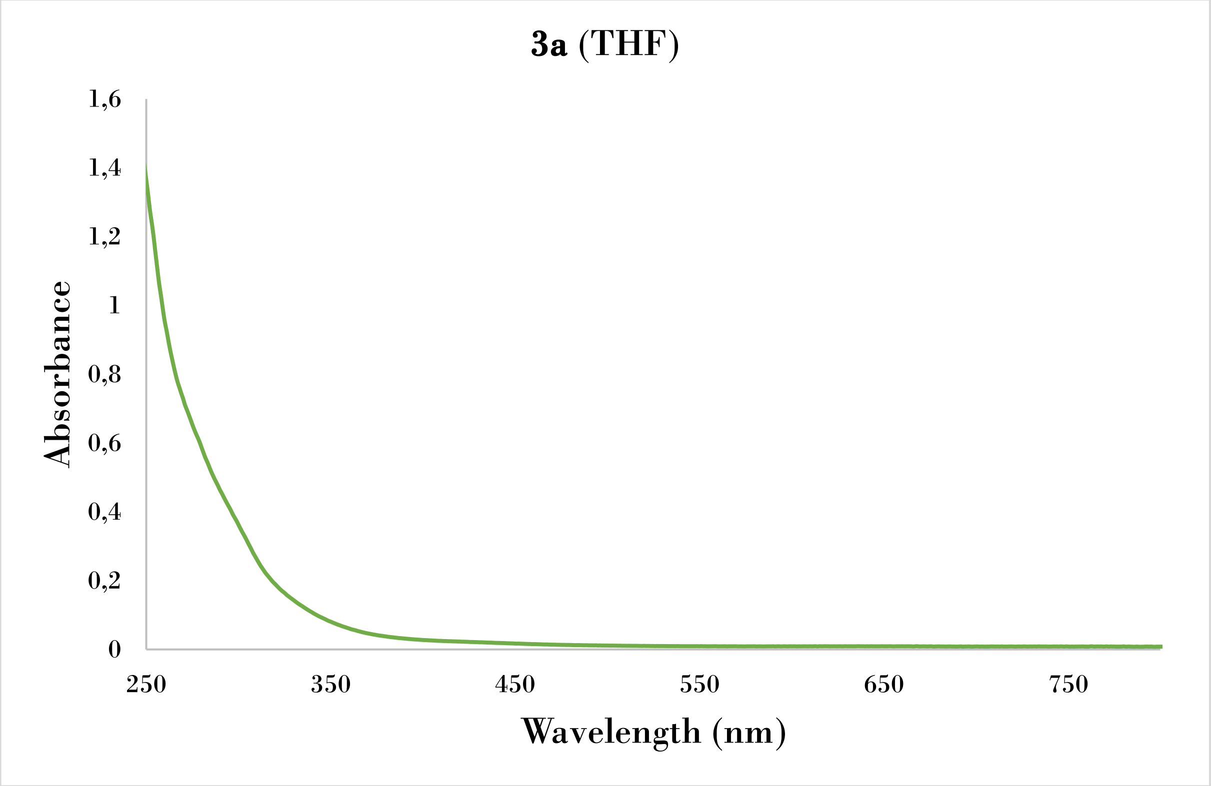

Figure S21: UV-vis (THF, 10 mm cell)

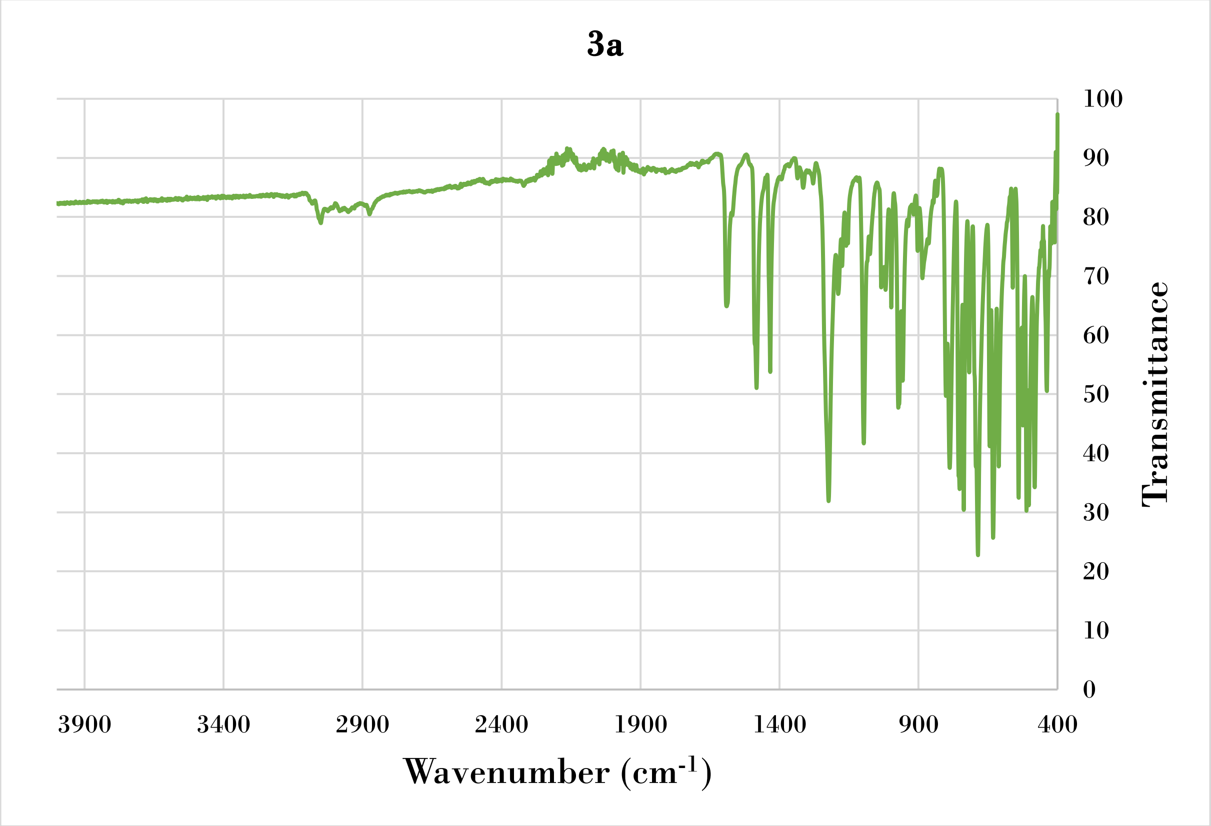

Figure S22: IR (ATR)

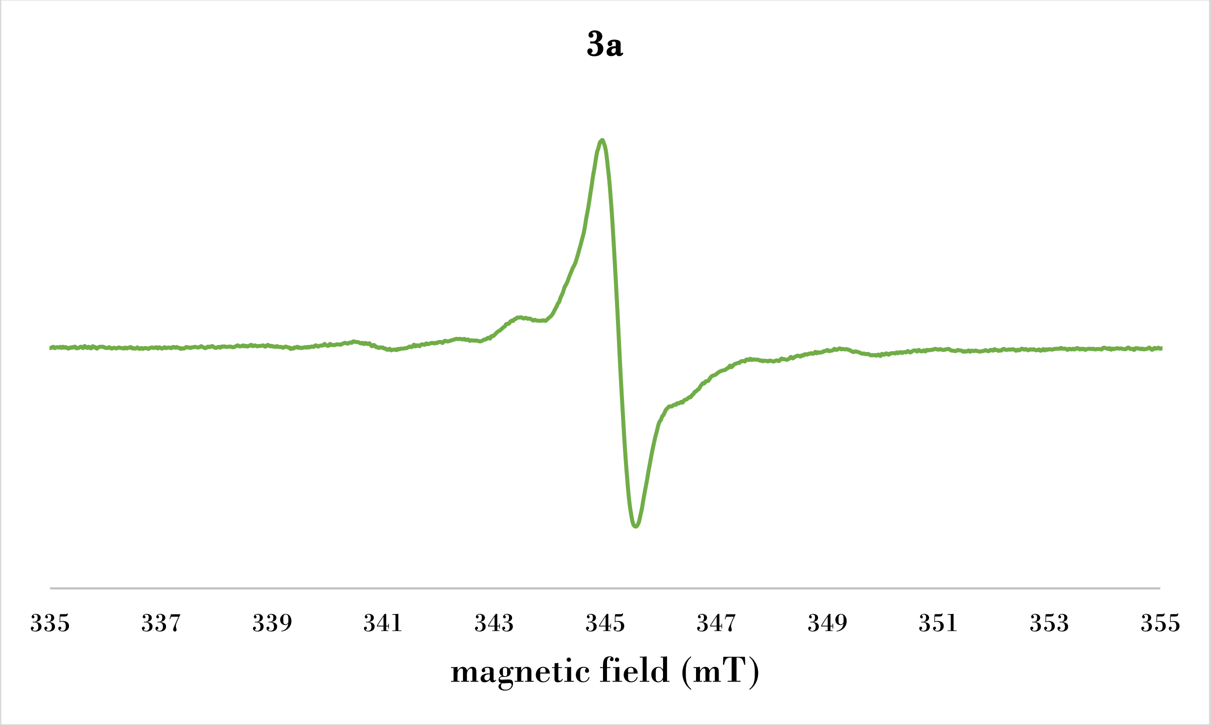

Figure S23: EPR (THF, 295 K)

*Synthesis of complex **3b***

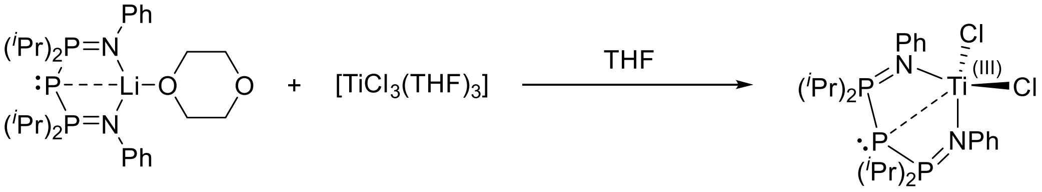

2b

3b *(0.367 g, 52%)*

In an Ar glovebox, proligand **2b** (0.537 g, 1.20 mmol) and [TiCl$_3$(THF)$_3$] (0.371 g, 1.20 mmol) were suspended in THF (5 mL). The reaction mixture turned quickly into a clear emerald green solution. After stirring overnight, a bright yellow precipitate appeared. The suspension was filtered over a sintered glass frit (porosity grade 4), the solid was rinsed with cold THF (2 x 1.5 mL) and dried on the frit, yielding **3b** as a bright yellow powder (0.367 g, yield 52%). Single crystals suitable for X-ray diffraction were grown by cooling a saturated THF solution of **3b** at -20 °C.

Elemental Analysis: calculated for $C_{24}H_{38}Cl_2N_2P_3Ti$: C, 50.91; H, 6.76; N, 4.95. Found: C, 50.65; H, 6.82; N, 4.85.

UV-vis (0.1 mm cell): λ_1 = 291 nm (shoulder, ε = 4900 $M^{-1}.cm^{-1}$).

IR (ATR): 2962 (w), 2929 (w), 1589 (m), 1483 (m), 1454 (w), 1446 (w), 1388 (w), 1446 (w), 1388 (w), 1367 (w), 1233 (m), 1224 (s), 1073 (w), 1034 (w), 1026 (w), 958 (s), 904 (w), 874 (w), 814 (m), 802 (vs), 753 (m), 743 (m), 701 (m), 693 (m), 670 (m), 656 (m), 641 (s), 618 (w), 606 (w), 543 (m), 527 (m), 501 (m), 479 (m), 478 (m), 458 (w) cm^{-1}.

EPR (THF, 295 K): g = 1.9520, ($A^{47/49Ti}$) = 15.7 x 10^{-4} cm^{-1}.

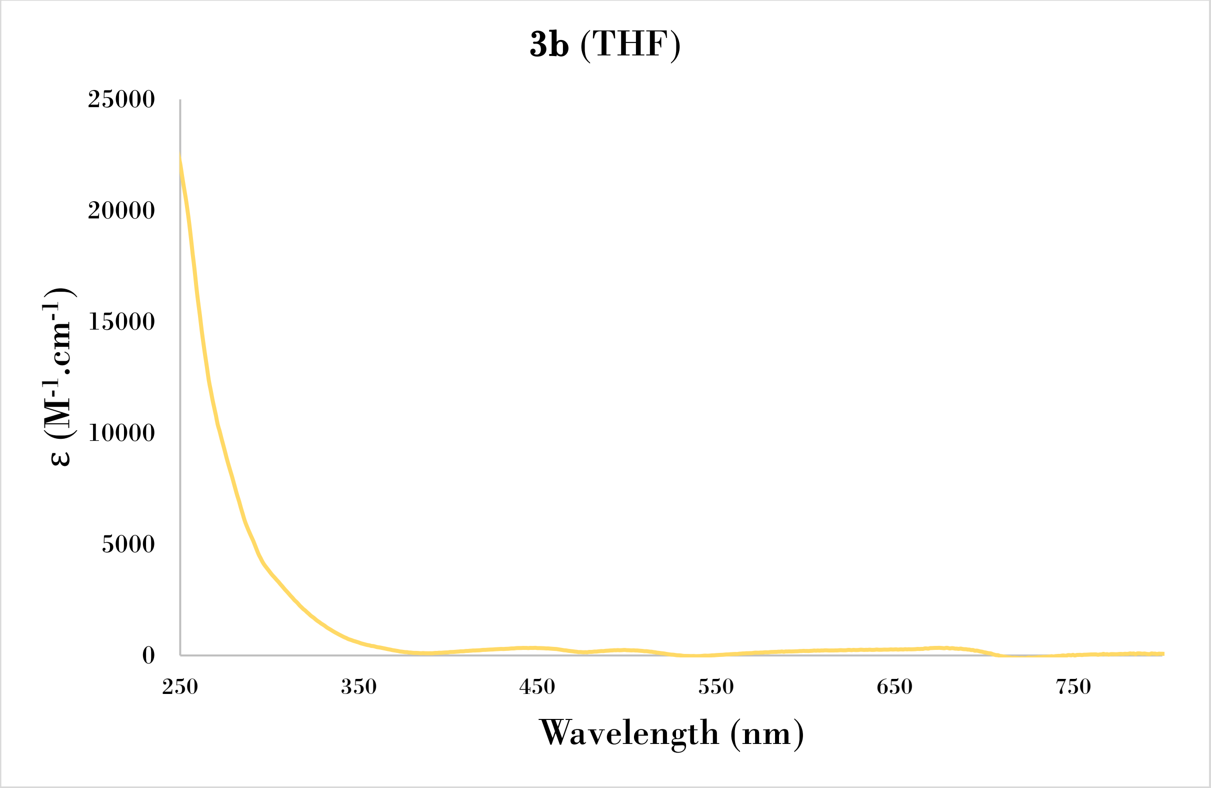

Figure S24: UV-vis (THF, 0.1 mm cell)

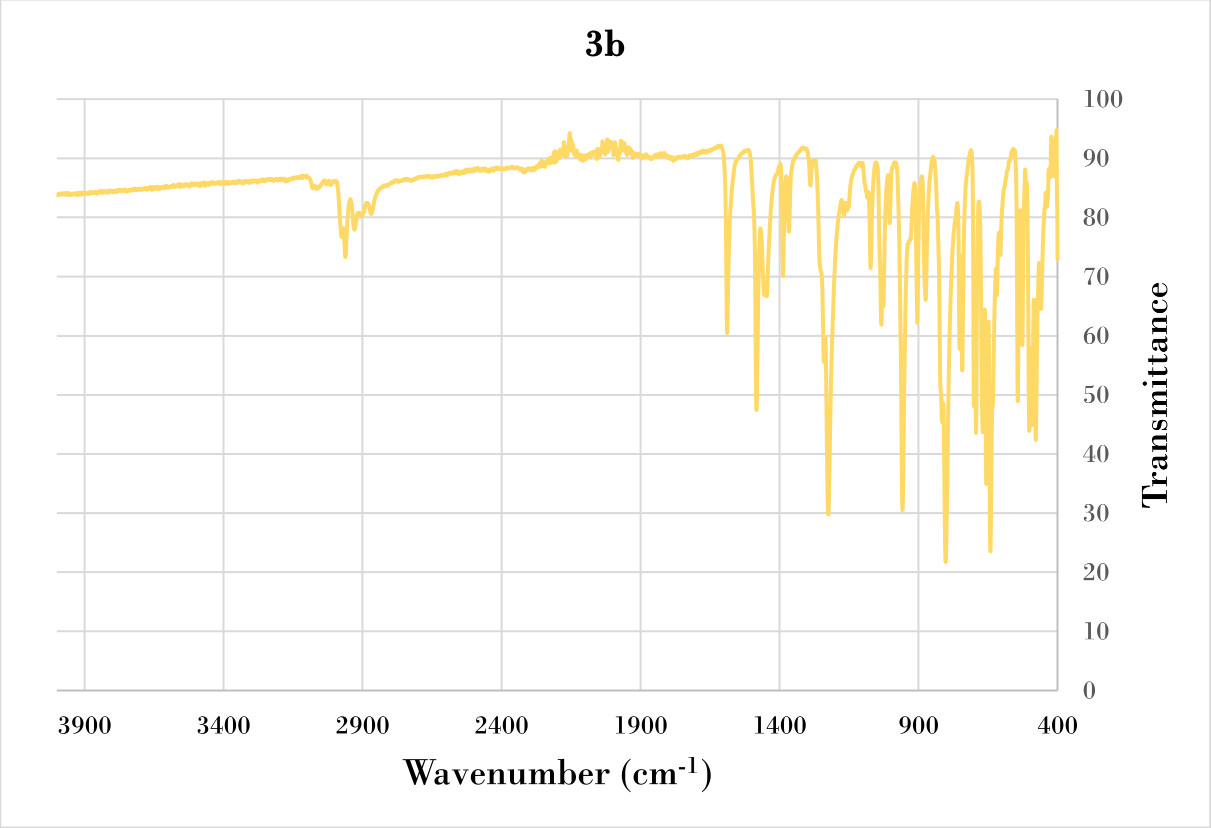

Figure S25: IR (ATR)

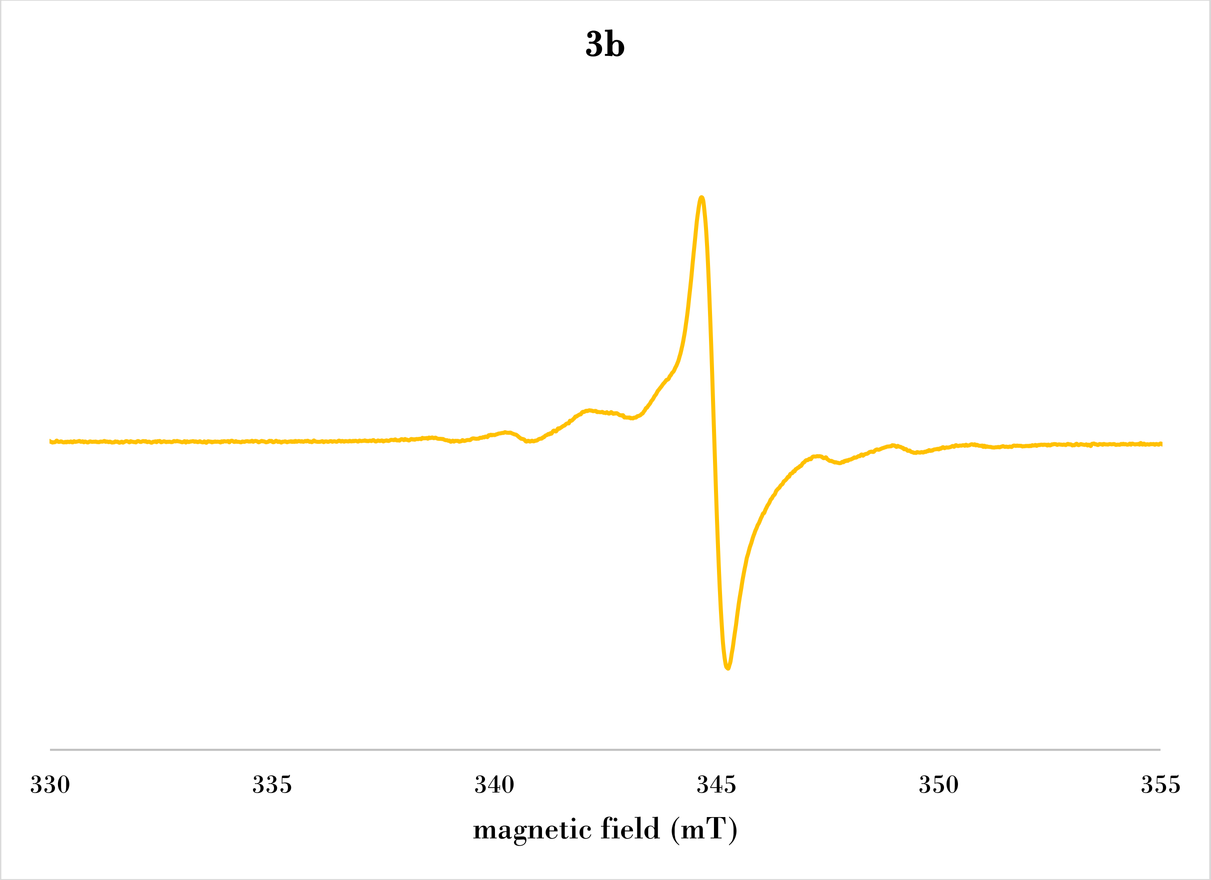

Figure S26: EPR (THF, 295 K)

*Synthesis of complex **4a***

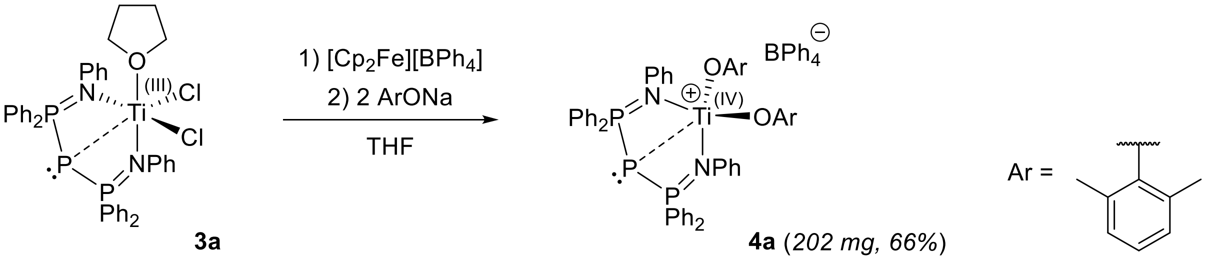

In an Ar glovebox, complex **3a** (194 mg, 0.250 mmol) and [Cp_2Fe][BPh_4] (126 mg, 0.250 mmol) were mixed in THF (3 mL). The reaction mixture turned quickly red. Sodium 3,5-dimethylphenolate etherate was added and the mixture was stirred for 5 min. The resulting solution was evaporated to dryness and the residue was triturated in toluene to remove ferrocene. The residue was dissolved in 3 mL of CH_2Cl_2, filtered over a plug of diatomaceous earth, and an orange solid was precipitated by addition to 50 mL of pentane under vigorous agitation. The solid was filtered over a sintered glass frit, suspended and washed with toluene (3 x 5 mL), then pentane (3 x 5 mL). After drying on the frit under vacuum for 20 min, complex **4a** was obtained as an orange powder containing 50 mol% of CH_2Cl_2 and 15 mol% of pentane (202 mg, yield 66%). Single crystals suitable for X-ray diffraction were obtained by diffusion of pentane into a CH_2Cl_2 solution of **4a** at -20 °C.

Elemental Analysis: a satisfactory elemental analysis could not be obtained; carbon was always too low. This problem has been encountered previously with BPh_4^- salts of Ti, see: *Chem. Eur. J.* **2019**, *25*, 2803-2815 and *Organometallics* **2015**, *34*, 2000-2011.

UV-vis (CH_2Cl_2, 10 mm cell): λ_1 = 391 nm (shoulder, ε = 1000 $M^{-1}.cm^{-1}$).

IR (ATR): 3053 (w), 3031 (w), 1579 (w), 1479 (w), 1434 (w), 1424 (w), 1264 (w), 1211 (b, m), 1199 (m), 1199 (m), 1095 (m), 1032 (b, w), 996 (w), 953 (m), 911 (m), 808 (m), 768 (w), 767 (w), 739 (m), 729 (s), 761 (s), 686 (vs), 656 (m) cm^{-1}.

^{1}H NMR (600 MHz, CD_2Cl_2, 260 K): δ =7.67 (m, 2H, *p* of PPh_2), 7.58 (m, 4H, *m* of PPh_2), 7.46 (m, 4H, *o* of PPh_2 overlapping with *p* of PPh_2), 7.42 (m, 2H, *p* of PPh_2 overlapping with *o* of PPh_2), 7.35 (m, 4H, m of PPh2), 7.29 (m, 8H, *o* of BPh), 7.20-7.12 (m, 6H, *o* of PPh_2 overlapping with *m* of OAr), 7.01 (m, 8H, *m* of BPh overlapping with *p* of OAr, *m* of NPh and *m* of OAr), 6.99-6.91 (m, 7H, *p* of OAr, *m* of NPh and *m* of OAr overlapping with *p* of NPh and *m* of BPh), 6.86 (m, 4H, *p* of BPh), 6.77-6.71 (m, 7H, *o* of NPh overlapping with *m* of OAr and *p* of OAr), 2.33 (s, 6H, $C\mathit{H}_3$ of OAr), 1.89 (s, 6H, $C\mathit{H}_3$ of OAr).

^{1}H-^{1}H COSY (600 MHz, CD_2Cl_2, 260 K)[selected cross-peaks]: COSY was uninformative due to the overlap of multiple signals in the aromatic region.

^{1}H-^{13}C HMBC (600 MHz / 151 MHz, CD_2Cl_2, 260 K)[selected cross-peaks]: δ = 7.67 / 132.2 (*p* of PPh_2 / *m* of PPh_2), 7.58 / 134.8 (*m* of PPh_2 / *p* of PPh_2), 7.58 / 127.4 (*m* of PPh_2 / *i* of PPh_2), 7.46 / 129.8 (*o* of PPh_2 / *o* of PPh_2), 7.46 / 127.4 (*o* of PPh_2 / *i* of PPh_2), 7.42 / 132.0 (*p* of PPh_2 / *m* of PPh_2), 7.35 / 134.2 (*m* of PPh_2 / *p* of PPh_2), 7.35 / 122.3 (*m* of PPh_2 / *i* of PPh_2), 7.29 / 164.0 (*o* of BPh / *i* of BPh), 7.29 / 135.9 (*o* of BPh / *o* of BPh), 7.29 / 126.0-125.7 (*o* of BPh / *m* of BPh), 7.29 / 121.9 (*o* of BPh / *p* of BPh), 7.20-7.12 / 166.2 (*m* of OAr / *i* of OAr), 7.20-7.12 / 18.3 (*m* of OAr / $\mathit{C}H_3$ of OAr), 7.01 / 164.0 (*m* of BPh / *i* of BPh), 7.01 / 135.9 (*m* of BPh / *o* of BPh), 7.01 / 126.0-125.7 (*m* of BPh / *m* of BPh), 7.01 / 121.9 (*m* of BPh / *p* of BPh), 6.99-6.91 / 146.7 (*m* of NPh / *i* of NPh), 6.86 / 135.9 (*p* of BPh / *o* of BPh), 6.86 / 126.0-125.7 (*p* of BPh / *m* of BPh), 6.77-6.71 / 166.2 (*m* of OAr and / or *p* of OAr / *i* of OAr), 6.77-6.71 / 146.7 (*m* of NPh / *i* of NPh), 6.77-6.71 / 17.0 (*m* of OAr / $\mathit{C}H_3$ of OAr), 2.33 / 166.2 ($C\mathit{H}_3$ of OAr / *i* of OAr), 2.33 / 128.9 ($C\mathit{H}_3$ of OAr / *m* of OAr), 2.33 / 126.5 ($C\mathit{H}_3$ of OAr / *o* of OAr), 1.89 / 166.2 ($C\mathit{H}_3$ of OAr / *i* of OAr), 1.89 / 129.2 ($C\mathit{H}_3$ of OAr / *o* of OAr), 1.89 / 128.0 ($C\mathit{H}_3$ of OAr / *o* of OAr).

^{13}C{^{1}H} NMR (151 MHz, CD_2Cl_2, 260 K): δ = 166.2 (m, *i* of OAr), 164.0 (m, *i* of BPh), 146.7 (m, *i* of NPh), 135.9 (s, *o* of BPh), 134.8 (s, *p* of PPh_2), 134.2 (s, *p* of PPh_2), 132.2 (m, *m* of PPh_2), 132.0 (m, *m* of PPh_2), 129.8 (m, *o* of PPh_2), 129.4 (s, *o* of OAr), 129.2 (s, *m* of NPh), 128.9 (s, *m* of OAr), 128.0 (s, *m* of OAr), 127.4 (m, *i* of PPh_2), 126.5 (s, *o* of OAr), 126.0-125.7 (m, *m* of BPh overlapping with *p* of NPh), 124.2 (s, *p* of OAr), 123.4 (m, *o* of NPh overlapping with *p* of OAr), 123.3 (s, *p* of OAr overlapping with *o* of NPh), 122.3 (m, *i* of PPh_2), 121.9 (s, *p* of BPh), 18.3 (s, $\mathit{C}H_3$ of OAr), 17.0 (s, $\mathit{C}H_3$ of OAr).

^{31}P{^{1}H} NMR (243 MHz, CD_2Cl_2, 260 K): δ = 32.5 (d, $^1J_{PP}$ = 381 Hz, $\mathit{P}Ph_2$), -212.9 (t, $^1J_{PP}$ = 381 Hz, central *P*).

^{11}B{^{1}H} NMR (194 MHz, CD_2Cl_2, 298 K): δ = -6.6.

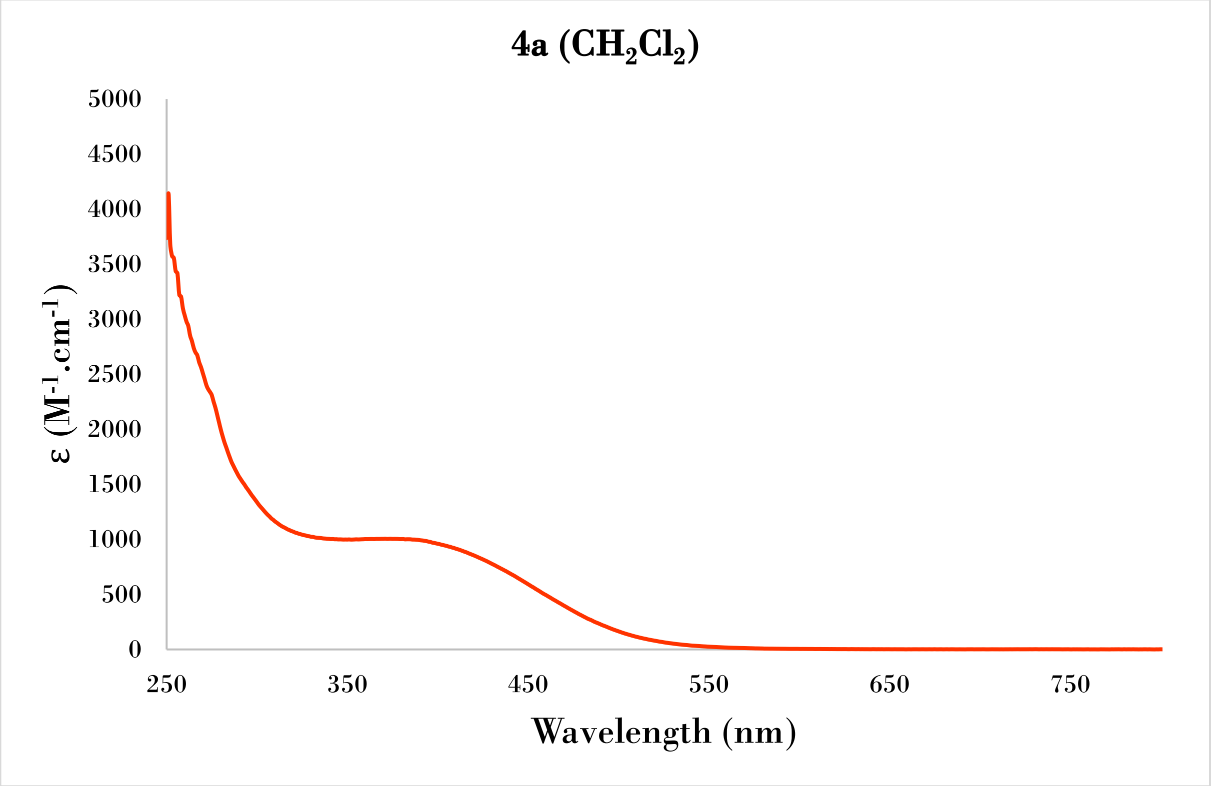

Figure S27: UV-vis (CH_2Cl_2, 10 mm cell)

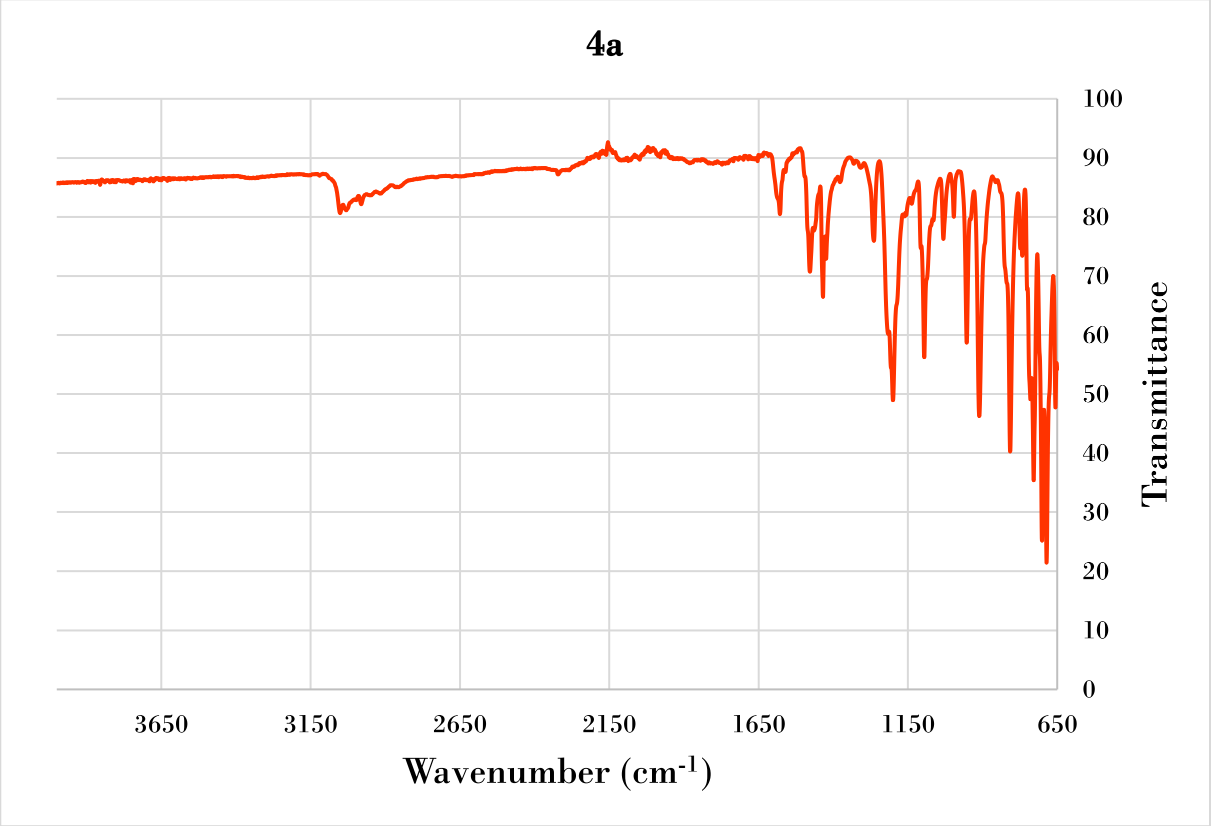

Figure S28: IR (ATR)

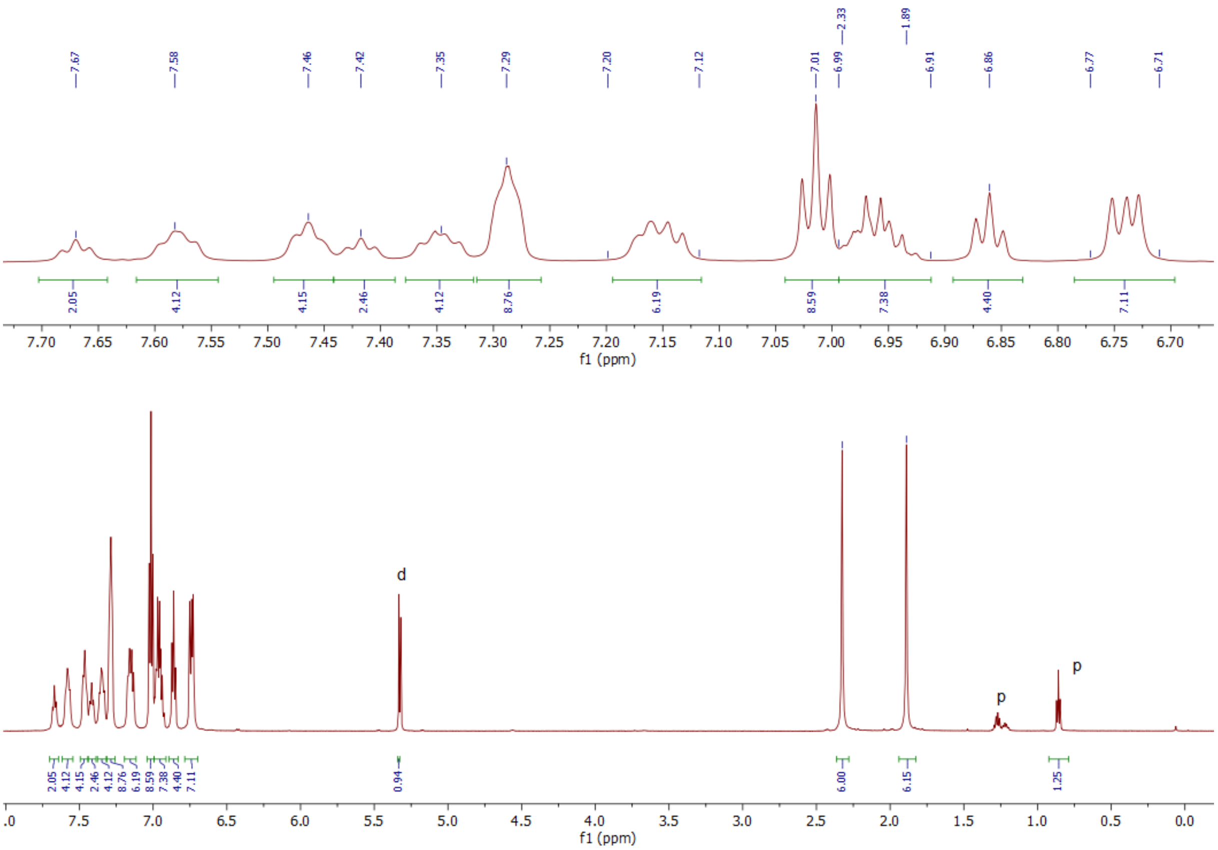

Figure S29: ^{1}H NMR (600 MHz, CD_2Cl_2, 260 K)(p: pentane; d: dichloromethane)

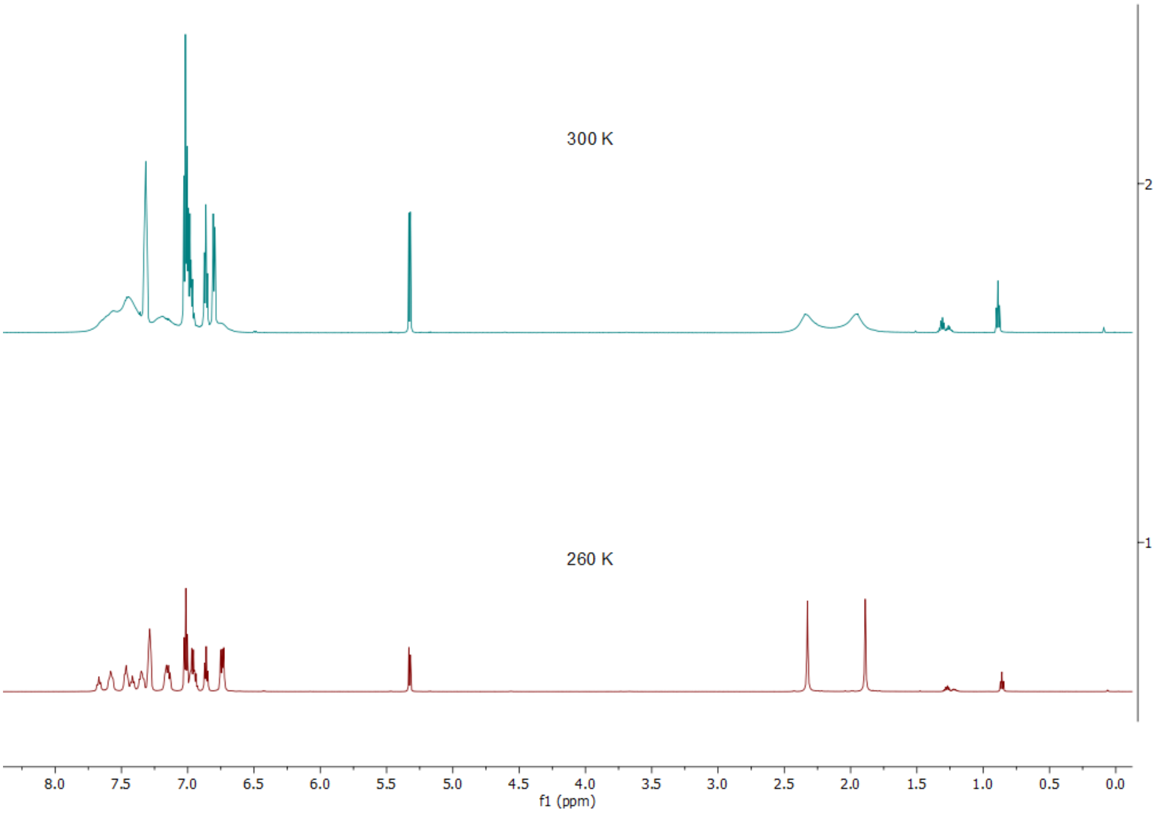

Figure S30: ^{1}H NMR (600 MHz, CD_2Cl_2, 300 K vs 260 K)

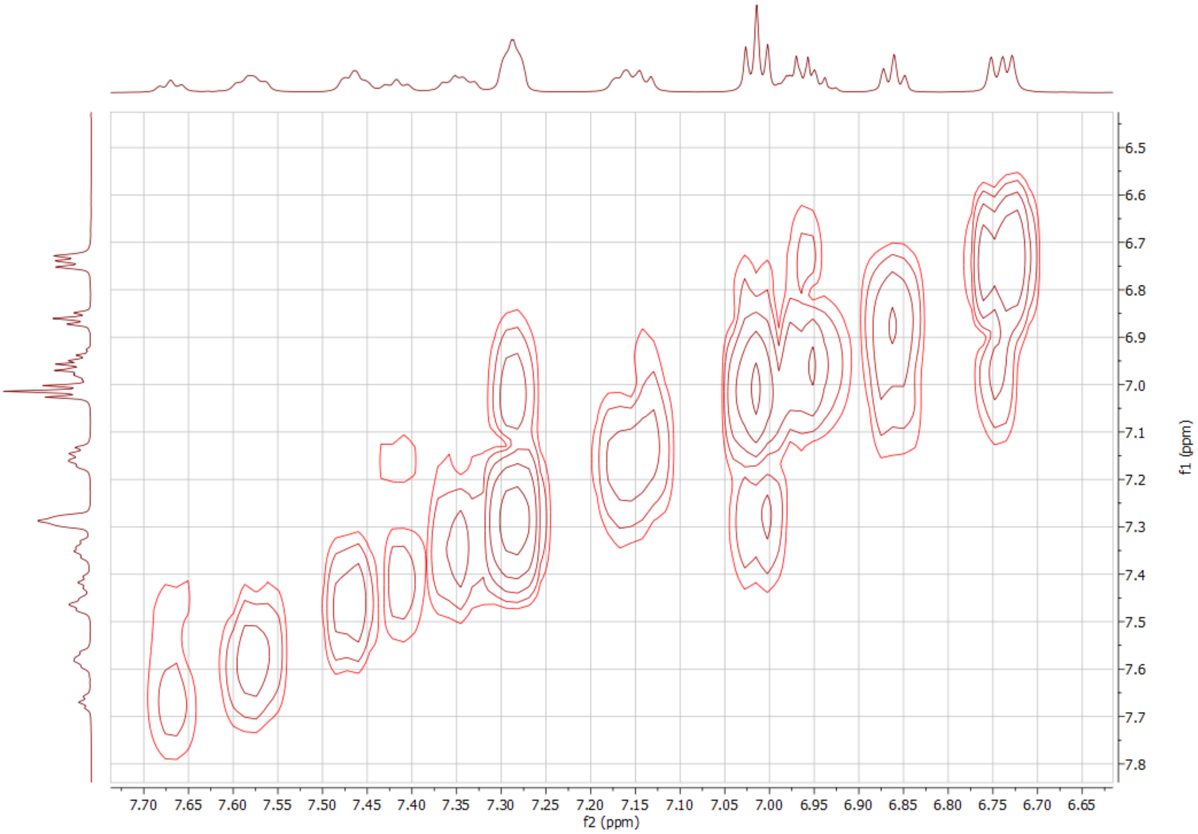

Figure S31: ^{1}H-^{1}H COSY (600 MHz, CD_2Cl_2, 260 K)

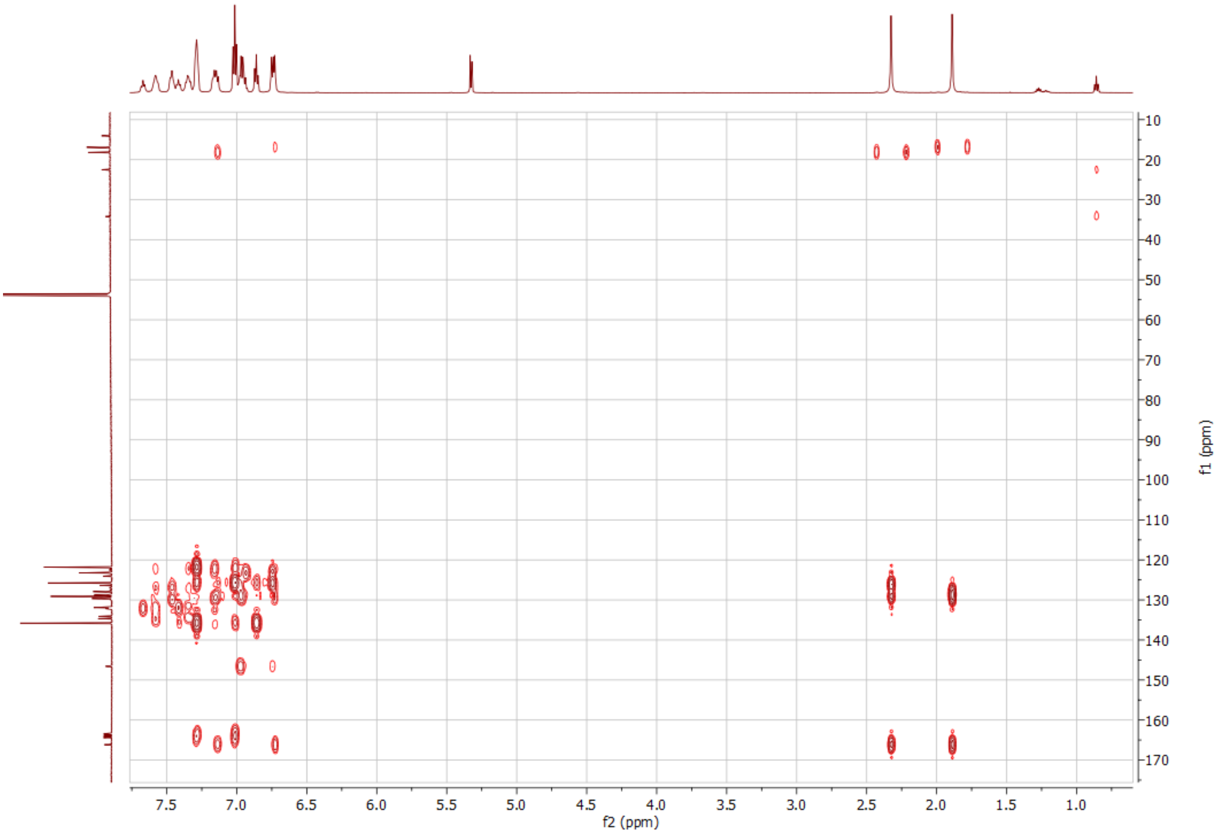

Figure S32: ^{1}H-^{13}C HMBC (600 MHz / 151 MHz, CD_2Cl_2, 260 K)(whole spectrum)

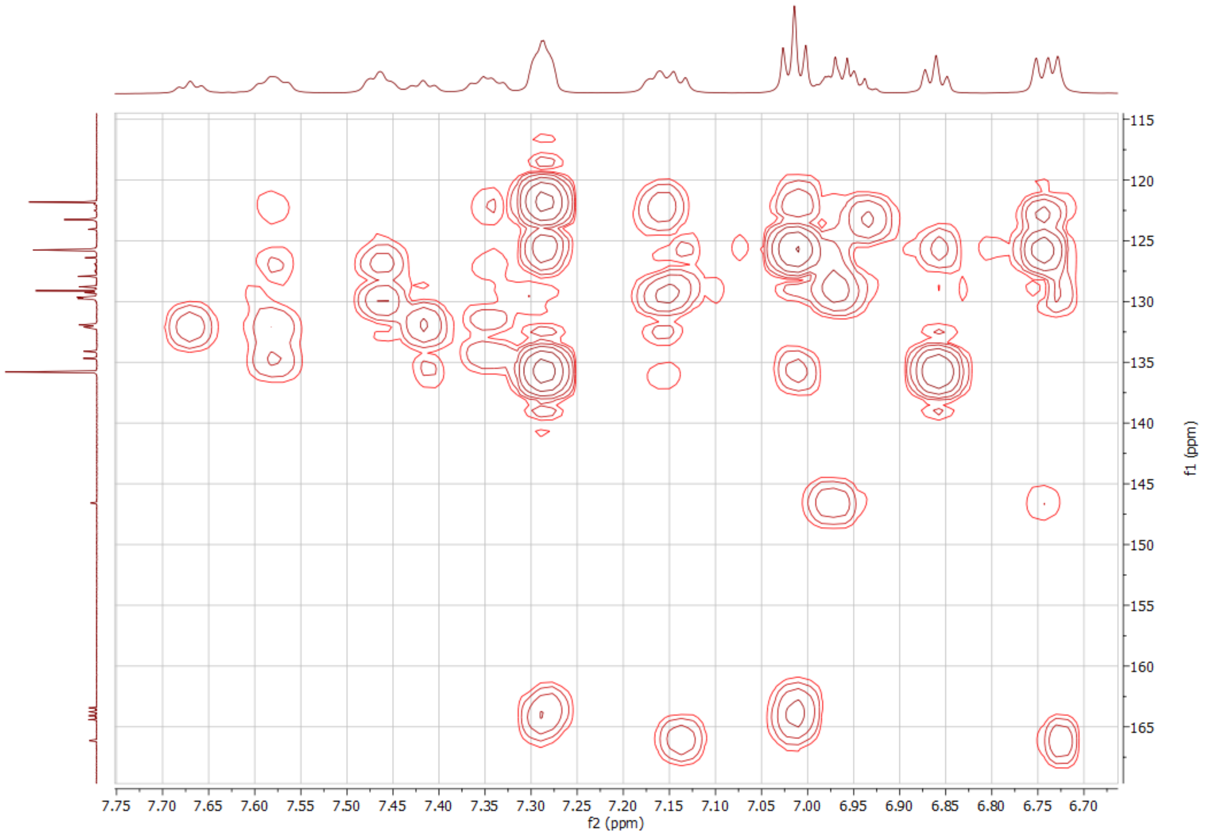

Figure S33: ^{1}H-^{13}C HMBC (600 MHz / 151 MHz, CD_2Cl_2, 260 K)(zoom)

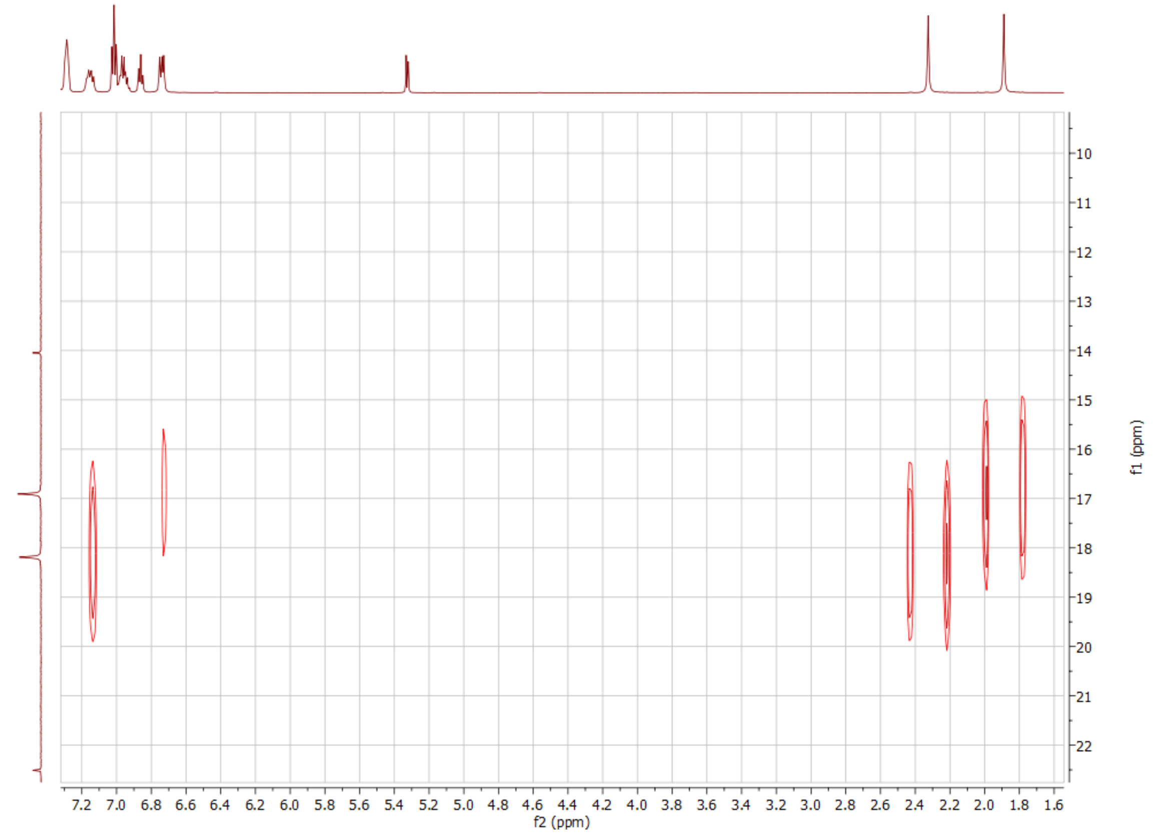

Figure S34: ^{1}H-^{13}C HMBC (600 MHz / 151 MHz, CD_2Cl_2, 260 K)(zoom)

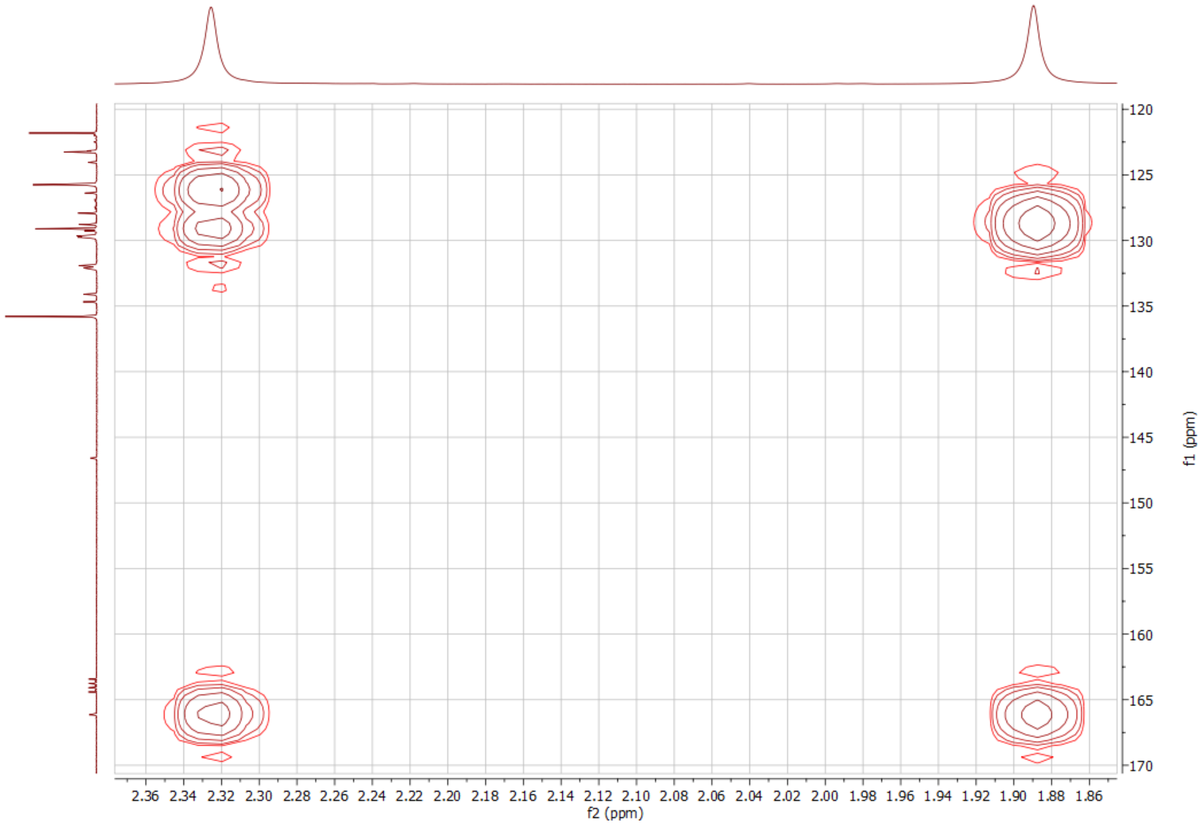

Figure S35: ^{1}H-^{13}C HMBC (600 MHz / 151 MHz, CD$_2$Cl$_2$, 260 K)(zoom)

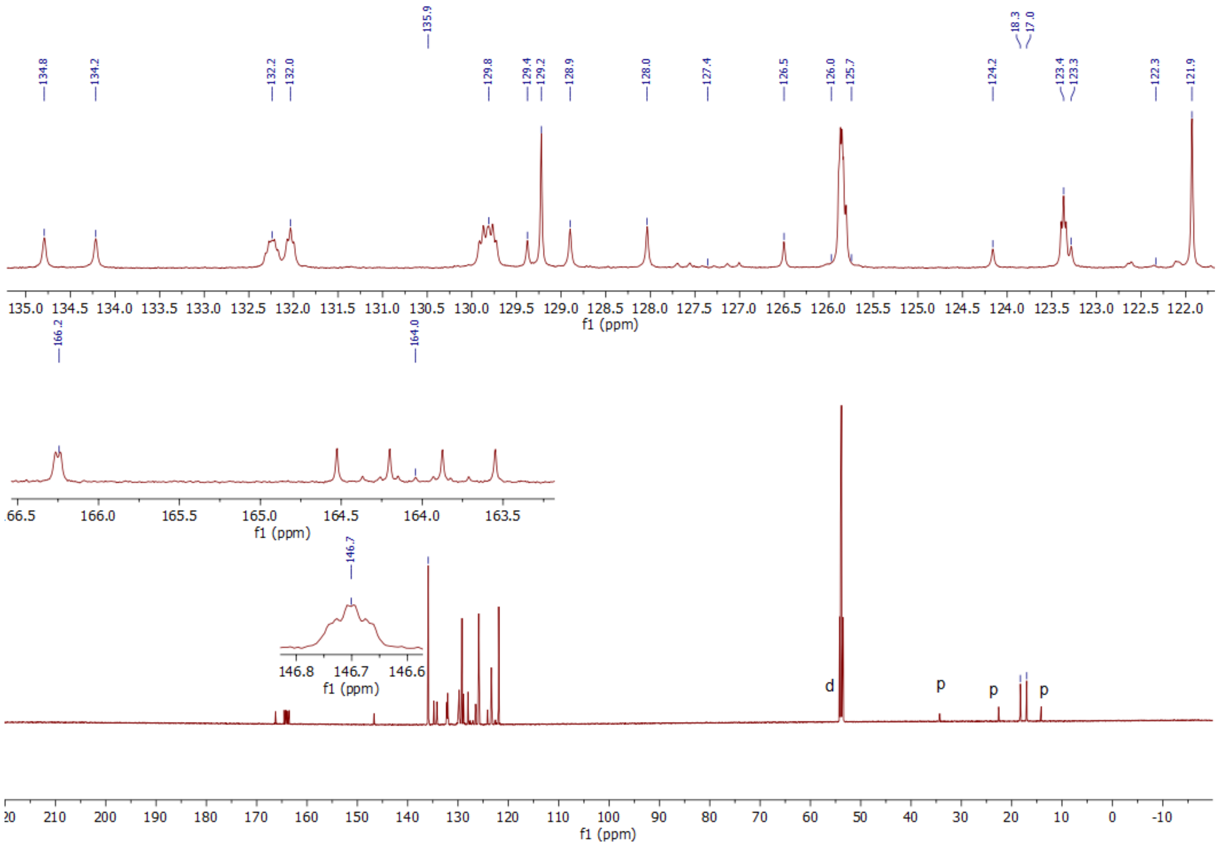

Figure S36: ^{13}C{^{1}H} NMR (151 MHz, CD$_2$Cl$_2$, 260 K)

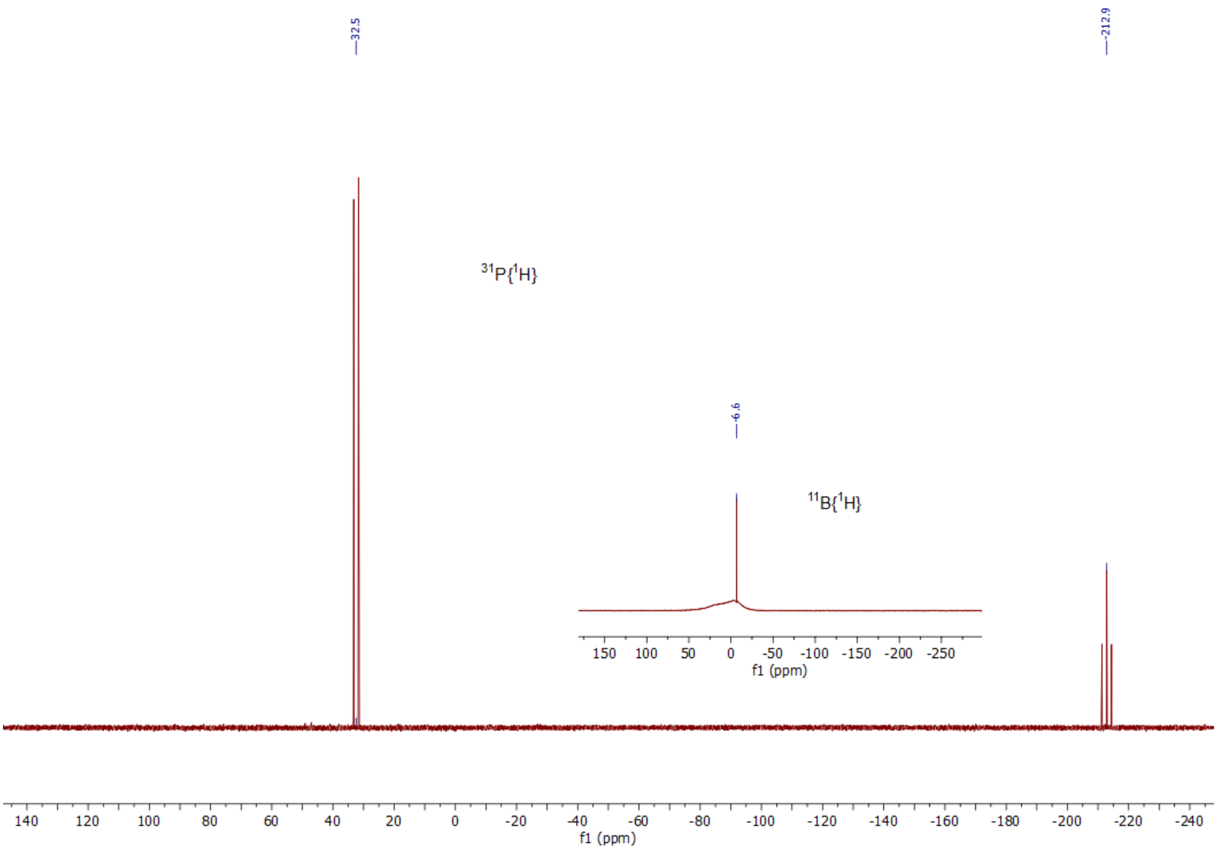

Figure S37: ^{31}P{^{1}H} NMR (243 MHz, CD_2Cl_2, 260 K); ^{11}B{^{1}H} NMR (160 MHz, CD_2Cl_2, 298 K)

*Synthesis of complex **5a***

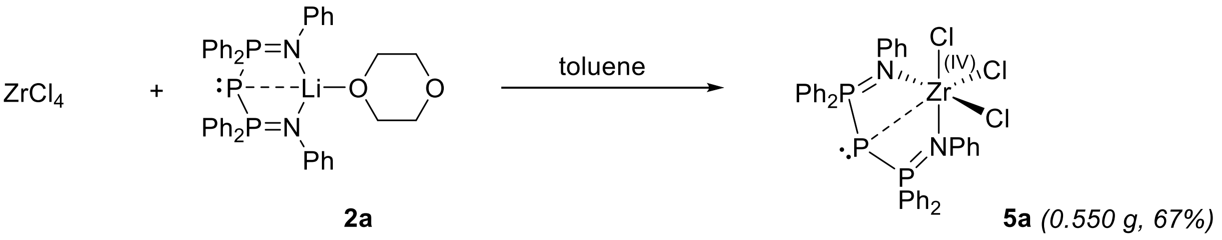

In an Ar glovebox, zirconium tetrachloride (233 mg, 1.00 mmol) and proligand **2a** (679 mg, 1.00 mmol) were suspended in toluene. The reaction mixture was stirred for 14 h, then filtered on a sintered glass frit and the resulting solid was rinsed with toluene (3 x 3 mL). The solid was suspended in 10 mL of CH_2Cl_2, filtered over a pad of diatomaceous earth, and the filtrate was evaporated to dryness. The residue was triturated in 5 mL of pentane, filtered on a sintered glass frit and dried on the frit, yielding **5a** as a white powder containing 50 mol% of CH_2Cl_2 (550 mg, yield 67%). Single crystals suitable for X-ray diffraction were grown by slow diffusion of pentane into a CH_2Cl_2 solution of **5a** at -20 °C.

Elemental Analysis: calculated for $C_{36}H_{30}Cl_3N_2P_3Zr(CH_2Cl_2)_{0.5}$: C, 53.23; H, 3.79; N, 3.40. Found: C, 54.63; H, 4.18; N, 3.46.

UV-vis (CH_2Cl_2, 0.1 mm cell): λ_1 = 306 nm (shoulder, ε = 9600 $M^{-1}.cm^{-1}$).

IR (ATR): 2964 (w), 1588 (w), 1483 (w), 1447 (w), 1446 (w), 1388 (w), 1368 (w), 1350 (w), 1240 (m), 1211 (m), 1169 (w), 1129 (w), 1073 (w), 1031 (w), 1026 (w), 1004 (w), 958 (m), 940 (w), 905 (w), 877 (b, w), 813 (b, m), 755 (w), 699 (m), 676 (m), 650 (m), 621 (w), 527 (m), 502 (w), 496 (w), 478 (w) cm^{-1}.

^{1}H NMR (500 MHz, CD_2Cl_2, 291 K): δ = 7.68 (m, 4H, *o* of PPh_2), 7.62 (m, 2H, *p* of PPh_2), 7.46 (m, 4H, *m* of PPh_2), 7.31 (m, 4H, *o* of PPh_2), 7.23 (m, 2H, *p* of PPh_2), 7.18 (m, 4H, *m* of NPh), 7.09 (m, 4H, *o* of NPh overlapping with *p* of NPh), 7.06 (m, 2H, *p* of NPh), 7.01 (m, 4H, *m* of PPh_2).

^{1}H-^{1}H COSY (500 MHz, CD_2Cl_2, 291 K)[selected cross-peaks]: 7.68 / 7.46 (*o* of PPh_2 / *m* of PPh_2), 7.62 / 7.46 (*p* of PPh_2 / *m* of PPh_2), 7.46 / 7.68 (*m* of PPh_2 / *o* of PPh_2), 7.46 / 7.62 (*m* of PPh_2 / *p* of PPh_2), 7.31 / 7.01 (*o* of PPh_2 / *m* of PPh_2), 7.23 / 7.01 (*p* of PPh_2 / *m* of PPh_2), 7.18 / 7.09 (*m* of NPh / *o* of NPh), 7.18 / 7.06 (*m* of NPh / *p* of NPh), 7.09 / 7.18 (*o* of NPh / *m* of NPh), 7.06 / 7.18 (*p* of NPh / *m* of NPh), 7.01 / 7.31 (*m* of PPh_2 / *o* of PPh_2), 7.01 / 7.23 (*m* of PPh_2 / *p* of PPh_2).

^{1}H-^{13}C HMBC (500 MHz / 126 MHz, CD_2Cl_2, 291 K)[selected cross-peaks]: 7.62 / 133.6 (*p* of PPh_2 / *o* of PPh_2), 7.46 / 130.7 (*m* of PPh_2 / *i* of PPh_2), 7.31 / 133.0 (*o* of PPh_2 / *p* of PPh_2), 7.23 / 132.6 (*p* of PPh_2 / *o* of PPh_2), 7.18 / 147.3 (*m* of NPh / *i* of NPh), 7.18 / 129.0 (*m* of NPh / *m* of NPh), 7.09 / 147.3 (*o* of NPh / *i* of NPh), 7.09 / 125.1 (*o* of NPh / *p* of NPh), 7.06 / 127.7 (*p* of NPh / *o* of NPh), 7.01 / 129.2 (*m* of PPh_2 / *m* of PPh_2), 7.01 / 126.8 (*m* of PPh_2 / *i* of PPh_2).

^{13}C{^{1}H} NMR (126 MHz, CD_2Cl_2, 291 K): δ = 147.3 (m, *i* of NPh), 133.7 s, *p* of PPh_2 overlapping with *o* of PPh_2), 133.6 (m, *o* of PPh_2 overlapping with *p* of PPh_2), 133.0 (m, *p* of PPh_2), 132.6 (m, *o* of PPh_2), 130.7 (m, *i* of PPh_2), 129.2 (m, *m* of PPh_2), 129.0 (s, *m* of NPh overlapping with *m* of PPh_2), 128.9 (m, *m* of PPh_2 overlapping with *m* of NPh), 127.7 (m, *o* of NPh), 126.8 (m, *i* of PPh_2), 125.1 (s, *p* of NPh).

^{31}P{^{1}H} NMR (202 MHz, CD_2Cl_2, 291 K): δ = 27.2 (d, $^1J_{PP}$ = 351 Hz, *P*Ph_2), -210.2 (t, $^1J_{PP}$ = 351 Hz, central *P*).

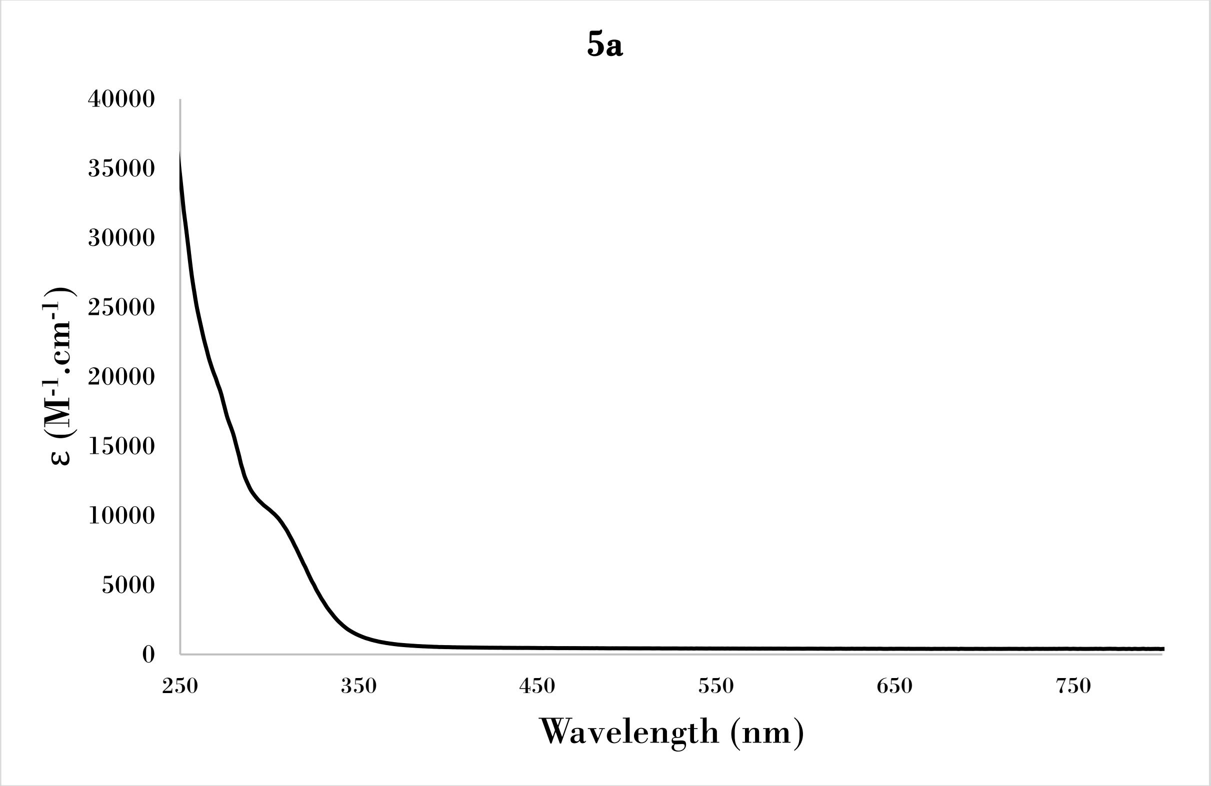

Figure S38: UV-vis (CH_2Cl_2, 0.1 mm cell)

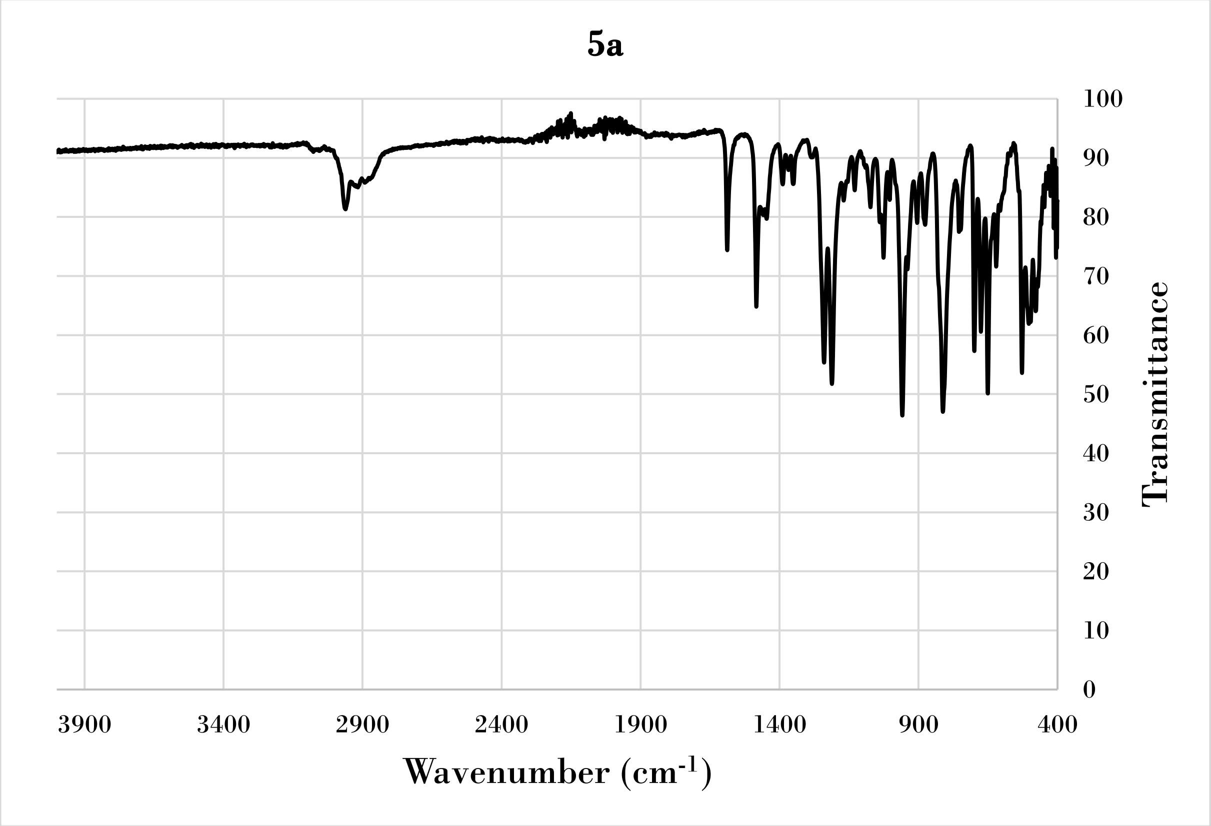

Figure S39: IR (ATR)

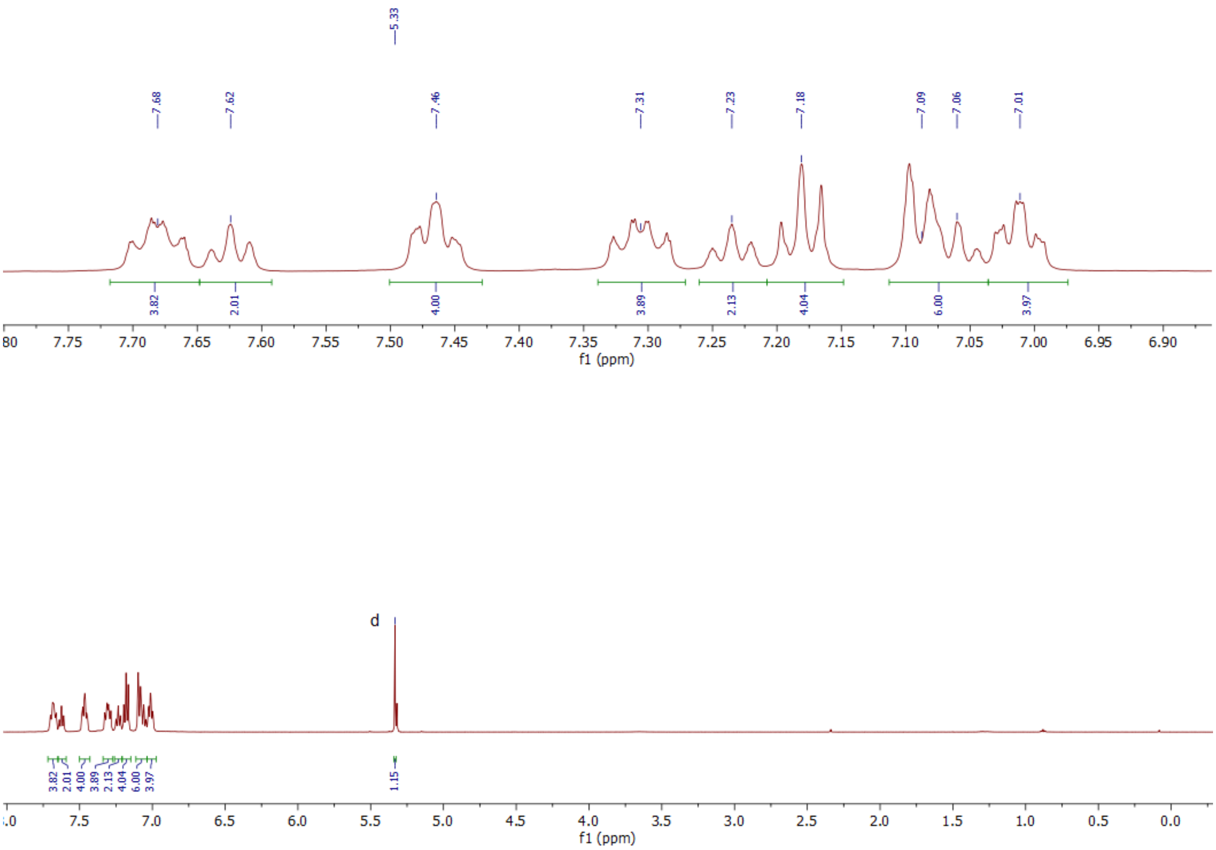

Figure S40: ^{1}H NMR (500 MHz, CD_2Cl_2, 291 K)(d: dichloromethane)

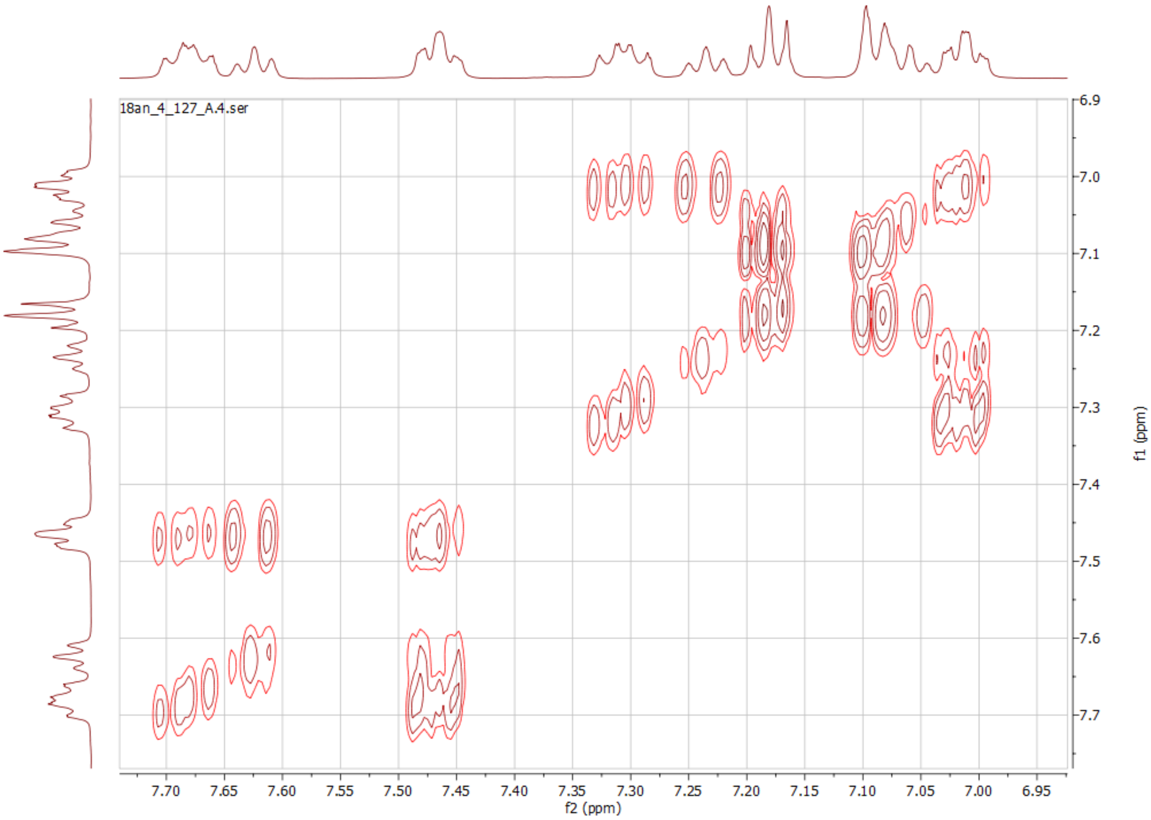

Figure S41: ^{1}H-^{1}H COSY (500 MHz, CD_2Cl_2, 291 K)(aromatic region)

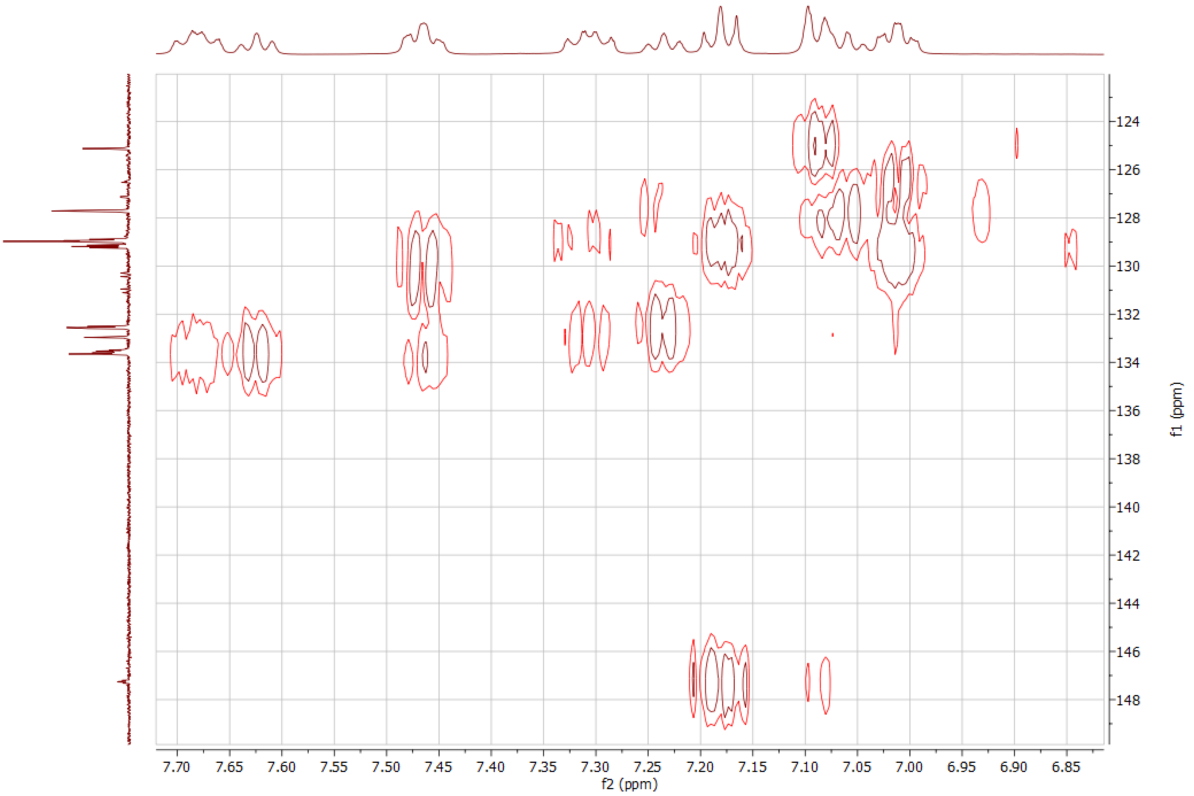

Figure S42: ^{1}H-^{13}C HMBC (500 MHz / 126 MHz, CD_2Cl_2, 291 K)(aromatic region)

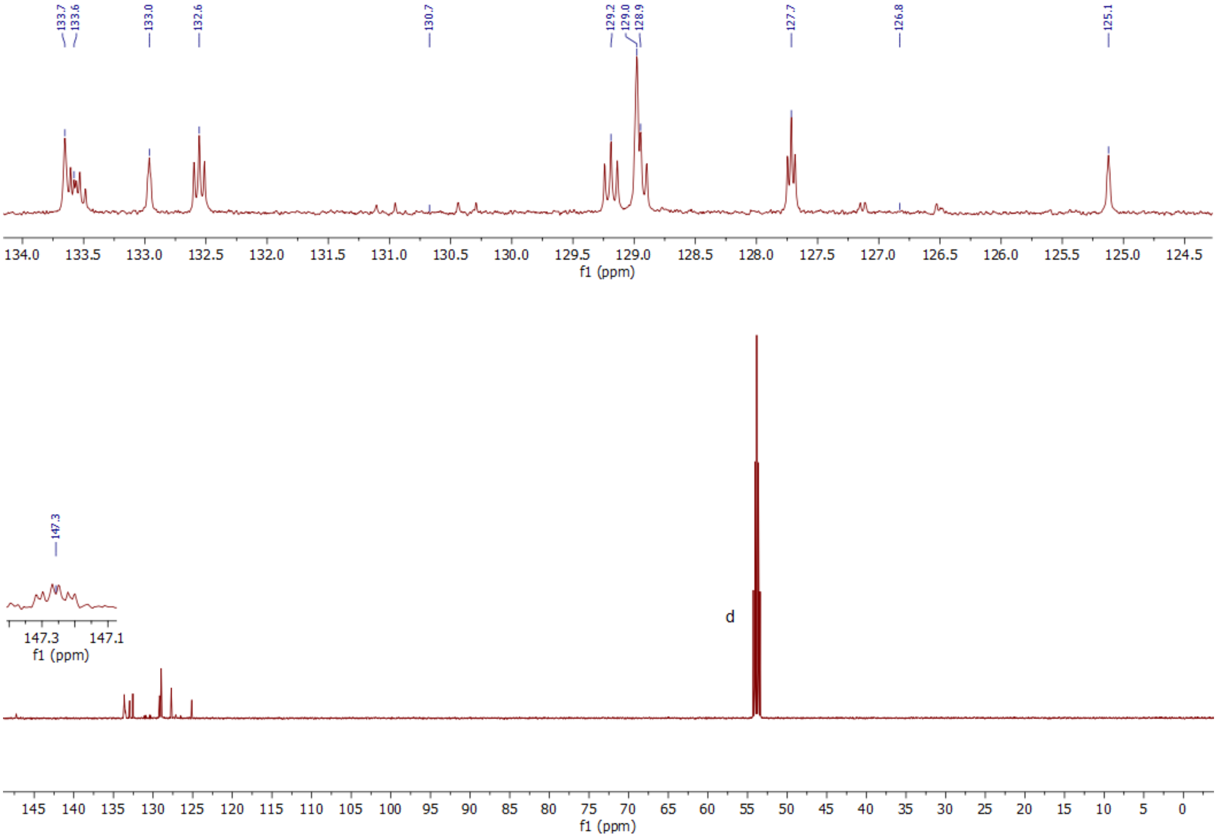

Figure S43: $^{13}C\{^{1}H\}$ NMR (126 MHz, CD_2Cl_2, 291 K)(d: dichloromethane)

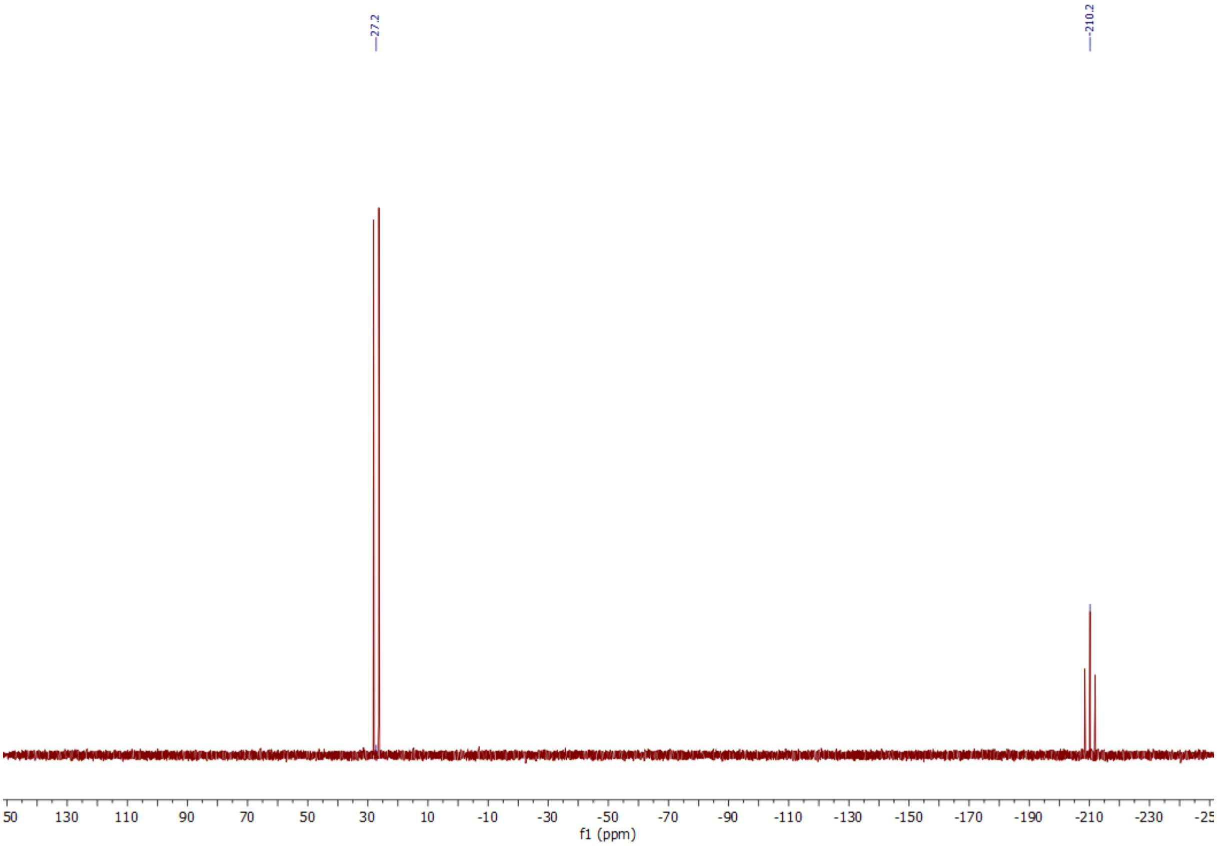

Figure S44: ^{31}**P{**^{1}**H} NMR (202 MHz,** CD_2Cl_2**, 291 K)**

*Synthesis of complex **5b***

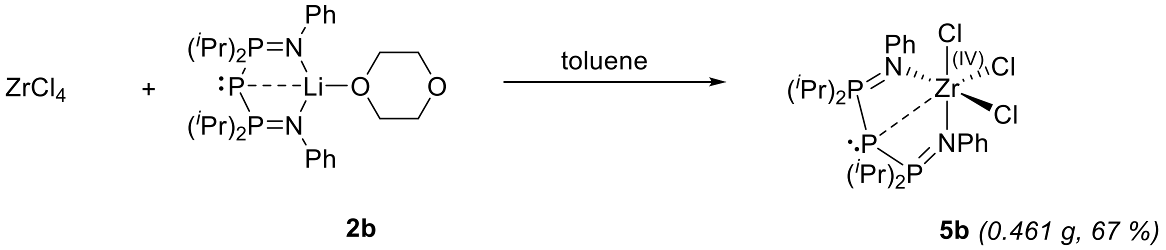

In an Ar glovebox, zirconium tetrachloride (233 mg, 1.0 mmol) and proligand **2b** (602 mg, 1.0 mmol) were suspended in dry toluene. The reaction mixture was stirred overnight, then filtered on a sintered glass frit and the resulting solid was rinsed with toluene (3 x 3 mL). The solid was suspended in 10 mL of CH_2Cl_2, filtered over a pad of diatomaceous earth, and the filtrate was evaporated to dryness. The residue was triturated in 5 mL of pentane, filtered on a sintered glass frit, rinsed with 2x5 mL of pentane and dried on the frit, yielding **5a** as a white powder (461 mg, yield 67%). Single crystals suitable for X-ray diffraction were grown by slow diffusion of pentane into a CH_2Cl_2 solution of **5b** at -20 °C.

Elemental Analysis: calculated for $C_{24}H_{38}Cl_3N_2P_3Zr$: C, 44.69; H, 5.94; N, 4.34. Found: C, 44.50; H, 5.93; N, 4.37.

UV-vis (CH_2Cl_2**, 0.1 mm cell):** λ_1 = 280 nm (shoulder, ε = 7200 $M^{-1}.cm^{-1}$), λ_2 = 306 nm (shoulder, ε = 4600 $M^{-1}.cm^{-1}$).

IR (ATR): 2970 (w), 2932 (w), 2873 (w), 1589 (m), 1483 (m), 1458 (w), 1457 (w), 1445 (w), 1389 (w), 1370 (w), 1237 (w), 1213 (s), 1174 (w), 1154 (w), 1090 (w), 1072 (w), 1034 (w), 1028 (w), 1002 (w), 959 (s), 931 (w), 910 (w), 872 (w), 836 (w), 813 (s), 789 (s), 755 (m), 735 (w), 703 (m), 697 (m), 667 (m), 629 (s), 541 (m), 506 (w), 499 (m), 486 (m) cm^{-1}.

^{1}H NMR (500 MHz, CD$_2$Cl$_2$, 298 K): δ = 7.35-7.29 (m, 8H, *o* of NPh overlapping with *m* of NPh), 7.15 (m, 2H, *p* of NPh), 2.95 (bs, 4H, CH of ^{i}Pr), 1.48 (m, 12H, CH_3 of ^{i}Pr), 1.31 (m, 12H, CH_3 of ^{i}Pr).

^{1}H-^{1}H COSY (500 MHz, CD$_2$Cl$_2$, 298 K): COSY was uninformative due to the overlap of signals in the aromatic region and the broadness of the signal of CH of ^{i}Pr.

^{1}H-^{13}C HMBC (500 MHz / 126 MHz, CD$_2$Cl$_2$, 298 K)[selected cross-peaks]: 7.35-7.29 / 148.5 (*o* of NPh and/or *m* of NPh / *i* of NPh), 7.35-7.29 / 129.2 (*o* of NPh and/or *m* of NPh / *m* of NPh), 7.35-7.29 / 125.5 (*o* of NPh and/or *m* of NPh / *p* of NPh), 7.15 / 127.8 (*p* of NPh / *o* of NPh), 1.48 / 33.3 (CH_3 of ^{i}Pr / *C*H of ^{i}Pr), 1.48 / 18.2 (CH_3 of ^{i}Pr / *C*H$_3$ of ^{i}Pr), 1.31 / 33.3 (CH_3 of ^{i}Pr / *C*H of ^{i}Pr), 1.31 / 19.4 (CH_3 of ^{i}Pr / *C*H$_3$ of ^{i}Pr).

^{13}C{^{1}H} NMR (126 MHz, CD$_2$Cl$_2$, 298 K): δ = 148.5 (m, *i* of NPh), 129.2 (m, *m* of NPh), 127.8 (m, *o* of NPh), 125.5 (m, *p* of NPh), 33.3 (bs, *C*H of ^{i}Pr), 19.4 (m, *C*H$_3$ of ^{i}Pr), 18.2 (m, *C*H$_3$ of ^{i}Pr).

^{31}P{^{1}H} NMR (202 MHz, CD$_2$Cl$_2$, 298 K): δ = 56.9 (d, $^1J_{PP}$ = 384 Hz, *P*^{i}Pr$_2$), -223.0 (t, $^1J_{PP}$ = 384 Hz, central *P*).

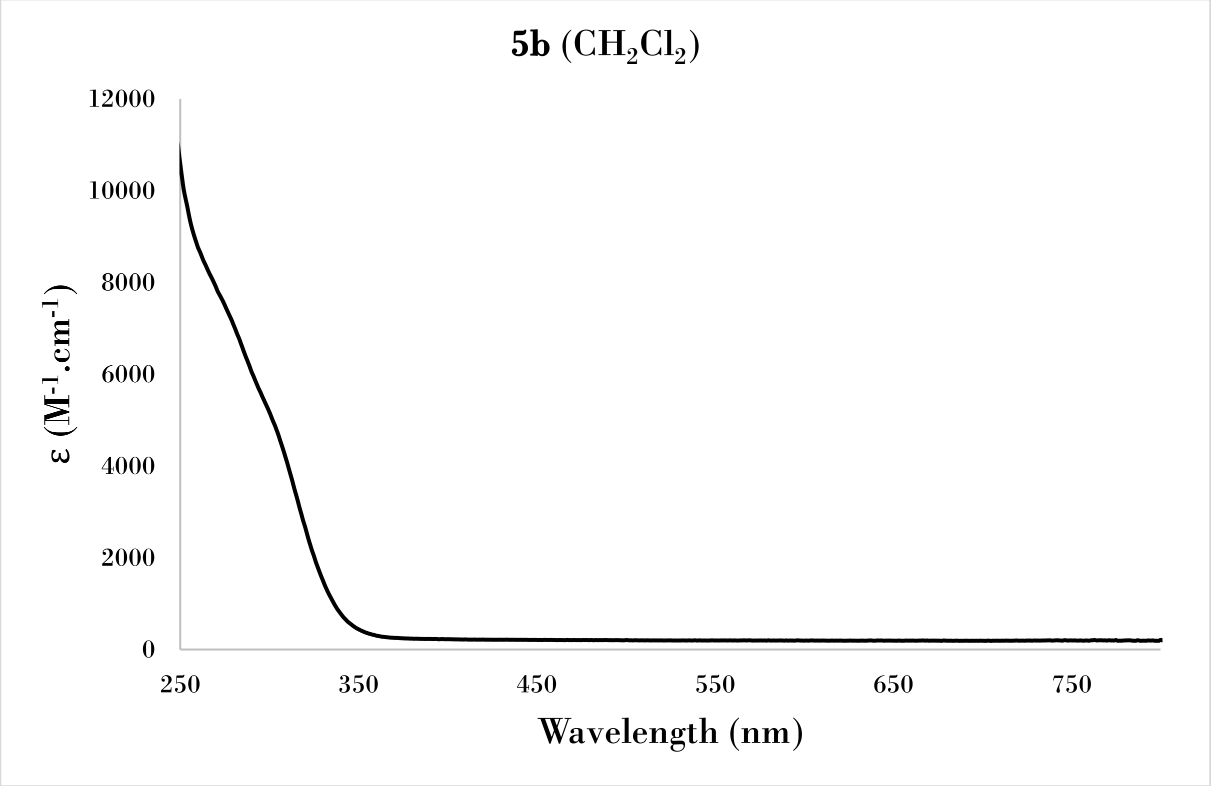

Figure S45: UV-vis (CH$_2$Cl$_2$, 0.1 mm cell)

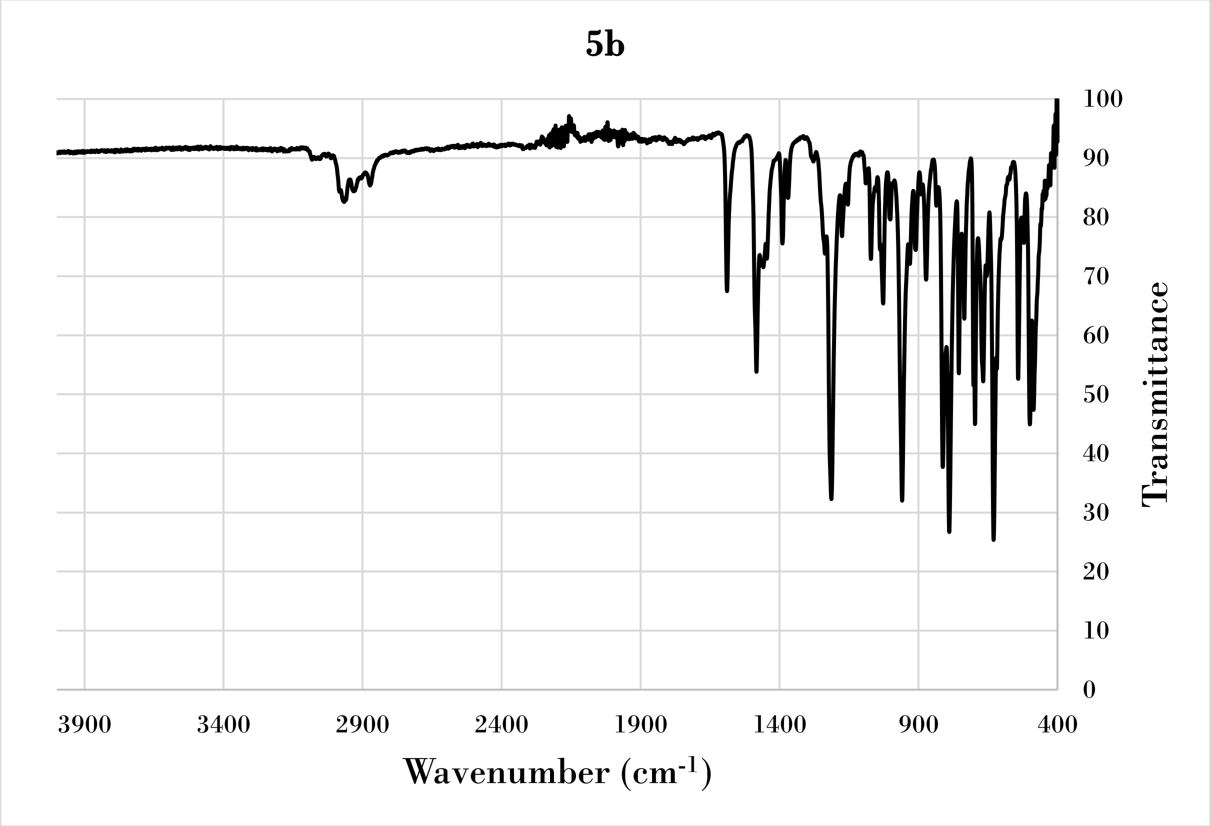

Figure S46: IR (ATR)

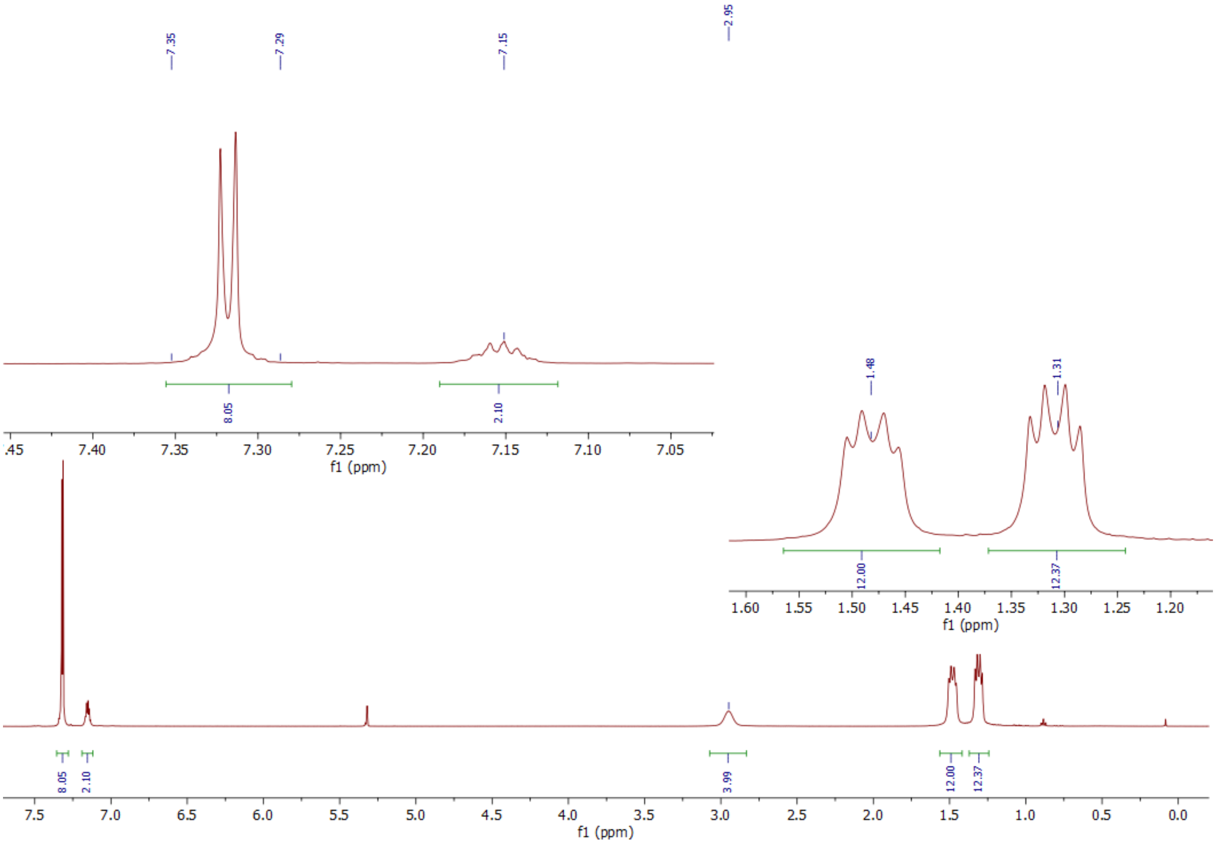

Figure S47: ^{1}H NMR (500 MHz, CD_2Cl_2, 298 K)

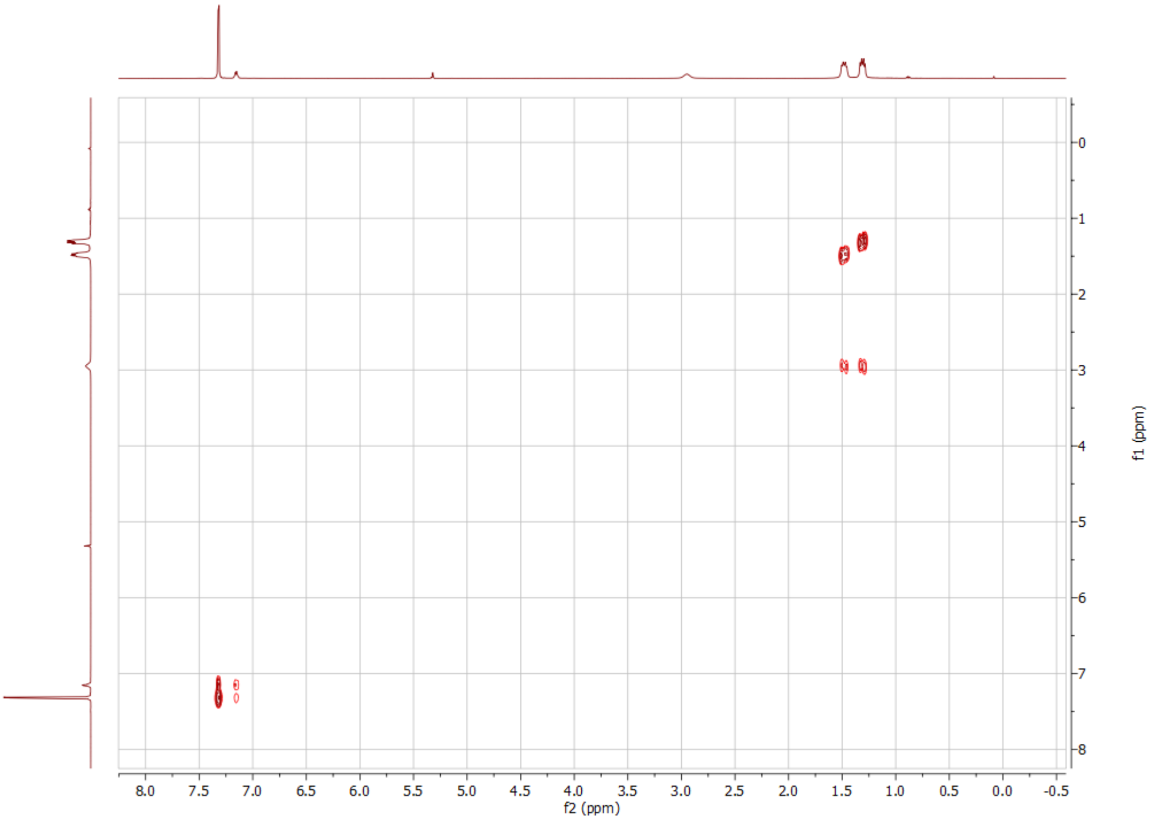

Figure S48: ^{1}H-^{1}H COSY (500 MHz, CD_2Cl_2, 298 K)

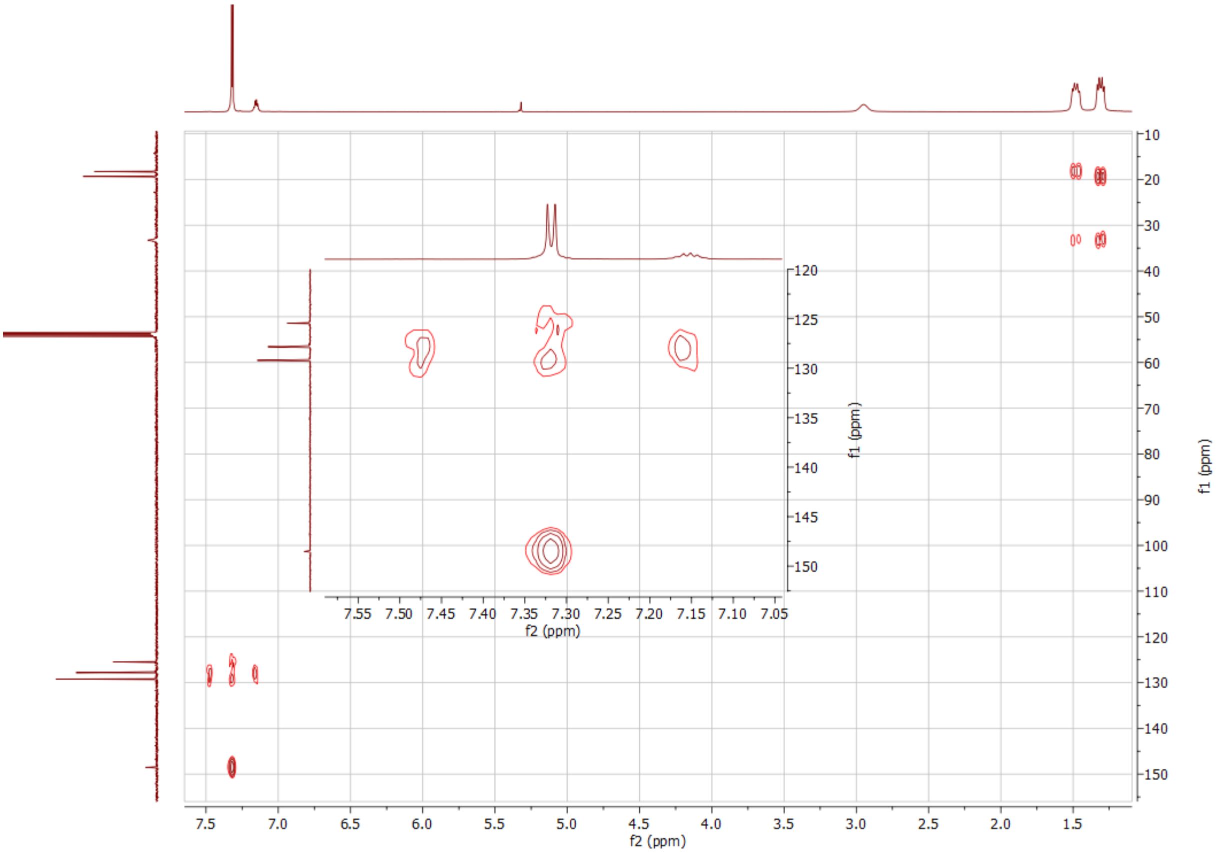

Figure S49: ^{1}H-^{13}C HMBC (500 MHz / 126 MHz, CD_2Cl_2, 298 K)

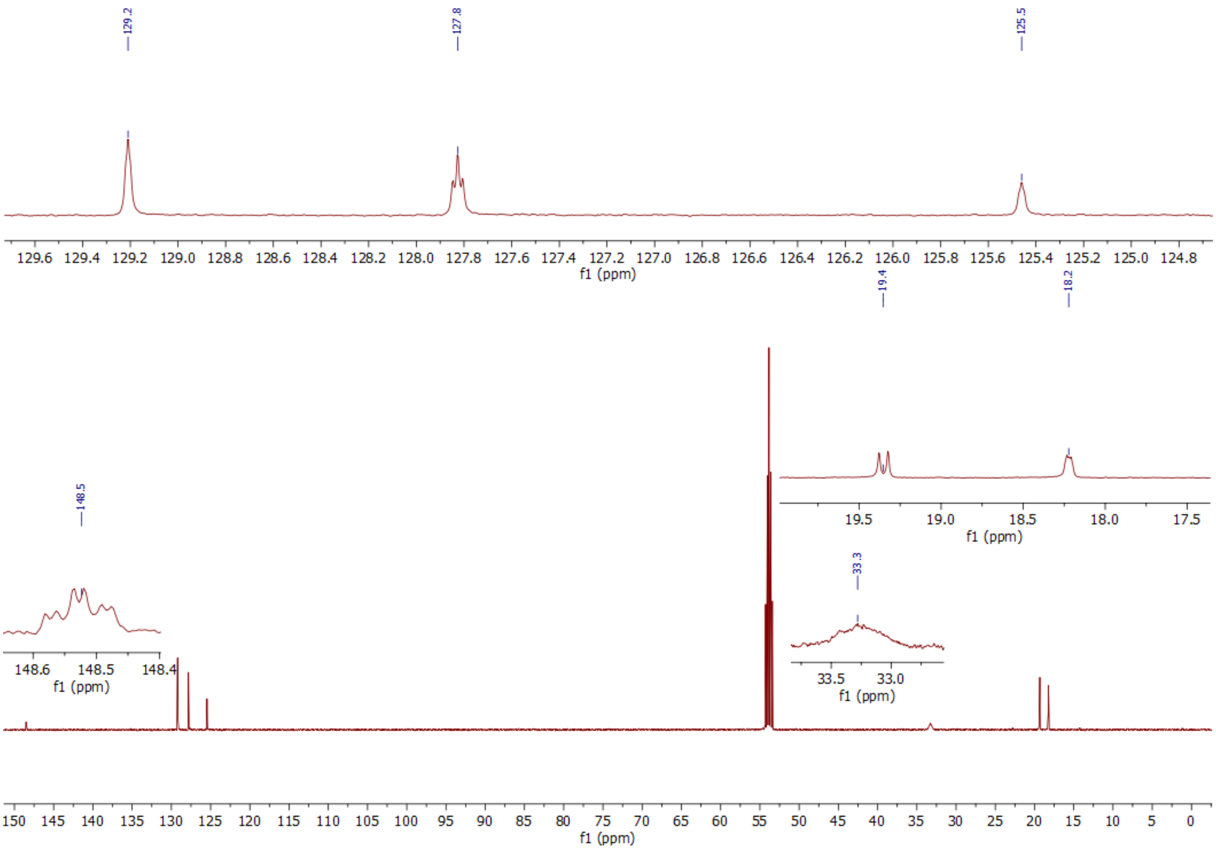

Figure S50: $^{13}C\{^1H\}$ NMR (126 MHz, CD_2Cl_2, 298 K)

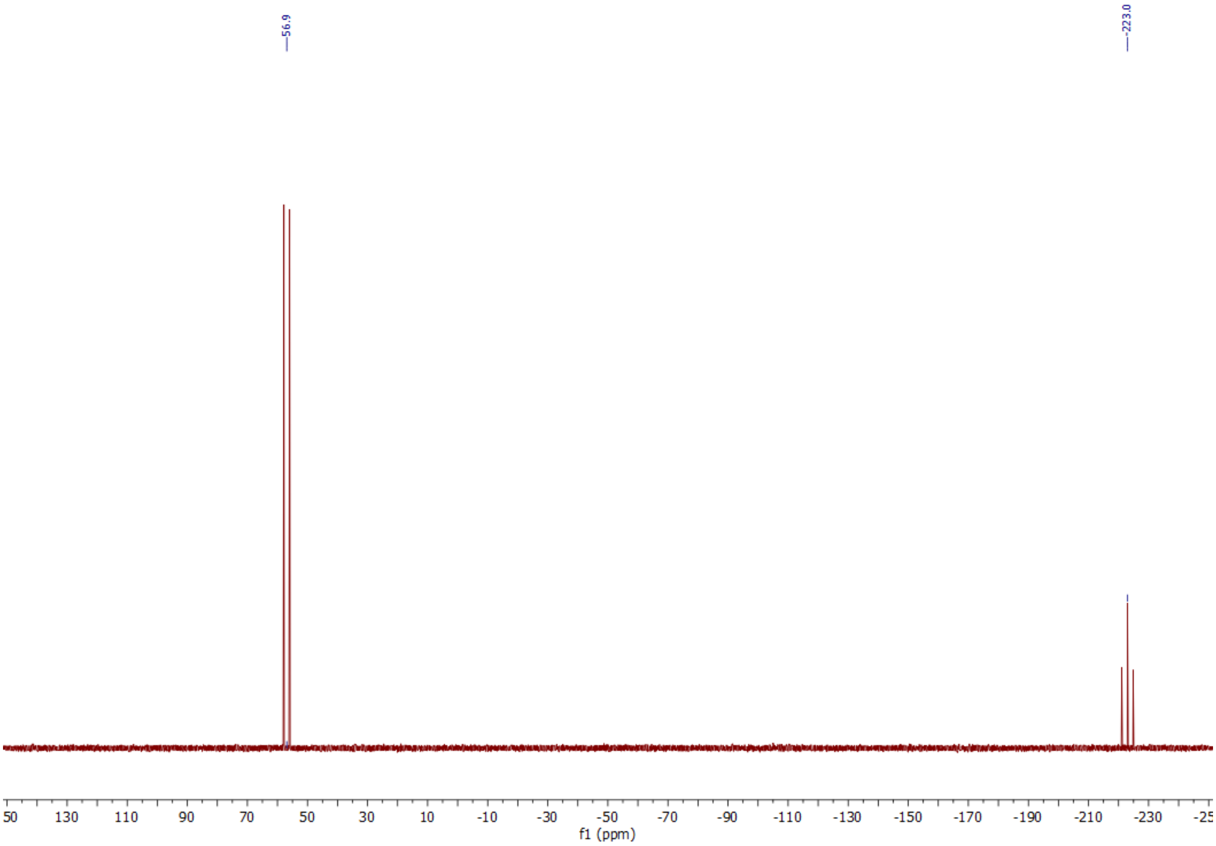

Figure S51: $^{31}P\{^1H\}$ NMR (202 MHz, CD_2Cl_2, 298 K)

Synthesis of complex ***6a-Py***

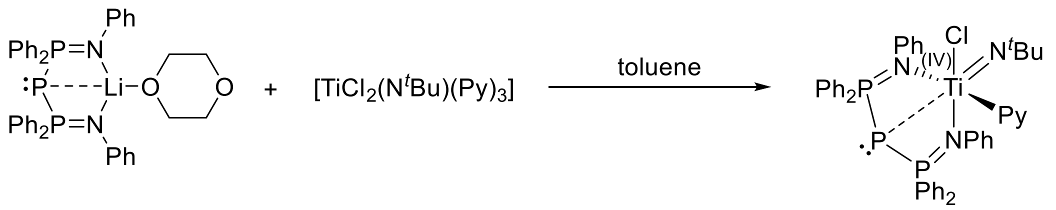

2a **6a-py** *(1.21 g, 50%)*

In an Ar glovebox, [TiCl$_2$(N^{t}Bu)(Py)$_3$] (1.28 g, 3.00 mmol) and proligand **2a** (2.06 g, 3.00 mmol) were suspended in toluene (50 mL). The reaction mixture was stirred for 2 h 30, during which it turned gradually yellow. It was filtered over a sintered glass frit, and the resulting solid was dissolved in CH$_2$Cl$_2$ and filtered over a pad of diatomaceous earth. The filtrate was evaporated to dryness outside of the glovebox. Upon returning to the glovebox, the resulting solid was stirred in 20 mL of pentane overnight. The suspension was filtered over a sintered glass frit, and the resulting solid was suspended in 5 mL of pentane and filtered, then dried on the frit. Complex **6a-py** was obtained as a yellow powder (1.21 g, yield 50%). Single crystals suitable for X-ray diffraction were grown by slow diffusion of pentane into a CH$_2$Cl$_2$ solution of **6a-Py** at -20 °C.

Elemental Analysis: calculated for C$_{45}$H$_{44}$ClN$_4$P$_3$Ti: C, 66.15; H, 5.43; N, 6.86. Found: C, 66.35; H, 5.49; N, 6.71.

UV-vis (CH$_2$Cl$_2$, 0.1 mm cell): $\lambda_1 = 277$ nm (shoulder, $\varepsilon = 19000$ M^{-1}.cm^{-1}).

IR (ATR): 3057 (w), 2956 (w), 2911 (w), 1586 (m), 1481 (m), 1435 (m), 1347 (w), 1241 (m), 1226 (m), 1097 (m), 1068 (w), 1028 (w), 1005 (w), 973 (m), 800 (m), 790 (s), 746 (m), 737 (m), 714 (m), 698 (m), 685 (s), 631 (s), 612 (m), 560 (w), 535 (s), 517 (s), 508 (s), 477 (m), 449 (m) cm^{-1}.

^{1}H NMR (500 MHz, CD$_2$Cl$_2$, 292 K): $\delta = 9.17$ (m, 2H, *H*2 of Py), 7.68 (m, 1H, *H*4 of Py), 7.55 (m, 4H, *o* of PPh$_2$), 7.48 (m, 4H, *o* of NPh), 7.40 (m, 2H, *p* of PPh$_2$), 7.32-7.19 (m, 10H, *o* of PPh$_2$ overlapping with *m* of PPh$_2$ and *H*3 of Py), 7.16-7.09 (m, 6H, *p* of PPh$_2$ overlapping with *m* of NPh), 6.94 (m, 2H, *p* of NPh), 6.89 (m, 4H, *m* of PPh$_2$), 0.60 (s, 9H, C*H*$_3$ of N^{t}Bu).

^{1}H-^{1}H COSY (500 MHz, CD$_2$Cl$_2$, 292 K)[selected cross-peaks]: 9.17 / 7.32-7.19 (*H*2 of Py / *H*3 of Py), 7.68 / 7.32-7.19 (*H*4 of Py / *H*3 of Py), 7.48 / 7.16-7.09 (*o* of NPh / *m* of NPh), 7.40 / 7.32-7.19 (*p* of PPh$_2$ / *o* of PPh$_2$ and/or *m* of PPh$_2$), 7.32-7.19 / 9.17 (*H*3 of Py / *H*2 of Py), 7.32-7.19 / 7.69 (*H*3 of Py / *H*4 of Py), 7.32-7.19 / 7.40 (*o* of PPh$_2$ and/or *m* of PPh$_2$ / *p* of PPh$_2$), 7.32-7.19 / 6.89 (*o* of PPh$_2$ / *m* of PPh$_2$), 7.16-7.09 / 7.48 (*m* of NPh / *o* of NPh), 7.16-7.09 / 6.94 (*m* of NPh / *p* of NPh), 7.16-7.09 / 6.89 (*p* of PPh$_2$ / *m* of PPh$_2$), 6.94 / 7.16-7.09 (*p* of NPh / *m* of NPh), 6.89 / 7.32-7.19 (*m* of PPh$_2$ / *o* of PPh$_2$), 6.89 / 7.16-7.09 (*m* of PPh$_2$ / *p* of PPh$_2$).

^{1}H-^{13}C HMBC (500 MHz / 126 MHz, CD$_2$Cl$_2$, 292 K)[selected cross-peaks]: 9.17 / 152.0 (*H*2 of Py / *C*2 of Py), 9.17 / 137.6 (*H*2 of Py / *C*4 of Py), 9.17 / 123.7 (*H*2 of Py / *C*3 of Py), 7.68 / 152.0 (*H*4 of Py / *C*2 of Py), 7.55 / 132.4 (*o* of PPh$_2$ / *o* of PPh$_2$), 7.48 / 153.1 (*o* of NPh / *i* of NPh), 7.48 / 126.7 (*o* of NPh / *o* of NPh), 7.48 / 122.2 (*o* of NPh / *p* of NPh), 7.40 / 132.4 (*p* of PPh$_2$ / *o* of PPh$_2$), 7.32-7.19 / 152.0 (*H*3 of Py / *C*2 of Py), 7.32-7.19 / 123.7 (*H*3 of Py / *C*3 of Py), 7.16-7.09 / 153.1 (*m* of NPh / *i* of NPh), 7.16-7.09 / 132.9 (*p* of PPh$_2$ / *o* of PPh$_2$), 0.60 / 71.1 (C*H*$_3$ of N^{t}Bu / C of N^{t}Bu), 0.60 / 30.3 (C*H*$_3$ of N^{t}Bu / *C*H$_3$ of N^{t}Bu).

$^{13}C\{^1H\}$ NMR (126 MHz, CD_2Cl_2, 292 K): δ = 153.1 (m, *i* of NPh), 152.0 (s, *C*2 of Py), 137.6 (s, *C*4 of Py), 134.4 (m, *i* of PPh_2), 132.9 (m, *o* of PPh_2), 132.4 (m, *o* of PPh_2), 131.8 (s, *p* of PPh_2), 131.1 (s, *p* of PPh_2), 130.0 (m, *i* of PPh_2), 128.4 (m, *m* of PPh_2 overlapping with *m* of NPh), 128.3 (s, *m* of NPh overlapping with two *m* of PPh_2), 128.2 (m, *m* of PPh_2 overlapping with *m* of NPh), 126.7 (m, *o* of NPh), 123.7 (s, *C*3 of Py), 122.2 (s, *p* of NPh), 71.1 (s, *C* of N^tBu), 30.3 (s, CH_3 of N^tBu).

$^{31}P\{^1H\}$ NMR (202 MHz, CD_2Cl_2, 292 K): δ = 34.5 (d, $^1J_{PP}$ = 390 Hz, PPh_2), -189.3 (t, $^1J_{PP}$ = 390 Hz, central *P*).

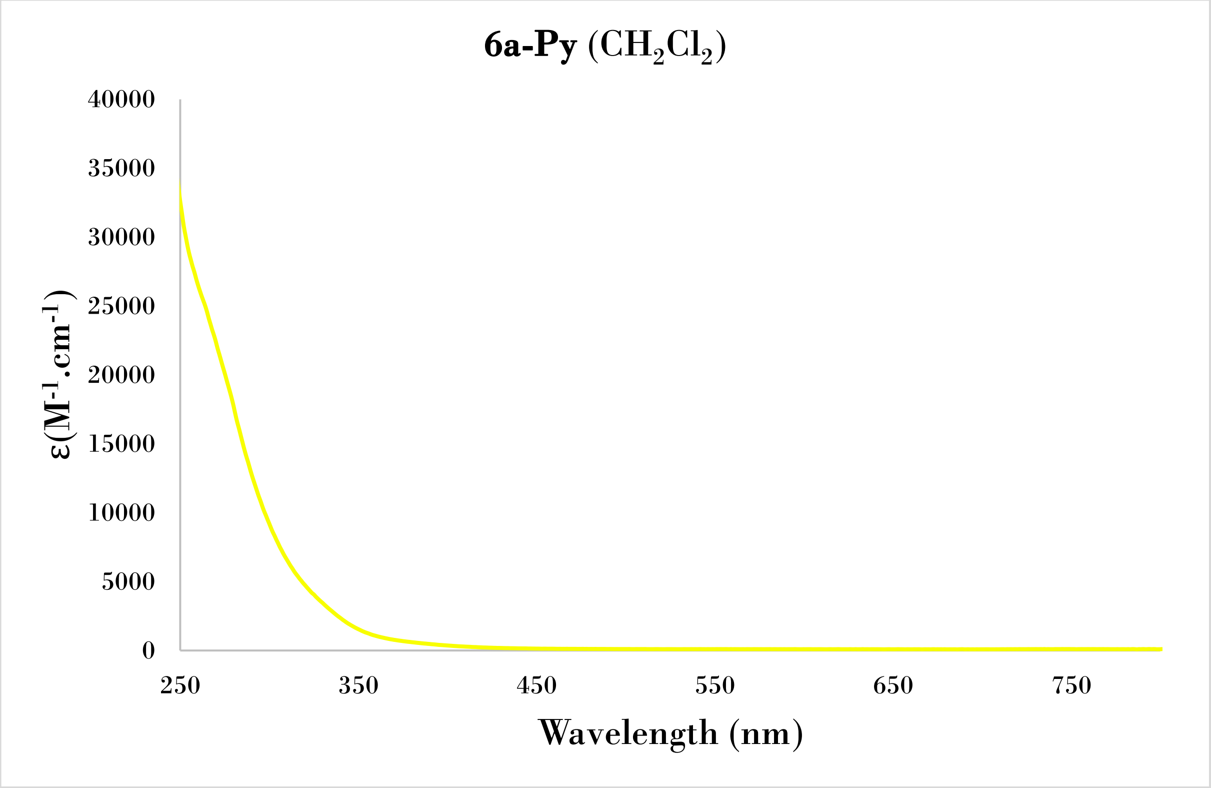

Figure S52: UV-vis (CH_2Cl_2, 0.1 mm cell)

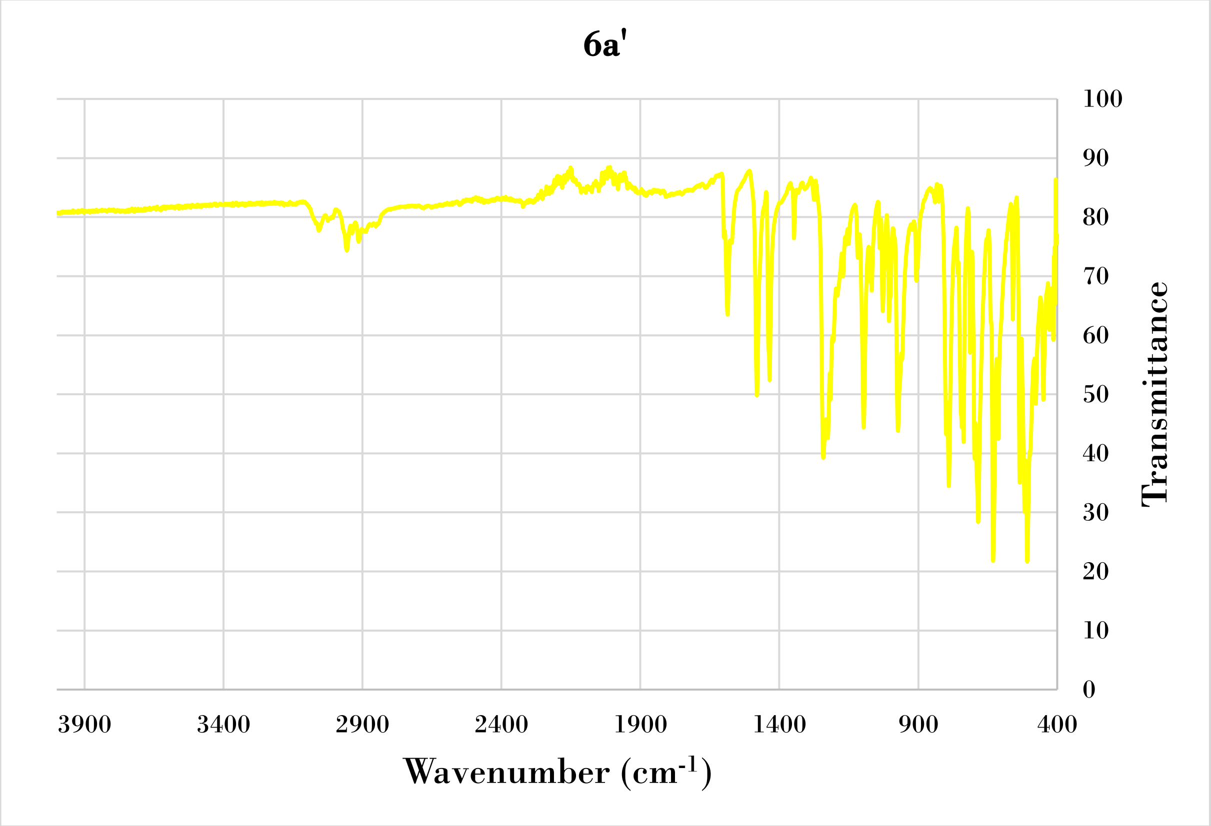

Figure S53: IR (ATR)

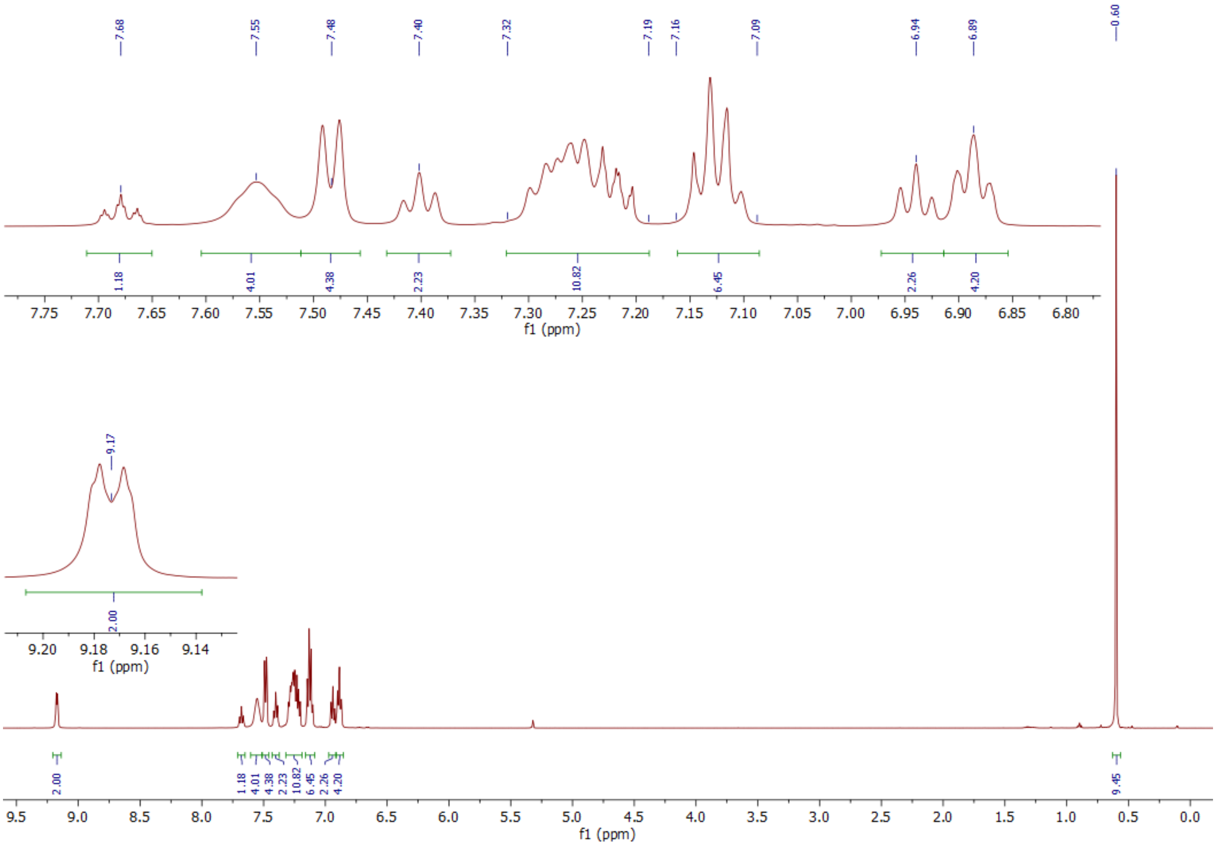

Figure S54: ^{1}**H NMR (500 MHz,** CD_2Cl_2**, 292 K)**

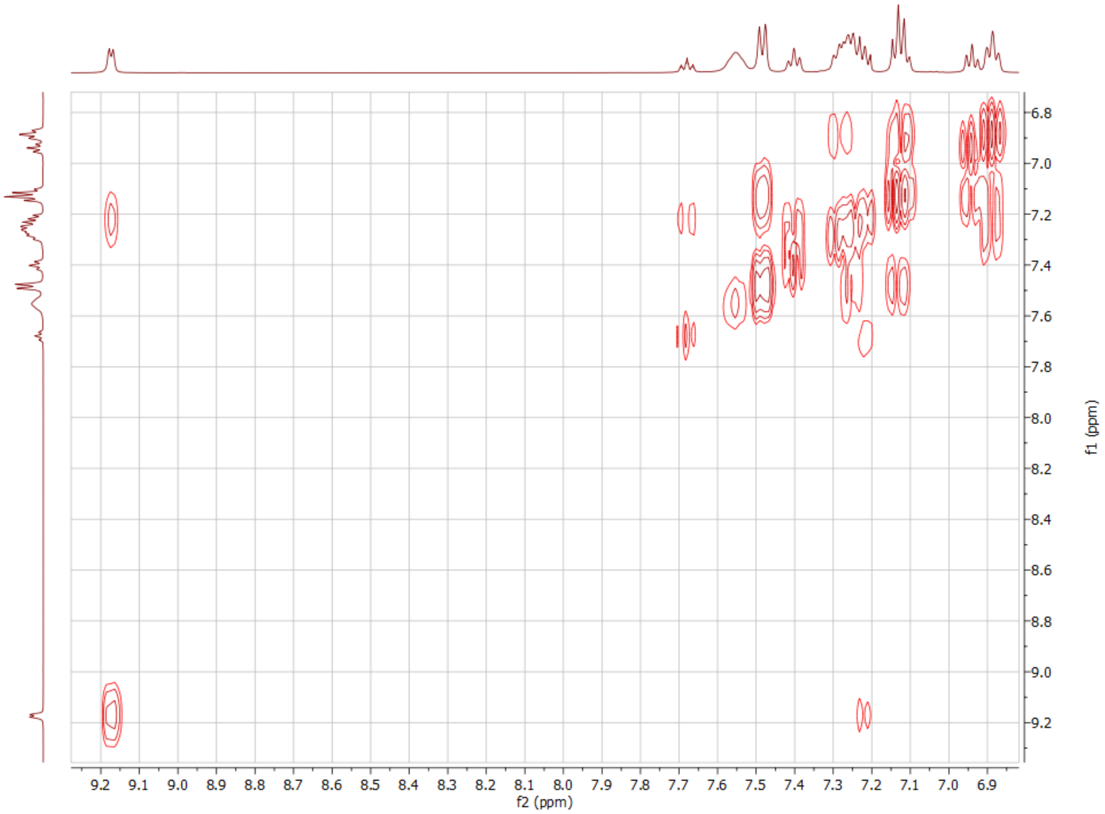

Figure S55: ^{1}H-^{1}H COSY (500 MHz, CD_2Cl_2, 292 K)(aromatic region)

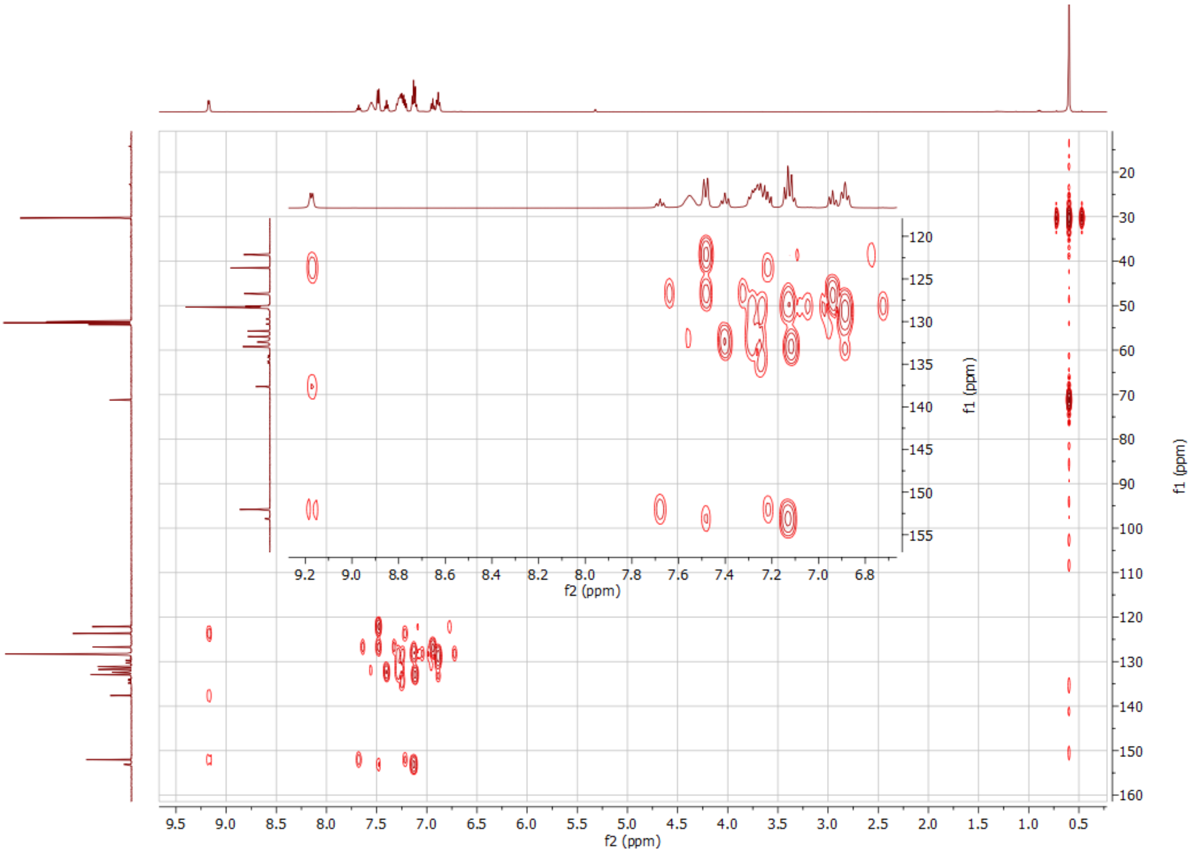

Figure S56: ^{1}H-^{13}C HMBC (500 MHz / 126 MHz, CD_2Cl_2, 292 K)

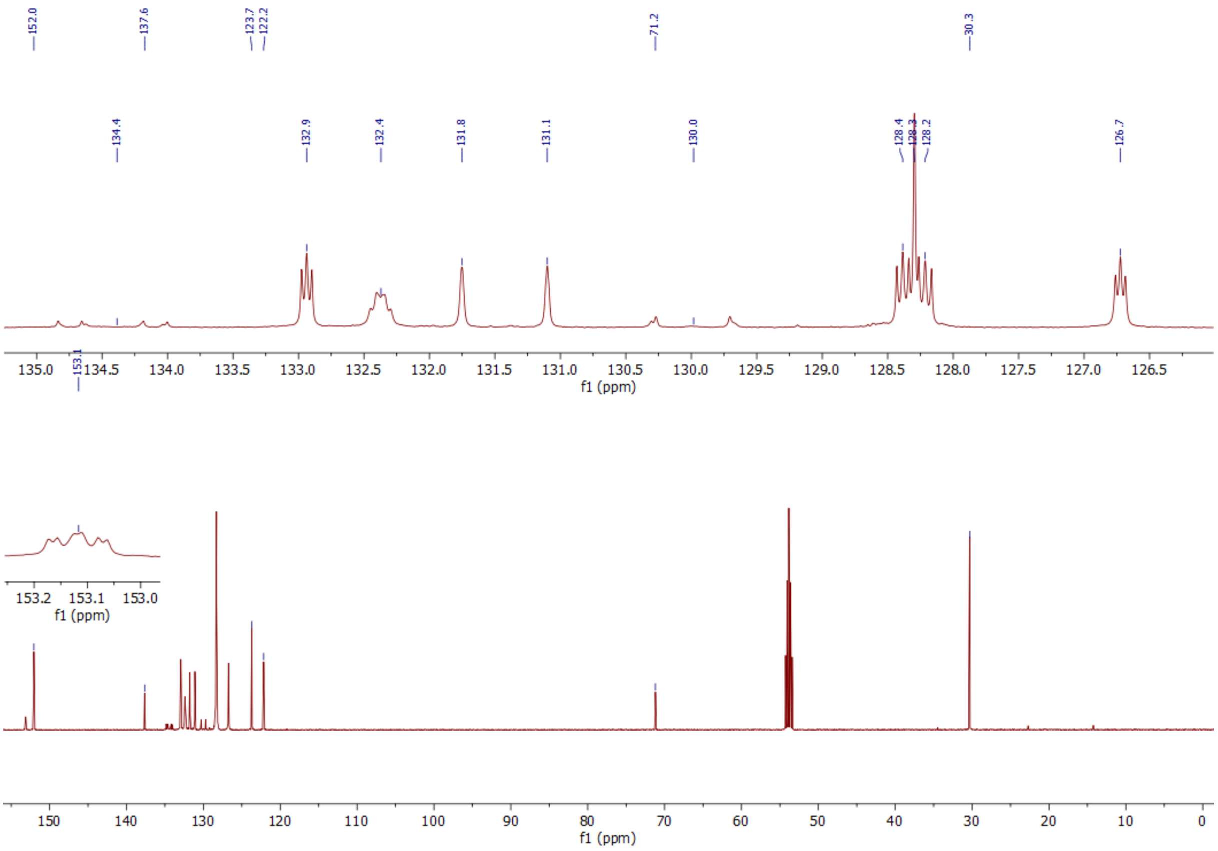

Figure S57: $^{13}C\{^{1}H\}$ NMR (126 MHz, CD_2Cl_2, 292 K)

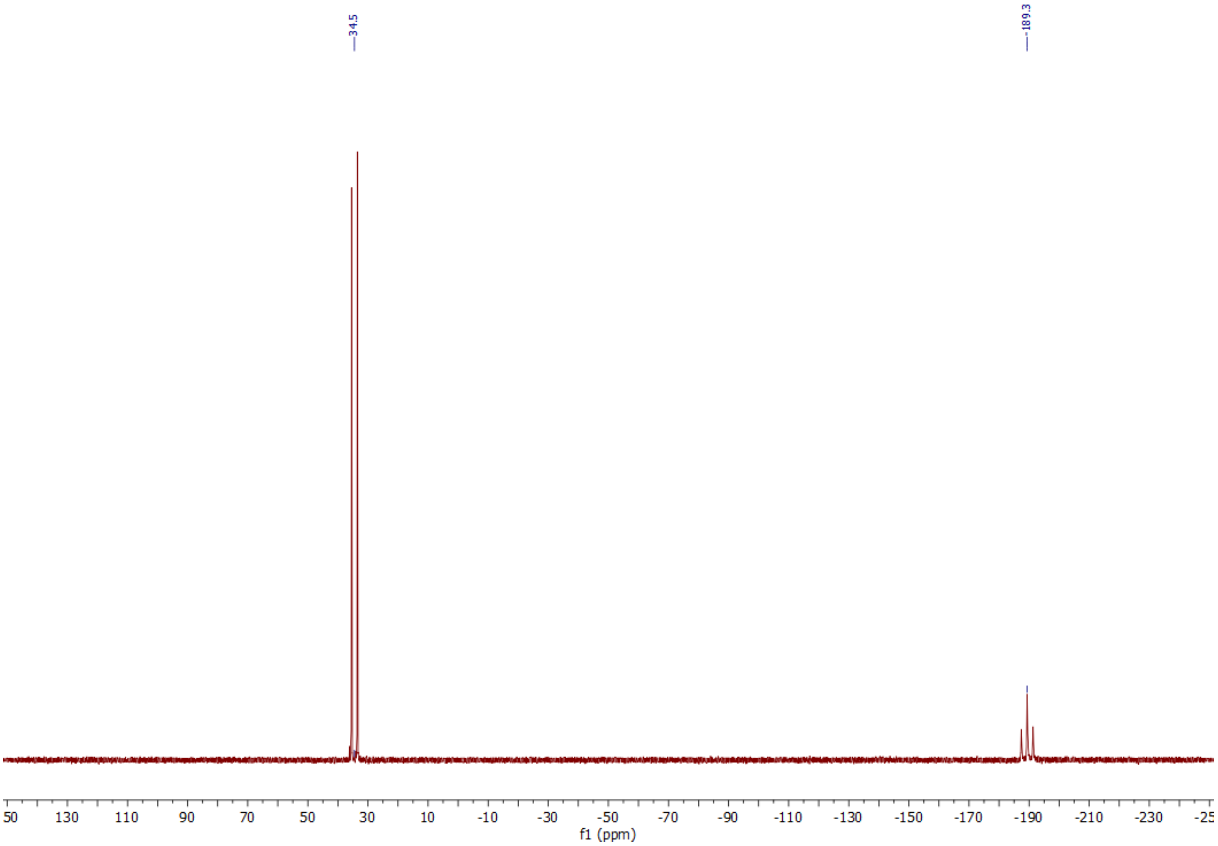

Figure S58: $^{31}P\{^{1}H\}$ NMR (202 MHz, CD_2Cl_2, 292 K)

*Synthesis of complex **6a***

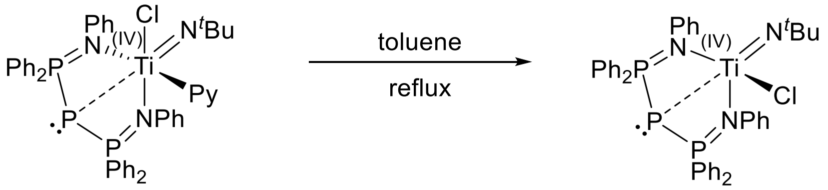

6a'

6a *(0.320 g, 74%)*

In an Ar glovebox, complex **6a-Py** (0.37 g, 0.45 mmol) was suspended in toluene (40 mL) in a Schlenk flask. Outside of the box, the vessel was connected to a Schlenk line and the reaction mixture was heated until a light reflux was observed. An oil bubbler was used to prevent any build-up of pressure during heating. The solid dissolved gradually, and the solution became paler. The oil bubbler war closed and the reaction mixture was allowed to cool to room temperature. Pentane (100 mL) was added to precipitate a microcrystalline solid, which was filtered on a sintered glass frit in the glovebox. The solid was dried under vacuum at a Schlenk line, yielding **6a** as a pale yellow powder containing 100 mol% of toluene (320 mg, yield 74%). Single crystals suitable for X-ray diffraction were obtained by slow diffusion of pentane into a CH_2Cl_2 solution of **6a** at -20 °C.

Elemental Analysis: calculated for $C_{40}H_{39}ClN_3P_3Ti(C_8H_8)$: C, 68.00; H, 5.71; N, 5.06. Found: C, 67.78; H, 6.10; N, 5.02.

UV-vis (CH_2Cl_2, 0.1 mm cell): λ = 270 nm (shoulder, ε = 17600 $M^{-1}.cm^{-1}$).

IR (ATR): 3058 (w), 2960 (w), 2858 (w), 1586 (w), 1483 (m), 1433 (m), 1350 (w), 1237 (m), 1209 (m), 1188 (w), 1123 (w), 1095 (m), 1072 (w), 1071 (w), 1027 (w), 997 (w), 953 (m), 936 (m), 907 w), 890 (w), 819 (m), 802 (m), 753 (m), 743 (m), 731 (m), 718 (m), 686 (s), 649 (s), 617 (w), 559 (w), 540 (m), 522 (m), 510 (m), 485 (m), 466 (m), 443 (m), 441 (m), 419 (w), 414 (m) cm^{-1}.

^{1}H NMR (500 MHz, CD_2Cl_2, 292 K): δ = 7.73 (m, 4H, *o* of PPh$_2$), 7.51 (m, 2H, *p* of PPh$_2$), 7.41 (m, 8H, *o* of PPh$_2$ overlapping with *m* of PPh$_2$), 7.32-7.23 (m, 4H, *p* of PPh$_2$ overlapping with toluene signal), 7.23-7.04 (m, 15H, *o* of NPh overlapping with toluene signal, *m* of PPh$_2$ and *m* of NPh), 6.94 (m, 2H, *p* of NPh), 0.57 (s, 9H, C*H*$_3$ of N^{t}Bu).

^{1}H-^{1}H COSY (500 MHz, CD_2Cl_2, 292 K): COSY was uninformative due to the overlap of signals in the aromatic region.

^{1}H-^{13}C HMBC (500 MHz / 126 MHz, CD_2Cl_2, 292 K)[selected cross-peaks]: 7.23-7.04 / 126.0 (*o* of NPh / *o* of NPh), 7.23-7.04 / 123.4 (*o* of NPh / *p* of NPh), 7.23-7.04 / 152.3 (*o* of NPh / *i* of NPh), 6.94 / 126.0 (*p* of NPh / *o* of NPh), 0.57/ 71.3 (C*H*$_3$ of N^{t}Bu / C of N^{t}Bu), 0.57 / 30.4 (C*H*$_3$ of N^{t}Bu / *C*H$_3$ of N^{t}Bu).

^{13}C{^{1}H} NMR (126 MHz, CD_2Cl_2, 292 K): δ = 152.3 (m, *i* of NPh), 133.1 (m, *o* of PPh$_2$), 132.7 (s, *p* of PPh$_2$), 132.5 (m, *i* of PPh$_2$), 132.1 (m, *o* of PPh$_2$), 131.9 (s, *p* of PPh$_2$), 129.1 (m, *m* of PPh$_2$), 128.7 (m, *m* of PPh$_2$), 128.5 (m, *m* of NPh overlapping with toluene signal), 127.9 (m, *i* of PPh$_2$), 126.0 (m, *o* of NPh), 123.4 (s, *p* of NPh), 71.3 (s, *C* of N^{t}Bu), 30.4 (s, *C*H$_3$ of N^{t}Bu).

$^{31}P\{^1H\}$ NMR (202 MHz, CD_2Cl_2, 292 K): δ = 37.4 (d, $^1J_{PP}$ = 416 Hz, *P*Ph$_2$), -179.2 (t, $^1J_{PP}$ = 416 Hz, central *P*).

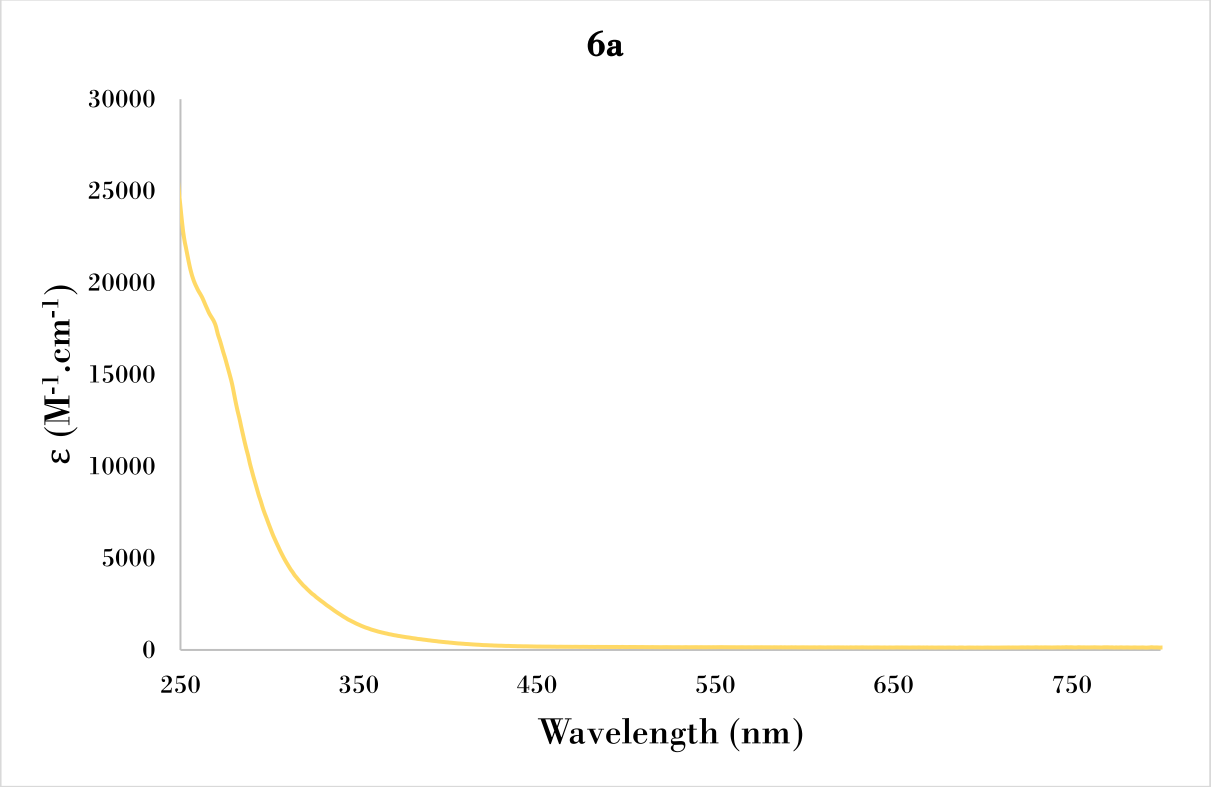

Figure S59: UV-vis (CH_2Cl_2, 0.1 mm cell)

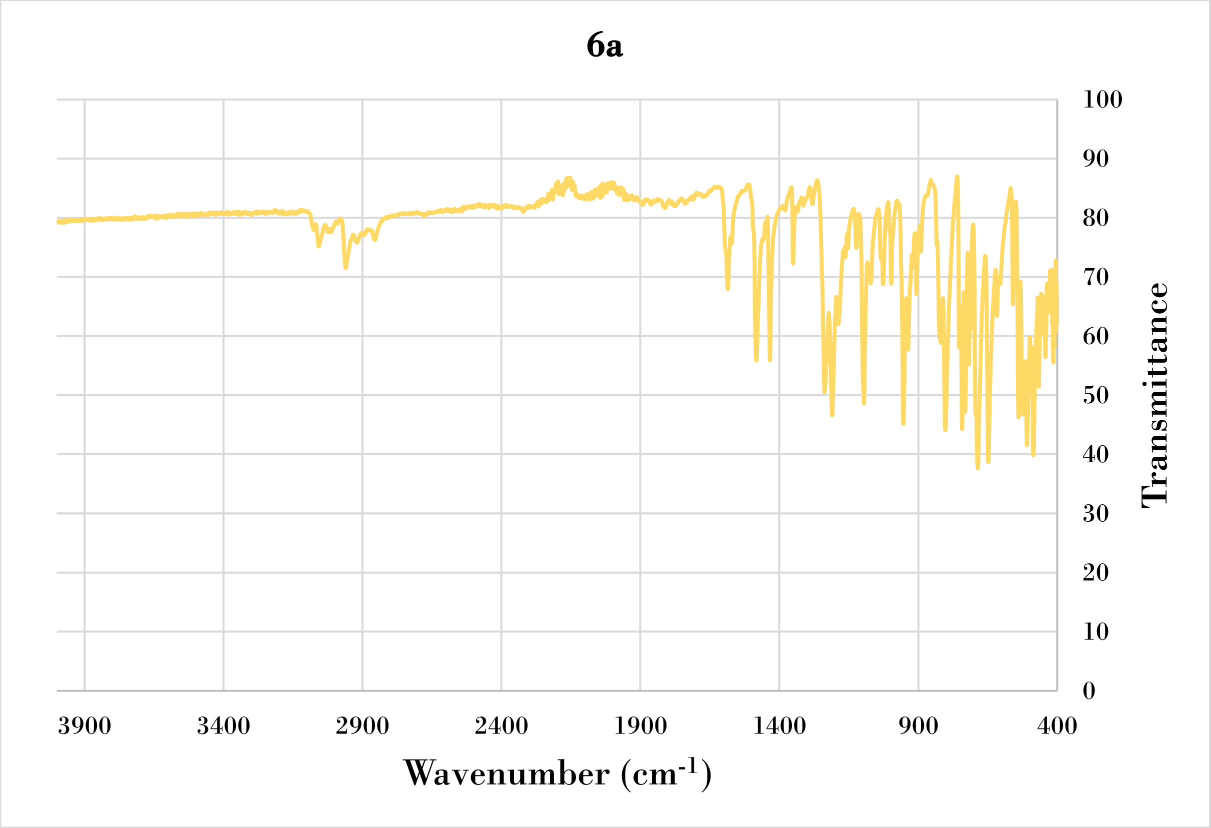

Figure S60: IR (ATR)

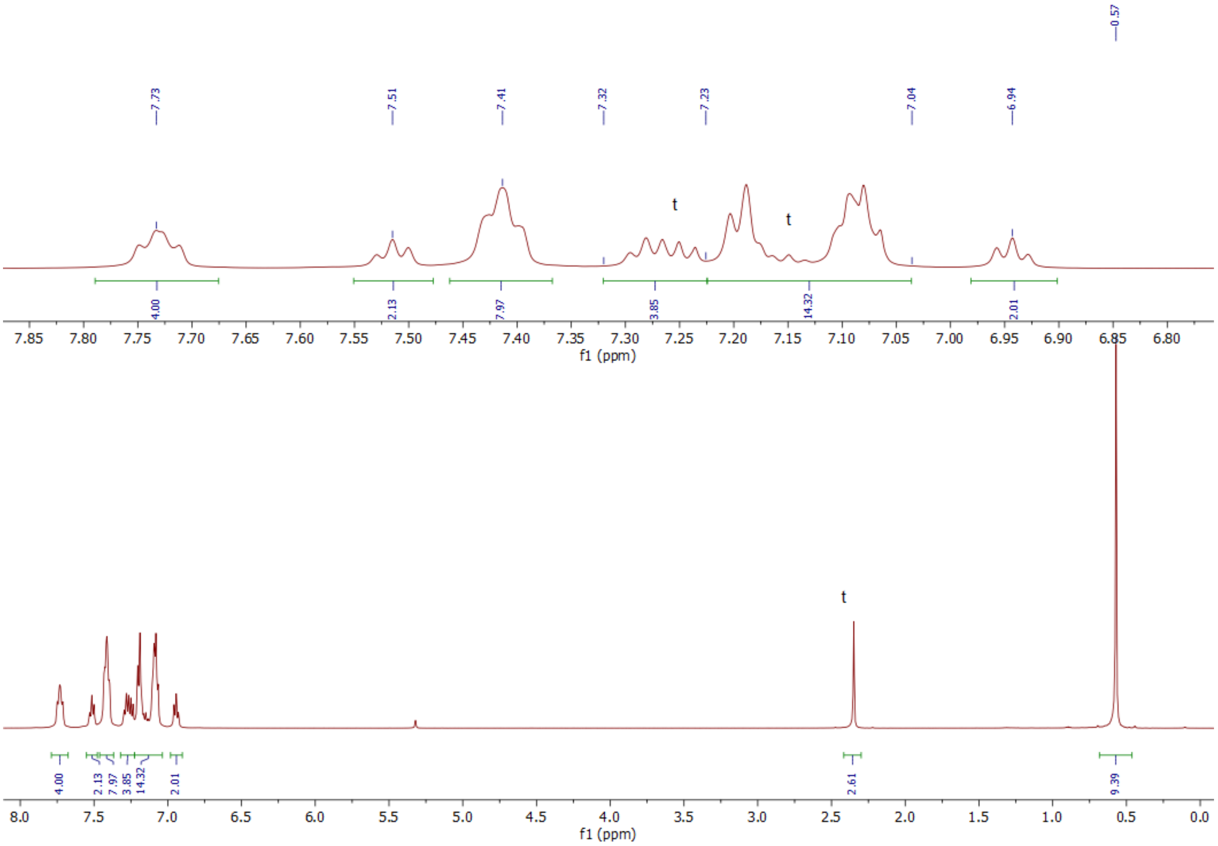

Figure S61: ^{1}H NMR (500 MHz, CD_2Cl_2, 292 K)(t: toluene)

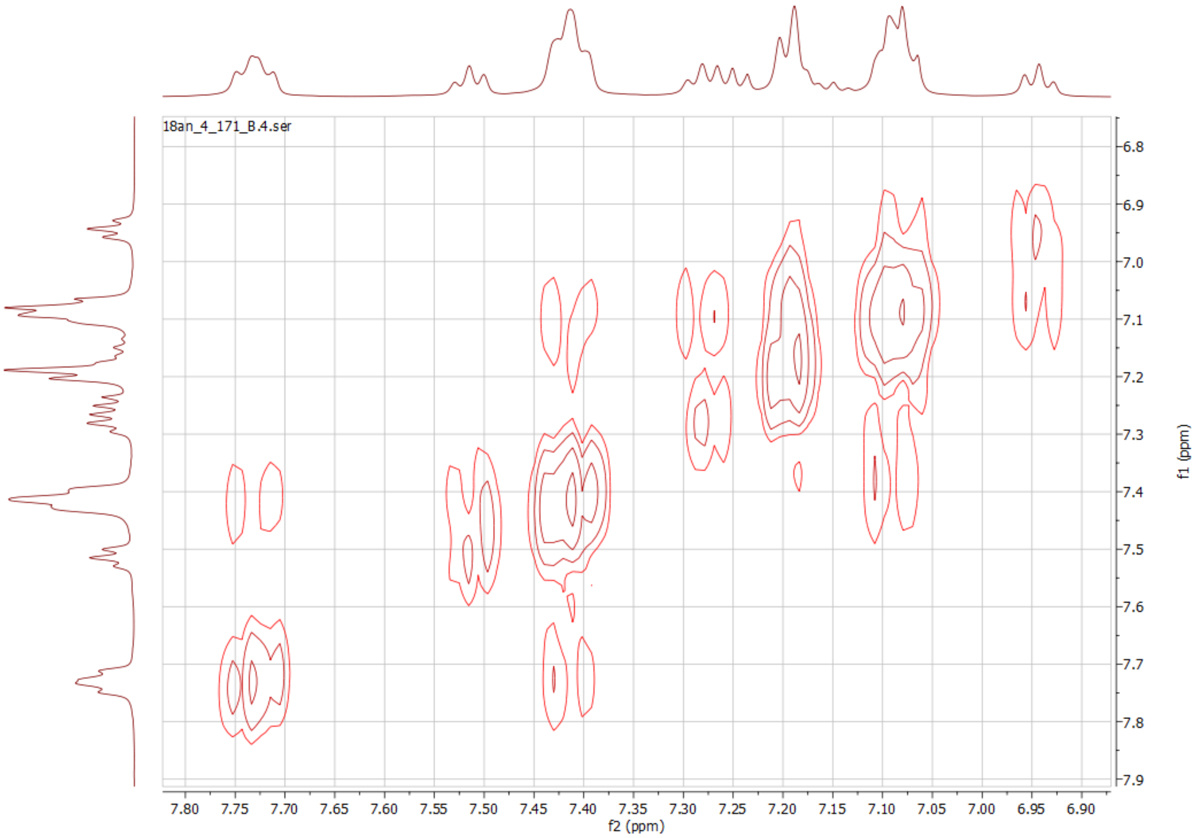

Figure S62: ^{1}H-^{1}H COSY (500 MHz, CD_2Cl_2, 292 K)(aromatic region)

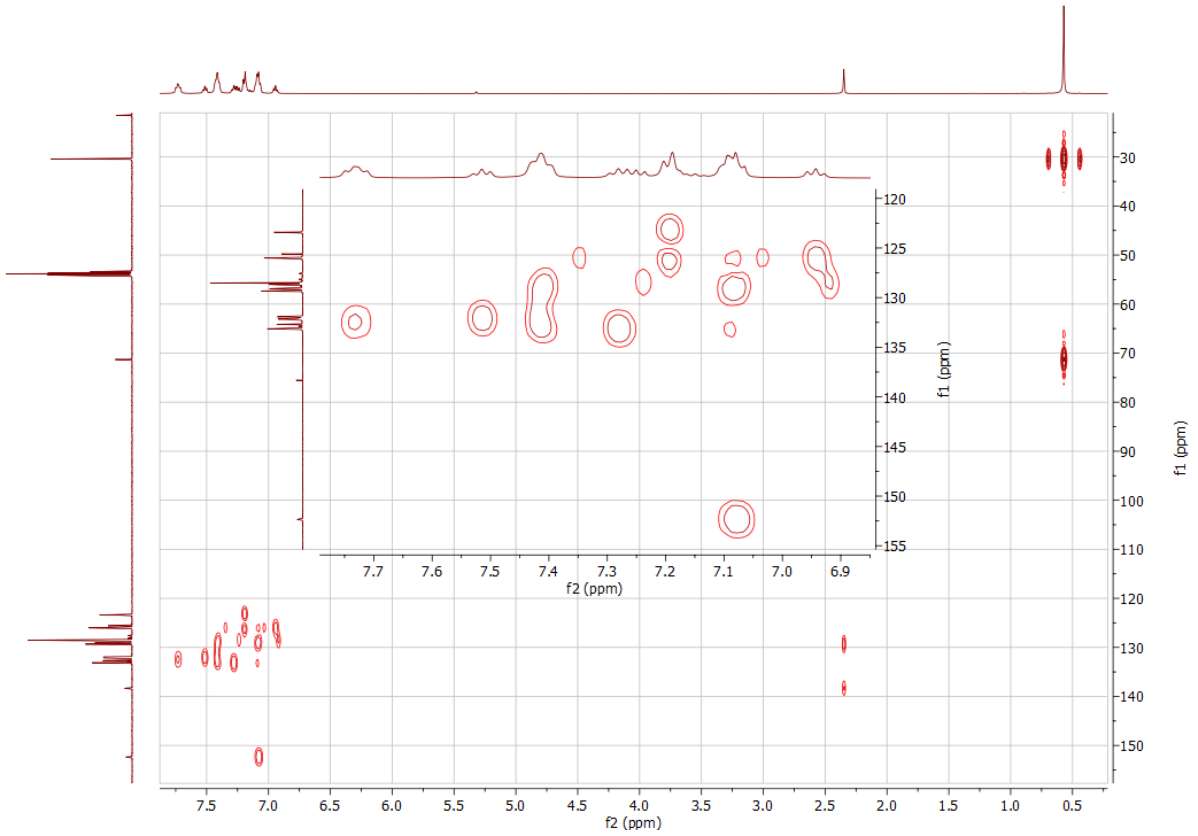

Figure S63: ^{1}H-^{13}C HMBC (500 MHz / 126 MHz, CD_2Cl_2, 292 K)

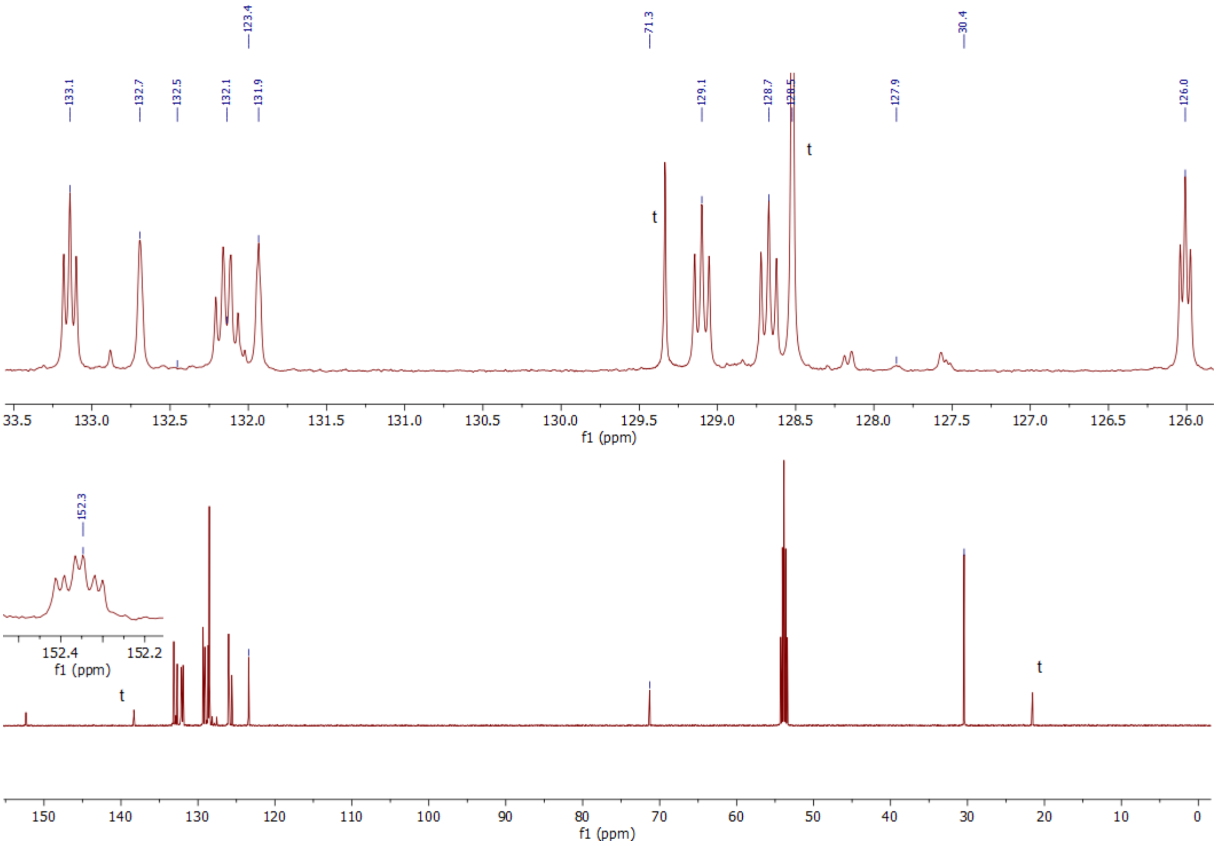

Figure S64: $^{13}C\{^{1}H\}$ **NMR (126 MHz, CD_2Cl_2, 292 K)(t: toluene)**

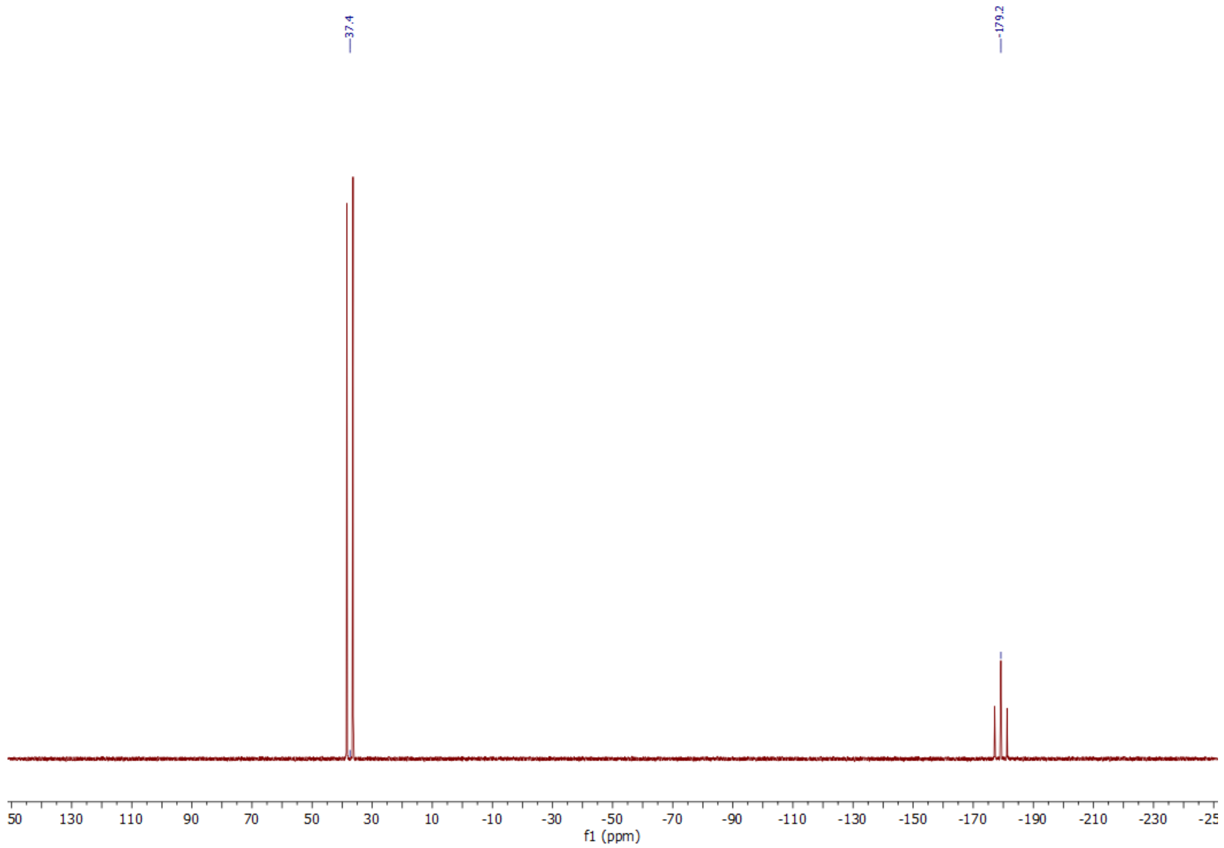

Figure S65: $^{31}P\{^{1}H\}$ **NMR (202 MHz, CD_2Cl_2, 292 K)**

Synthesis of complex ***6b***

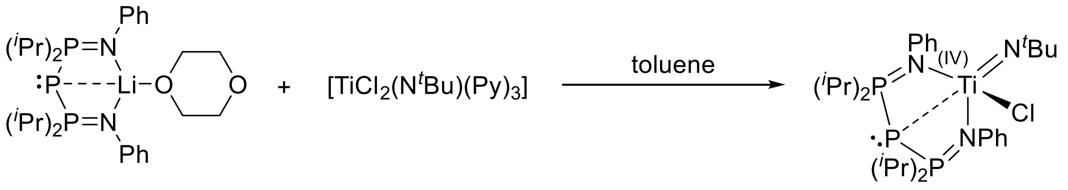

2b

6b *(0.705 g, 81%)*

In an Ar glovebox, $[TiCl_2(N^tBu)(Py)_3]$ (620 mg, 1.45 mmol) and proligand **2b** (827 mg, 1.52 mmol) were suspended in toluene (50 mL). The reaction mixture was filtered over a pad of diatomaceous earth. The filtrate was evaporated to dryness outside of the glovebox. Upon returning to the glovebox, the resulting solid was stirred in 30 mL of pentane for 5 min. The suspension was filtered over a sintered glass frit, and the resulting solid was suspended three times in pentane (5 mL) and filtered, then dried on the frit. Complex **6b** was obtained as a pale yellow powder (705 mg, yield 81%). Single crystals suitable for X-ray diffraction were grown by slow diffusion of pentane into a CH_2Cl_2 solution of **6b** at -20 °C.

Elemental Analysis: calculated for $C_{28}H_{47}ClN_3P_3Ti$: C, 55.87; H, 7.87; N, 6.98. Found: C, 55.86; H, 8.44; N, 7.25.

UV-vis (CH$_2$Cl$_2$, 0.1 mm cell): λ_1 = 279 nm (shoulder, ε = 5600 M^{-1}.cm^{-1}), λ_2 = 344 nm (local maximum, ε = 800 M^{-1}.cm^{-1}).

IR (ATR): 2962 (w), 2912 (w), 2872 (w), 1588 (m), 1485 (m), 1457 (m), 1385 (w), 1366 (w), 1348 (w), 1241 (m), 1229 (m), 1220 (m), 1169 (w), 1122 (w), 1070 (w), 1030 (w), 1026 (m), 955 (s), 902 (m), 879 (w), 820 (m), 804 (s), 746 (m), 696 (s), 683 (m), 655 (s), 642 (m), 622 (m), 606 (w), 536 (w), 529 (m), 476 (m) cm^{-1}.

^{1}H NMR (600 MHz, CD$_2$Cl$_2$, 298 K): δ = 7.35 (m, 4H, *o* of NPh), 7.25 (m, 4H, *m* of NPh), 7.06 (m, 2H, *p* of NPh), 2.59 (m, 2H, C*H* of ^{i}Pr), 2.50 (m, 2H, C*H* of ^{i}Pr), 1.43 (m, 6H, CH_3 of ^{i}Pr overlapping with CH_3 of ^{i}Pr), 1.38 (m, 6H, CH_3 of ^{i}Pr overlapping with CH_3 of ^{i}Pr), 1.25 (m, 6H, CH_3 of ^{i}Pr), 1.04 (m, 6H, CH_3 of ^{i}Pr), 0.20 (s, 9H, CH_3 of N^{t}Bu).

^{1}H-^{1}H COSY (600 MHz, CD$_2$Cl$_2$, 298 K)[selected cross-peaks]: 7.35 / 7.25 (*o* of NPh / *m* of NPh), 7.25 / 7.35 (*m* of NPh / *o* of NPh), 7.25 / 7.06 (*m* of NPh / *p* of NPh), 7.06 / 7.25 (*p* of NPh / *m* of NPh), 2.50 / 1.43 (C*H* of ^{i}Pr / CH_3 of ^{i}Pr), 2.50 / 1.25 (C*H* of ^{i}Pr / CH_3 of ^{i}Pr), 1.43 / 2.50 (CH_3 of ^{i}Pr / C*H* of ^{i}Pr), 1.25 / 2.50 (CH_3 of ^{i}Pr / C*H* of ^{i}Pr). Note: cross peaks between C*H* of ^{i}Pr at 2.59 ppm and CH_3 of ^{i}Pr at 1.38 and 1.04 ppm were observed, but only under the diagonal.

^{1}H-^{13}C HMBC (600 MHz / 151 MHz, CD$_2$Cl$_2$, 298 K)[selected cross-peaks]: 7.35 / 153.3 (*o* of NPh / *i* of NPh), 7.35 / 127.1 (*o* of NPh / *o* of NPh), 7.35 / 124.0 (*o* of NPh / *p* of NPh), 7.26 / 153.3 (*m* of / *i* of NPh), 7.26 / 128.9 (*m* of NPh / *m* of NPh), 7.06 / 127.1 (*p* of NPh / *o* of NPh), 2.59 / 19.5 (C*H* of ^{i}Pr / *C*H$_3$ of ^{i}Pr), 2.59 / 17.2 (C*H* of ^{i}Pr / *C*H$_3$ of ^{i}Pr), 2.50 / 18.1 (C*H* of ^{i}Pr / *C*H$_3$ of ^{i}Pr), 2.50 / 17.9 (C*H* of ^{i}Pr / *C*H$_3$ of ^{i}Pr), 1.43 / 30.4 (CH_3 of ^{i}Pr / *C*H of ^{i}Pr), 1.43 / 17.9 (CH_3 of ^{i}Pr / *C*H$_3$ of ^{i}Pr), 1.38 / 31.4 (CH_3 of ^{i}Pr / *C*H of ^{i}Pr), 1.38 / 17.2 (CH_3 of ^{i}Pr / *C*H$_3$ of ^{i}Pr), 1.25 / 30.4 (CH_3 of ^{i}Pr / *C*H of ^{i}Pr), 1.25 / 18.1 (CH_3 of ^{i}Pr / *C*H$_3$ of ^{i}Pr), 1.04 / 31.4 (CH_3 of ^{i}Pr / *C*H of ^{i}Pr), 1.04 / 19.5 (CH_3 of ^{i}Pr / *C*H$_3$ of ^{i}Pr), 0.20 / 70.1 (CH_3 of N^{t}Bu / *C* of N^{t}Bu), 0.20 / 30.2 (CH_3 of N^{t}Bu / *C*H$_3$ of N^{t}Bu).

^{13}C{^{1}H} NMR (151 MHz, CD$_2$Cl$_2$, 298 K): δ = 153.3 (m, *i* of NPh), 128.9 (s, *m* of NPh), 127.1 (m, *o* of NPh), 124.0 (m, *p* of NPh), 70.1 (s, *C* of N^{t}Bu), 31.4 (m, *C*H of ^{i}Pr), 30.4 (m, *C*H of ^{i}Pr), 30.2 (s, *C*H$_3$ of N^{t}Bu), 19.5 (m, *C*H$_3$ of ^{i}Pr), 18.1 (m, *C*H$_3$ of ^{i}Pr), 17.9 (m, *C*H$_3$ of ^{i}Pr), 17.2 (m, *C*H$_3$ of ^{i}Pr).

^{31}P{^{1}H} NMR (243 MHz, CD$_2$Cl$_2$, 298 K): δ = 67.7 (d, $^1J_{\mathrm{PP}}$ = 474 Hz, *P*^{i}Pr$_2$), -241.0 (t, $^1J_{\mathrm{PP}}$ = 474 Hz, central *P*).

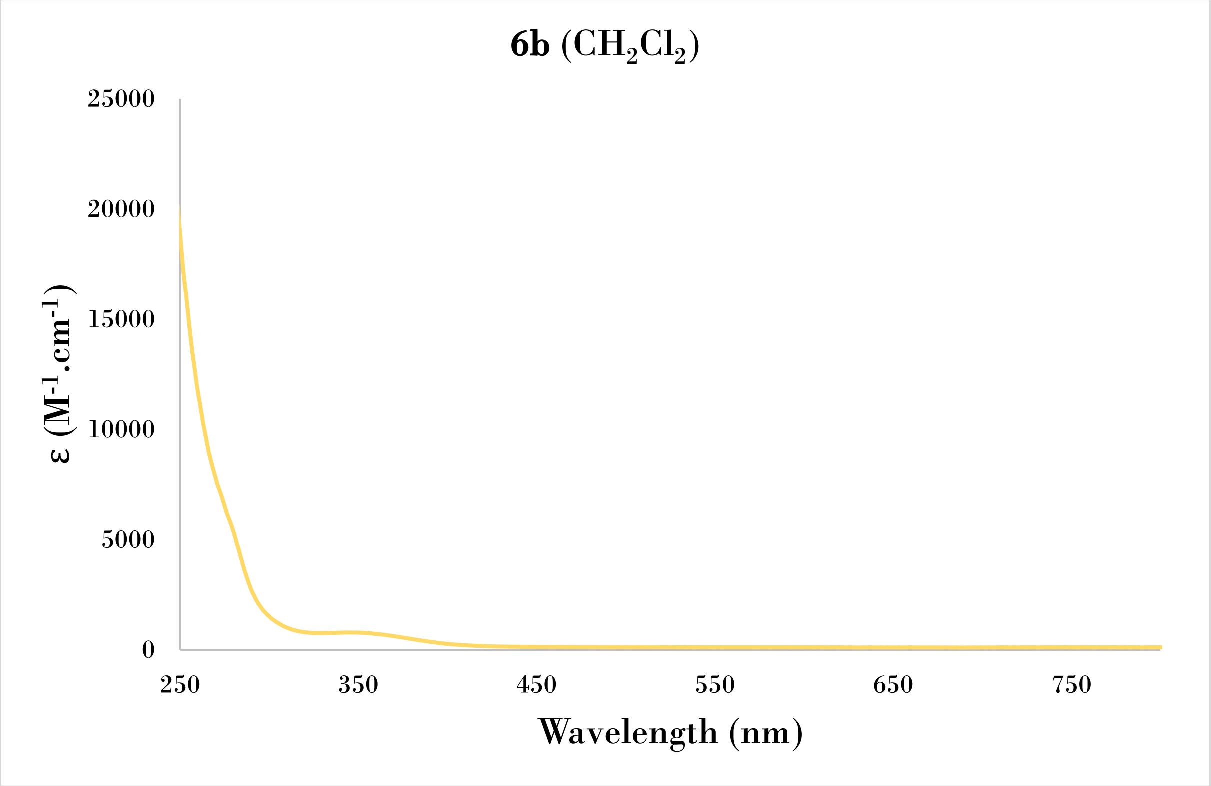

Figure S66: UV-vis (CH_2Cl_2, 0.1 mm cell)

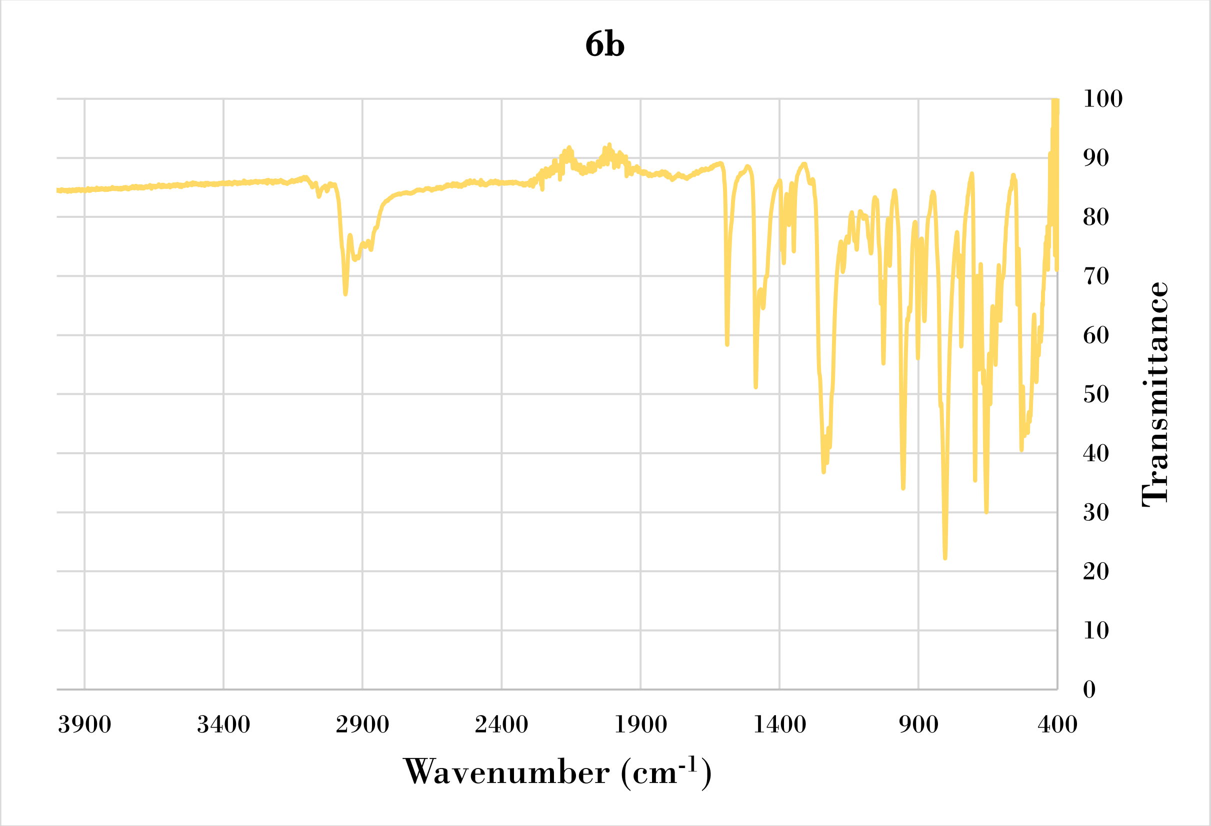

Figure S67: IR (ATR)

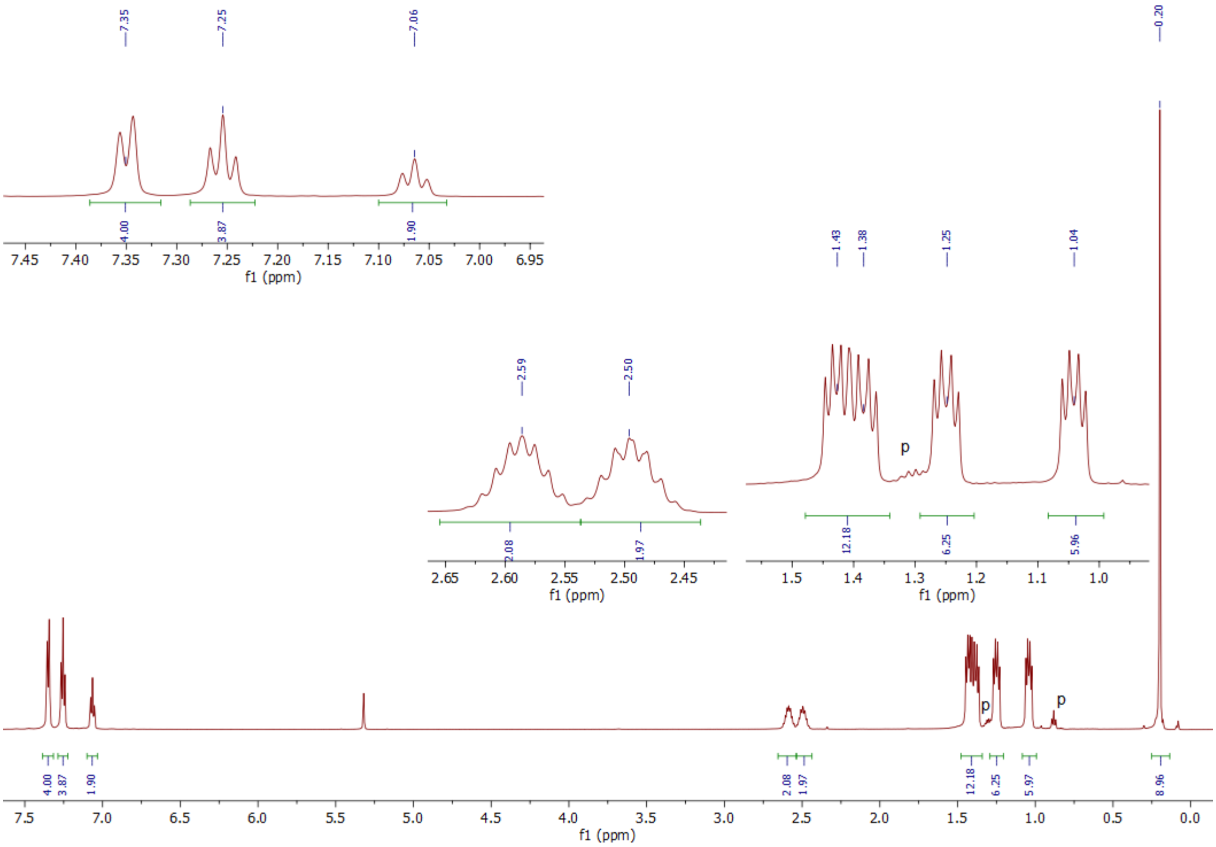

Figure S68: ^{1}H NMR (600 MHz, CD_2Cl_2, 298 K)(p: pentane)

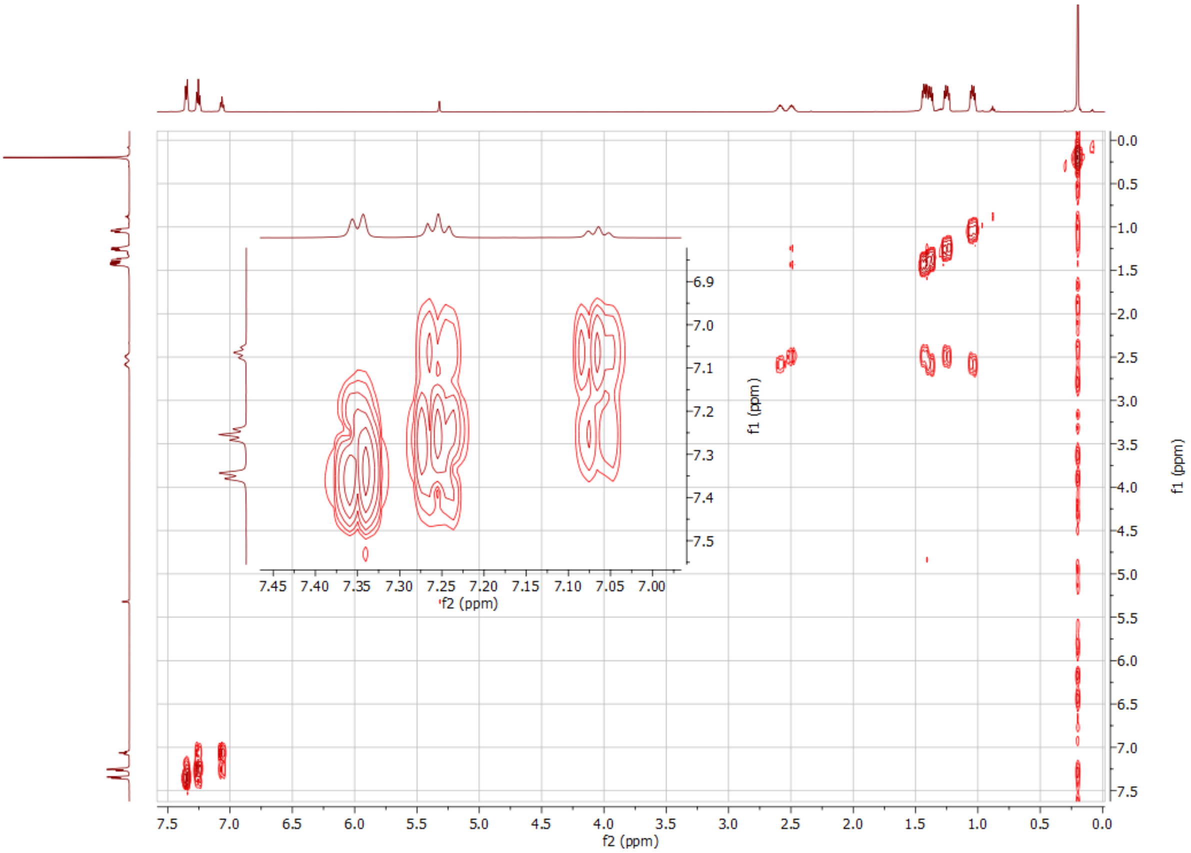

Figure S69: ^{1}H-^{1}H COSY (600 MHz, CD_2Cl_2, 298 K)(aromatic region)

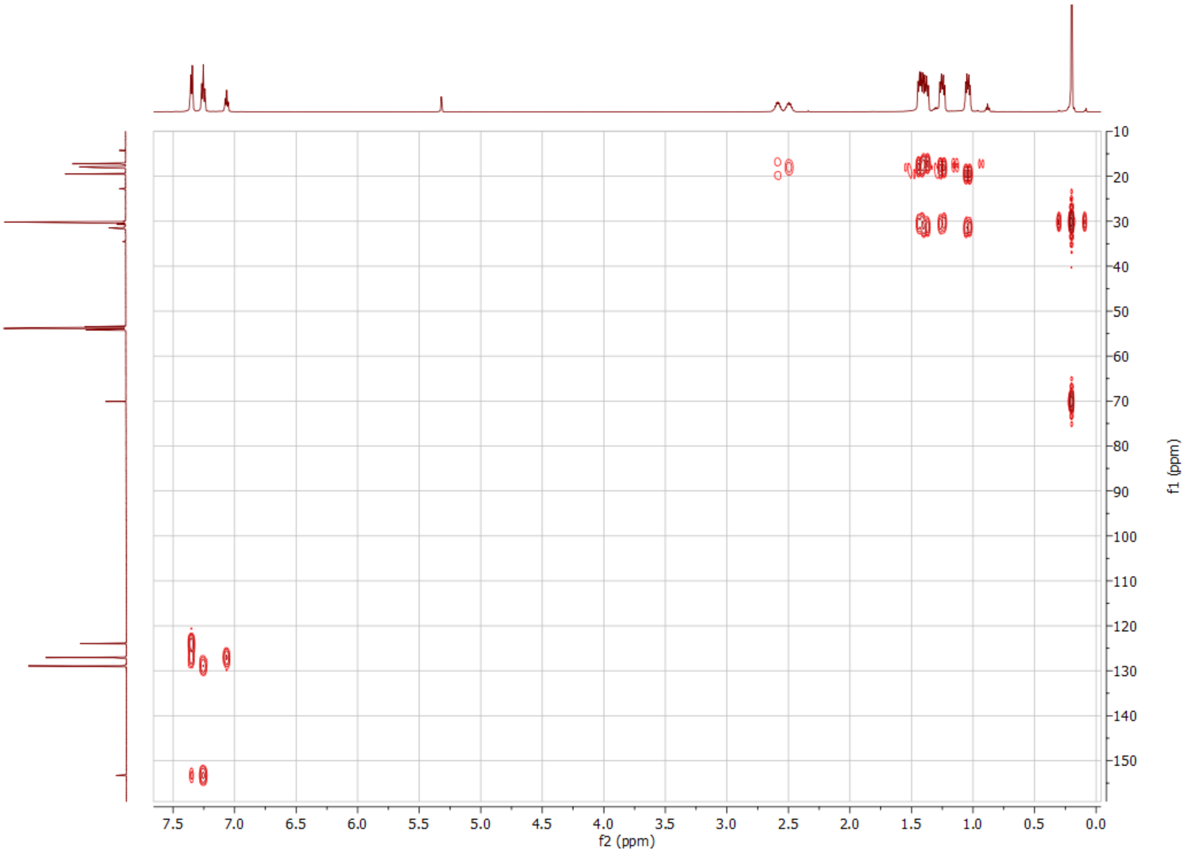

Figure S70: ^{1}H-^{13}C HMBC (600 MHz / 151 MHz, CD$_2$Cl$_2$, 298 K)(whole spectrum)

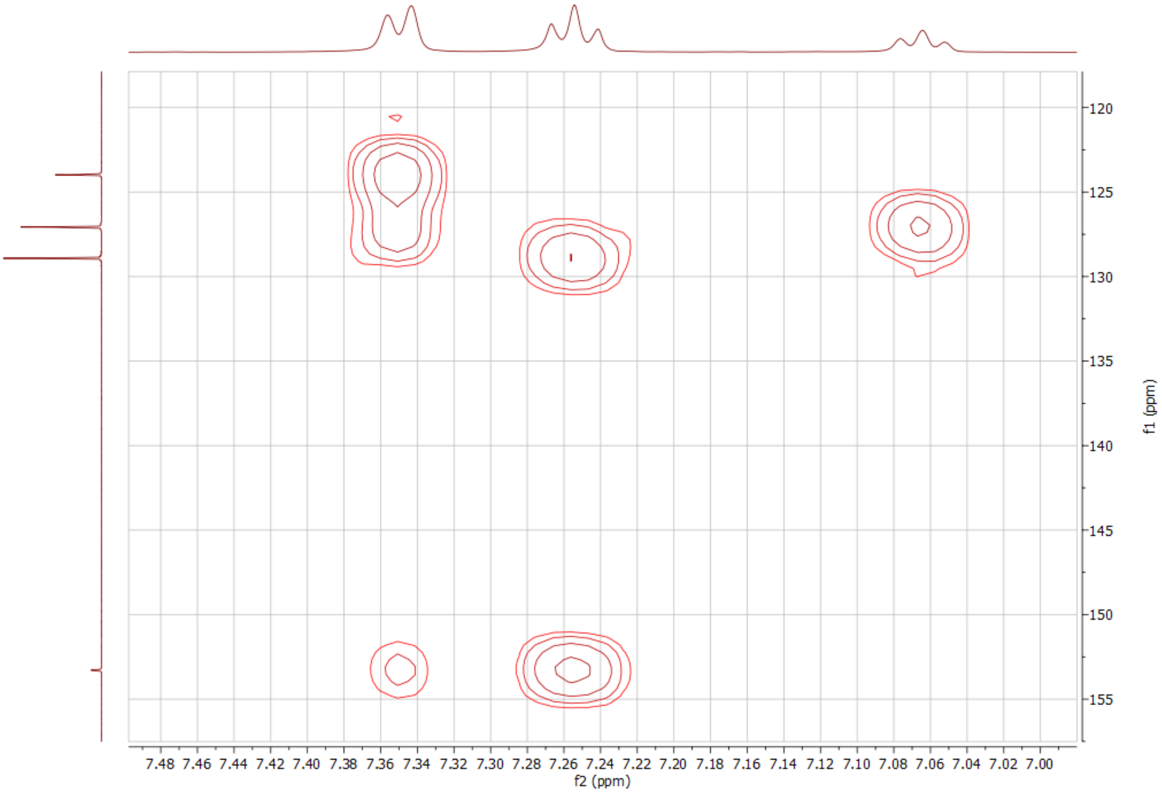

Figure S71: ^{1}H-^{13}C HMBC (600 MHz / 151 MHz, CD$_2$Cl$_2$, 298 K)(zoom)

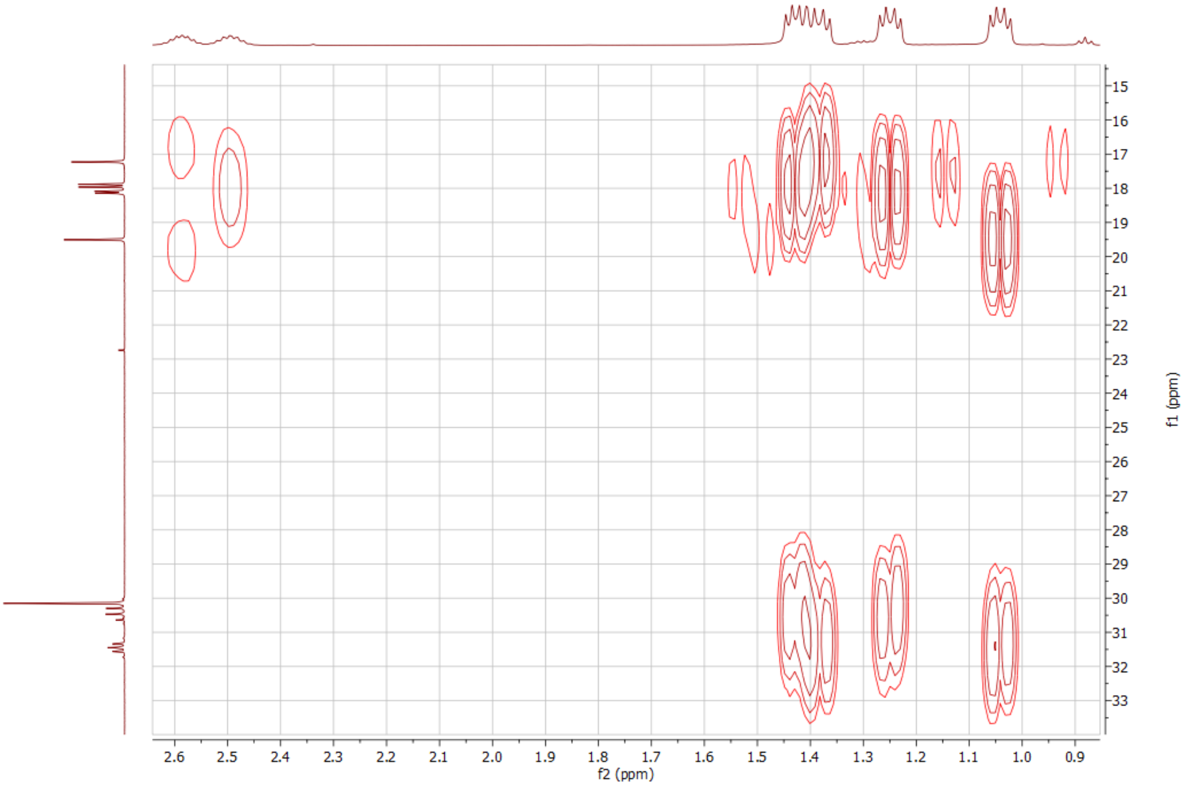

Figure S72: ^{1}H-^{13}C HMBC (600 MHz / 151 MHz, CD_2Cl_2, 298 K)(zoom)

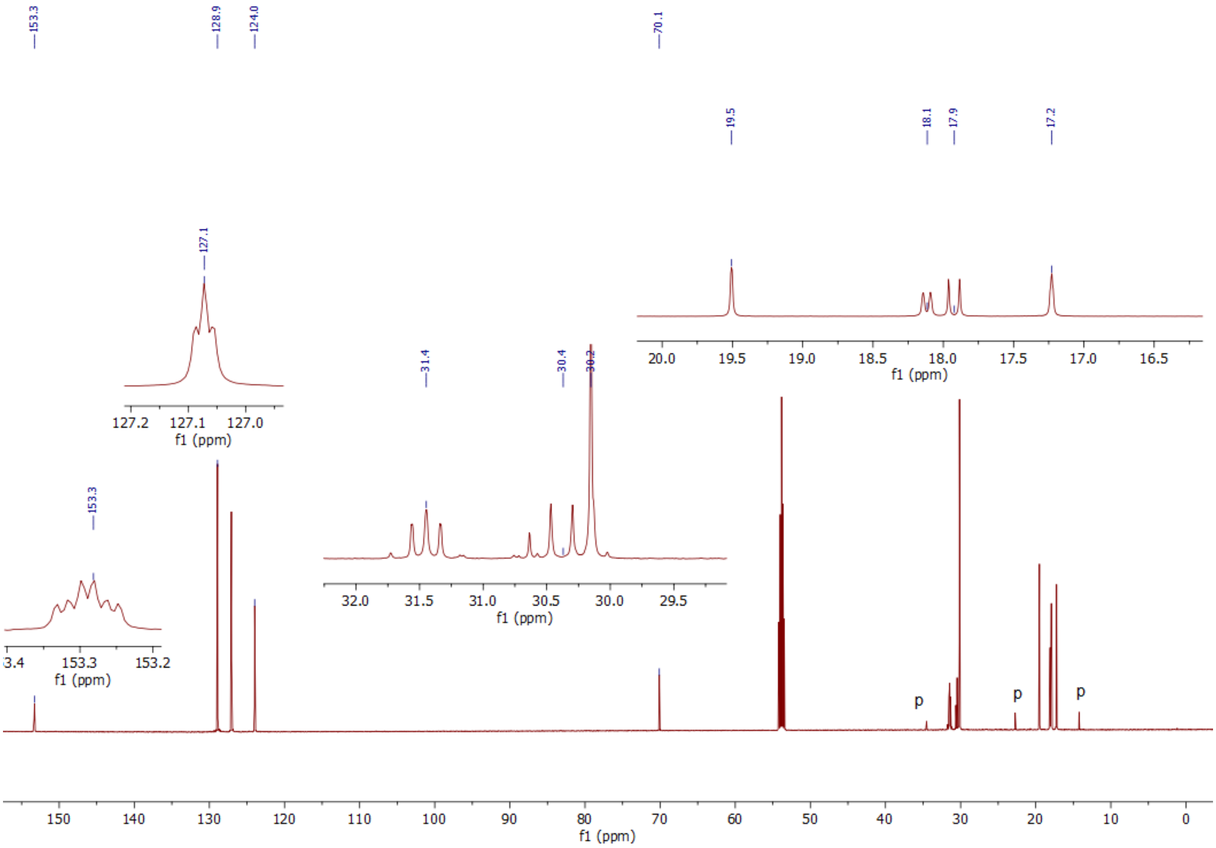

Figure S73: ^{13}C{^{1}H} NMR (151 MHz, CD_2Cl_2, 298 K)(p: pentane)

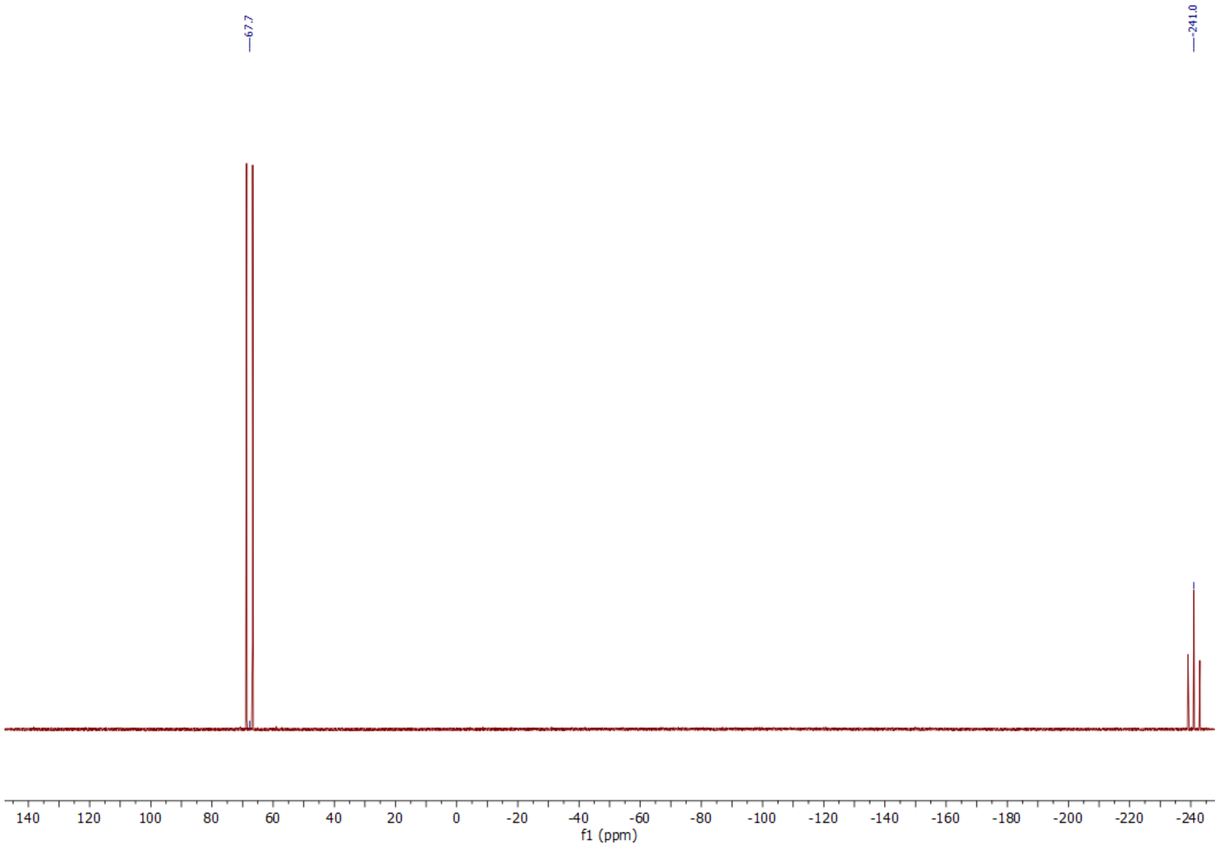

Figure S74: ^{31}**P{**^{1}**H} NMR (243 MHz,** CD_2Cl_2**, 298 K)**

Synthesis of complex ***7b***

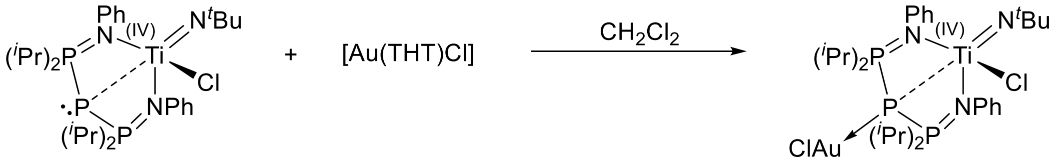

6b

7b *(0.300 g, 48%)*

In an Ar glovebox, [Au(THT)Cl] (240 mg, 0.750 mmol) and complex **6b** (451 mg, 0.750 mmol) were suspended in CH_2Cl_2 and the reaction mixture was stirred for 5 min, then evaporated to dryness outside of the glovebox. Upon returning to the glovebox, the resulting solid was stirred in 10 mL of pentane for 15 min. The suspension was filtered over a sintered glass frit, and the resulting solid was suspended in 5 mL of pentane and filtered, then dried on the frit. Analysis of the solid by ^{1}H NMR spectroscopy revealed the presence of residual THT, pentane and CH_2Cl_2. The solid was heated under vacuum in a warm bath (40 °C) for 1 h, thus drastically reducing the content of pentane and CH_2Cl_2, but not THT. The solid was stirred in 5 mL of pentane for 1 h, filtered over a sintered glass frit and dried on the frit, affording complex **7b** was obtained as a white powder (300 mg, yield 48%). The moderate yield is essentially due to the solubility of **7b** in pentane, since it is the only observable product by ^{1}H and ^{31}P NMR spectroscopy when the reaction is performed in situ on an analytical scale. Single crystals suitable for X-ray diffraction were grown by slow diffusion of pentane into a CH_2Cl_2 solution of **7b** at -20 °C. Complex **7b** slowly degrades in solutions of CD_2Cl_2 or C_6D_6 at room temperature, but can be stored for several months in the solid state at -20 °C under argon without significant degradation.

Elemental Analysis: calculated for $C_{28}H_{47}AuCl_2N_3P_3Ti$: C, 40.31; H, 5.68; N, 5.04. Found: C, 40.21; H, 5.60; N, 4.86.

UV-vis (CH_2Cl_2, 0.1 mm cell): λ_1 = 280 nm (shoulder, ε = 7500 $M^{-1}.cm^{-1}$), λ_2 = 377 nm (shoulder, ε = 900 $M^{-1}.cm^{-1}$).

IR (ATR): 3056 (w), 1587 (w), 1482 (m), 1433 (m), 1329 (w), 1306 (w), 1265 (w), 1214 (m), 1210 (m), 1189 (w), 1095 (m), 1093 (m), 1073 (w), 1026 (w), 1005 (w), 997 (w), 964 (s), 910 (w), 802 (m), 793 (s), 790 (s), 740 (s), 716 (m), 691 (m), 684 (s), 631 (s), 613 (m), 557 (m), 533 (s), 505 (vs), 491 (s), 459 (m), 423 (w) cm^{-1}.

^{1}H NMR (600 MHz, CD_2Cl_2, 298 K): δ = 7.36 (m, 4H, *o* of NPh), 7.31 (m, 4H, *m* of NPh), 7.14 (m, 2H, *p* of NPh), 2.90 (bs, 2H, C*H* of ^{i}Pr), 2.67 (m, 2H, C*H* of ^{i}Pr), 1.74 (bs, 6H, CH_3 of ^{i}Pr), 1.50 (m, 6H, CH_3 of ^{i}Pr), 1.35 (m, 6H, CH_3 of ^{i}Pr), 1.20 (m, 6H, CH_3 of ^{i}Pr), 0.08 (s, 9H, CH_3 of N^{t}Bu).

^{1}H-^{1}H COSY (600 MHz, CD_2Cl_2, 298 K)[selected cross-peaks]: 7.36 / 7.31 (*o* of NPh / *m* of NPh), 7.31 / 7.36 (*m* of NPh / *o* of NPh), 7.31 / 7.14 (*m* of NPh / *p* of NPh), 7.14 / 7.31 (*p* of NPh / *m* of NPh). Note: cross peaks between C*H* of ^{i}Pr and CH_3 of ^{i}Pr were observed, but only under the diagonal.

^{1}H-^{13}C HMBC (600 MHz / 151 MHz, CD_2Cl_2, 298 K)[selected cross-peaks]: 7.36 / 127.2 (*o* of NPh / *o* of NPh), 7.35 / 125.2 (*o* of NPh / *p* of NPh), 7.31 / 150.7 (*m* of NPh / *i* of NPh), 7.31 / 129.5 (*m* of NPh / *m* of NPh), 7.14 / 127.2 (*p* of NPh / *o* of NPh), 1.35 / 18.1 (CH_3 of ^{i}Pr / CH_3 of ^{i}Pr), 0.08 / 73.1 (CH_3 of N^{t}Bu / *C* of N^{t}Bu), 0.08 / 29.7 (CH_3 of N^{t}Bu / CH_3 of N^{t}Bu).

^{13}C{^{1}H} NMR (151 MHz, CD_2Cl_2, 298 K): δ = 150.7 (bs, *i* of NPh), 129.5 (bs, *m* of NPh), 127.2 (bs, *o* of NPh), 125.2 (bs, *p* of NPh), 73.1 (bs, *C* of N^{t}Bu), 31.5 (bs, *C*H of ^{i}Pr), 30.2 (bs, *C*H of ^{i}Pr), 29.7 (bs, CH_3 of N^{t}Bu), 20.0 (m, CH_3 of ^{i}Pr), 18.1 (m, CH_3 of ^{i}Pr), 17.7 (m, two overlapping CH_3 of ^{i}Pr).

^{31}P{^{1}H} NMR (243 MHz, CD_2Cl_2, 298 K): δ = 73.7 (d, $^{1}J_{PP}$ = 347 Hz, $P^{i}Pr_2$), -160.4 (t, $^{1}J_{PP}$ = 347 Hz, central *P*).

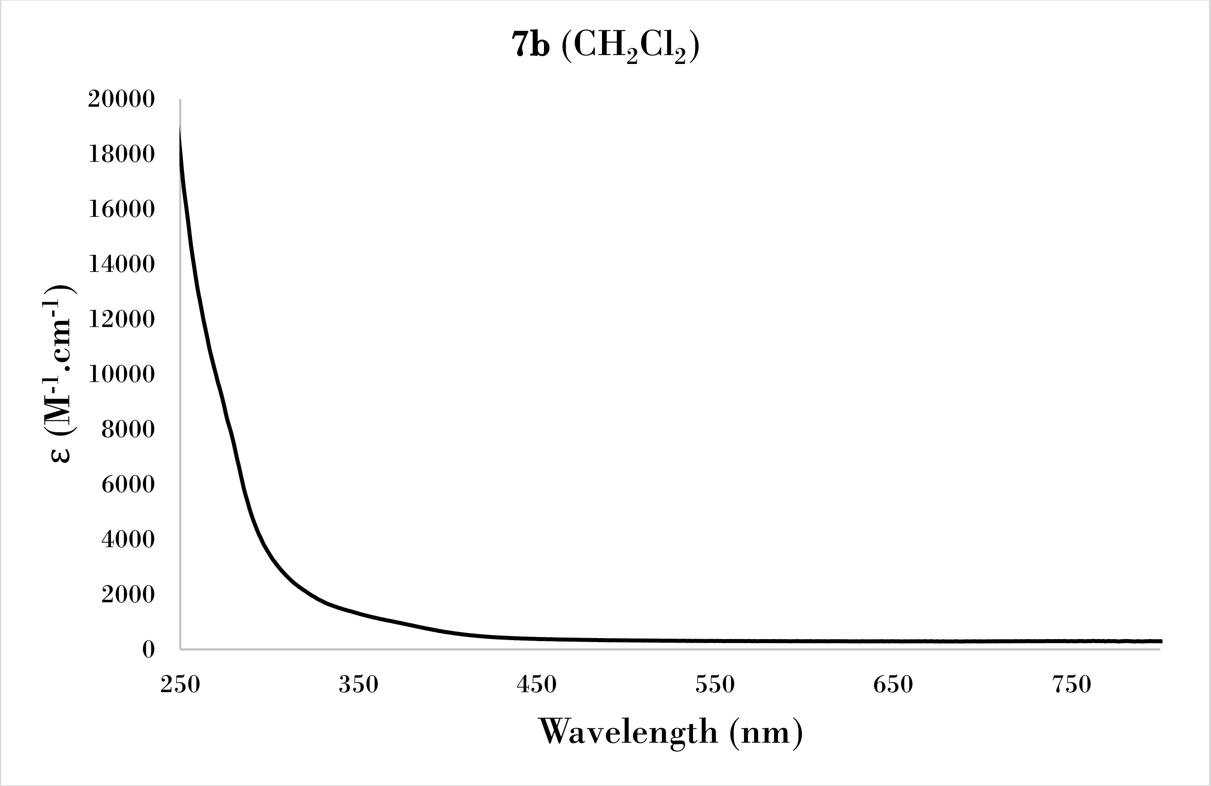

Figure S75: UV-vis (CH_2Cl_2, 0.1 mm cell)

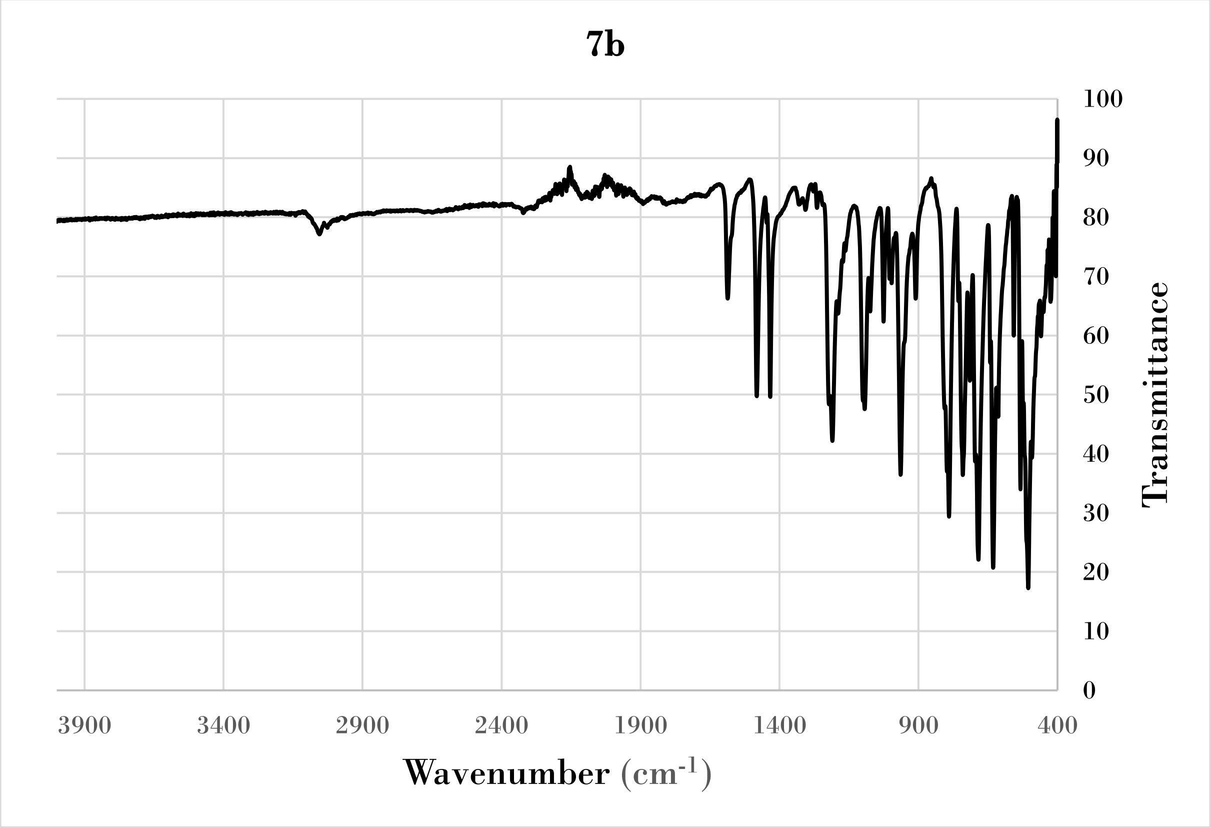

Figure S76: IR (ATR)

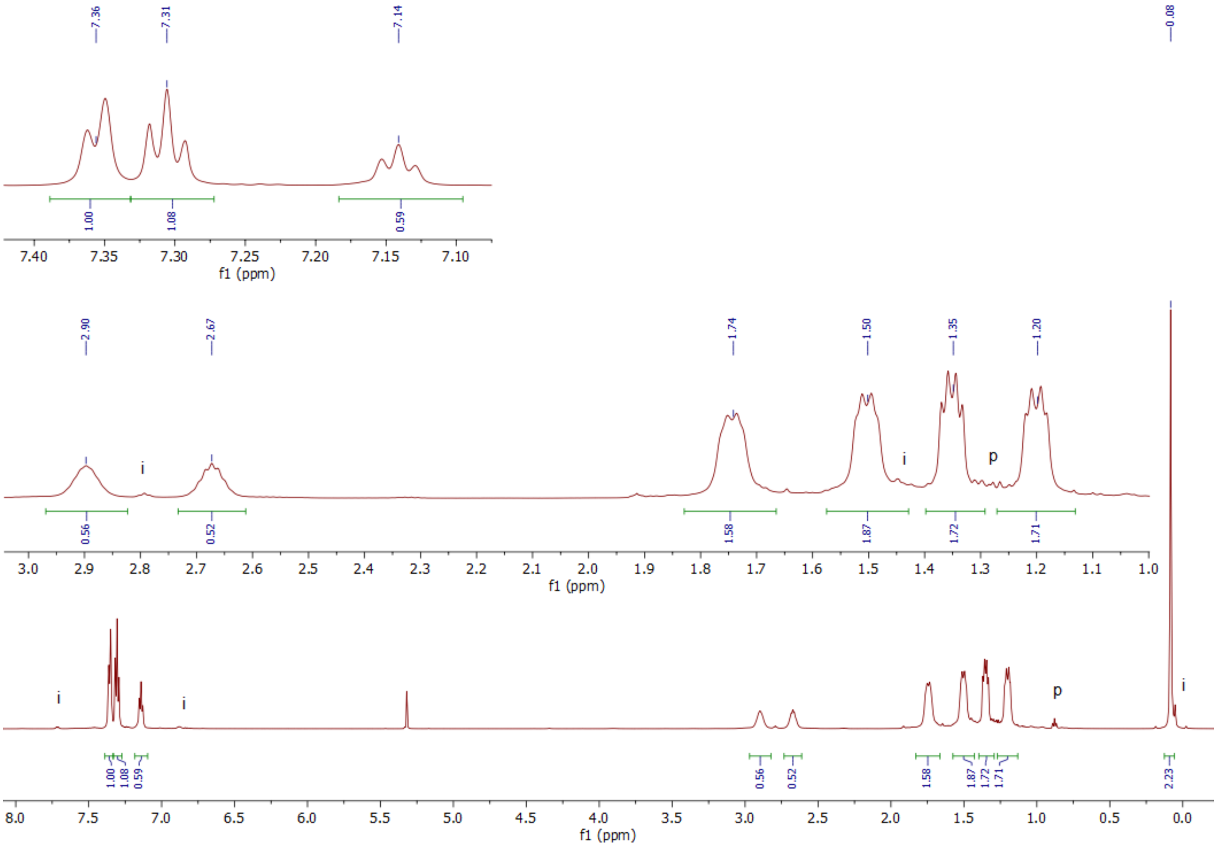

Figure S77: ^{1}H NMR (600 MHz, CD_2Cl_2, 298 K)(p: pentane; i: impurity)

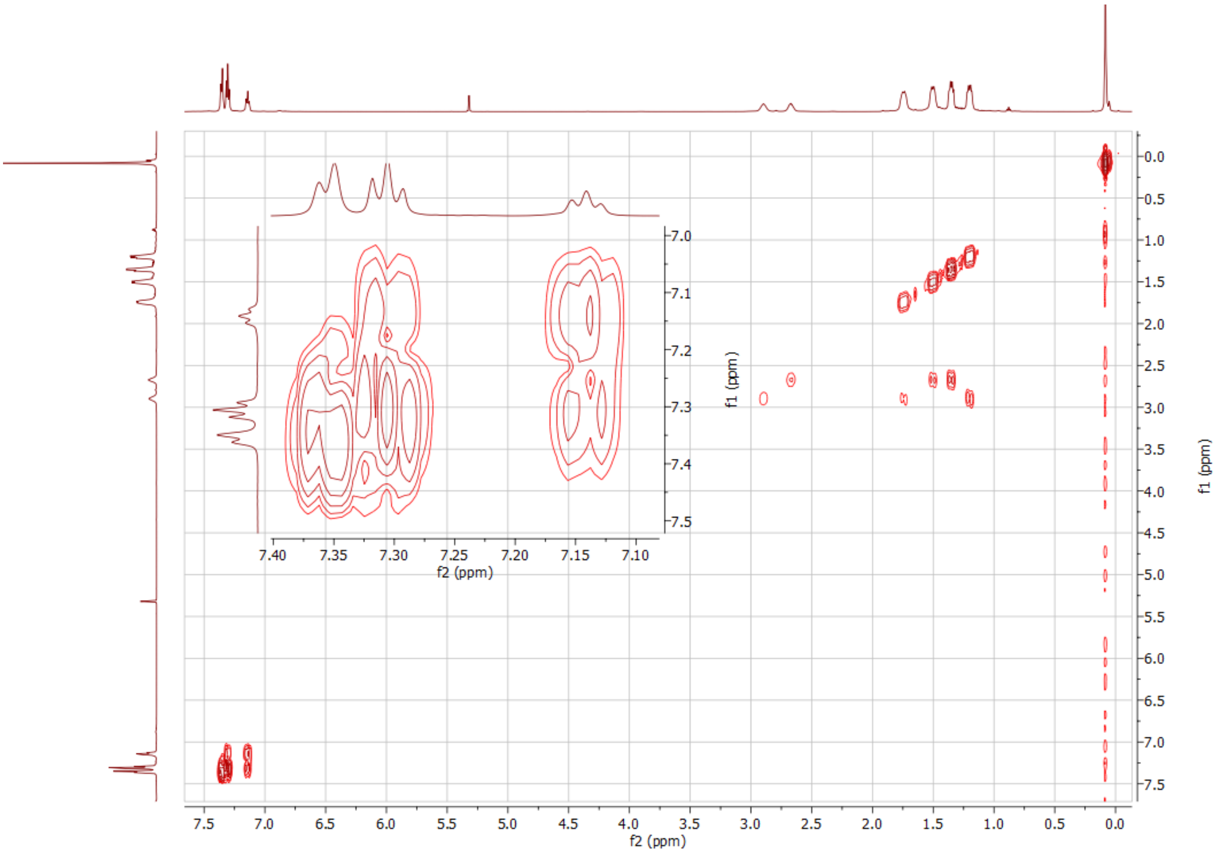

Figure S78: ^{1}H-^{1}H COSY (600 MHz, CD_2Cl_2, 298 K)(aromatic region)

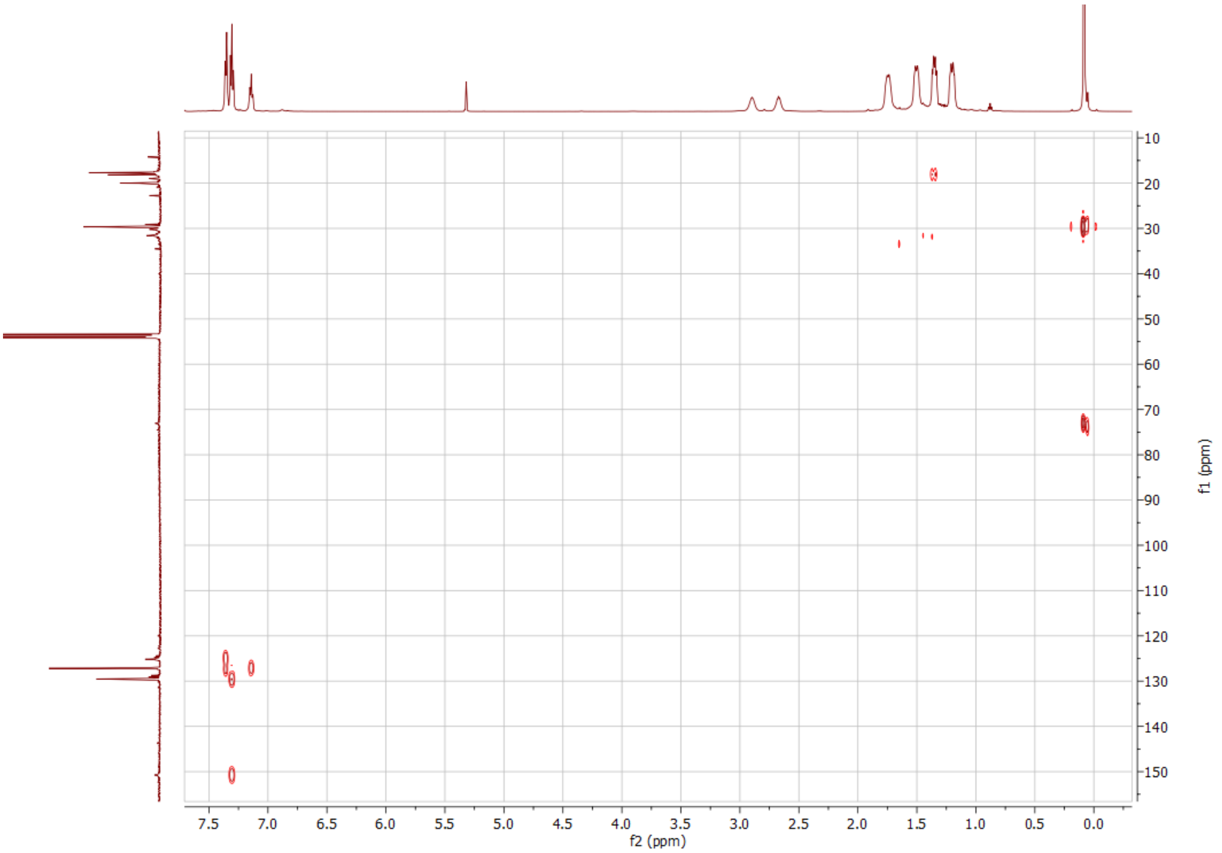

Figure S79: ^{1}H-^{13}C HMBC (600 MHz / 151 MHz, CD_2Cl_2, 298 K)(whole spectrum)

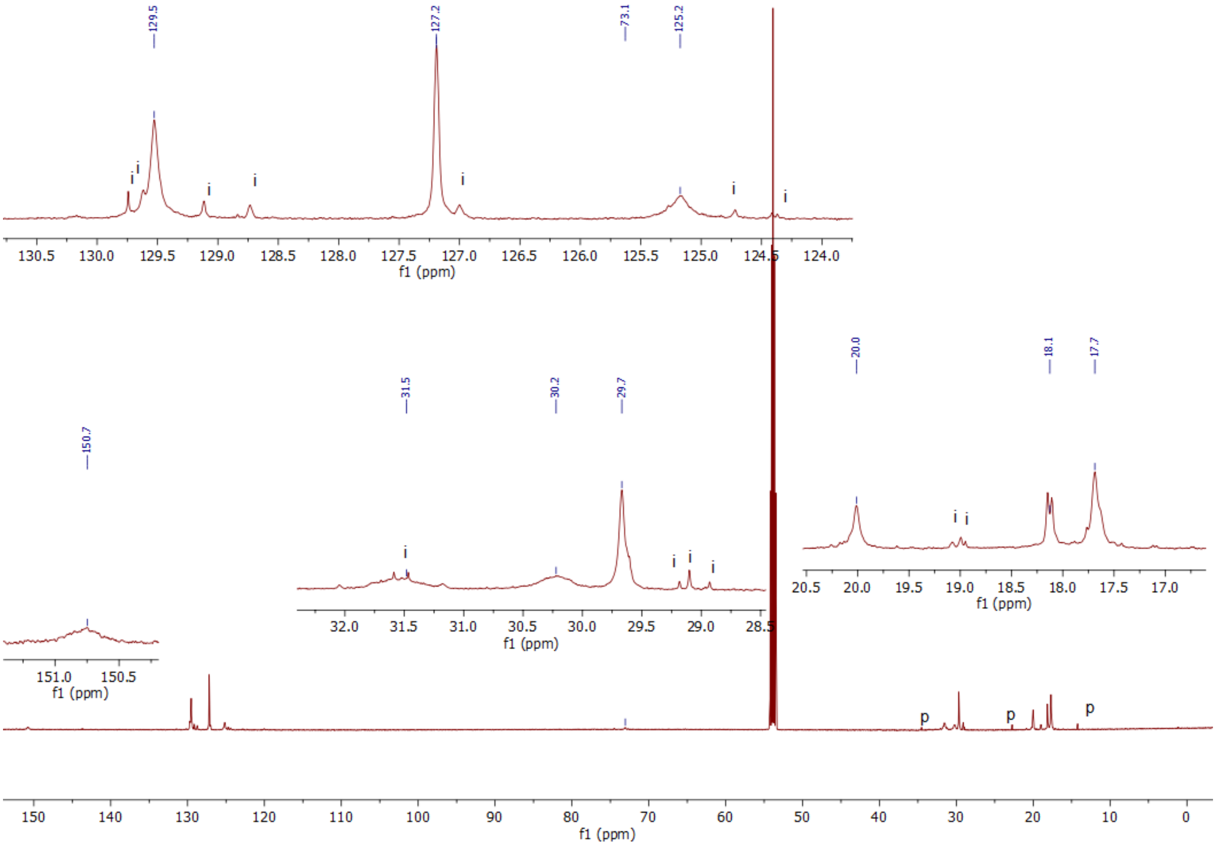

Figure S80: ^{13}C{^{1}H} NMR (151 MHz, CD_2Cl_2, 298 K)(p: pentane; i: impurity)

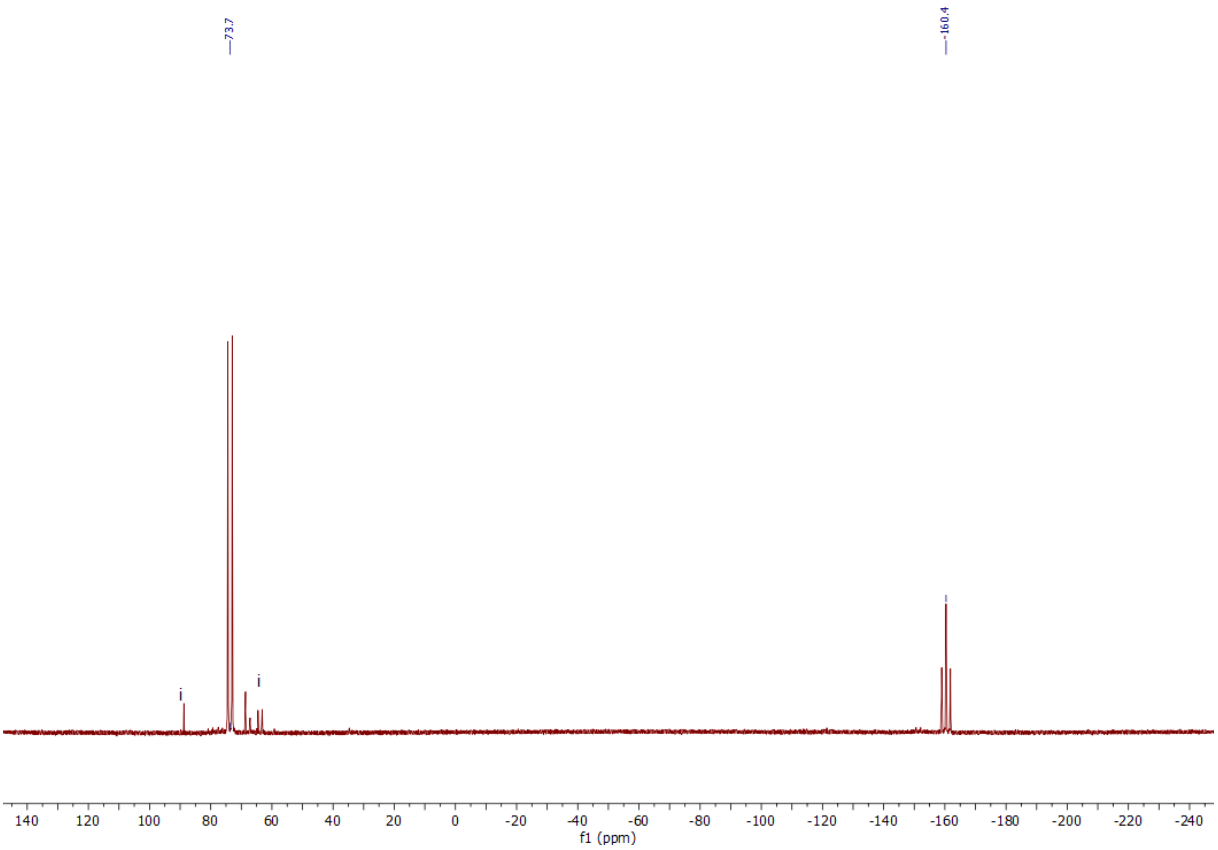

Figure S81: ^{31}**P{**^{1}**H} NMR (243 MHz, CD₂Cl₂, 298 K)(i: impurity)**

*Synthesis of complex **8b***

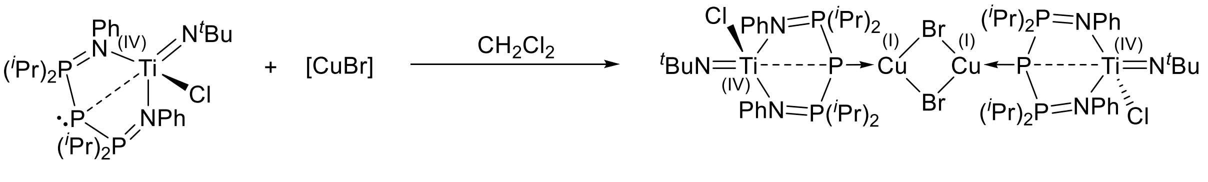

6b

8b *(0.152 g, 78%)*

In an Ar glovebox, [CuBr] (36 mg, 0.25 mmol) and complex **6b** (151 mg, 0.250 mmol) were suspended in CH_2Cl_2 and the reaction mixture was stirred for 10 min, during which it turned orange-brown. A small amount of white solid was removed by filtration over a pad of diatomaceous earth. The reaction mixture was then evaporated to dryness outside of the glovebox. Upon returning to the glovebox, the resulting solid was stirred in 10 mL of pentane, and the suspension was filtered over a sintered glass frit. The resulting solid was suspended three times in pentane (5 mL) and filtered, then dried on the frit. Complex **8b** was obtained as a light brown powder containing 50 mol% of pentane (152 mg, yield 78%). Single crystals suitable for X-ray diffraction were grown by slow diffusion of pentane into a CH_2Cl_2 solution of **8b** at -20 °C.

Elemental Analysis: calculated for $C_{28}H_{47}BrClCuN_3P_3Ti(C_5H_{12})_{0.5}$: C, 46.88; H, 6.84; N, 5.38. Found: C, 46.60; H, 7.30; N, 5.39.

UV-vis (CH_2Cl_2, 0.1 mm cell): λ_1 = 280 nm (shoulder, ε = 8100 $M^{-1}.cm^{-1}$), λ_2 = 366 nm (shoulder, ε = 1000 $M^{-1}.cm^{-1}$).

IR (ATR): 2960 (w), 2915 (w), 2866 (w), 1589 (m), 1483 (m), 1457 (b, w), 1446 (w), 1386 (w), 1364 (w), 1350 (w), 1248 (m), 1222 (s), 1132 (w), 1071 (w), 1036 (w), 1027 (m), 1004 (w), 960 (s), 903 (m), 882 (w), 873 (w), 808 (s), 743 (w), 695 (m), 677 (m), 651 (m), 625 (m), 605 (w), 527 (m), 511 (m), 497 (m), 483 (m), 461 (m) cm^{-1}.

^{1}H NMR (500 MHz, CD$_2$Cl$_2$, 290 K): δ = 7.37 (m, 4H, *o* of NPh), 7.30 (m, 4H, *m* of NPh), 7.13 (m, 2H, *p* of NPh), 2.81-2.65 (m, 4H, two overlapping CH of ^{i}Pr), 1.60 (m, 6H, CH_3 of ^{i}Pr), 1.49 (m, 6H, CH_3 of ^{i}Pr), 1.34 (m, 6H, CH_3 of ^{i}Pr overlapping with pentane signal), 1.10 (m, 6H, CH_3 of ^{i}Pr), 0.22 (s, 9H, CH_3 of N^{t}Bu).

^{1}H-^{1}H COSY (500 MHz, CD$_2$Cl$_2$, 290 K)[selected cross-peaks]: 7.37 / 7.30 (*o* of NPh / *m* of NPh), 7.30 / 7.37 (*m* of NPh / *o* of NPh), 7.30 / 7.13 (*m* of NPh / *p* of NPh), 7.13 / 7.30 (*p* of NPh / *m* of NPh). Note: cross peaks between CH of ^{i}Pr and CH_3 of ^{i}Pr were observed, but only under the diagonal.

^{1}H-^{13}C HMBC (500 MHz / 126 MHz, CD$_2$Cl$_2$, 290 K)[selected cross-peaks]: 7.37 / 151.5 (*o* of NPh / *i* of NPh), 7.37 / 126.8 (*o* of NPh / *o* of NPh), 7.37 / 125.0 (*o* of NPh / *p* of NPh), 7.30 / 151.5 (*m* of NPh / *i* of NPh), 7.30 / 129.4 (*m* of NPh / *m* of NPh), 7.30 / 125.0 (*m* of NPh / *p* of NPh), 7.13 / 126.9 (*p* of NPh / *o* of NPh), 2.81-2.65 / 19.8 (CH of ^{i}Pr / CH$_3$ of ^{i}Pr), 1.60 / 30.5 (CH_3 of ^{i}Pr / CH of ^{i}Pr), 1.60 / 18.0 (CH_3 of ^{i}Pr / CH$_3$ of ^{i}Pr), 1.49 / 31.2 (CH_3 of ^{i}Pr / CH of ^{i}Pr), 1.49 / 17.6 (CH_3 of ^{i}Pr / CH$_3$ of ^{i}Pr), 1.34 / 30.4 (CH_3 of ^{i}Pr / CH of ^{i}Pr), 1.34 / 19.0 (CH_3 of ^{i}Pr / CH$_3$ of ^{i}Pr), 1.10 / 31.2 (CH_3 of ^{i}Pr / CH of ^{i}Pr), 1.10 / 19.8 (CH_3 of ^{i}Pr / CH$_3$ of ^{i}Pr), 0.22 / 72.3 (CH_3 of N^{t}Bu / C of N^{t}Bu), 0.22 / 30.0 (CH_3 of N^{t}Bu / CH$_3$ of N^{t}Bu).

^{13}C{^{1}H} NMR (126 MHz, CD$_2$Cl$_2$, 290 K): δ = 151.5 (bs, *i* of NPh), 129.4 (s, *m* of NPh), 126.9 (m, *o* of NPh), 125.0 (s, *p* of NPh), 72.3 (s, C of N^{t}Bu), 31.2 (m, CH of ^{i}Pr), 30.5 (m, CH of ^{i}Pr), 30.0 (s, CH$_3$ of N^{t}Bu), 19.8 (m, CH$_3$ of ^{i}Pr), 19.0 (m, CH$_3$ of ^{i}Pr), 18.0 (m, CH$_3$ of ^{i}Pr), 17.6 (m, CH$_3$ of ^{i}Pr).

^{31}P{^{1}H} NMR (202 MHz, CD$_2$Cl$_2$, 290 K): δ = 70.2 (d, $^1J_{\mathrm{PP}}$ = 414 Hz, P^iPr$_2$), -212.8 (bs, central P).

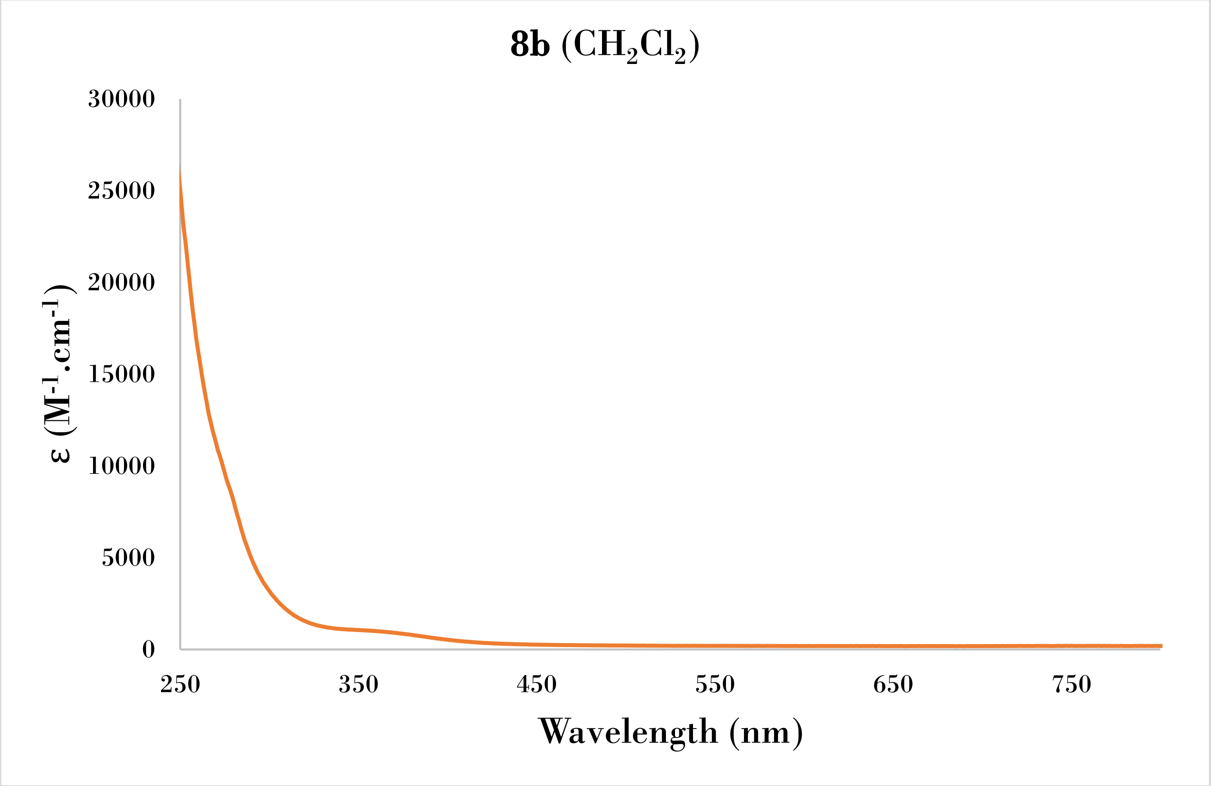

Figure S82: UV-vis (CH_2Cl_2, 0.1 mm cell)

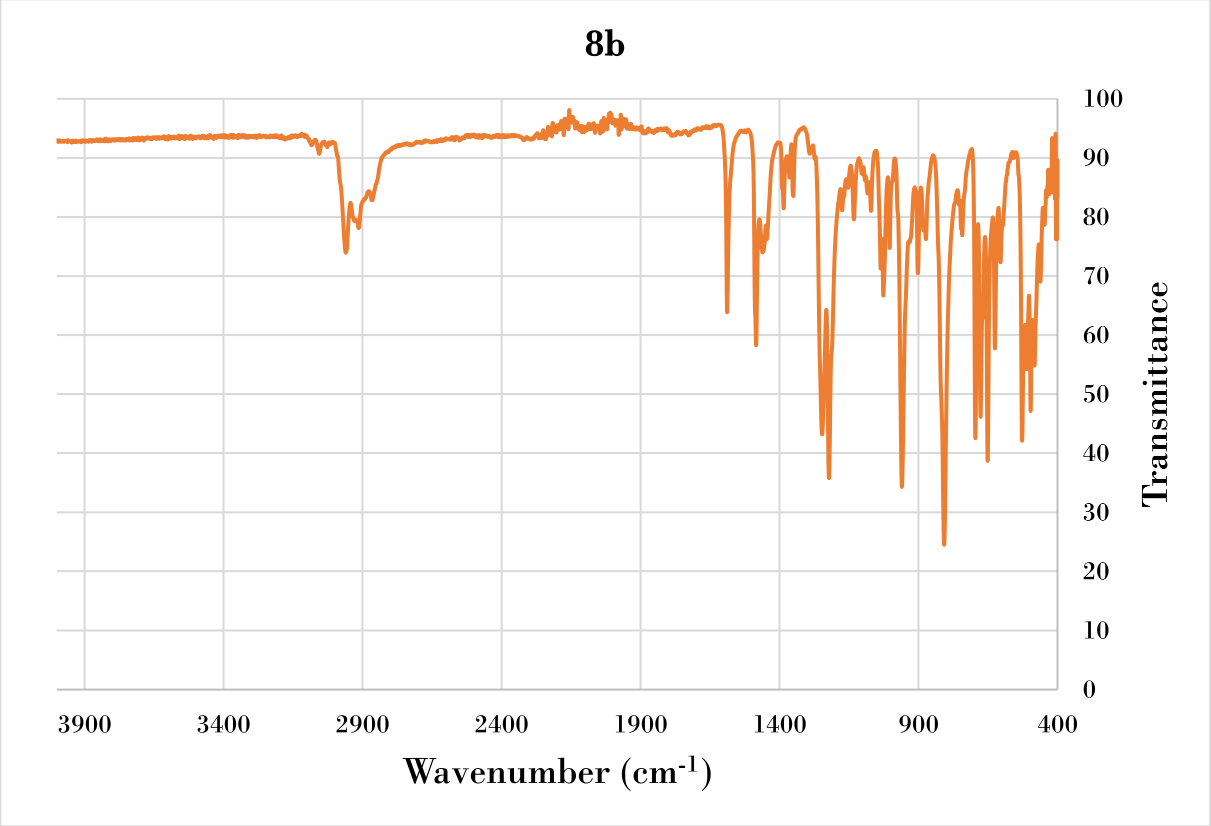

Figure S83: IR (ATR)

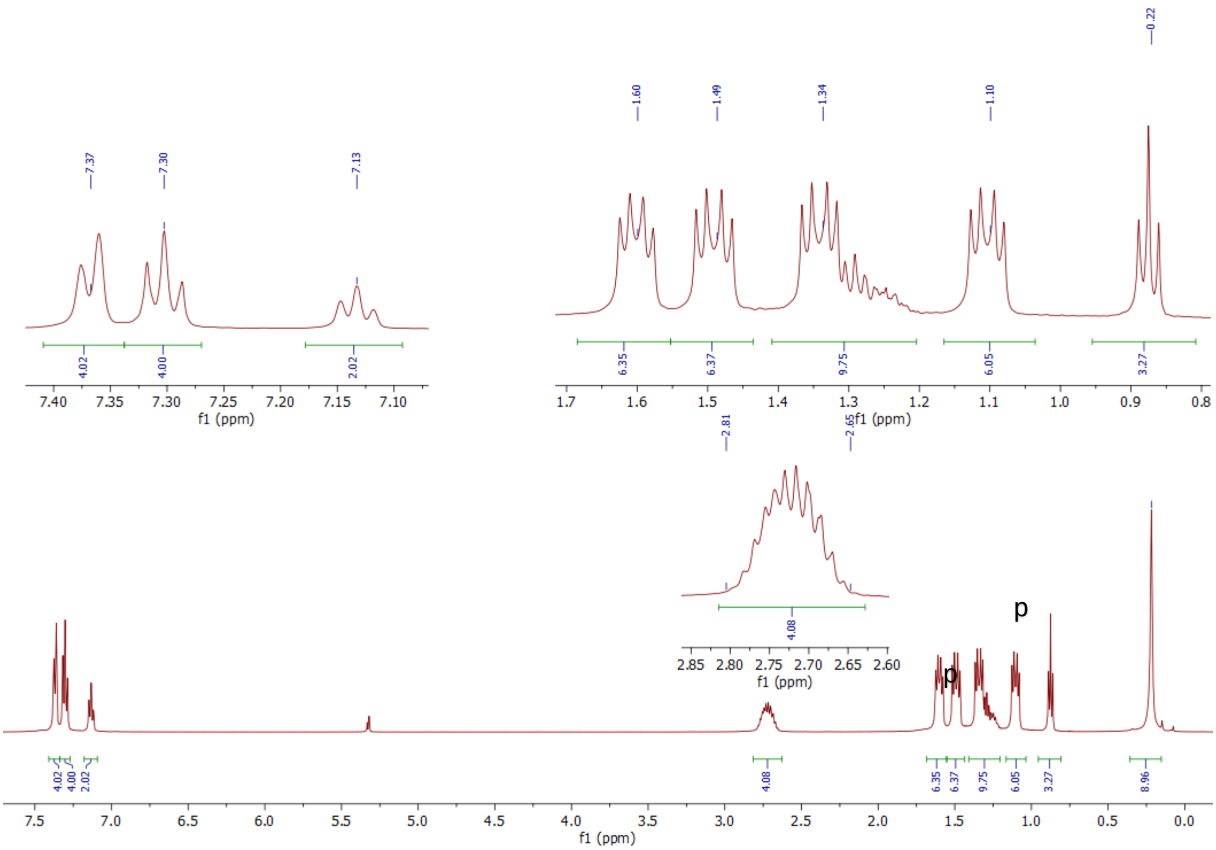

Figure S84: ^{1}H NMR (500 MHz, CD_2Cl_2, 290 K)(p: pentane)

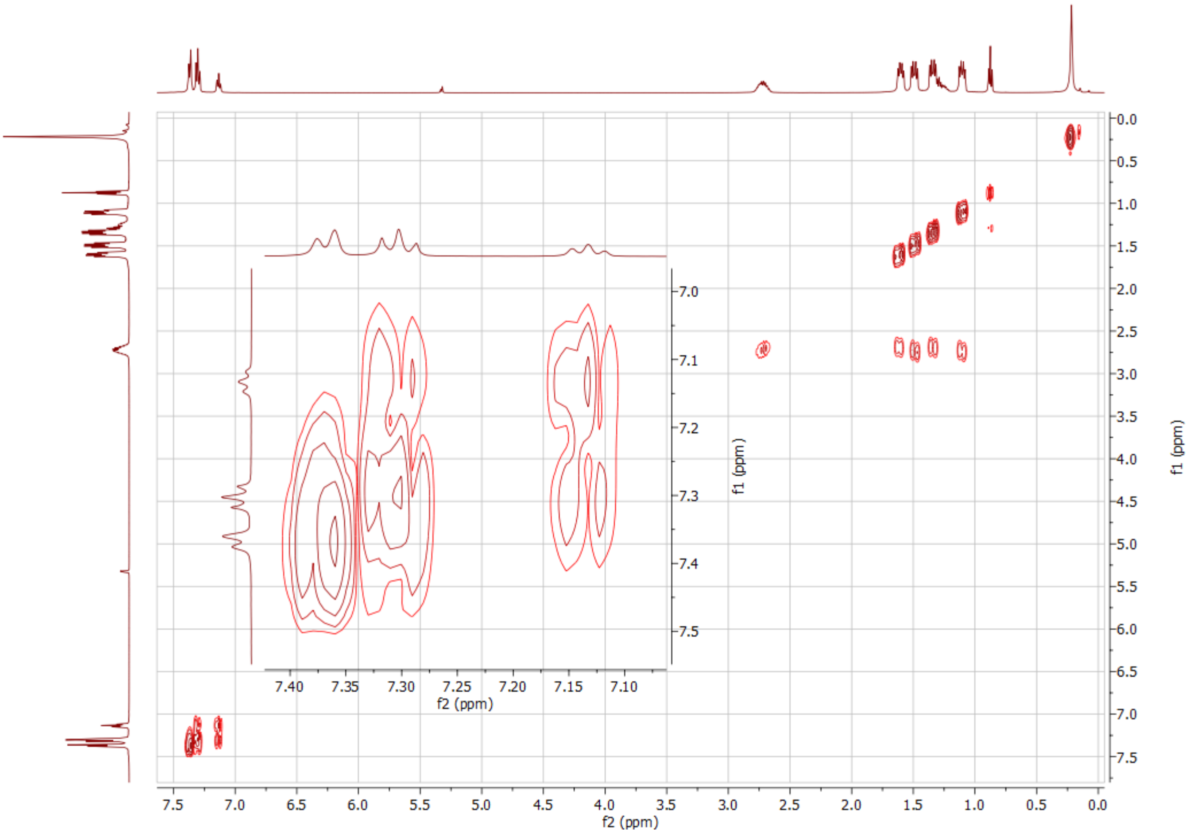

Figure S85: ^{1}H-^{1}H COSY (500 MHz, CD_2Cl_2, 290 K)(aromatic region)

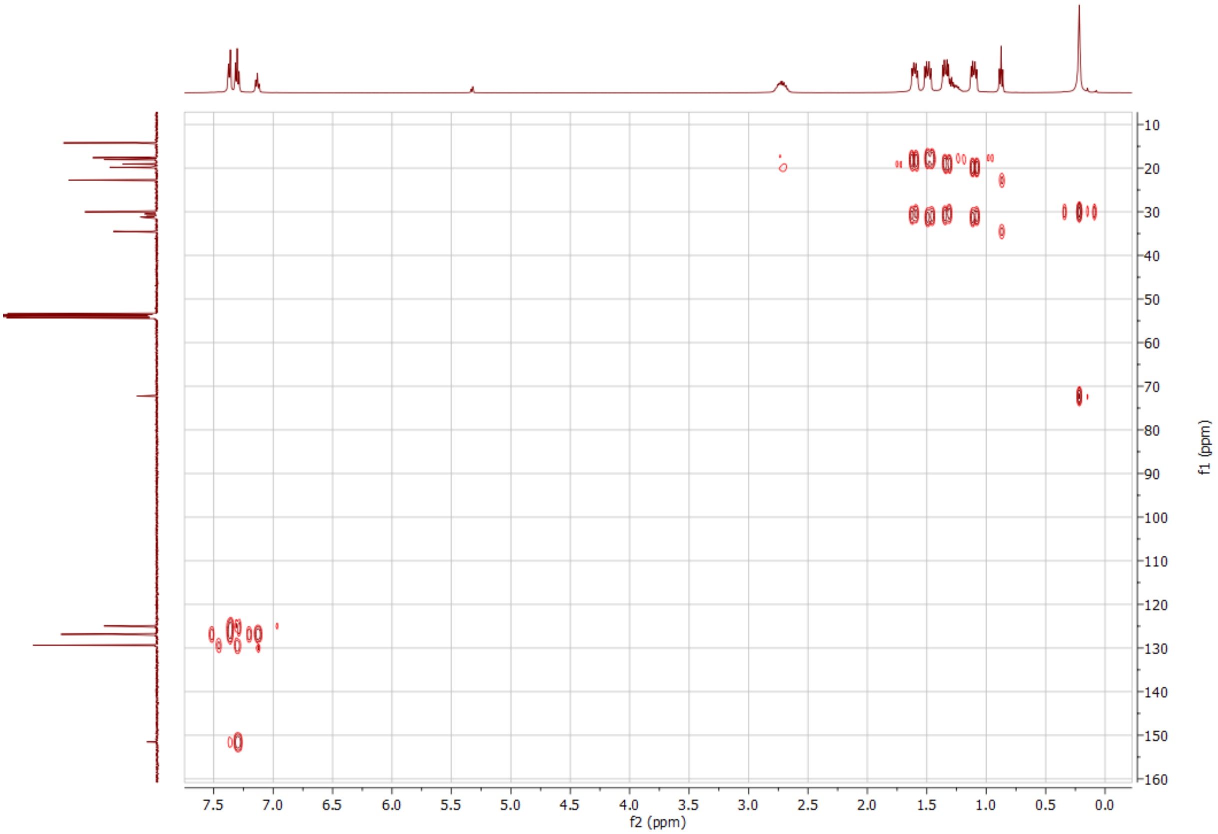

Figure S86: ^{1}H-^{13}C HMBC (500 MHz / 126 MHz, CD_2Cl_2, 290 K)(whole spectrum)

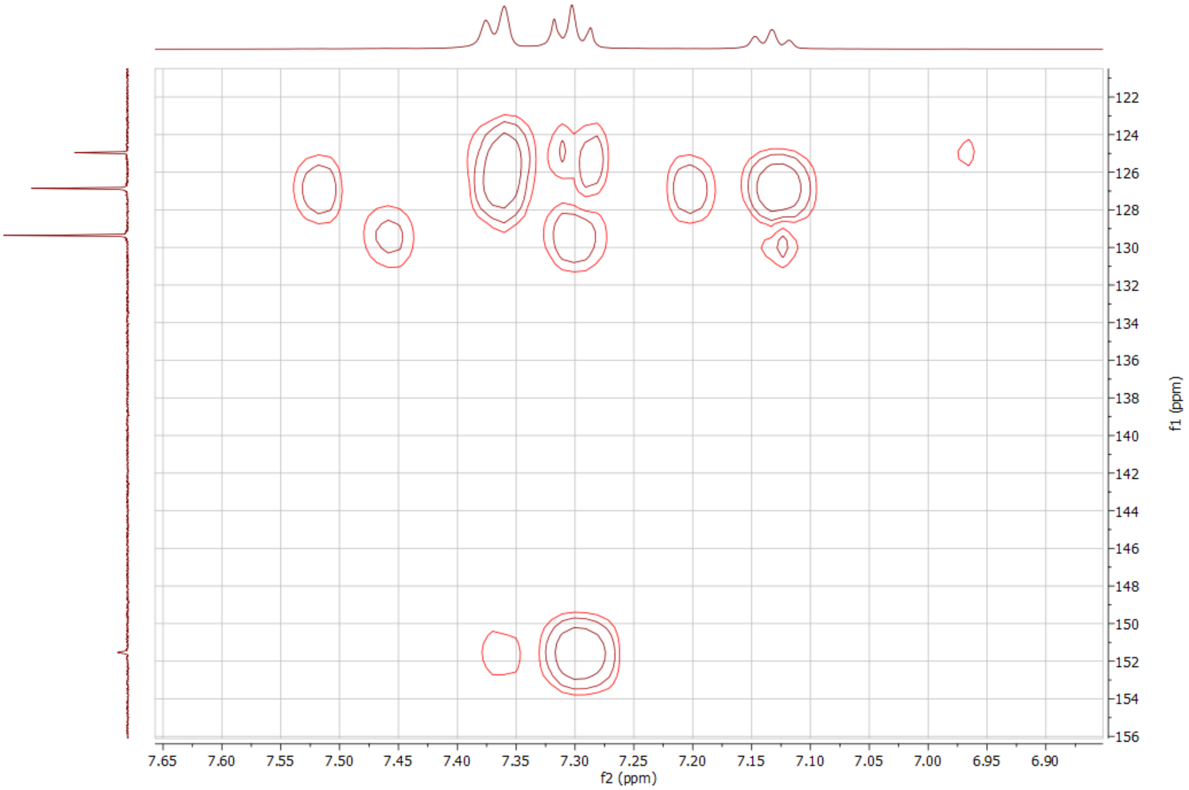

Figure S87: ^{1}H-^{13}C HMBC (500 MHz / 126 MHz, CD_2Cl_2, 290 K)(zoom)

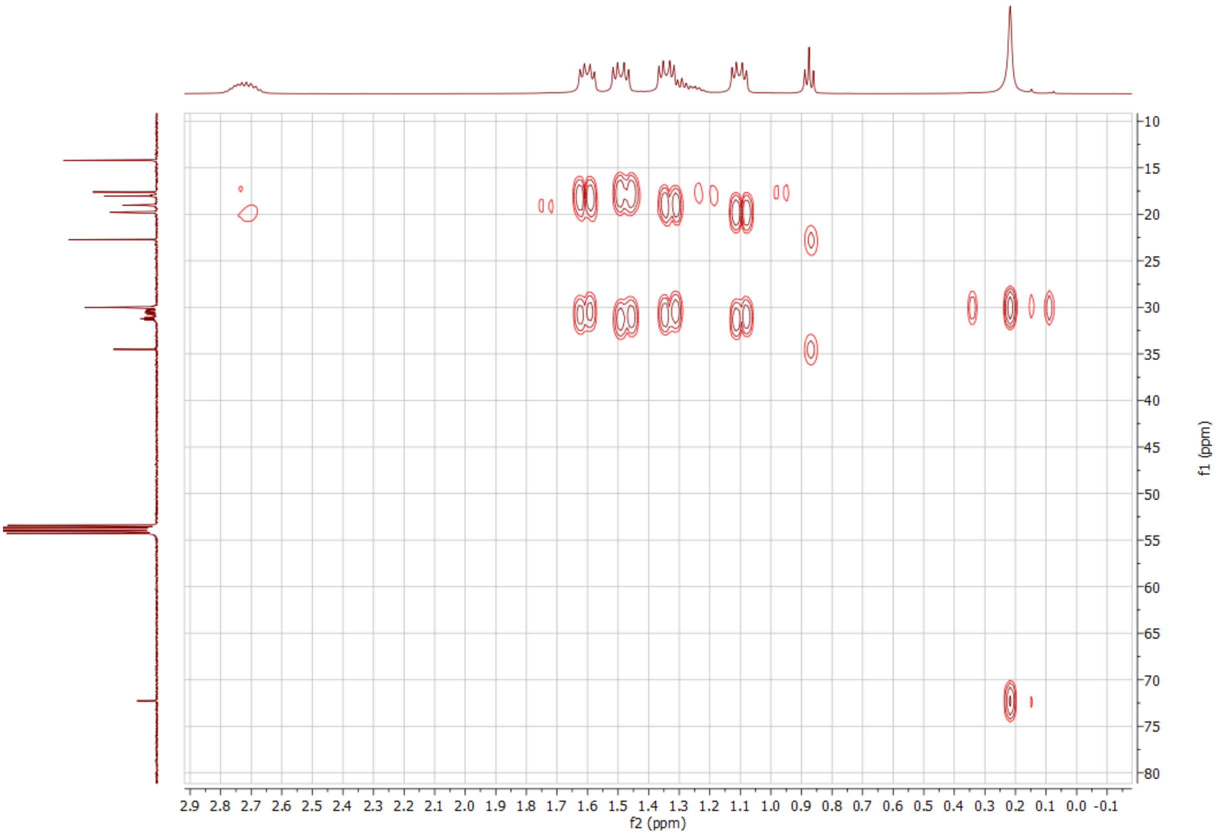

Figure S88: ^{1}H-^{13}C HMBC (500 MHz / 126 MHz, CD$_2$Cl$_2$, 290 K)(zoom)

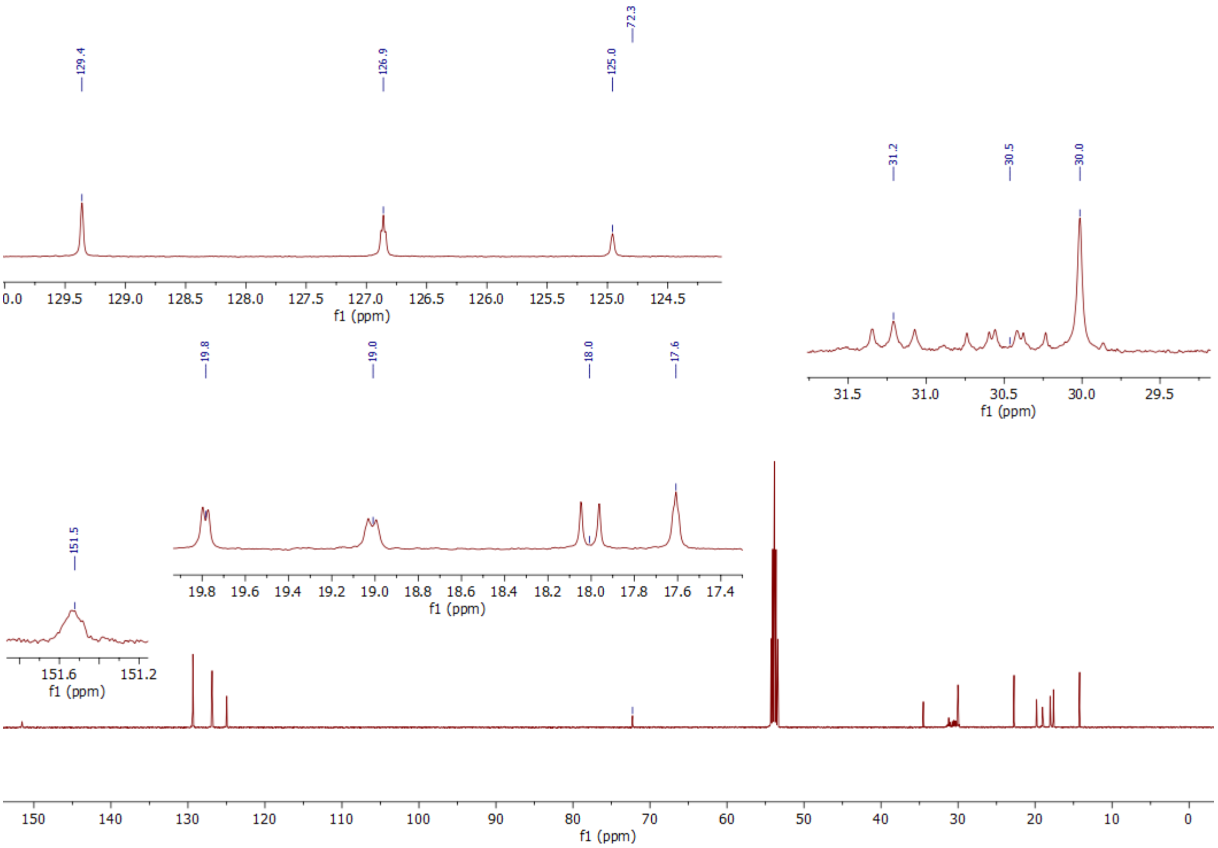

Figure S89: ^{13}C{^{1}H} NMR (126 MHz, CD$_2$Cl$_2$, 290 K)(p: pentane)

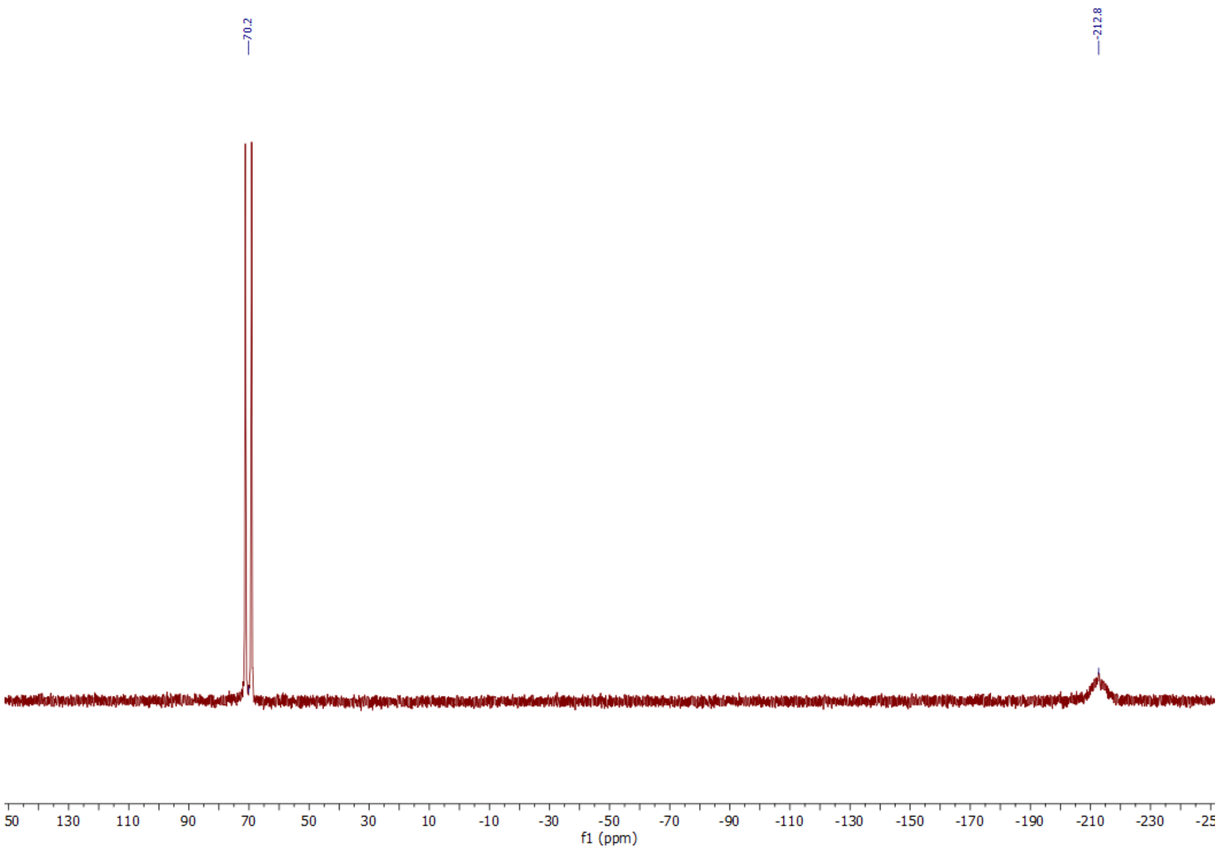

Figure S90: $^{31}P\{^1H\}$ NMR (202 MHz, CD_2Cl_2, 290 K)

*Synthesis of complex **9b***

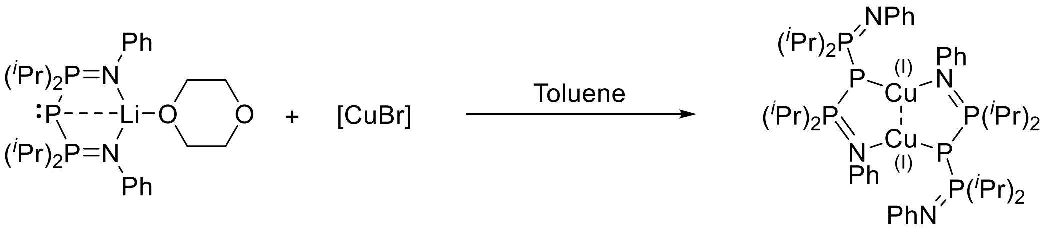

2b **9b** *(0.121 g, 67%)*

In an Ar glovebox, proligand **2b** (200 mg, 0.33 mmol) and [CuBr] (48 mg, 0.33 mmol) were suspended in toluene (25 mL). The resulting beige slurry was stirred at room temperature for 5 days. Volatiles were removed under vacuum outside of the glovebox. The resulting beige solid was suspended in 20 mL of CH_2Cl_2 and the suspension was filtered over a pad of diatomaceous earth. The filtrate was evaporated to dryness. The solid residue was stirred in 20 mL of pentane overnight. Upon returning in the glovebox, the yellow slurry was filtered over a sintered glass frit and dried under vacuum, yielding complex **9b** as a white powder containing 80 mol% of pentane (121 mg, yield 67%). Single crystals suitable for X-ray diffraction were obtained by slow diffusion of pentane into a CH_2Cl_2 solution of **9b** at -20 °C.

Elemental Analysis: calculated for $C_{48}H_{76}Cu_2N_4P_6(C_5H_{12})_{0.8}$: C, 57.84; H, 7.99; N, 5.19. Found: C, 57.42; H, 8.13; N, 4.95.

UV-vis (Toluene, 10 mm cell): λ_1 = 339 nm (local maximum, ε = 16000 $M^{-1}.cm^{-1}$).

UV-vis (CH_2Cl_2, 10 mm cell): λ_1 = 269 nm (local maximum, ε = 43000 $M^{-1}.cm^{-}$), 337 nm (local maximum, ε = 18000 $M^{-1}.cm^{-1}$).

UV-vis (THF, 10 mm cell): λ_1 = 264 nm (local maximum, ε = 63000 $M^{-1}.cm^{-}$), 339 nm (local maximum, ε = 19000 $M^{-1}.cm^{-1}$).

IR (ATR): 2957 (w), 2925 (w), 2866 (w), 1585 (m), 1557 (w), 1485 (s), 1472 (s), 1386 (w), 1335 (s), 1272 (m), 1255 (s), 1235 (s), 1171 (m), 1147 (w), 1088 (b, w), 1069 (m), 1051 (m), 1030 (s), 1008 (m), 1001 (m), 968 (s), 923 (w), 900 (w), 875 (m), 800 (s), 746 (s), 694 (s), 683 (s), 673 (s), 637 (m), 621 (m), 562 (w), 524 (s), 496 (s) cm^{-1}.

^{1}H NMR (500 MHz, CD_2Cl_2, 298 K): δ = 7.05 (m, 8H, *m* of NPh), 6.86 (m, 8H, *o* of NPh), 6.71 (m, 4H, *p* of NPh), 2.62 (m, 8H, two overlapping C*H* of ^{i}Pr), 1.29 (m, 48H, CH_3 of ^{i}Pr overlapping with pentane signal).

^{1}H-^{1}H COSY (500 MHz, CD_2Cl_2, 298 K)[selected cross-peaks]: 7.05 / 6.86 (*m* of NPh / *o* of NPh), 7.05 / 6.71 (*m* of NPh / *p* of NPh), 6.86 / 7.05 (*o* of NPh / *m* of NPh), 6.71 / 7.05 (*p* of NPh / *m* of NPh). Note: cross peaks between C*H* of ^{i}Pr and CH_3 of ^{i}Pr were observed, but only under the diagonal.

^{1}H-^{13}C HMBC (500 MHz / 126 MHz, CD_2Cl_2, 298 K)[selected cross-peaks]: 7.05 / 151.9 (*m* of NPh / *i* of NPh), 7.05 / 129.0 (*m* of NPh / *m* of NPh), 6.86 / 125.0 (*o* of NPh / *o* of NPh), 6.86 / 119.1 (*o* of NPh / *p* of NPh), 6.71 / 125.0 (*p* of NPh / *o* of NPh), 2.60 / 18.1 (C*H* of ^{i}Pr / *C*H_3 of ^{i}Pr), 1.30 / 32.2 (CH_3 of ^{i}Pr / *C*H of ^{i}Pr), 1.30 / 18.3 (CH_3 of ^{i}Pr / *C*H_3 of ^{i}Pr).

^{13}C{^{1}H} NMR (126 MHz, CD_2Cl_2, 298 K): δ = 151.9 (m, *i* of NPh), 129.0 (s, *m* of NPh), 125.0 (m, *o* of NPh), 119.1 (s, *p* of NPh), 32.2 (m, *C*H of ^{i}Pr), 31.9 (m, *C*H of ^{i}Pr), 18.3 (m, *C*H_3 of ^{i}Pr).

^{31}P{^{1}H} NMR (202 MHz, CD_2Cl_2, 298 K): δ = 59.2 (broad d, $^1J_{PP}$ = 349 Hz, *P*^{i}Pr$_2$), -146.2 (t, $^1J_{PP}$ = 349 Hz, central *P*).

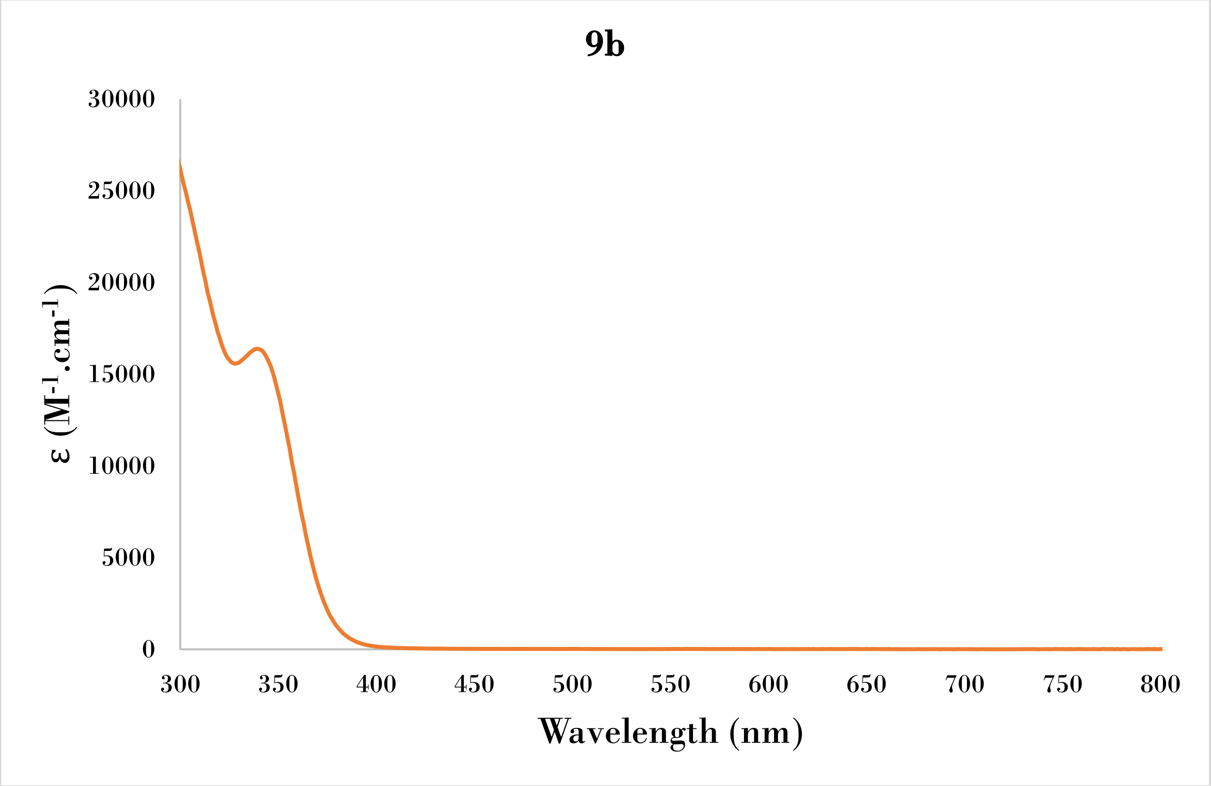

Figure S91: UV-vis (Toluene, 10 mm cell)

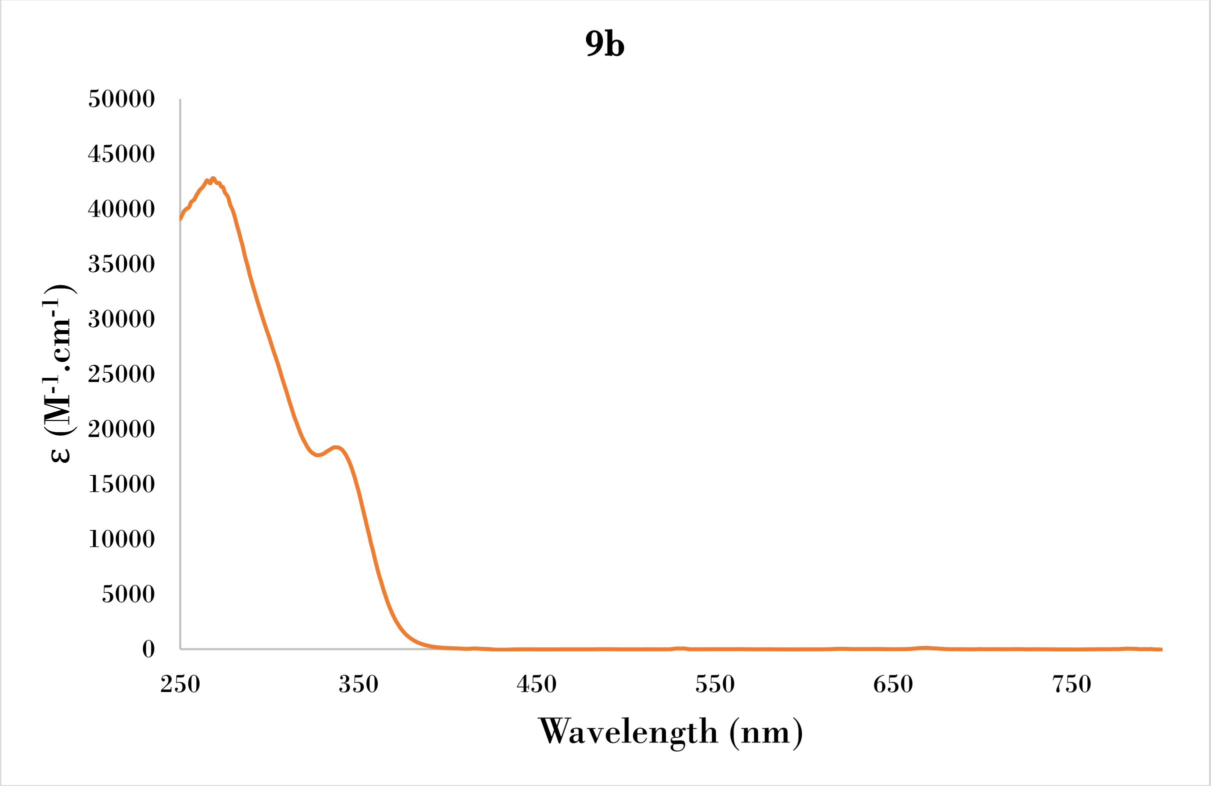

Figure S92: UV-vis (CH_2Cl_2, 10 mm cell)

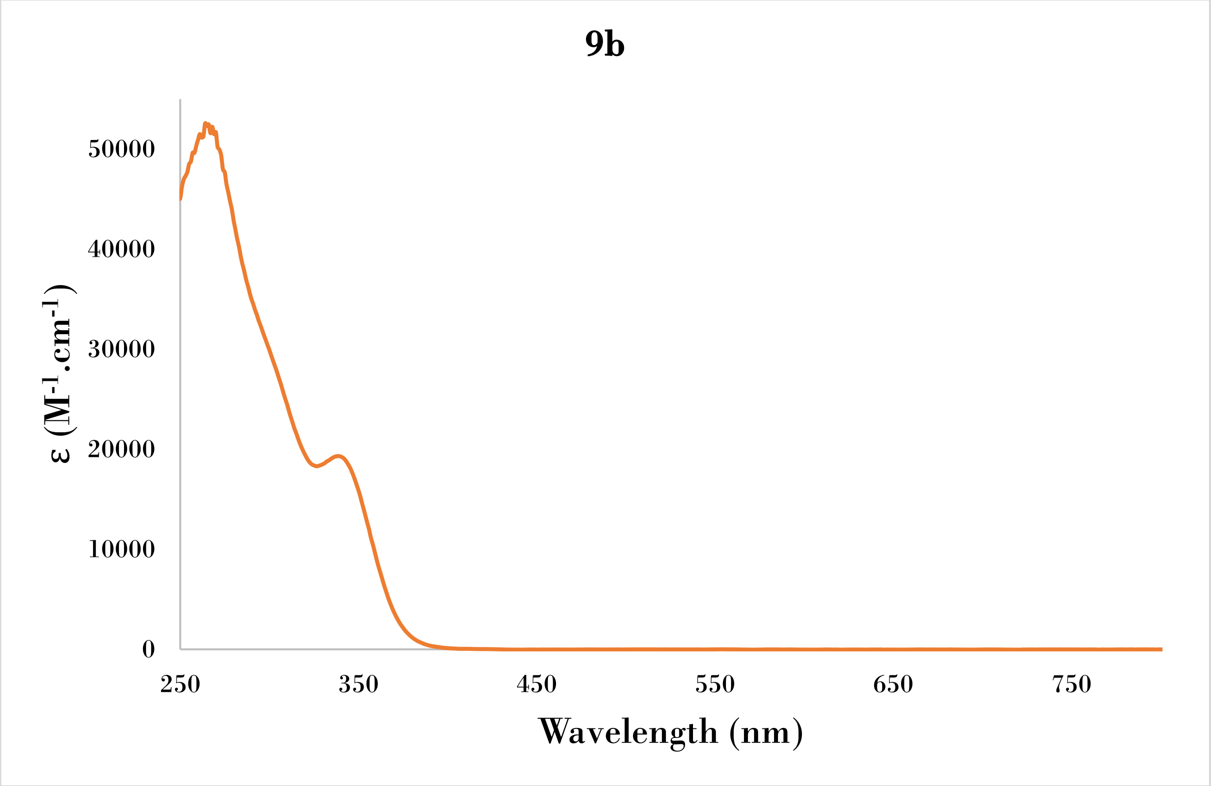

Figure S93: UV-vis (THF, 10 mm cell)

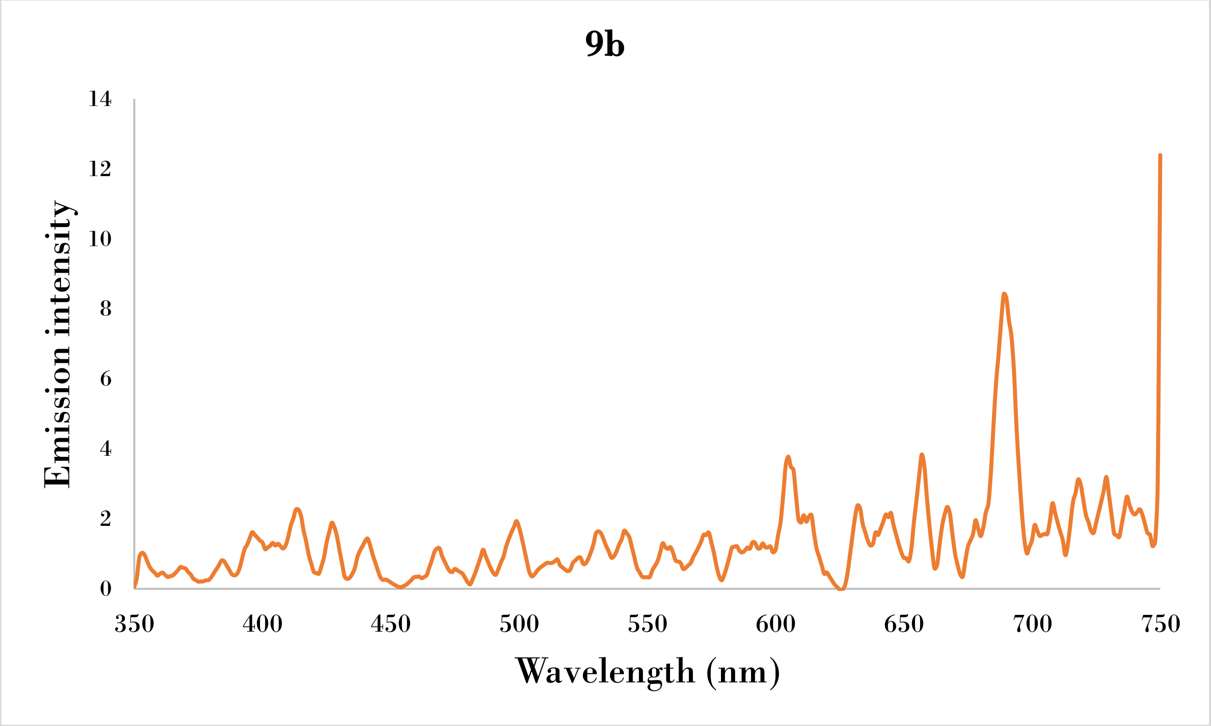

Figure S94: Emission spectrum in CH_2Cl_2 at 298 K (Excitation wavelength: 335 nm)

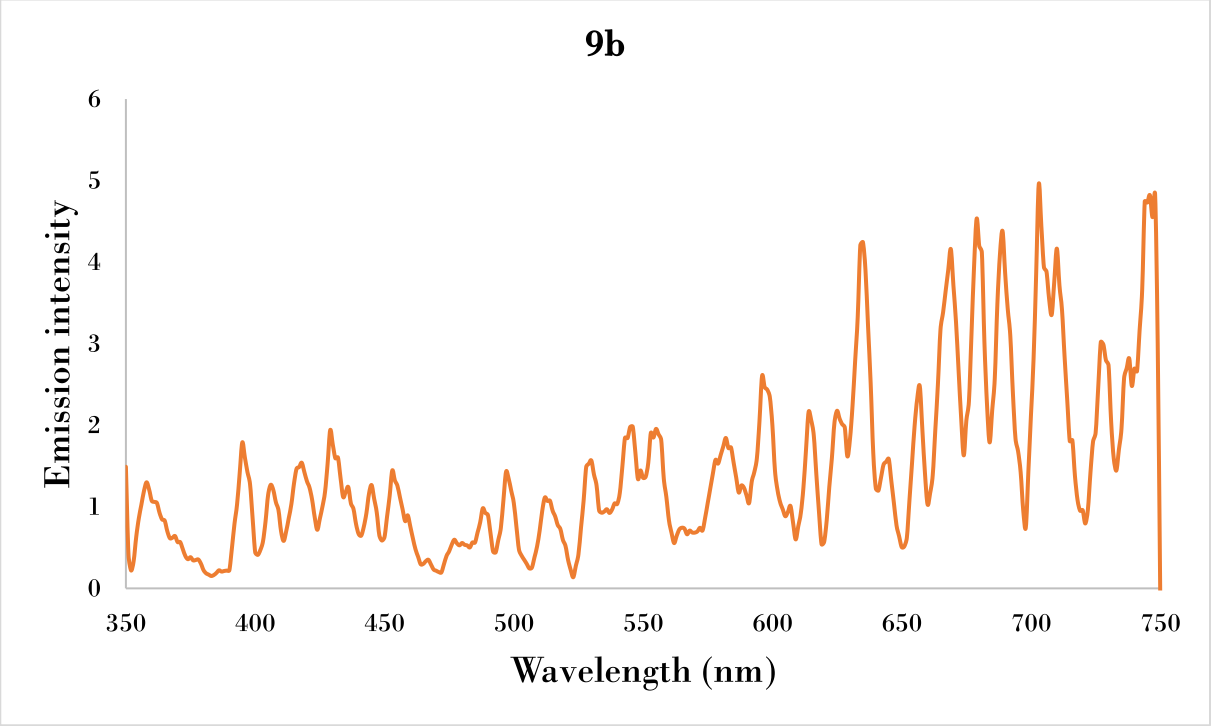

Figure S95: Emission spectrum in THF at 298 K (Excitation wavelength: 335 nm)

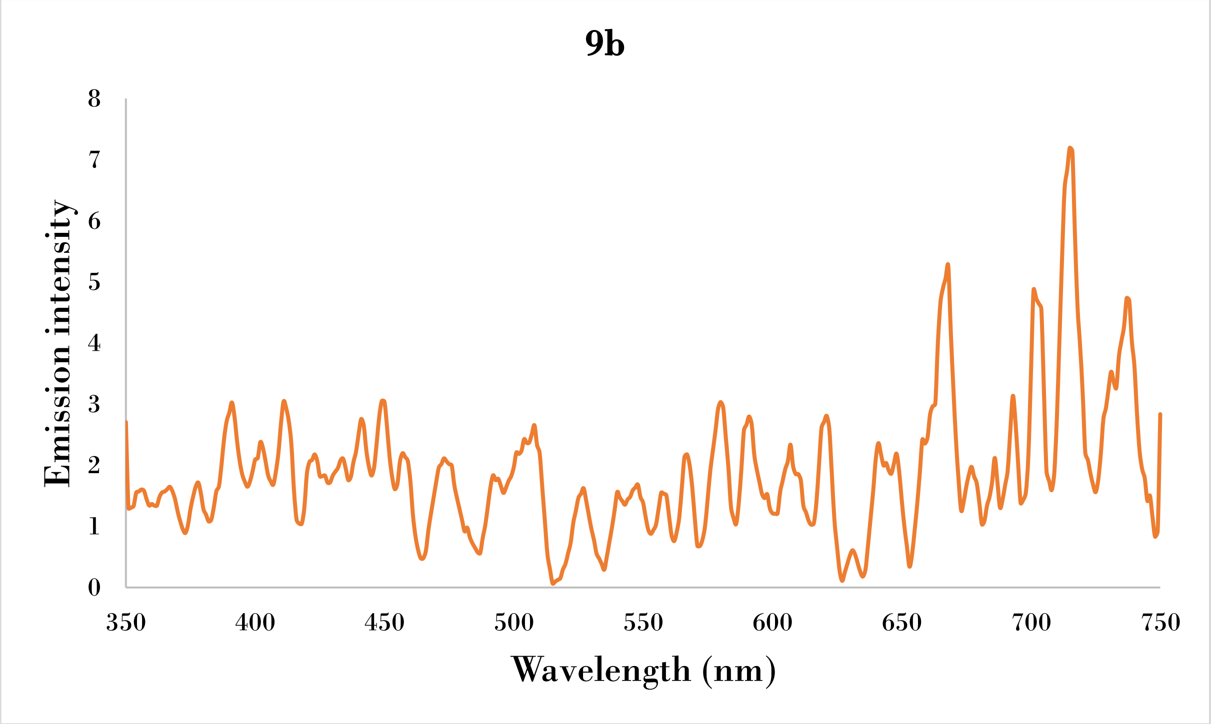

Figure S96: Solid state emission spectrum at 298 K (Excitation wavelength: 335 nm)

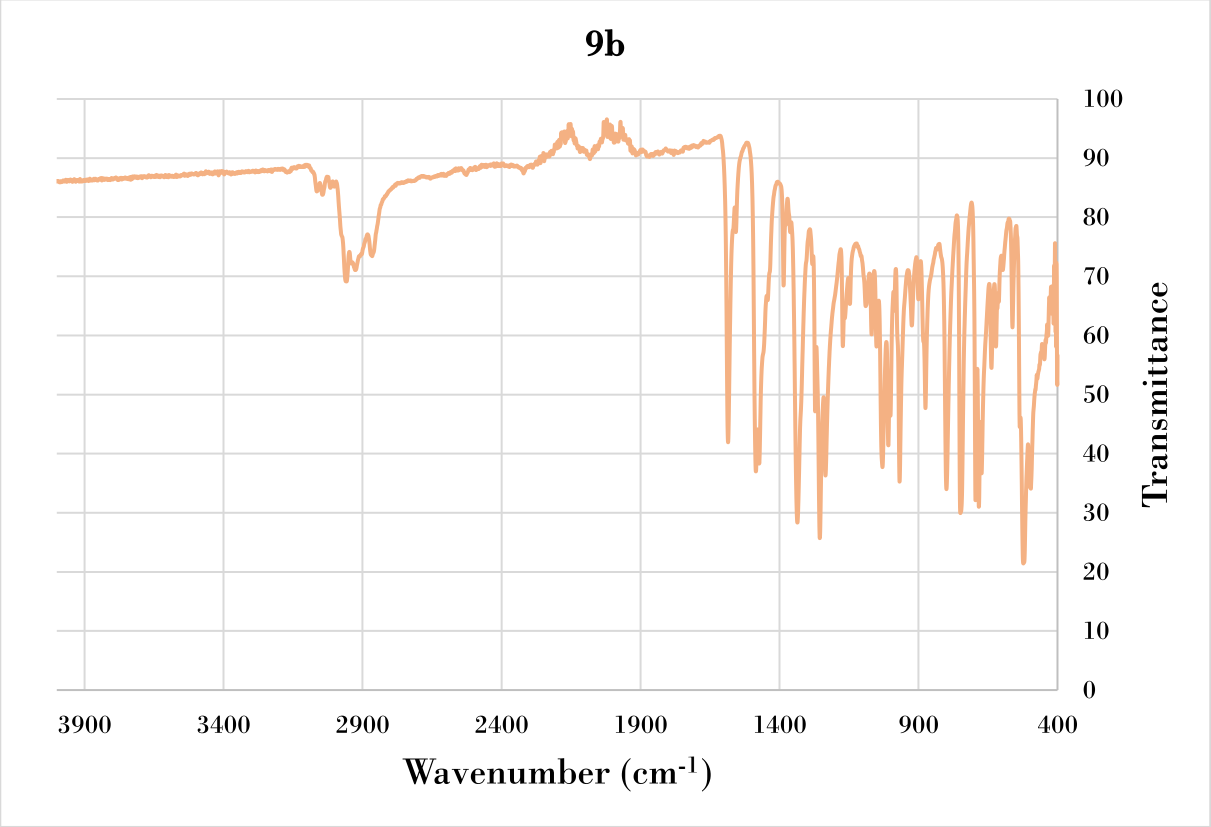

Figure S97: IR (ATR)

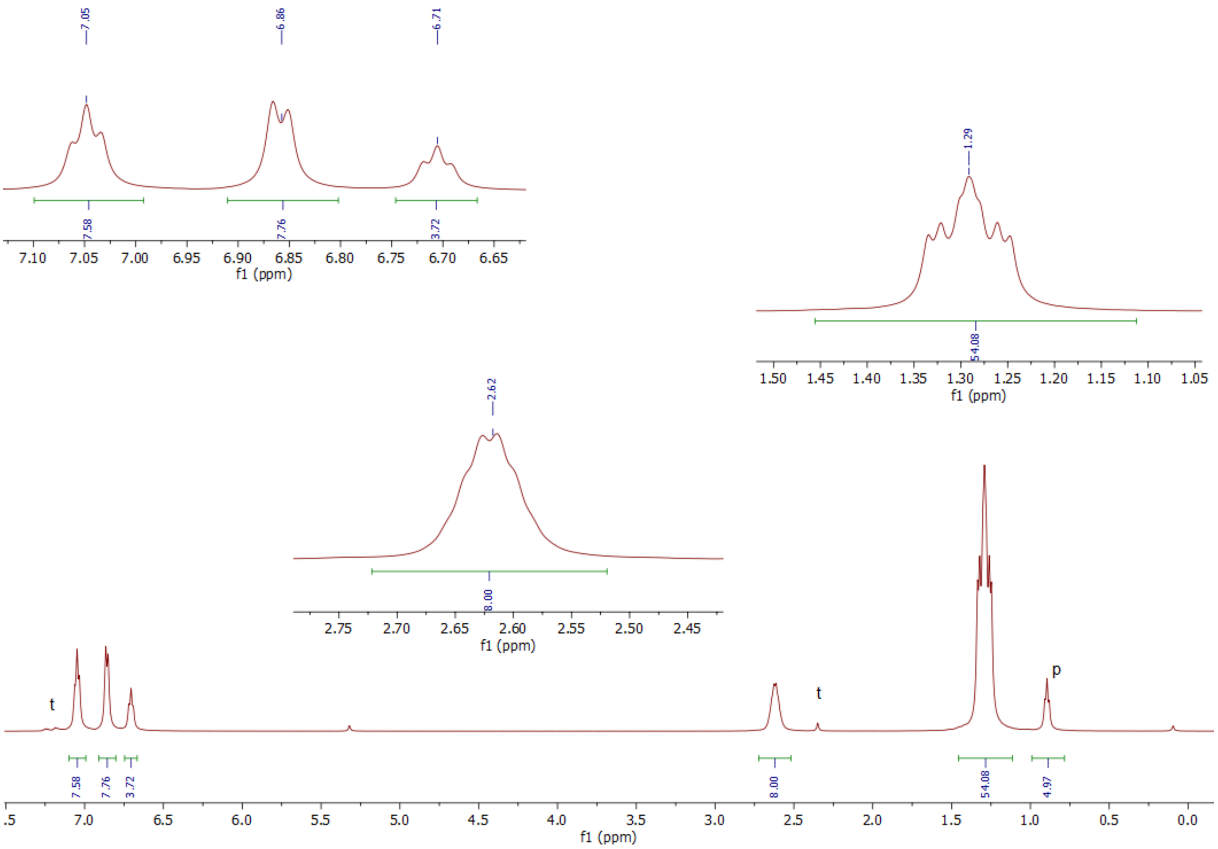

Figure S98: ^{1}H NMR (500 MHz, CD_2Cl_2, 298 K)(p: pentane; t: toluene)

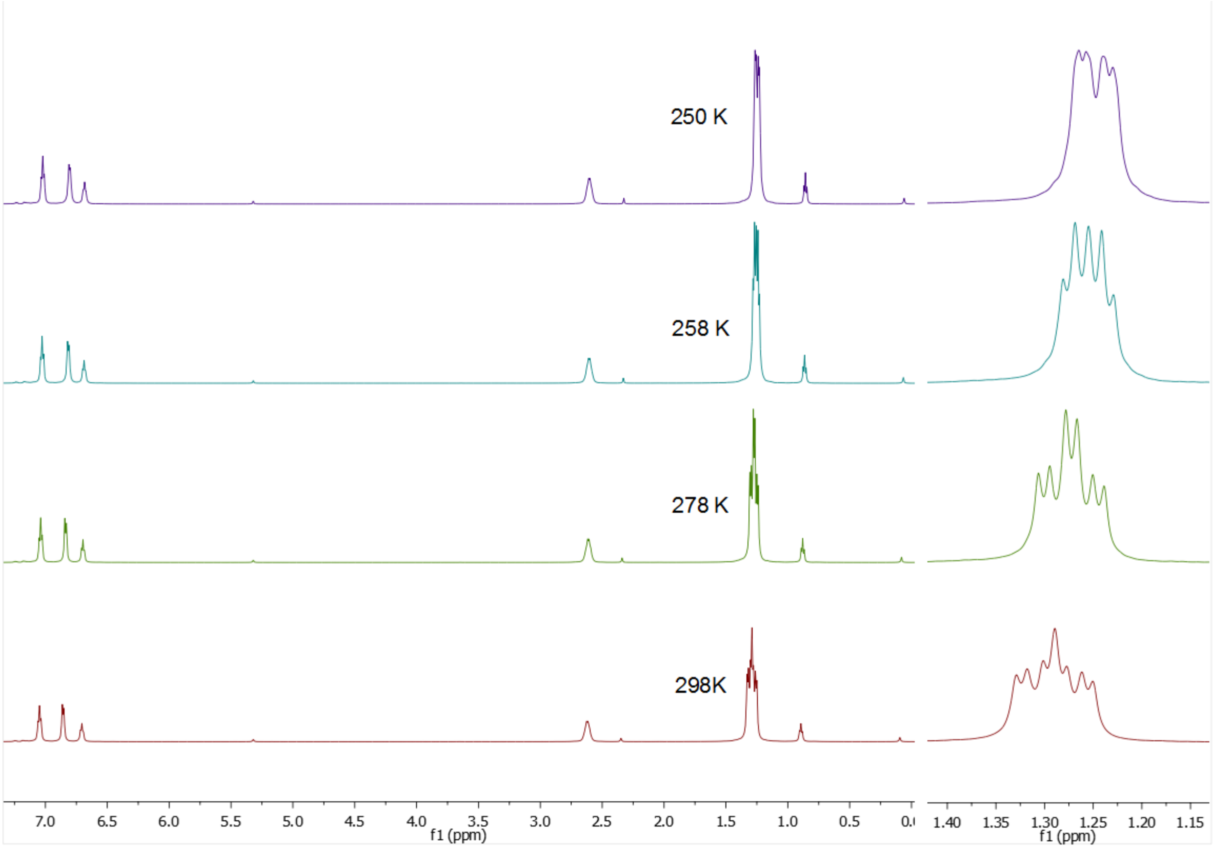

Figure S99: ^{1}H NMR (500 MHz, CD_2Cl_2, 250-298 K)

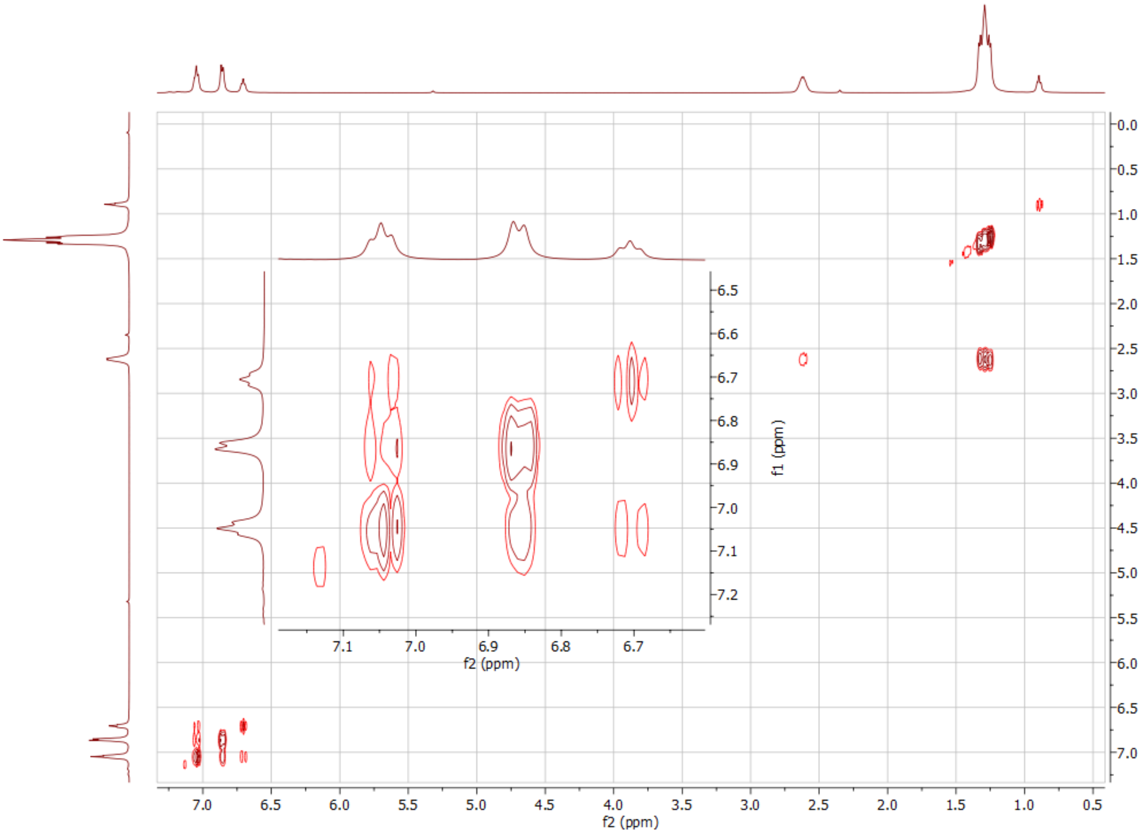

Figure S100: ^{1}H-^{1}H COSY (500 MHz, CD_2Cl_2, 298 K)

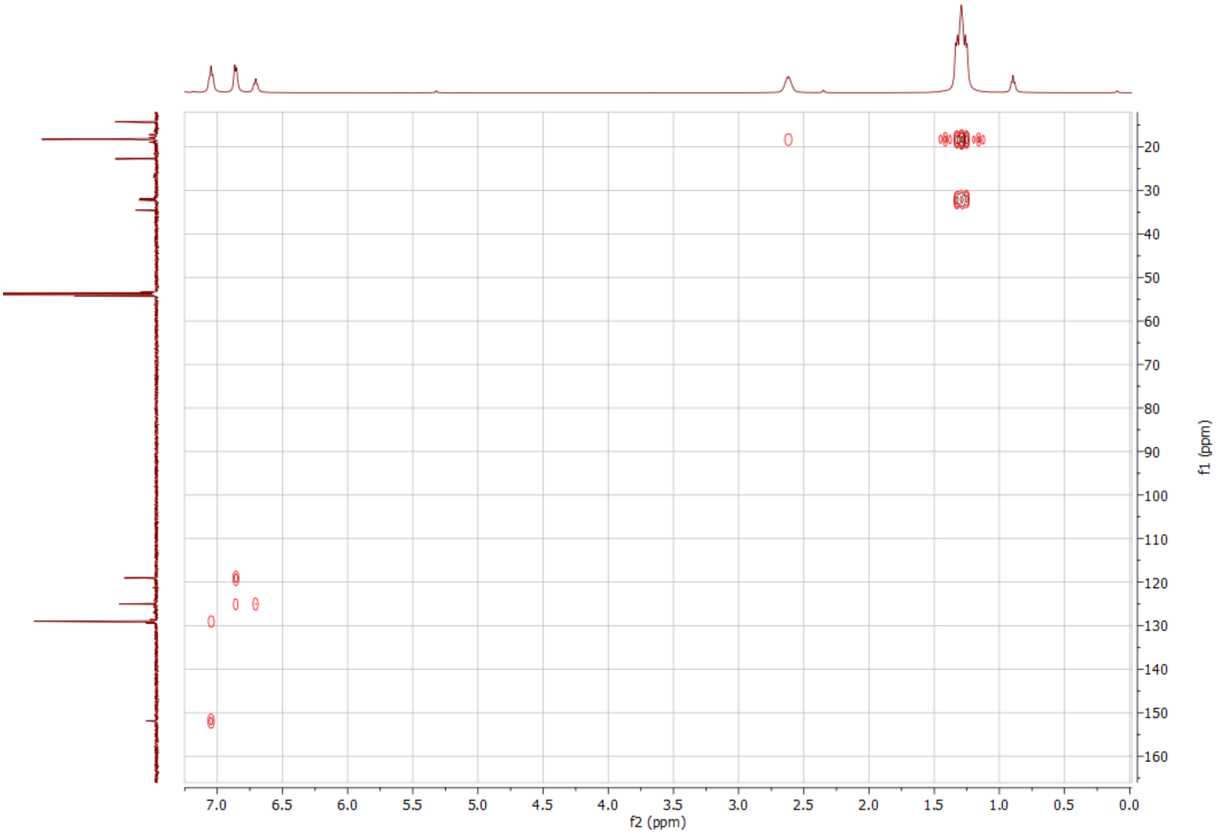

Figure S101: ^{1}H-^{13}C HMBC (500 MHz / 126 MHz, CD_2Cl_2, 298 K)(whole spectrum)

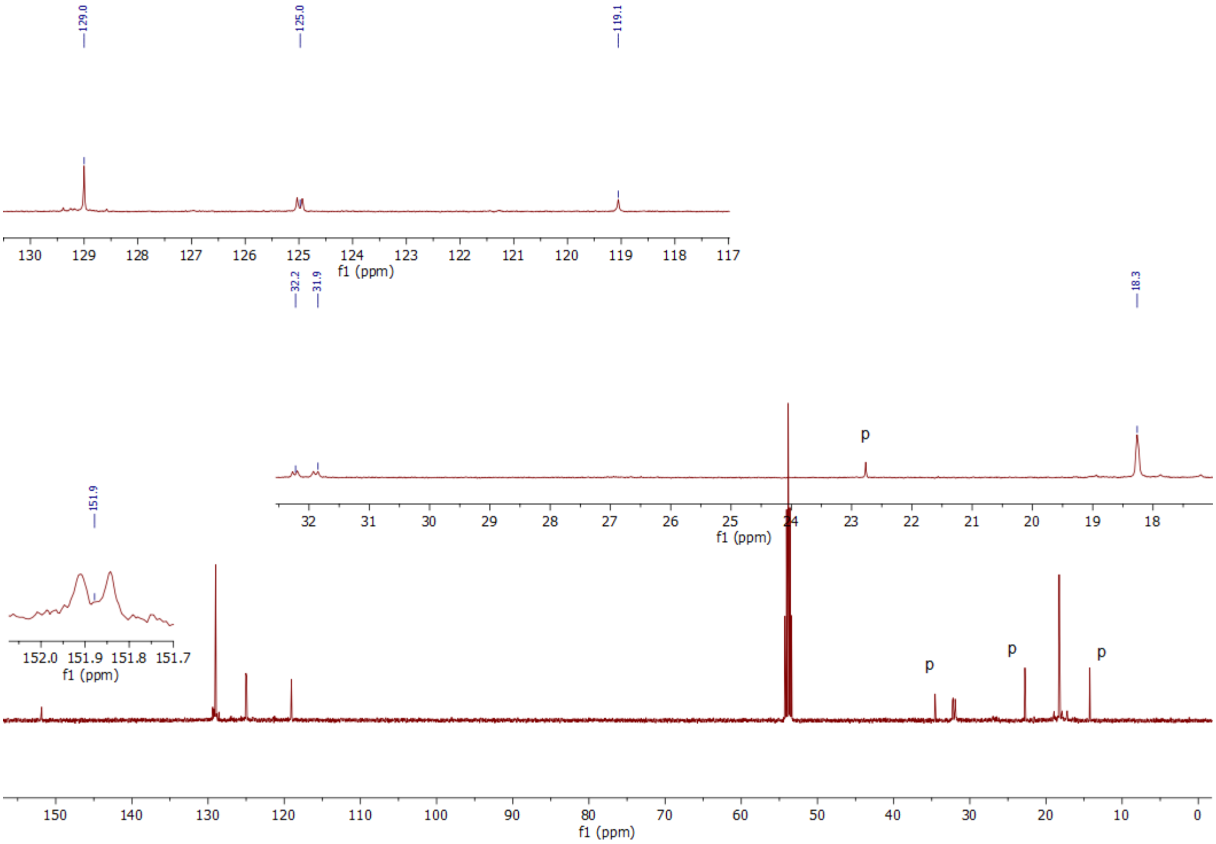

Figure S102: $^{13}C\{^{1}H\}$ **NMR (126 MHz,** CD_2Cl_2**, 298 K)(p: pentane)**

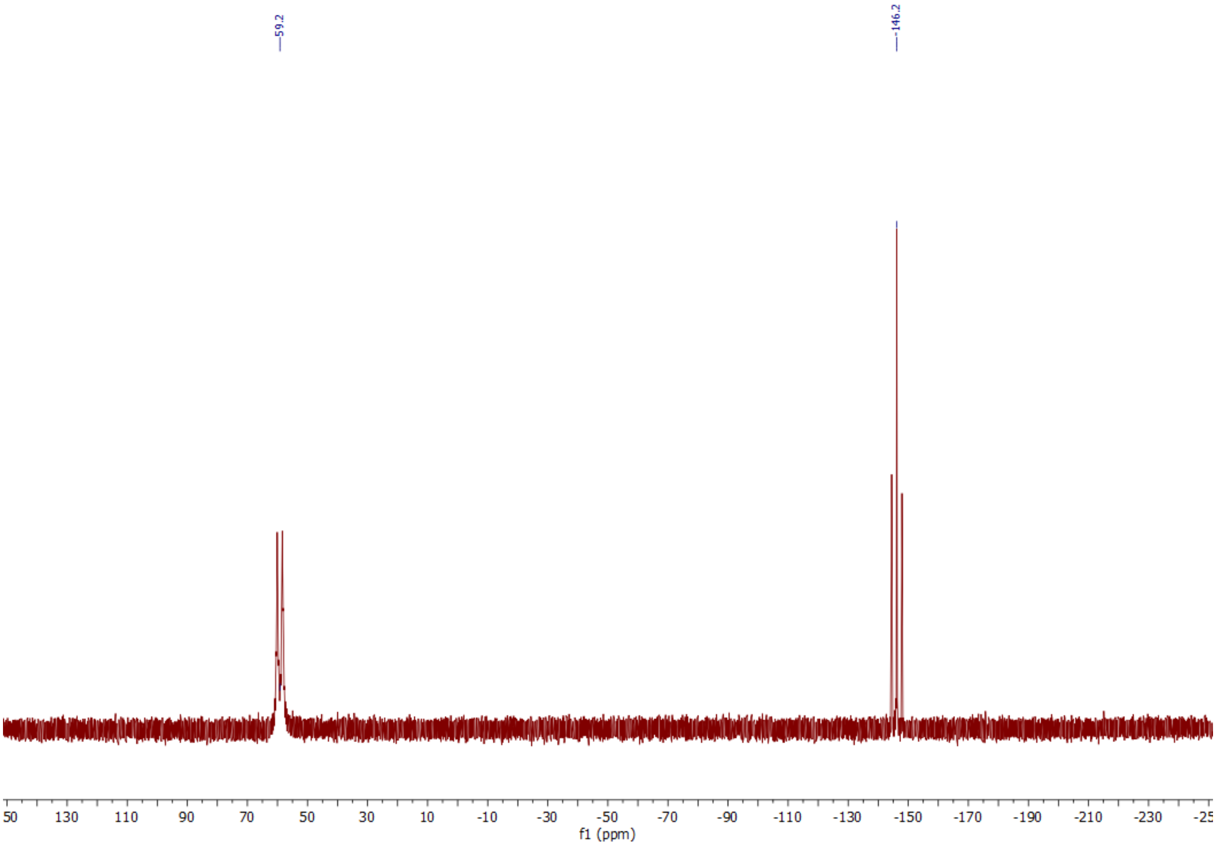

Figure S103: $^{31}P\{^{1}H\}$ **NMR (202 MHz,** CD_2Cl_2**, 298 K)**

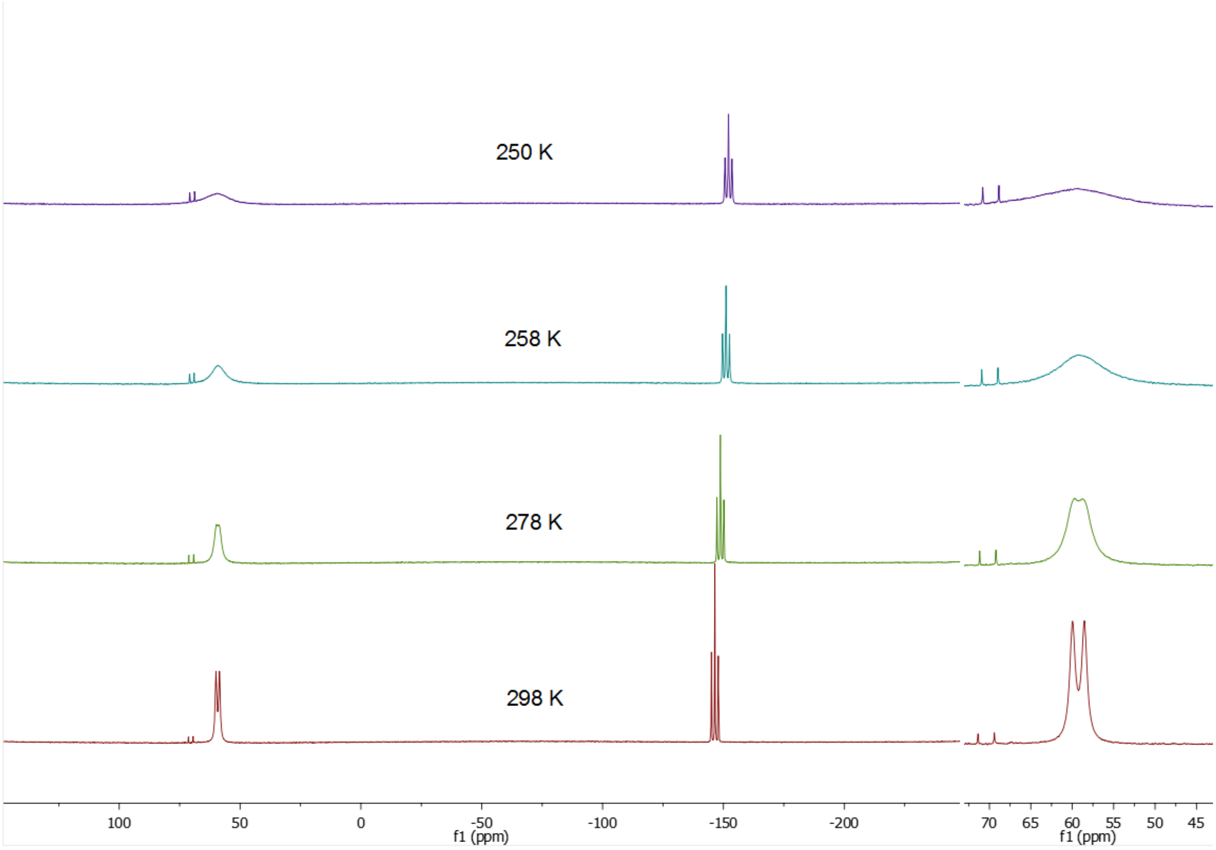

Figure S104: $^{31}P\{^1H\}$ **NMR (202 MHz,** CD_2Cl_2**, 250-298 K)**

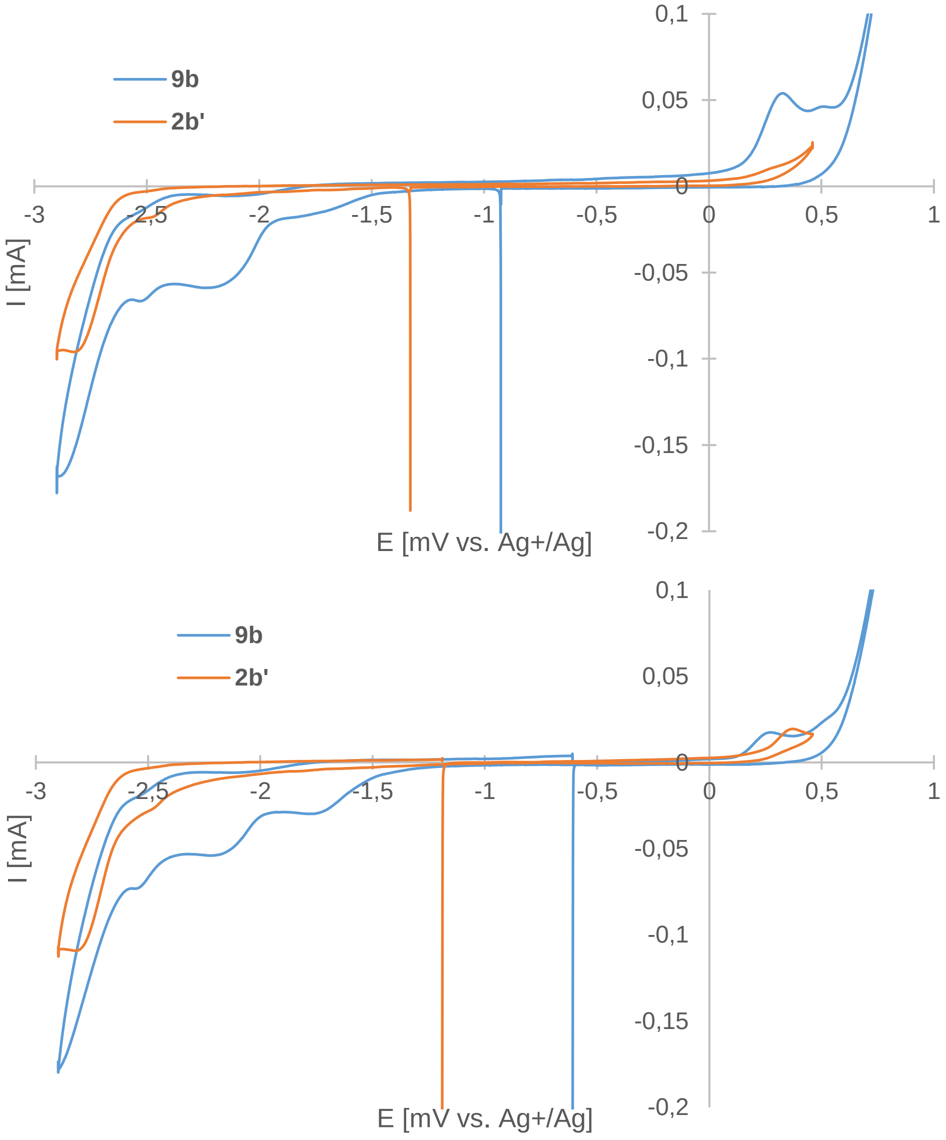

Figure S105: cyclic voltammograms of 9b and 2b (THF 0.1M NaBPh$_4$; concentration: 3 ×10^{-3} M; working electrode: glassy carbon Ø = 3 mm; scan rate = 100 mV s^{-1})

III. Attempted syntheses and failed experiments

*Attempted synthesis of **4b***

In an Ar glovebox, complex **3a** (200 mg, 0.35 mmol) and [Cp_2Fe][BPh_4] (178 mg, 0.35 mmol) were mixed in THF (3 mL). The reaction mixture turned quickly red. Sodium 3,5-dimethylphenolate etherate was added and the mixture was stirred for 5 min. The resulting solution was evaporated to dryness and the residue was dissolved in 3 mL of CH_2Cl_2, filtered over a plug of diatomaceous earth, and an orange solid was precipitated by addition to 50 mL of pentane under vigorous agitation. The resulting solid was dissolved in 3 mL of CH_2Cl_2 and the precipitation procedure was repeated. The resulting solid was extracted with pentane and the supernatant solution was discarded. A gum was obtained (242 mg), which could not be purified further.

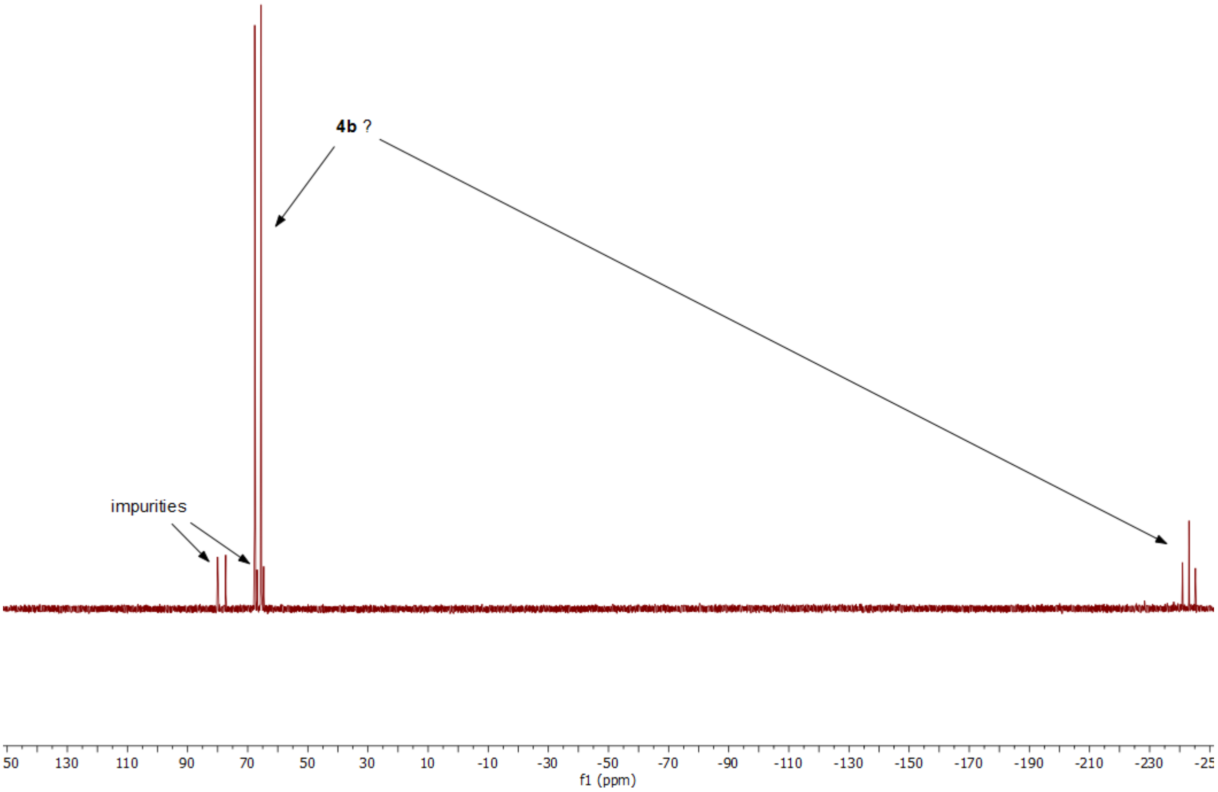

Figure S106: $^{31}P\{^1H\}$ NMR (202 MHz, CD_2Cl_2, 298 K)

*Reaction of **4a** with ferrocene carboxaldehyde*

In an Ar glovebox, complex **4a** (31.2 mg, 0.025 mmol) and FcCHO (5.4 mg, 0.025 mmol) were mixed in CD_2Cl_2. The mixture was analysed by ^1H and ^{31}P NMR spectroscopy.

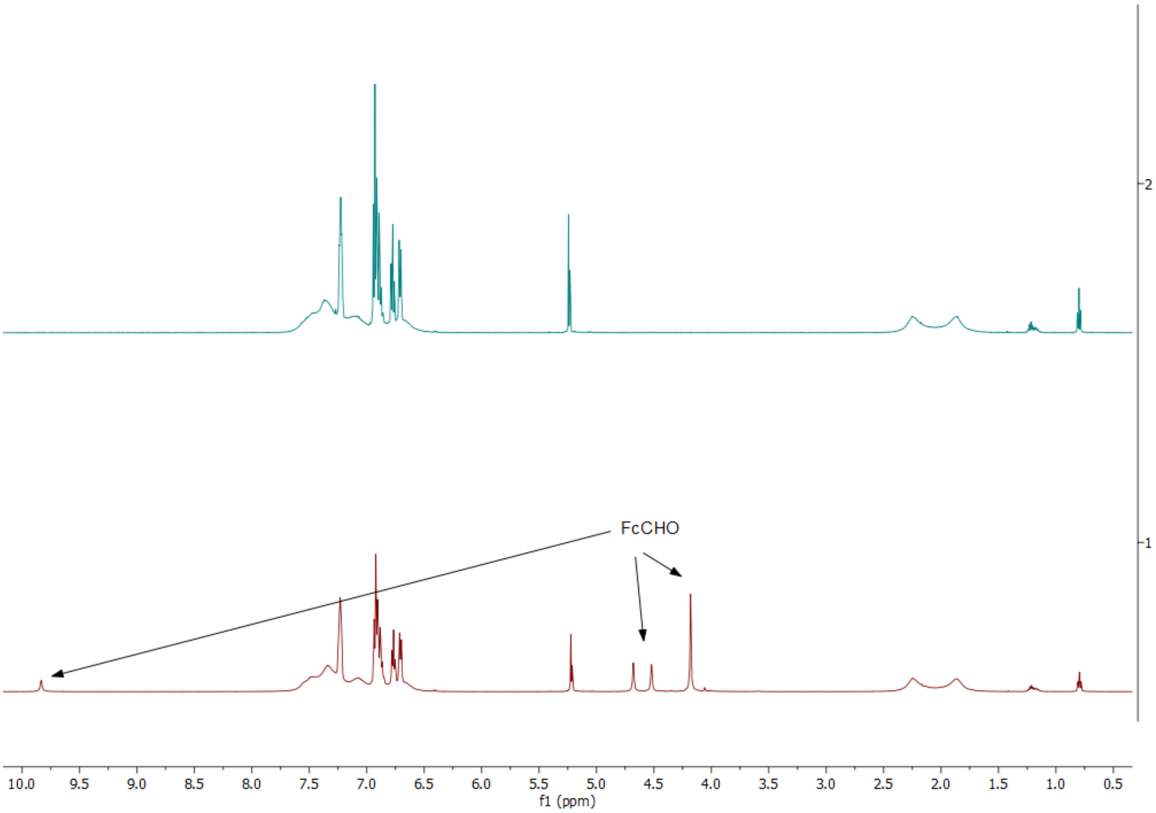

Figure S107: ^{1}**H NMR (500 MHz,** CD_2Cl_2**, 298 K)**

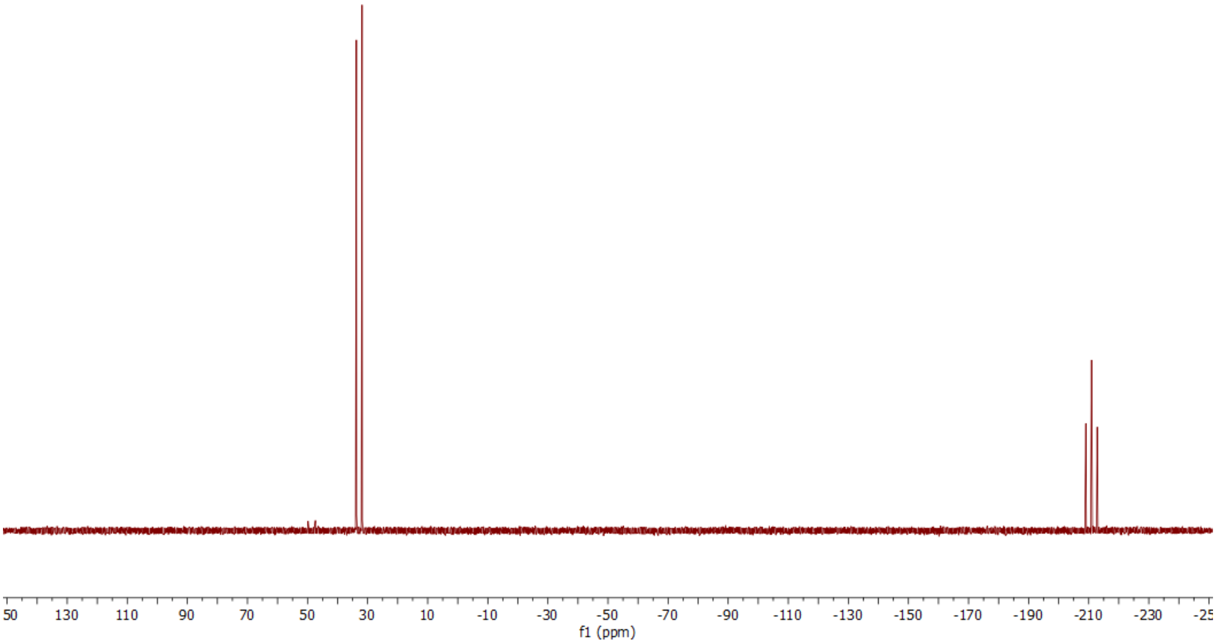

Figure S108: ^{31}**P{**^{1}**H} NMR (202 MHz,** CD_2Cl_2**, 298 K)**

Attempted syntheses of the Zr analogues of ***4a***

In an Ar glovebox, complexes **5** (**5a**: 380 mg, 0.46 mmol; **5b**; 323 mg, 0.50 mmol) were dissolved in CH_2Cl_2 and sodium 2,6-dimethylphenate etherate (2.0 eq) was added in 6 portions. The mixture was stirred in the glovebox for at least 15 mins and evaporated to dryness. The residue was triturated in pentane and dried under vacuum yielding white powders (260 and 245 mg, respectively). The $^{31}P\{^1H\}$ NMR spectra revealed the presence of impurities that could not be removed.

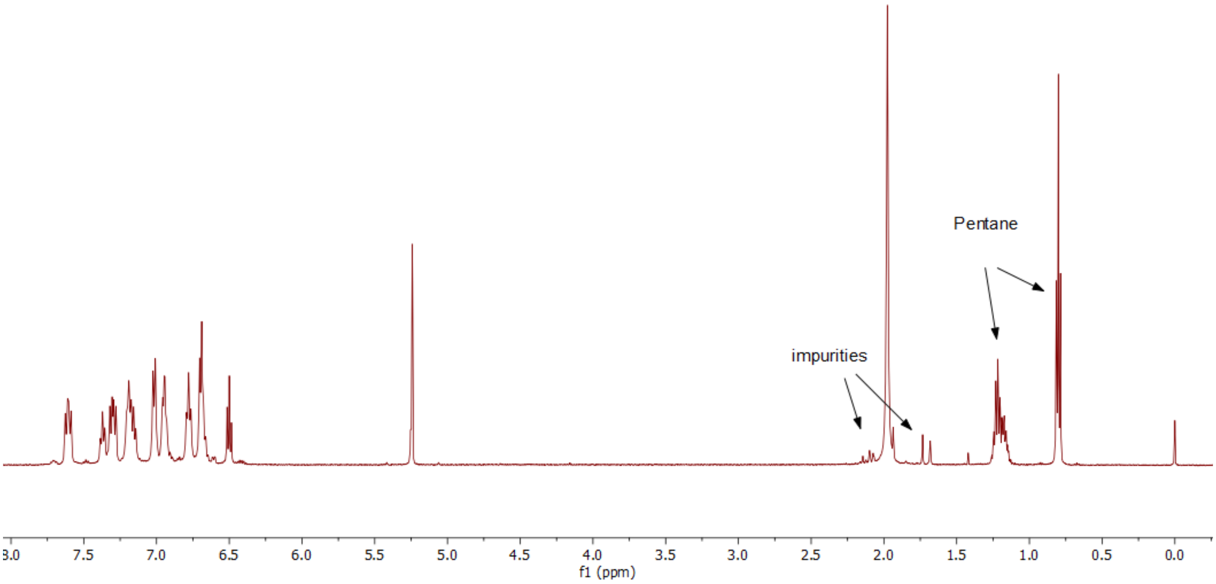

Figure S109: ^{1}H NMR (500 MHz, CD_2Cl_2, 298 K) of experiment a (NB: the $^{31}P\{^1H\}$ NMR spectrum was uninformative due to the fluxionality of the signal of the lateral phosphorus)

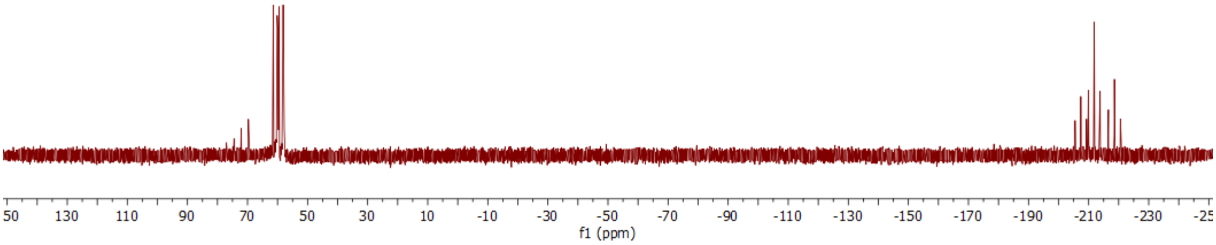

Figure S110: $^{31}P\{^1H\}$ NMR (202 MHz, CD_2Cl_2, 298 K) of experiment b

*Reaction of **5a** with ferrocene carboxaldehyde*

In an Ar glovebox, complex **5a** (32.3 mg, 0.05 mmol) and FcCHO (10.7 mg, 0.05 mmol) were mixed in C_6D_5Br. The mixture was analysed by ^{1}H and ^{31}P NMR spectroscopy, no reaction was observed. The mixture was heated to 60 °C overnight, resulting in product degradation.

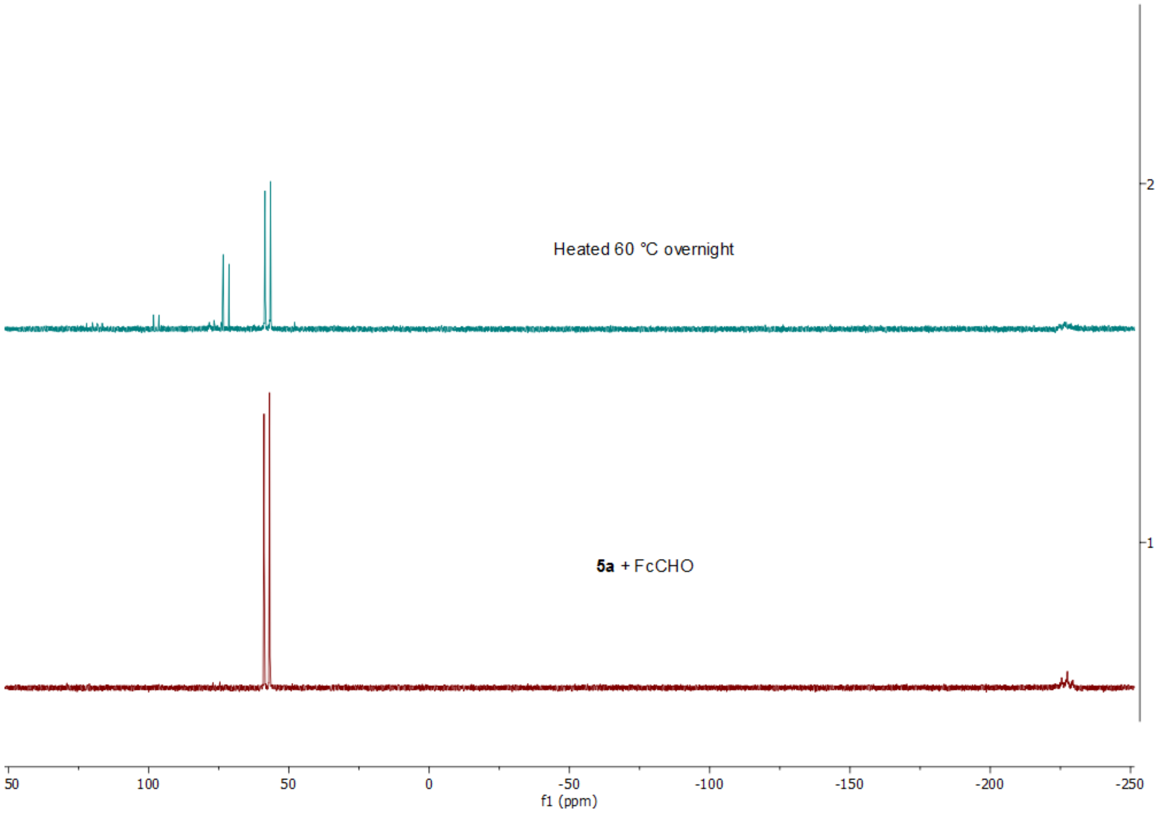

Figure S111: $^{31}P\{^1H\}$ NMR (202 MHz, C_6D_5Br, 298 K)

Attempted synthesis of 7a

In an Ar glovebox, complex **6a** (41.5 mg, 0.05 mmol) and [Au(THT)Cl] (16 mg, 0.05 mmol) were mixed in CD_2Cl_2. The reaction mixture was analysed by ^1H and $^{31}P\{^1H\}$ NMR spectroscopy, showing only the presence of the reactants.

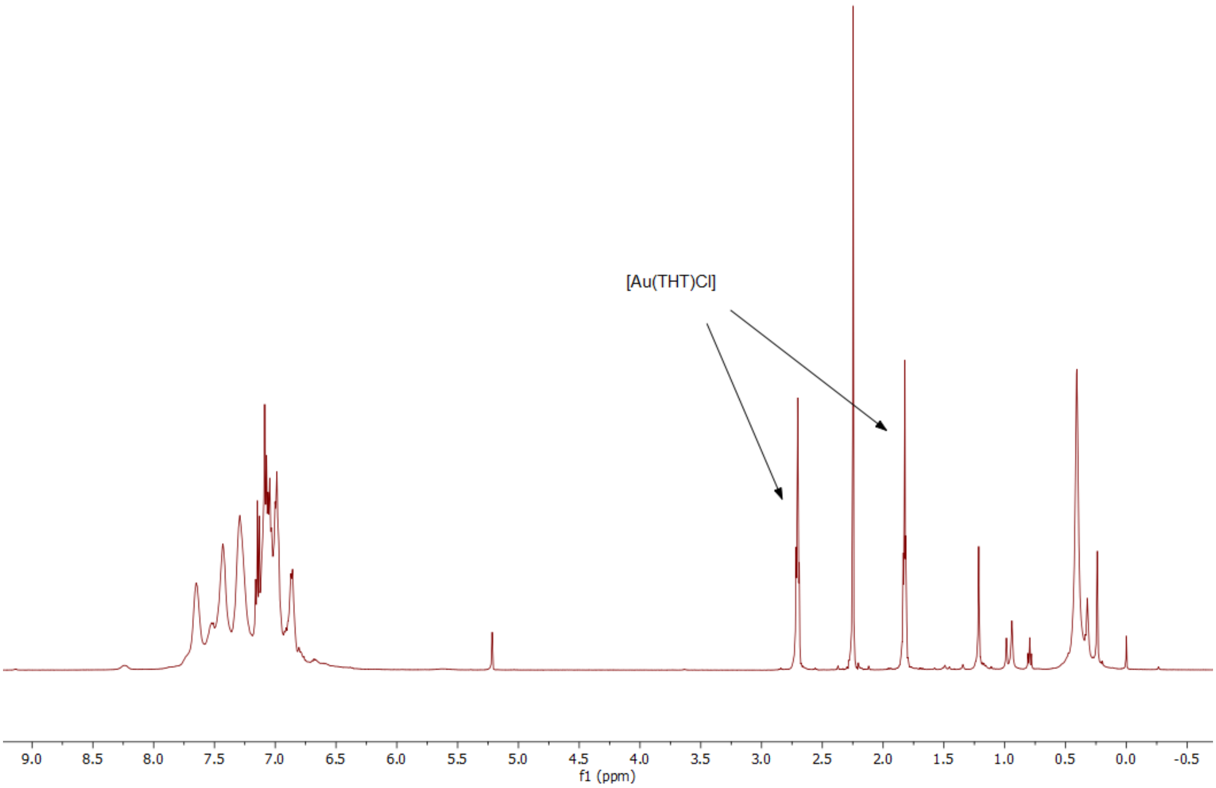

Figure S112: ^{1}H NMR (500 MHz, CD_2Cl_2, 298 K)

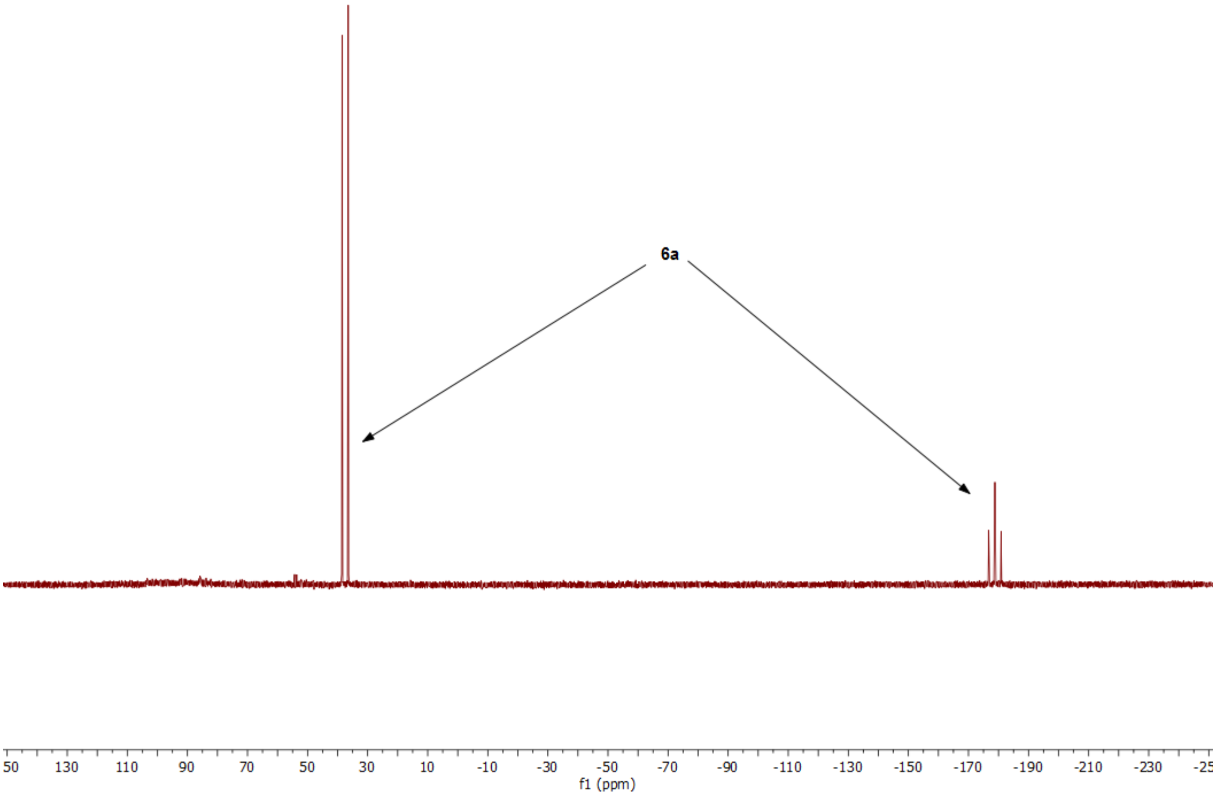

Figure S113: ^{31}P{^{1}H} NMR (202 MHz, CD_2Cl_2, 298 K)

*Attempted double metalation of **6b** with CuBr*

In an Ar glovebox, complex **6b** (30.1 mg, 0.05 mmol) and CuBr (14.4 mg, 0.1 mmol) were mixed in CD_2Cl_2. A small amount of white solid (probably CuBr) remained insoluble. The reaction mixture was analysed by ^1H and $^{31}P\{^1H\}$ NMR spectroscopy, showing only the presence of complex **7b**.

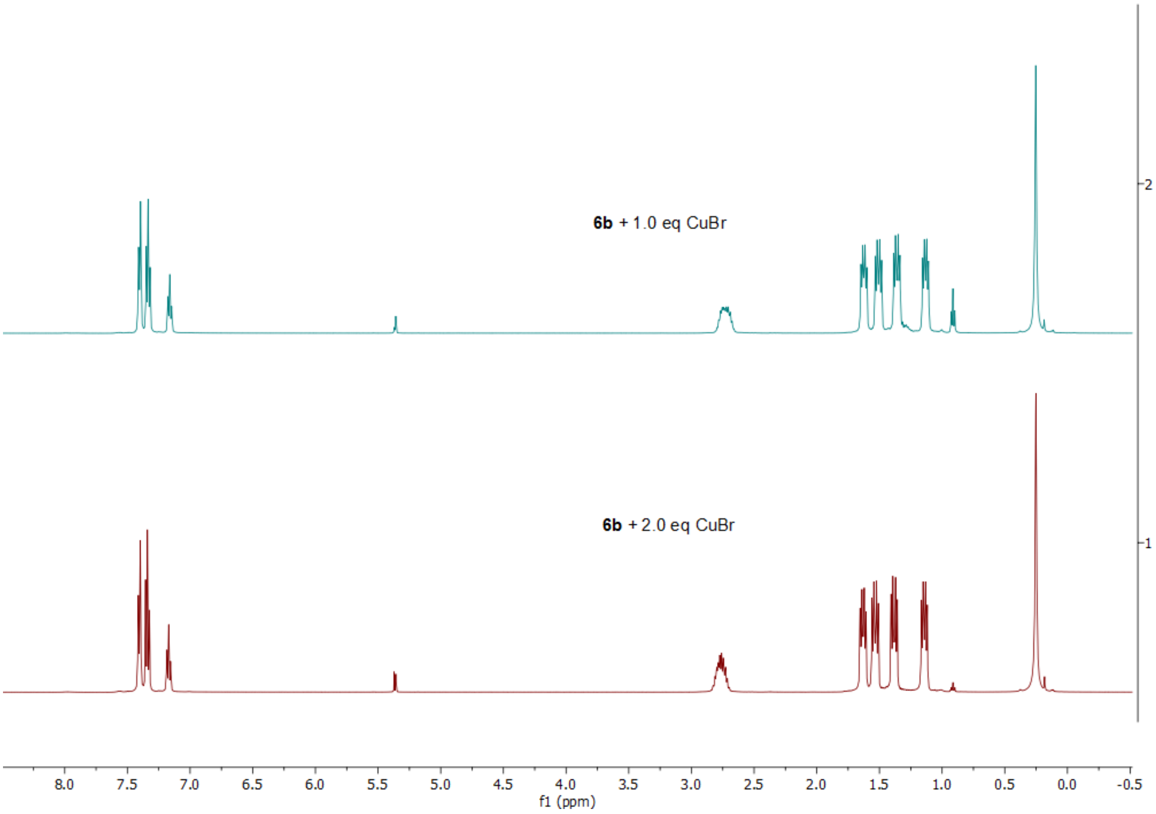

Figure S114: ^1H **NMR (500 MHz,** CD_2Cl_2**, 298 K)**

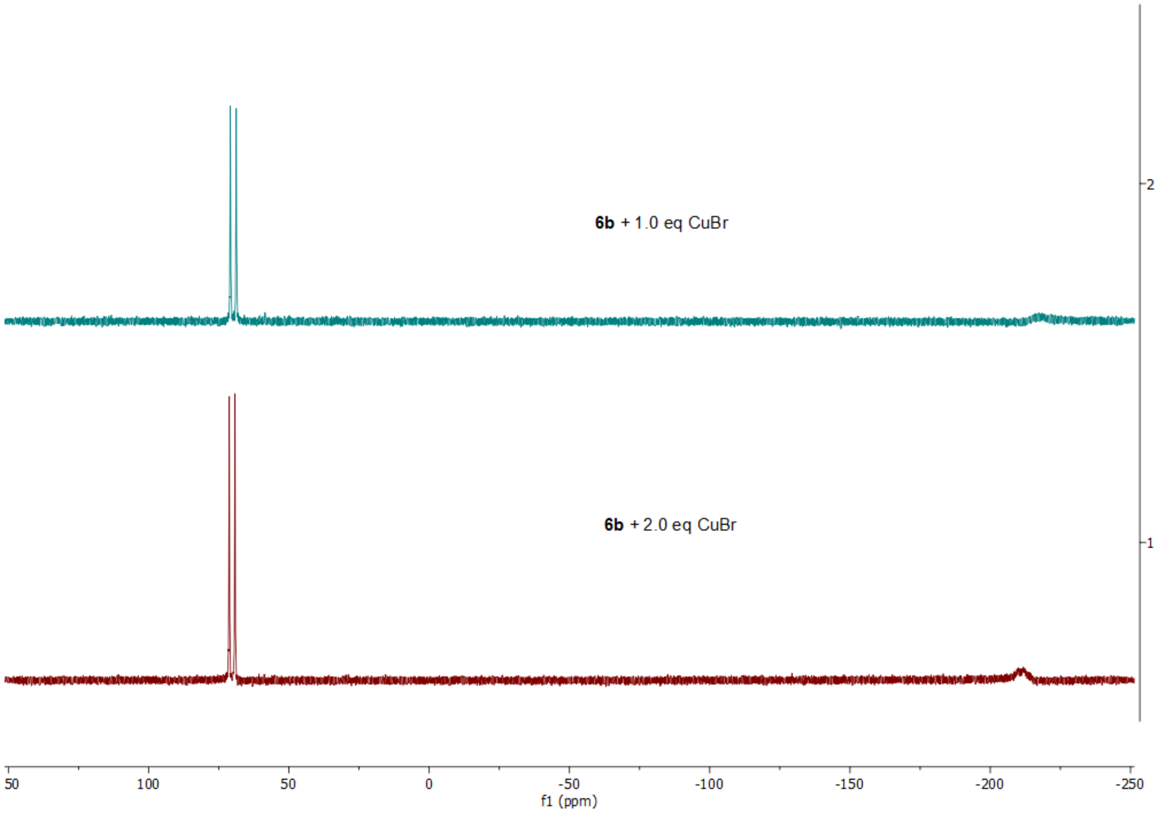

Figure S115: $^{31}P\{^1H\}$ NMR (202 MHz, CD_2Cl_2, 298 K)

*Reaction of **2a** and **2b'** with [Au(THT)Cl]*

In an Ar glovebox, complexes **2** (0.05 mmol) and [Au(THT)Cl] (16.0 mg, 0.1 mmol) were mixed in C_6D_6. For **2a**, the reaction mixture was filtered over a plug of diatomaceous earth placed over a borosilicate fibre filter. Both mixtures were analysed by ^1H and $^{31}P\{^1H\}$ NMR spectroscopy, showing a complex mixture (only the $^{31}P\{^1H\}$ spectrum are shown).

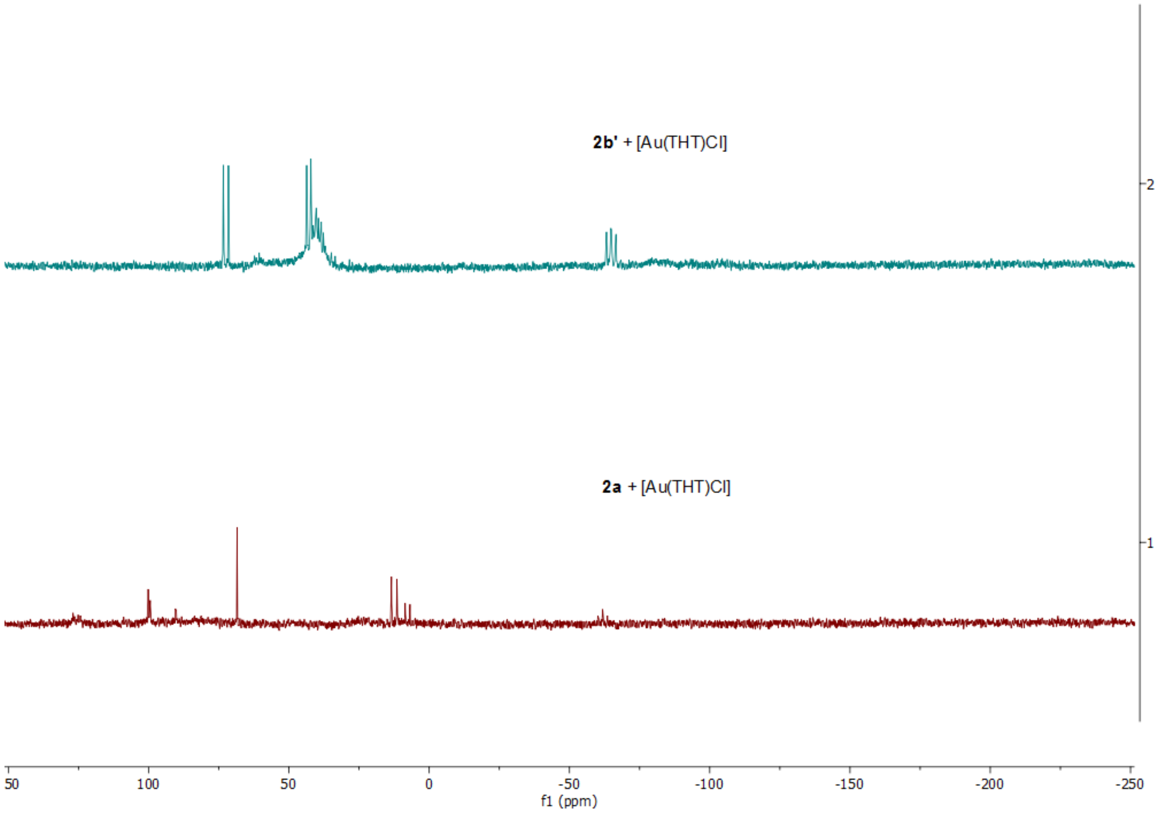

Figure S116: $^{31}P\{^{1}H\}$ NMR (202 MHz, C_6D_6, 298 K)

Attempted synthesis of ***9a***

In an Ar glovebox, complex **2a** (68 mg, 0.1 mmol) and CuBr (14.4 mg, 0.1 mmol) were mixed in C_6D_6 and the mixture was stirred for 4 days, after which it was filtered over diatomaceous earth placed over a borosilicate fibre filter. The orange solution was analysed by ^{1}H and $^{31}P\{^{1}H\}$ NMR spectroscopy, showing a complex mixture (only the ^{1}H NMR spectrum is shown). The plug of diatomaceous earth was extracted with d_8-THF. No product could be detected by ^{1}H and $^{31}P\{^{1}H\}$ NMR spectroscopy.

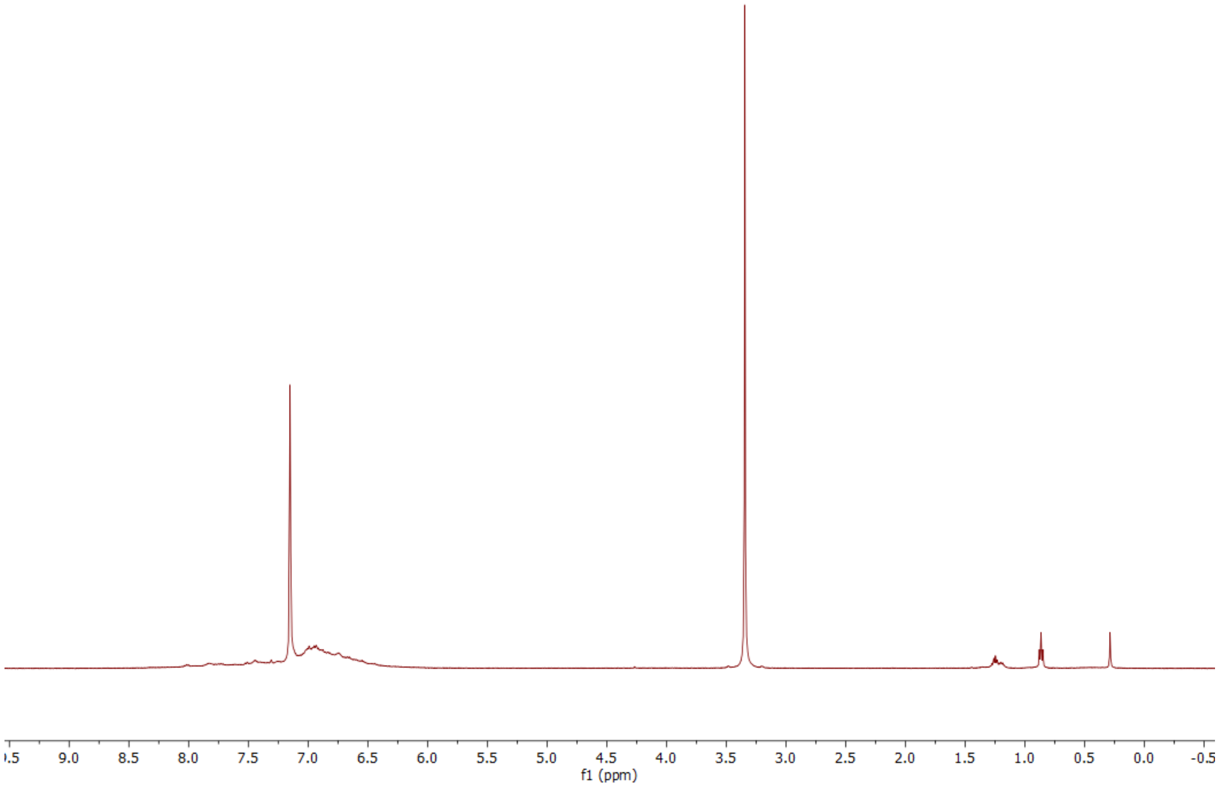

Figure S117: ^{1}H NMR (500 MHz, C_6D_6, 298 K)

IV. Computational studies

Computational details

All calculations were performed using the Gaussian 16[14] package and the B3PW91 hybrid functional[15] on the real experimental systems. The gold and copper atoms were described with the LANL2DZ[16] pseudopotential. The 6-31+G** basis set were employed for all other atoms. Optimizations were carried out without any symmetry restrictions taking into solvent effect

---

[14] Gaussian 16, Revision C.01, M. J. Frisch, G. W. Trucks, H. B. Schlegel, G. E. Scuseria, M. A. Robb, J. R. Cheeseman, G. Scalmani, V. Barone, G. A. Petersson, H. Nakatsuji, X. Li, M. Caricato, A. V. Marenich, J. Bloino, B. G. Janesko, R. Gomperts, B. Mennucci, H. P. Hratchian, J. V. Ortiz, A. F. Izmaylov, J. L. Sonnenberg, D. Williams-Young, F. Ding, F. Lipparini, F. Egidi, J. Goings, B. Peng, A. Petrone, T. Henderson, D. Ranasinghe, V. G. Zakrzewski, J. Gao, N. Rega, G. Zheng, W. Liang, M. Hada, M. Ehara, K. Toyota, R. Fukuda, J. Hasegawa, M. Ishida, T. Nakajima, Y. Honda, O. Kitao, H. Nakai, T. Vreven, K. Throssell, J. A. Montgomery, Jr., J. E. Peralta, F. Ogliaro, M. J. Bearpark, J. J. Heyd, E. N. Brothers, K. N. Kudin, V. N. Staroverov, T. A. Keith, R. Kobayashi, J. Normand, K. Raghavachari, A. P. Rendell, J. C. Burant, S. S. Iyengar, J. Tomasi, M. Cossi, J. M. Millam, M. Klene, C. Adamo, R. Cammi, J. W. Ochterski, R. L. Martin, K. Morokuma, O. Farkas, J. B. Foresman, and D. J. Fox, Gaussian, Inc., Wallingford CT, 2016.

[15] a) A. D. Becke, *J. Chem. Phys.* **1993**, *98*, 5648-5652; b) J. P. Perdew, in *Electronic Structure of Solids '91*, Ed. P. Ziesche and H. Eschrig, Akademie Verlag, Berlin, **1991**, 11.

[16] P. J. Hay and W. R. Wadt, *J. Chem. Phys.* **1985**, *82*, 299-310.

(Toluene) by means of the continuum standard solvation PCM model.[17]All stationary points computed were fully optimized. All total energies and Gibbs free energies have been zero-point energy (ZPE) and temperature corrected using unscaled density functional frequencies.

ELF Bonding basins

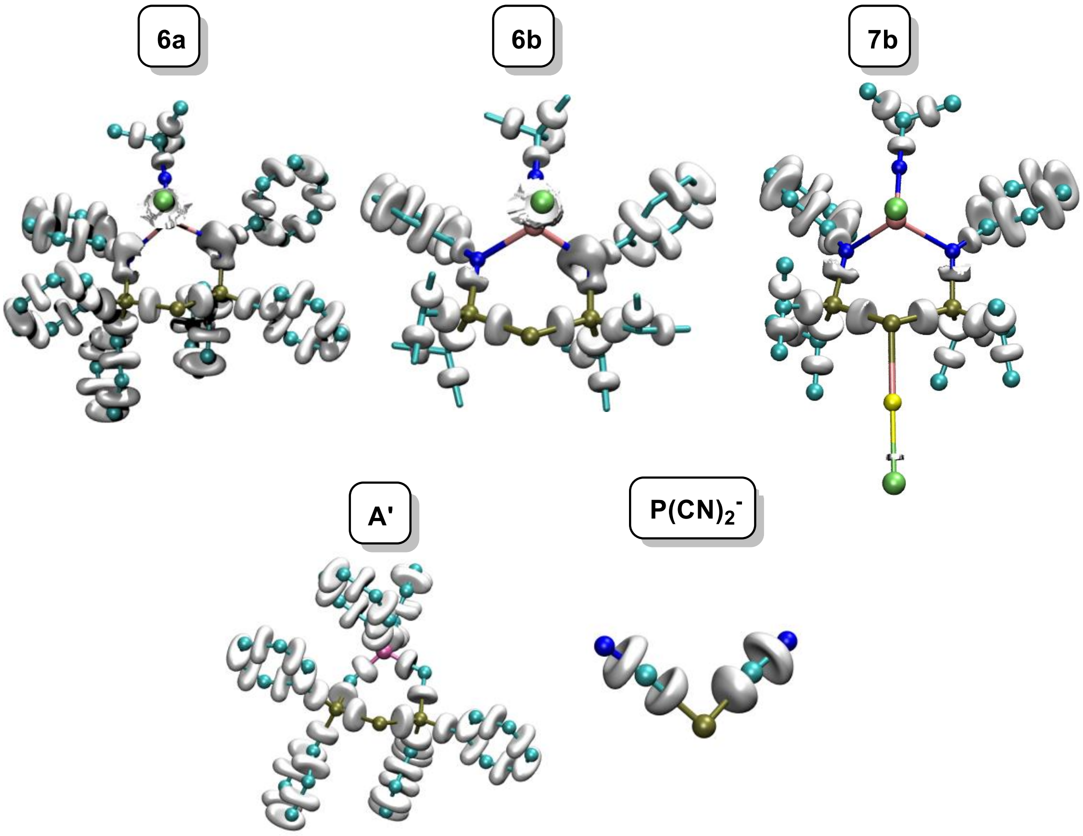

Figure S118: ELF bonding basins

AIM analysis

In order to gain insight into the nature of the chemical bonding we performed Atoms In Molecules analysis (QTAIM)[18] using AIMALL[19] software and Electronic Localized Function analysis using TopChem package.[20] The Electrostatic Potential Surface (ESP) map and NCIPLOT have been plotted with VMD software.[21]

---

[17] J. Tomasi, B. Mennucci and R. Cammi, *Chem. Rev.* **2005**, *105*, 2999-3094.

[18] a) R. F. W. Bader, *Chem. Rev.* **1991**, *91*, 893-928; b) R. F. W. Bader, in Atoms in Molecules, a Quantum Theory, Oxford University Press, New York, 1990.

[19] AIMAll (version 17.11.14B), T-A. Keith, TK Gristmill Software, Overland Park KS, USA, 2014.

[20] D. Kozlowski and J. Pilmé, *J. Comput. Chem.* **2011**, *32*, 3207-3217.

[21] a) W. Humphrey, A. Dalke and K. Schulten, *J. Mol. Graphics* **1996**, *14*, 33-38. b) http://www.ks.uiuc.edu/Research/vmd/.

The AIM analysis was computed at PCM-(Toluene)-B3PW91-D3/def2-SVP-RIFIT(Au or Cu), 6-31+G(other atoms)//PCM(Toluene)-B3PW91-D3/LANL2DZ(Au), 6-31+G**(other atoms) level of theory. Values are expressed in e.Å^{-3} (ρ); e.Å^{-5} ($\nabla^2\rho$); E_h.Å^{-3} (G, V, H); E_h.e^{-1} (G/ρ, H/ρ); ε and DI are dimensionless. Values in grey were exported to Table 3 in the paper.**

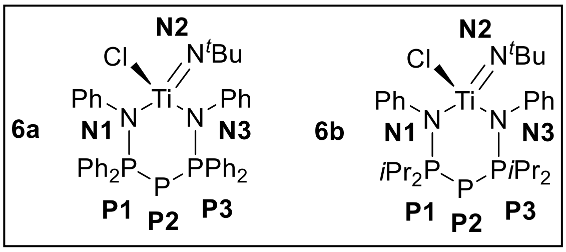

6a	ρ	$\nabla^2\rho$	ε	DI(A|B)	G	V	H	G/ρ	H/ρ
N2–Ti	1.458	18.195	0.021	1.759	2.220	-3.158	-0.945	1.518	-0.645
N3–Ti	0.614	8.266	0.119	0.512	0.661	-0.749	-0.088	1.079	-0.138
N3–P3	1.221	13.278	0.101	0.777	1.917	-2.909	-0.985	1.57	-0.809
N1–P1	1.215	13.134	0.116	0.799	1.903	-2.888	-0.985	1.563	-0.807
N1–Ti	0.607	8.338	0.102	0.516	0.668	-0.749	-0.081	1.093	-0.134
P2–P3	0.844	-4.386	0.254	1.011	0.236	-0.776	-0.540	0.278	-0.642
P2–P1	0.857	-4.531	0.302	1.022	0.243	-0.810	-0.567	0.287	-0.658
P2–Ti	0.115	0.940	2.527	0.085	0.074	-0.081	-0.007	0.647	-0.071
Cl–Ti	0.459	5.254	0.005	0.543	0.418	-0.472	-0.054	0.923	-0.117

6b	ρ	$\nabla^2\rho$	ε	DI(A|B)	G	V	H	G/ρ	H/ρ
N2–Ti	1.458	18.387	0.012	1.753	2.220	-3.158	-0.931	1.526	-0.642
N1–P1	1.201	13.013	0.138	0.802	1.876	-2.841	-0.965	1.557	-0.8
N1–Ti	0.641	8.676	0.112	0.534	0.709	-0.810	-0.101	1.105	-0.157
N3–Ti	0.641	8.555	0.118	0.53	0.702	-0.803	-0.101	1.09	-0.159
N3–P3	1.208	13.230	0.119	0.797	1.890	-2.848	-0.958	1.567	-0.798
P1–P2	0.844	-4.362	0.269	1.042	0.223	-0.749	-0.526	0.263	-0.626
P2–P3	0.837	-4.241	0.247	1.033	0.216	-0.736	-0.513	0.262	-0.617
Cl–Ti	0.459	5.278	0.005	0.539	0.425	-0.479	-0.054	0.928	-0.117

A'

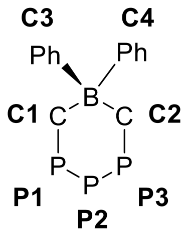

A'	ρ	∇²ρ	ε	DI(A|B)	G	V	H	G/ρ	H/ρ
C1–P1	1.161	-4.844	0.05	0.831	0.844	-2.025	-1.181	0.724	-1.016
C2–P3	1.181	-4.145	0.046	0.828	0.911	-2.112	-1.201	0.774	-1.02
P2–P3	0.857	-4.579	0.311	1.044	0.256	-0.830	-0.574	0.298	-0.670
P2–P1	0.837	-4.265	0.257	1.027	0.236	-0.776	-0.540	0.286	-0.644
C2–B	0.918	1.012	0.047	0.395	0.891	-1.714	-0.823	0.968	-0.892
C1–B	0.945	1.470	0.064	0.394	0.945	-1.782	-0.844	1.000	-0.891
B–C3	1.066	-0.313	0.056	0.425	0.992	-2.004	-1.012	0.931	-0.951
B–C4	1.059	-0.193	0.017	0.419	0.992	-1.998	-1.006	0.937	-0.950

7a

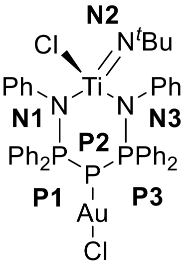

7b

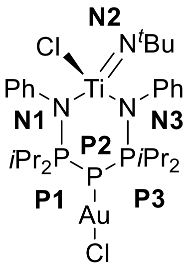

7a	ρ	∇²ρ	ε	DI(A|B)	G	V	H	G/ρ	H/ρ
N1–Ti	1.491	18.460	0.03	1.749	2.274	-3.253	-0.979	1.524	-0.658
N3–Ti	0.607	8.169	0.116	0.505	0.655	-0.736	-0.081	1.072	-0.132
N1–Ti	0.601	8.290	0.101	0.503	0.655	-0.729	-0.074	1.093	-0.123
N3–P3	1.228	14.218	0.061	0.789	1.971	-2.949	-0.979	1.608	-0.796
P2–P3	0.790	-3.109	0.197	0.815	0.223	-0.668	-0.445	0.284	-0.559
P2–P1	0.790	-3.253	0.258	0.871	0.223	-0.668	-0.445	0.280	-0.567
N1–P1	1.215	13.688	0.095	0.805	1.930	-2.902	-0.972	1.586	-0.798
Cl–Ti	0.466	5.446	0.019	0.544	0.439	-0.493	-0.061	0.936	-0.123
P2–Au	0.803	4.868	0.608	1.296	0.722	-1.100	-0.378	0.896	-0.472
Au–Cl	0.763	12.339	0.202	0.921	1.032	-1.201	-0.169	1.357	-0.220
P2–Ti	0.121	0.988	0.518	0.086	0.081	-0.088	-0.007	0.631	-0.074

7b	ρ	$\nabla^2\rho$	ε	DI(A|B)	G	V	H	G/ρ	H/ρ
Ti–P2	0.135	1.060	0.337	0.099	0.081	-0.094	-0.007	0.627	-0.070
Ti–Cl	0.459	5.398	0.027	0.527	0.432	-0.486	-0.054	0.939	-0.117
Ti–N2	1.478	18.749	0.026	1.733	2.274	-3.239	-0.965	1.539	-0.651
Au–P2	0.783	6.434	2.278	1.331	0.803	-1.147	-0.351	1.024	-0.447
Au–Cl	0.749	12.772	0.345	0.894	1.046	-1.201	-0.155	1.405	-0.207
Ti–N1	0.601	8.194	0.082	0.498	0.648	-0.722	-0.074	1.083	-0.124
P2–P1	0.776	-3.061	0.289	0.869	0.223	-0.668	-0.439	0.290	-0.564
N1–P1	1.201	14.025	0.136	0.818	1.930	-2.875	-0.945	1.602	-0.786
Ti–N3	0.655	8.555	0.112	0.534	0.709	-0.817	-0.108	1.082	-0.165
P2–P3	0.776	-3.012	0.227	0.876	0.223	-0.661	-0.439	0.290	-0.562
N3–P3	1.201	13.688	0.078	0.800	1.910	-2.861	-0.952	1.588	-0.791

9b

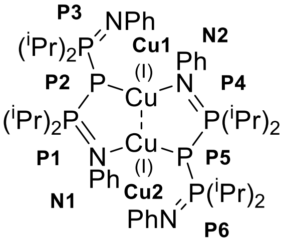

9b	ρ	$\nabla^2\rho$	ε	DI(A|B)	G	V	H	G/ρ	H/ρ
P2–P3	0.769	-3.350	0.180	0.910	0.169	-0.567	-0.398	0.215	-0.519
P2–Cu1	0.547	4.338	0.039	0.509	0.520	-0.742	-0.216	0.957	-0.399
P5–P6	0.769	-3.350	0.180	0.910	0.169	-0.567	-0.398	0.215	-0.519
P4–P5	0.817	-3.928	0.257	0.986	0.196	-0.661	-0.472	0.238	-0.574
P1–P2	0.817	-3.928	0.257	0.986	0.196	-0.661	-0.472	0.238	-0.574
N2–P4	1.228	14.821	0.119	0.815	2.011	-2.990	-0.979	1.636	-0.793
N3–P4	1.228	14.821	0.119	0.815	2.011	-2.990	-0.979	1.636	-0.793
Cu1–N2	0.675	12.073	0.080	0.419	1.059	-1.269	-0.209	1.564	-0.312
Cu2–P5	0.547	4.338	0.039	0.509	0.520	-0.742	-0.216	0.957	-0.399
Cu2–N3	0.675	12.073	0.080	0.419	1.059	-1.269	-0.209	1.564	-0.312
Cu2–Cu1	0.142	2.097	0.399	0.101	0.148	-0.155	-0.007	1.079	-0.040

Charge analysis

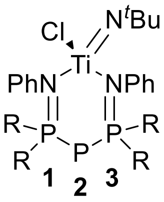

Atomic charges analysis - Bader charges					
	P1	**P2**	**P3**	Au	Cl
6a[1]	2.11	-0.06	2.13	--	--
6b[1]	1.98	-0.15	2.02	--	--
7a[2]	2.16	-0.30	2.15	1.21	(-0.71)
7b[2]	1.99	-0.29	2.01	1.07	(-0.74)

1. Level of theory: PCM(Toluene)-B3PW91-D3, 6-31+G**(other atoms) level of theory. 2. Level of theory: PCM(Toluene)-B3PW91-D3/def2-SVP-RIFIT(Au), 6-31+G**(other atoms)// PCM(Toluene)-B3PW91-D3/LANL2DZ(Au), 6-31+G**(other atoms) level of theory

P-Cu/Au bonds

According to the topological indexes at the BCP, the interaction between the central phosphorus and the coinage metal (**7b**: Au; **9b**: Cu) corresponds to donor-acceptor interactions between heavy atoms: the small density, the positive Laplacian, the **G/ρ** ratio close to unity and the negative **H/ρ** ratio are all consistent with this view.[22]

Moreover, the **DI** for the P-Cu bond in **9b** is clearly inferior to the formal bond order (0.509 *vs* 1): again this is indicative of a dative bond. In the case of **9b** the **DI** for the P-Au bond is superior to the formal bond order (1.331 *vs* 1), whilst it is inferior for the P-P bonds (~0.87 vs 1). This suggests a significant amount of backdonation to the **BIPP** ligand.[23] Indeed, the crystal structure of **7b** reveals considerably elongated P-P bonds compared to the other κ^3-P,N,N **BIPP** complexes (Table 2).

Cu-Cu interaction

The crystal structure of **9b** indicates the presence of cuprophilic interaction between the d^{10} Cu atoms (d_{Cu-Cu} < 3.29 Å).[24] The topological indexes computed at the Cu-Cu BCP are consistent with those obtained by Silvi. for a binuclear Cu amidinate complex with a Cu-Cu distance of 2.414 Å (ρ = 0.040 a.u. ; $\nabla^2\rho$ = 0.116 a.u.; **H/ρ** = -0.044 a.u.; **DI** = 0.328). This is in line with a weakly covalent character for cuprophilic interactions.[25]

---

[22] Phosphorus is not considered as heavy according to QTAIM (< 4 atomic shells), but as highlighted by Sironi and Macchi: " properties shown by heavy atoms are *in pectore* recognizable also in early elements of the first three rows" (P. Macchi, D. M. Proserpio and A. Sironi, *J. Am. Chem. Soc.* **1998**, *120*, 13429-13435), which explains why the P-Cu and P-Au bonds display topological indexes corresponding heavy atoms.

[23] P. Macchi and A. Sironi, *Coord. Chem. Rev.* **2003**, *238-239*, 383-412.

[24] N. V. S. Harisomayajula, S. Makovetskyi and Y.-C. Tsai, *Chem. Eur. J.* **2019**, *25*, 8936-8954.

[25] a) B. S. Lim, A. Rahtu, J.-S. Park and R. G. Gordon, *Inorg. Chem.* **2003**, *42*, 7951-7958; b) C. Lepetit, P. Fau, K. Fajerwerg, M. L. Kahn and B. Silvi, *Coord. Chem. Rev.* **2017**, *345*, 150-181.

*Natural Transition Orbitals for **9b** and **D**$^+$*

Natural transition orbitals[26] were computed for **9b** and **D**$^+$ are are displayed below (cutoff=0.06).

9b

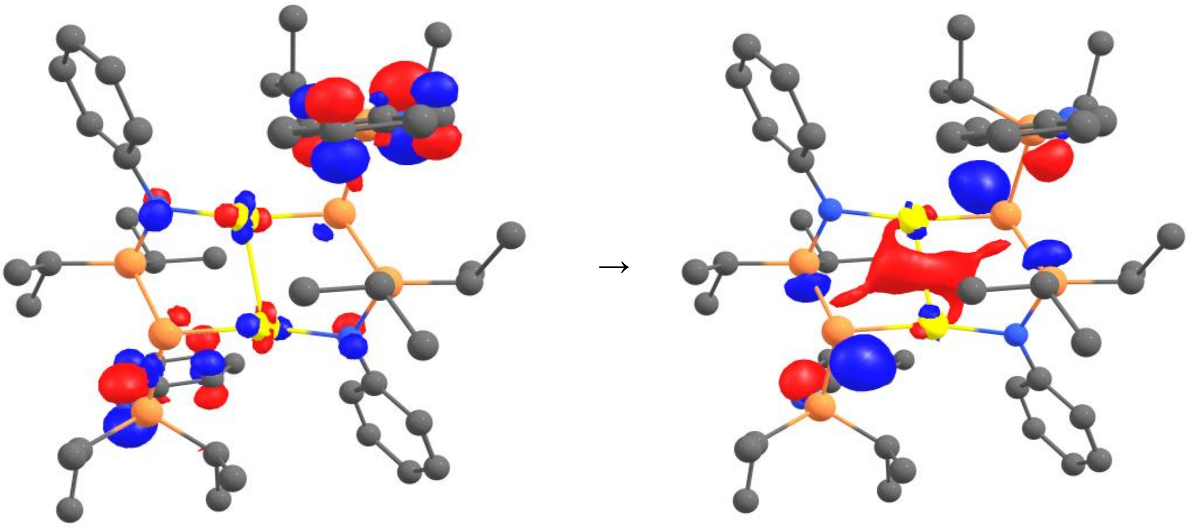

K$^+$

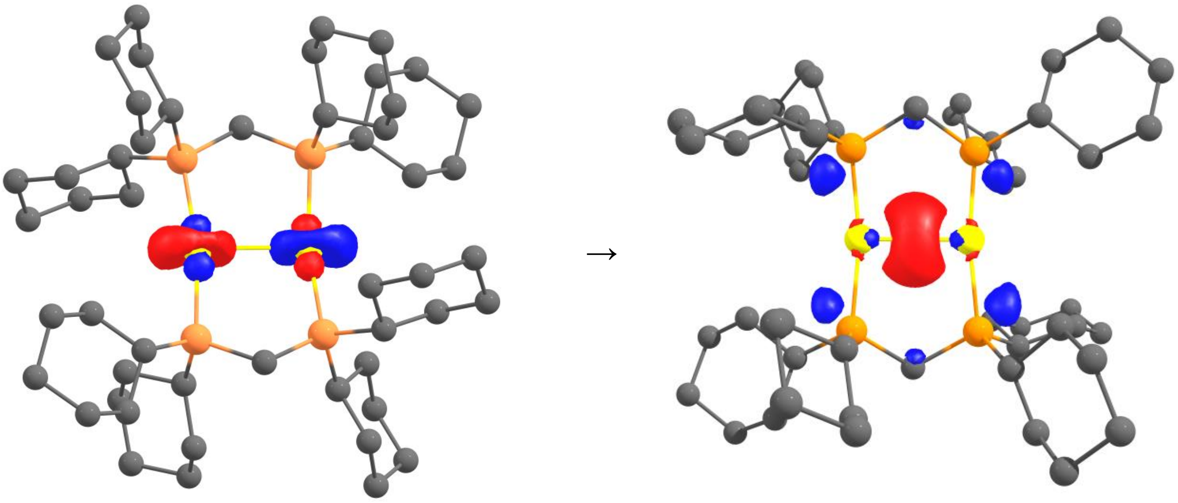

Figure S119. Natural Transition orbitals for 9b and D$^+$ (Color code: Copper atoms in yellow, Carbon atoms in gray and phosphorus atoms in orange. Hydrogen atoms are not displayed)

---

[26] R. L. Martin, *J. Chem. Phys.*, **2003**, *118*, 4775-4777.

Cartesian coordinates and energies in au

6a

Sum of electronic and zero-point Energies = -4044.696706

Sum of electronic and thermal Enthalpies = -4044.649590

Sum of electronic and thermal Free Energies = -4044.779069

C	0.63247	4.24378	-0.68336
C	1.56981	5.13943	0.14083
H	1.20874	5.21666	1.17046
H	1.61976	6.14515	-0.29229
H	2.57969	4.72081	0.15833
C	1.20768	4.04825	-2.09409
H	2.17690	3.54339	-2.03561
H	1.34220	5.01358	-2.59585
H	0.53107	3.43597	-2.69671
C	-0.76300	4.88313	-0.75492
H	-1.45114	4.24073	-1.30961
H	-0.71541	5.85981	-1.25077
H	-1.16101	5.02233	0.25488
C	3.15985	0.81900	-0.21426
C	3.90754	0.07805	-1.14243
H	3.53341	-0.86878	-1.51621
C	5.13314	0.55449	-1.60664
H	5.69271	-0.03691	-2.32623
C	5.63516	1.77652	-1.16229
H	6.58750	2.14684	-1.52960
C	4.89959	2.51386	-0.23099
H	5.27946	3.46338	0.13619
C	3.68397	2.03698	0.24620
H	3.11974	2.59963	0.98242
C	2.88295	-2.13255	1.01515
C	3.43221	-3.22575	0.34094
H	3.01131	-3.55644	-0.60284
C	4.54241	-3.87825	0.87424
H	4.97421	-4.72323	0.34625
C	5.10157	-3.44218	2.07544
H	5.96783	-3.95196	2.48660
C	4.55636	-2.34484	2.74453
H	4.99697	-1.99645	3.67357
C	3.45060	-1.68552	2.21607
H	3.03652	-0.81671	2.72083
C	0.97177	-1.81521	-1.21867
C	0.92698	-0.92355	-2.29407
H	1.21838	0.11040	-2.13808
C	0.50879	-1.36999	-3.54537
H	0.46911	-0.67606	-4.37962
C	0.13866	-2.70250	-3.72178
H	-0.19127	-3.04886	-4.69665
C	0.16838	-3.58952	-2.64404
H	-0.14840	-4.61892	-2.77539
C	0.57109	-3.14616	-1.38904
H	0.55238	-3.82157	-0.53886
C	-2.27989	-1.97977	-0.51417
C	-2.63181	-1.66907	-1.82938
H	-2.51853	-0.66075	-2.20532
C	-3.12921	-2.66844	-2.66596
H	-3.39328	-2.42244	-3.69007
C	-3.28141	-3.97068	-2.19633
H	-3.67109	-4.74375	-2.85227
C	-2.92297	-4.28405	-0.88304
H	-3.03029	-5.29951	-0.51337
C	-2.41909	-3.29452	-0.04645
H	-2.12296	-3.53746	0.97076
C	-3.06728	-0.55313	1.84954
C	-4.33407	-1.09096	1.59655
H	-4.50619	-1.68992	0.70863
C	-5.38125	-0.84370	2.48273
H	-6.36433	-1.25925	2.28222
C	-5.16793	-0.06261	3.61872
H	-5.98602	0.12848	4.30711
C	-3.90470	0.47698	3.86946
H	-3.73526	1.08984	4.74948
C	-2.85456	0.23823	2.98744
H	-1.87763	0.67667	3.17568
C	-2.14371	1.38431	-0.92967
C	-3.42376	1.80096	-0.54931
H	-3.77020	1.60993	0.46048
C	-4.23933	2.47665	-1.45784
H	-5.22887	2.79976	-1.14689
C	-3.78844	2.74864	-2.74908
H	-4.42415	3.27923	-3.45146
C	-2.50526	2.34354	-3.12587
H	-2.13536	2.56067	-4.12418
C	-1.69030	1.66749	-2.22386
H	-0.69084	1.35379	-2.49873
Cl	0.30011	2.24834	3.08519
N	0.52057	2.96203	-0.04464
N	1.91304	0.40359	0.29446
N	-1.27831	0.69951	-0.03278
P	-0.06202	-1.39864	1.90284
P	1.46425	-1.18616	0.40353
P	-1.68919	-0.73804	0.67583
Ti	0.33735	1.56967	0.85330

6b

Sum of electronic and zero-point Energies = -3592.377182

Sum of electronic and thermal Enthalpies = -3592.331955

Sum of electronic and thermal Free Energies = -3592.452805

C	1.05550	3.58072	0.38939
C	-0.18563	4.48330	0.45502
H	-0.92898	4.16283	-0.27962
H	0.08382	5.52655	0.25170

H	-0.64054	4.42676	1.44883
C	2.08758	4.02312	1.43690
H	1.66374	3.93627	2.44196
H	2.39277	5.06278	1.26907
H	2.97339	3.38386	1.38217
C	1.67347	3.63924	-1.01561
H	2.55035	2.98876	-1.07229
H	1.97709	4.66328	-1.26354
H	0.94388	3.30114	-1.75800
C	-2.19763	1.51104	-0.50061
C	-3.20999	2.22760	0.14771
H	-3.46893	1.96566	1.16886
C	-3.85696	3.27742	-0.50261
H	-4.63522	3.83124	0.01483
C	-3.50057	3.62417	-1.80663
H	-4.00242	4.44443	-2.31093
C	-2.48269	2.91886	-2.45247
H	-2.18591	3.19222	-3.46121
C	-1.83425	1.87123	-1.80323
H	-1.02204	1.33398	-2.28208
C	-3.46861	-1.20033	1.48126
H	-4.24551	-0.52078	1.10558
C	-2.95896	-0.66556	2.81772
H	-2.17585	-1.30559	3.23227
H	-3.78866	-0.62666	3.53145
H	-2.54115	0.33914	2.72437
C	-4.05371	-2.60652	1.61808
H	-4.50992	-2.96526	0.69300
H	-4.82948	-2.60277	2.39081
H	-3.28609	-3.32574	1.92051
C	-2.97705	-1.42040	-1.44742
H	-2.30913	-0.90088	-2.14464
C	-4.36536	-0.78351	-1.56567
H	-5.08852	-1.27274	-0.90636
H	-4.72328	-0.90811	-2.59334
H	-4.35680	0.28525	-1.34365
C	-3.01619	-2.90589	-1.80557
H	-2.06193	-3.40139	-1.61371
H	-3.26440	-3.01966	-2.86613
H	-3.77859	-3.43611	-1.22912
C	2.78530	0.13151	-0.48920
C	3.12062	0.22949	-1.84555
H	2.42261	-0.11373	-2.59948
C	4.32531	0.81348	-2.23706
H	4.56278	0.88717	-3.29478
C	5.20884	1.32085	-1.28508
H	6.14225	1.78214	-1.59316
C	4.87180	1.24344	0.06794
H	5.54114	1.64842	0.82168
C	3.67570	0.65129	0.46184
H	3.40230	0.60102	1.51137
C	2.36031	-3.08173	0.72007
H	1.91370	-4.08515	0.71840
C	2.50700	-2.59923	2.16403
H	2.93959	-1.59677	2.19575
H	3.17332	-3.27814	2.70610
H	1.54992	-2.55789	2.68785
C	3.71900	-3.12672	0.01371
H	3.66399	-3.54429	-0.99462
H	4.39775	-3.75969	0.59496
H	4.16578	-2.13119	-0.05062
C	1.23840	-2.53397	-1.94549
H	2.27615	-2.31039	-2.22327
C	0.30238	-1.69677	-2.81405
H	-0.71482	-2.08407	-2.75455
H	0.61360	-1.74832	-3.86221
H	0.28759	-0.64655	-2.50905
C	0.98518	-4.03168	-2.10710
H	1.74556	-4.64007	-1.61115
H	0.99029	-4.29294	-3.17040
H	0.01041	-4.30918	-1.69371
Cl	0.58056	0.43007	3.37119
N	0.66406	2.22914	0.66865
N	-1.52244	0.44927	0.15492
N	1.55476	-0.41148	-0.03738
P	-2.15049	-1.08440	0.18526
P	-0.66872	-2.47516	0.88403
P	1.14532	-2.00951	-0.17984
Ti	0.25844	0.66413	1.07331

7b

Sum of electronic and zero-point Energies = -4188.120247

Sum of electronic and thermal Enthalpies = -4188.070874

Sum of electronic and thermal Free Energies = -4188.203467

Au	-3.51003	0.14337	-0.25249
Ti	1.74164	-0.07332	-1.27749
Cl	1.26634	0.17221	-3.54033
N	3.39268	-0.12543	-1.10774
P	-1.29811	-0.01174	-0.82041
Cl	-5.79330	0.31462	0.29635
N	1.12841	-1.59583	-0.05787
P	-0.49789	-1.85863	0.04439
C	5.38561	-0.56721	0.19913
H	6.48138	-0.58831	0.17487
H	5.01978	-1.56649	0.44848
C	5.28212	-1.08277	-2.26107
H	4.94492	-2.09850	-2.03079
H	6.37479	-1.08813	-2.34859
H	4.85150	-0.78612	-3.22217
C	5.29694	1.31254	-1.47666
H	4.88502	1.63745	-2.43703
H	6.39103	1.35662	-1.52939
H	4.95487	2.00592	-0.70334
C	2.08270	-2.27867	0.74359
C	2.75974	-3.39825	0.24891
H	2.54297	-3.74205	-0.75733
C	3.70702	-4.05085	1.03598
H	4.22924	-4.91660	0.63873
C	3.98989	-3.59401	2.32513
H	4.72982	-4.10269	2.93547
C	3.32201	-2.47202	2.81873
H	3.54117	-2.10127	3.81612
C	2.37752	-1.81780	2.03125
H	1.85578	-0.94234	2.40486

C	-0.99769	-2.40867	1.74316
H	-0.52552	-1.65507	2.38615
C	-0.42122	-3.78981	2.09120
H	-0.90320	-4.57392	1.50019
H	-0.64223	-3.99526	3.14374
H	0.65719	-3.86108	1.95544
C	-2.50862	-2.41508	1.98866
H	-3.02574	-1.54082	1.58270
H	-2.69259	-2.44598	3.06688
H	-2.96944	-3.30438	1.55206
C	-1.04458	-3.15742	-1.15663
H	-0.79081	-4.09552	-0.64519
C	-2.54692	-3.13142	-1.45215
H	-3.16876	-3.13179	-0.55595
H	-2.80715	-4.01512	-2.04337
H	-2.81208	-2.25019	-2.04358
C	-0.23075	-3.06006	-2.44592
H	-0.41455	-2.11501	-2.96523
H	-0.52088	-3.87679	-3.11442
H	0.84271	-3.13214	-2.26147
C	4.82814	-0.11527	-1.15818
H	5.06862	0.12138	0.98638
N	1.24505	1.50893	-0.13935
P	-0.33863	1.58559	0.33238
C	2.21760	2.39415	0.40482
C	2.40558	3.66720	-0.14275
H	1.81179	3.96675	-1.00060
C	3.37010	4.52485	0.38863
H	3.51219	5.50866	-0.04947
C	4.15753	4.11766	1.46573
H	4.91032	4.78429	1.87558
C	3.98261	2.83926	2.00251
H	4.60405	2.50522	2.82873
C	3.02177	1.98253	1.47406
H	2.89622	0.97796	1.86204
C	-0.44038	1.57346	2.17867
H	0.34210	0.84662	2.43568
C	-0.05244	2.93664	2.76930
H	-0.82751	3.68444	2.58311
H	0.04610	2.82968	3.85449
H	0.89601	3.31404	2.38488
C	-1.77589	1.08824	2.73520
H	-2.04755	0.10531	2.35449
H	-1.70694	1.02557	3.82620
H	-2.59407	1.76842	2.48905
C	-1.08003	3.14331	-0.32215
H	-0.36534	3.88882	0.05656
C	-2.47687	3.49262	0.18521
H	-2.52367	3.59932	1.27021
H	-2.78226	4.44705	-0.25565
H	-3.21356	2.73996	-0.11411
C	-1.01637	3.12986	-1.85177
H	-1.78712	2.47326	-2.26703
H	-1.20012	4.14043	-2.22958
H	-0.04773	2.78893	-2.22616

9b

Sum of electronic and zero-point Energies = -4532.928638

Sum of electronic and thermal Enthalpies = -4532.853953

Sum of electronic and thermal Free Energies = -4533.043670

Cu	0.41738	-1.08856	0.54229
C	-1.11329	-3.21994	1.75916
N	-1.12590	-2.22339	0.78155
P	-2.33394	-1.77961	-0.23343
C	-0.63153	-2.88960	3.04019
H	-0.38144	-1.85046	3.23555
N	-4.23628	0.52982	-2.56553
P	-2.37638	0.34944	0.18862
C	-0.49071	-3.85533	4.03125
H	-0.09832	-3.56943	5.00347
P	-3.72922	1.33047	-1.27135
C	-0.85907	-5.17982	3.78114
H	-0.75341	-5.93641	4.55273
C	-1.36370	-5.51663	2.52409
H	-1.64991	-6.54348	2.31138
C	-1.48199	-4.55525	1.52042
H	-1.82808	-4.84622	0.53414
C	-3.93703	-2.56239	0.21866
H	-3.71010	-3.63126	0.31129
C	-4.40151	-2.05629	1.58468
H	-3.62707	-2.17603	2.34752
H	-5.28381	-2.62309	1.90000
H	-4.67019	-0.99726	1.53960
C	-4.98826	-2.36327	-0.87604
H	-5.07761	-1.31674	-1.18304
H	-5.96198	-2.70458	-0.50912
H	-4.75332	-2.93315	-1.77873
C	-1.94653	-2.27203	-1.96443
H	-2.72296	-1.80465	-2.57925
C	-1.99582	-3.79442	-2.11665
H	-1.20284	-4.26420	-1.52598
H	-1.82577	-4.05252	-3.16688
H	-2.95460	-4.22935	-1.82233
C	-0.58192	-1.75106	-2.40103
H	-0.49111	-0.66894	-2.26607
H	-0.43629	-1.96125	-3.46423
H	0.22037	-2.23271	-1.83259
C	-3.52789	0.17165	-3.68680
C	-4.15237	-0.71345	-4.59958
H	-5.15565	-1.05735	-4.36353
C	-3.50675	-1.14170	-5.75345
H	-4.01862	-1.82640	-6.42573
C	-2.21220	-0.70361	-6.05754
H	-1.70968	-1.03951	-6.95962
C	-1.58340	0.17583	-5.17580
H	-0.57547	0.52782	-5.38456
C	-2.22326	0.60520	-4.01649
H	-1.69945	1.27291	-3.34316
C	-2.82514	2.92912	-1.60730
H	-1.82280	2.57269	-1.88567
C	-2.64678	3.83165	-0.38795

H	-3.58064	4.33499	-0.12268
H	-1.90324	4.60123	-0.62083
H	-2.28864	3.28199	0.48831
C	-3.40022	3.67345	-2.81110
H	-3.55852	3.00508	-3.66092
H	-2.69326	4.45253	-3.11642
H	-4.35240	4.15393	-2.57214
C	-5.30729	1.62848	-0.35263
H	-5.72704	0.61372	-0.35711
C	-6.25163	2.53315	-1.14593
H	-5.92722	3.57742	-1.09974
H	-7.25723	2.48312	-0.71395
H	-6.30915	2.22673	-2.19324
C	-5.16379	2.08140	1.09899
H	-4.45011	1.46493	1.65228
H	-6.13744	2.00641	1.59520
H	-4.83886	3.12215	1.17058
Cu	-0.41738	1.08856	-0.54229
C	1.11329	3.21994	-1.75916
N	1.12590	2.22339	-0.78155
P	2.33394	1.77961	0.23343
C	0.63153	2.88960	-3.04019
H	0.38144	1.85046	-3.23555
N	4.23628	-0.52982	2.56553
P	2.37638	-0.34944	-0.18862
C	0.49071	3.85533	-4.03125
H	0.09832	3.56943	-5.00347
P	3.72922	-1.33047	1.27135
C	0.85907	5.17982	-3.78114
H	0.75341	5.93641	-4.55273
C	1.36370	5.51663	-2.52409
H	1.64991	6.54348	-2.31138
C	1.48199	4.55525	-1.52042
H	1.82808	4.84622	-0.53414
C	3.93703	2.56239	-0.21866
H	3.71010	3.63126	-0.31129
C	4.40151	2.05629	-1.58468
H	3.62707	2.17603	-2.34752
H	5.28381	2.62309	-1.90000
H	4.67019	0.99726	-1.53960
C	4.98826	2.36327	0.87604
H	5.07761	1.31674	1.18304
H	5.96198	2.70458	0.50912
H	4.75332	2.93315	1.77873
C	1.94653	2.27203	1.96443
H	2.72296	1.80465	2.57925
C	1.99582	3.79442	2.11665
H	1.20284	4.26420	1.52598
H	1.82577	4.05252	3.16688
H	2.95460	4.22935	1.82233
C	0.58192	1.75106	2.40103
H	0.49111	0.66894	2.26607
H	0.43629	1.96125	3.46423
H	-0.22037	2.23271	1.83259
C	3.52789	-0.17165	3.68680
C	4.15237	0.71345	4.59958
H	5.15565	1.05735	4.36353
C	3.50675	1.14170	5.75345
H	4.01862	1.82640	6.42573
C	2.21220	0.70361	6.05754
H	1.70968	1.03951	6.95962
C	1.58340	-0.17583	5.17580
H	0.57547	-0.52782	5.38456
C	2.22326	-0.60520	4.01649
H	1.69945	-1.27291	3.34316
C	2.82514	-2.92912	1.60730
H	1.82280	-2.57269	1.88567
C	2.64678	-3.83165	0.38795
H	3.58064	-4.33499	0.12268
H	1.90324	-4.60123	0.62083
H	2.28864	-3.28199	-0.48831
C	3.40022	-3.67345	2.81110
H	3.55852	-3.00508	3.66092
H	2.69326	-4.45253	3.11642
H	4.35240	-4.15393	2.57214
C	5.30729	-1.62848	0.35263
H	5.72704	-0.61372	0.35711
C	6.25163	-2.53315	1.14593
H	5.92722	-3.57742	1.09974
H	7.25723	-2.48312	0.71395
H	6.30915	-2.22673	2.19324
C	5.16379	-2.08140	-1.09899
H	4.45011	-1.46493	-1.65228
H	6.13744	-2.00641	-1.59520
H	4.83886	-3.12215	-1.17058

A

Sum of electronic and zero-point Energies = -2516.475369

Sum of electronic and thermal Enthalpies = -2516.437513

Sum of electronic and thermal Free Energies = -2516.546550

C	-2.86999	1.51664	-1.72083
C	-4.22126	1.51034	-1.36126
H	-4.54020	1.00905	-0.45279
C	-5.15832	2.14774	-2.17373
H	-6.20685	2.14124	-1.89114
C	-4.75208	2.78794	-3.34412
H	-5.48470	3.28173	-3.97559
C	-3.40321	2.79380	-3.70475
H	-3.08360	3.29000	-4.61618
C	-2.46230	2.16209	-2.89614
H	-1.41314	2.16297	-3.17999
C	-2.49973	-0.18057	0.61763
C	-2.59817	0.29533	1.93017
H	-2.17097	1.25369	2.20454
C	-3.22143	-0.48136	2.90607
H	-3.28187	-0.11286	3.92580
C	-3.75446	-1.72764	2.57624
H	-4.22803	-2.33506	3.34200
C	-3.66770	-2.19929	1.26588
H	-4.06521	-3.17556	1.00724
C	-3.03780	-1.43170	0.29163
H	-2.92464	-1.81000	-0.72023
C	-0.11634	-2.86349	0.30147
C	-0.15794	-3.16053	1.66673

H	0.25751	-2.46870	2.39182
C	-0.75264	-4.34259	2.10775
H	-0.79247	-4.55941	3.17117
C	-1.30106	-5.23505	1.18885
H	-1.77038	-6.15178	1.53397
C	-1.24961	-4.94711	-0.17719
H	-1.67629	-5.63929	-0.89728
C	-0.66321	-3.76523	-0.61844
H	-0.65439	-3.52170	-1.67752
C	2.25926	-1.75359	-0.90209
C	3.04136	-2.62727	-0.13626
H	2.64153	-3.06522	0.77420
C	4.33444	-2.93779	-0.54693
H	4.94240	-3.61186	0.04933
C	4.84427	-2.38809	-1.72548
H	5.85407	-2.63071	-2.04371
C	4.06057	-1.52532	-2.48935
H	4.45824	-1.08319	-3.39730
C	2.76888	-1.20389	-2.07892
H	2.16886	-0.49992	-2.64634
C	-0.58366	1.98770	0.11521
C	0.76396	-0.19400	1.11482
P	-0.52505	-0.55793	-1.98060
P	-1.60438	0.74021	-0.67612
P	0.60593	-1.29671	-0.30575
B	0.85845	1.41939	0.74483
H	-0.40228	2.74978	-0.65087
H	-1.20045	2.47495	0.87881
H	-0.08205	-0.41447	1.77171
H	1.67778	-0.50978	1.63270
C	2.11117	1.63145	-0.27029
C	3.40345	1.29960	0.17895
C	2.02210	2.11092	-1.58377
C	4.53249	1.42950	-0.62472
C	3.14400	2.25569	-2.40532
C	4.40766	1.91236	-1.92951
H	3.52693	0.93134	1.19602
H	1.05028	2.36427	-1.99848
H	5.50991	1.15053	-0.23860
H	3.02715	2.62985	-3.42009
H	5.28342	2.01546	-2.56498
C	1.09007	2.25391	2.12384
C	1.72991	3.50578	2.10479
C	0.59994	1.82717	3.36982
C	1.86920	4.28861	3.25111
C	0.73476	2.59589	4.52876
C	1.37084	3.83611	4.47459
H	2.13779	3.86987	1.16411
H	0.09818	0.86461	3.44997
H	2.37220	5.25130	3.19255
H	0.34605	2.22483	5.47475
H	1.48094	4.43906	5.37219

$P(CN)_2^-$

Sum of electronic and zero-point Energies = -527.023972

Sum of electronic and thermal Enthalpies = -527.018015

Sum of electronic and thermal Free Energies = -527.052011

P	-0.00000	0.00000	0.98754
C	0.00000	1.31494	-0.20056
N	0.00000	2.26857	-0.88617
C	-0.00000	-1.31494	-0.20056
N	-0.00000	-2.26857	-0.88617

V. Crystallographic studies

Additional bond distances and angles

2b': Li-O = 1.904(6). **3a**: Ti-Cl1 = 2.3688(6), Ti-Cl2 = 2.3542(6), Cl1-Ti-N2 = 164.21(4), Cl2-Ti-P2 = 161.358(18), N1-Ti-O = 170.28(5). **3b**: Ti-Cl1 = 2.3119(5), Ti-Cl2 = 2.3384(5), Cl1-Ti-N1/2 = 110.74(4)/ 134.39(4), Cl2-Ti-N1/2 = 100.71(4)/ 92.39(4), Cl2-Ti-P2 = 164.981(19). **4a**: Ti-O1 = 1.782(3), Ti-O2 = 1.770(3), O1-Ti-N1/2 = 124.02(13)/101.70(13), O2-Ti-N1/2 = 94.33(12)/ 101.70(13), O2-Ti-P2 = 164.15(9). **5a-1/5a-2** (labels are those of **5a-1**): Zr1-Cl1 = 2.4367(6)/2.4475(5), Zr1-Cl2 = 2.3734(5)/2.3734(5), Zr1-Cl3 = 2.4584(5)/2.4577(5), Cl1-Zr1-N1 = 160.18(4)/157.88(4), Cl2-Zr1-P2 = 160.49(2)/161.13(2), Cl3-Zr1-N2 = 164.23(4)/166.39(4). **5b**: Zr-Cl1 = 2.4704(4), Zr-Cl2 = 2.3958(4), Zr-Cl3 = 2.4397(4), Cl1-Zr-N2 = 159.19(3), Cl2-Zr-P2 = 152.12(2), Cl3-Zr-N1 = 173.50(4), Cl3-Zr-N2 = 84.95(4). **6a-Py**: Ti-N3 = 1.685(5), Ti-Cl = 2.422(2), Cl-Ti-N1 = 93.70(14), Cl-Ti-N2 = 154.30(14), N1-Ti-N4 = 162.1(2), N3-Ti-P2 = 167.66(18), Ti-N3-C1 = 163.7(4). **6a**: Ti-N3 = 1.6945(19), Ti-Cl = 2.3362(7), Cl-Ti-N1 = 117.41(6), Cl-Ti-N2 = 119.76(6), N3-Ti-P2 = 171.37(7), Ti-N3-C37 = 164.38(16). **6b-1/6b-2**: Ti-N3 = 1.6912(13)/1.7007(13), Ti-Cl = 2.3357(5)/2.3575(5), Cl-Ti-N1 = 123.85(4)/122.79(4), Cl-Ti-N2 = 112.84(4)/113.46(4), N3-Ti-P2 = 167.20(5)/167.63(5), Ti-N3-C1 = 174.81(12)/168.28(12). **7b** (^{i}: X, 3/2-Y, Z): Ti-N2 = 1.682(3), Ti-Cl1 = 2.3234(12), Au-Cl2 2.2934(10), Cl1-Ti-N1 = 120.20(7), Ti-N3-C1 = 169.7(3), P2-Ti-N2 = 167.55(13), Au-P2-Ti = 173.36(5), Cl2-Au-P2 = 176.43(4), $\Sigma\alpha$(P2) = 327.51(8). **8b** (^{i}: 1-X, 1-Y, 1-Z): Ti-N3 = 1.688(3), Ti-Cl1 = 2.3541(9), Cu-Br = 2.3807(6), Cu-Br^{i} = 2.4472(6), Cl1-Ti-N1 = 118.11(8), Cl1-Ti-N2 = 121.47 (8), Ti-N3-C25 = 174.7(3), P2-Ti-N3 = 164.42(10), Cu-P2-Ti = 172.66(4), Br-Cu-P2 = 135.78(3), Br^{i}-Cu-P2 = 122.43(3), $\Sigma\alpha$(P2) = 333.31(8), $\Sigma\alpha$(Cu) = 359.23(5). **9b**: (^{i} 3/2-X, 3/2-Y, 1-Z): Cu-Cu^{i} = 2.5759(4), P2^{i}-Cu-N1 = 165.25(5).

*Crystal data and structure refinement for **2b'***

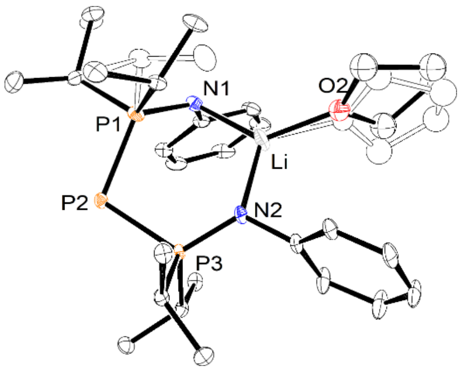

Fig S120: Crystal structure of 2b'

Table S1: Crystal data and structure refinement for 2b'

Identification code	2b'
Empirical formula	$C_{28}H_{46}LiN_2OP_3$
Formula weight	526.52

Temperature/K	100.0
Crystal system	monoclinic
Space group	$P2_1/n$
a/Å	10.215(4)
b/Å	30.038(9)
c/Å	10.723(4)
α/°	90
β/°	116.107(12)
γ/°	90
Volume/Å^3	2954.5(18)
Z	4
ρ_{calc}g/cm^3	1.184
μ/mm^{-1}	0.224
F(000)	1136.0
Crystal size/mm^3	0.34 × 0.33 × 0.2
Radiation	MoKα (λ = 0.71073)
2Θ range for data collection/°	5.87 to 55.094
Index ranges	$-13 \le h \le 13, -39 \le k \le 39, -13 \le l \le 13$
Reflections collected	48835
Independent reflections	6783 [R_{int} = 0.0267, R_{sigma} = 0.0167]
Data/restraints/parameters	6783/0/323
Goodness-of-fit on F^2	1.024
Final R indexes [I>=2σ (I)]	R_1 = 0.0680, wR_2 = 0.1758
Final R indexes [all data]	R_1 = 0.0759, wR_2 = 0.1835
Largest diff. peak/hole / e Å^{-3}	2.02/-1.18
CCDC	1985134

Special refinement details for **2b'**

The tetrahydrofuran molecule is not located very precisely. This tetrahydrofuran molecule was isotropically refined on two positions with a set of constraints (EADP) applied on the isotropic temperature factors. The occupations factors of the two components of the disorder converged to approximately the same values than for the disordered isopropyl groups. In view of the inter and intra-molecular interactions between these groups, the occupation factors for both groups (tetrahydrofuran and isopropyl) were set to the same value (0.63:037).

*Crystal data and structure refinement for **3a***

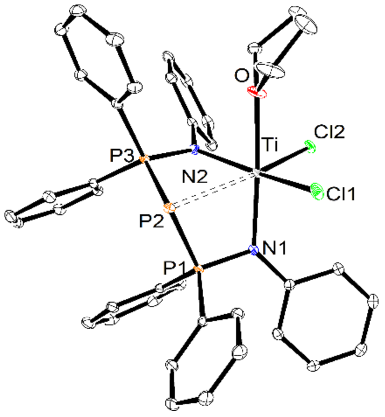

Fig S121: Crystal structure of 3a

Table S2: Crystal data and structure refinement for 3a

Identification code	3a
Internal reference	ad240717_0m
Empirical formula	$C_{40}H_{38}Cl_2N_2OP_3Ti$
Formula weight	774.43
Temperature/K	115
Crystal system	monoclinic
Space group	$P2_1/n$
a/Å	10.1219(16)
b/Å	16.662(3)
c/Å	22.432(4)
α/°	90
β/°	99.270(3)
γ/°	90
Volume/Å^3	3733.8(10)
Z	4
ρ_{calc}g/cm^3	1.378
μ/mm^{-1}	0.536
F(000)	1604.0
Crystal size/mm^3	0.3 × 0.25 × 0.22
Radiation	MoKα (λ = 0.71073)
2Θ range for data collection/°	4.754 to 54.988
Index ranges	$-13 \le h \le 12, -21 \le k \le 21, -29 \le l \le 28$
Reflections collected	47407
Independent reflections	8521 [R_{int} = 0.0354, R_{sigma} = 0.0247]
Data/restraints/parameters	8521/0/442
Goodness-of-fit on F^2	1.036
Final R indexes [I>=2σ (I)]	R_1 = 0.0316, wR_2 = 0.0721
Final R indexes [all data]	R_1 = 0.0419, wR_2 = 0.0784
Largest diff. peak/hole / e Å^{-3}	0.73/-0.54
CCDC	1985143

*Crystal data and structure refinement for **3b***

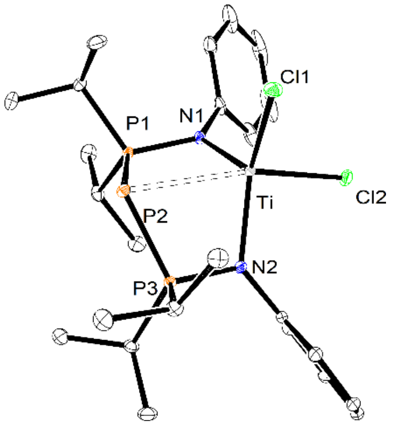

Fig S122: Crystal structure of 3b

Table S3: Crystal data and structure refinement for 3b

Identification code	3b
Internal reference	mo_matrix_0m with mo_ad150318_0m.hkl
Empirical formula	$C_{24}H_{38}Cl_2N_2P_3Ti$
Formula weight	566.27
Temperature/K	100
Crystal system	monoclinic
Space group	$P2_1/n$
a/Å	11.1686(13)
b/Å	15.390(2)
c/Å	16.608(2)
α/°	90
β/°	99.796(6)
γ/°	90
Volume/Å^3	2813.1(7)
Z	4
ρ_{calc}g/cm^3	1.337
μ/mm^{-1}	0.680
F(000)	1188.0
Crystal size/mm^3	0.32 × 0.32 × 0.075
Radiation	MoKα (λ = 0.71073)
2Θ range for data collection/°	6.264 to 55.166
Index ranges	$-14 \leq h \leq 14$, $-19 \leq k \leq 20$, $-17 \leq l \leq 21$
Reflections collected	50555
Independent reflections	6479 [R_{int} = 0.0306, R_{sigma} = 0.0195]
Data/restraints/parameters	6479/0/297
Goodness-of-fit on F^2	1.086
Final R indexes [I>=2σ (I)]	R_1 = 0.0295, wR_2 = 0.0624
Final R indexes [all data]	R_1 = 0.0395, wR_2 = 0.0685
Largest diff. peak/hole / e Å^{-3}	0.40/-0.28
CCDC	1985146

*Crystal data and structure refinement for **4a***

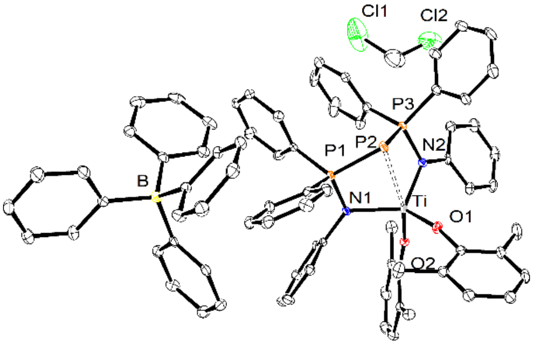

Fig S123: Crystal structure of 4a

Table S4: Crystal data and structure refinement for 4a

Identification code	4a
Internal reference	ad171017_0m_a
Empirical formula	$C_{77}H_{70}BCl_2N_2O_2P_3Ti$
Formula weight	1277.87
Temperature/K	115
Crystal system	triclinic
Space group	P-1
a/Å	11.7665(19)
b/Å	13.781(2)
c/Å	20.643(3)
α/°	82.299(4)
β/°	86.711(4)
γ/°	80.965(4)
Volume/Å^3	3273.8(9)
Z	2
ρ_{calc}g/cm^3	1.296
μ/mm^{-1}	0.335
F(000)	1336.0
Crystal size/mm^3	0.4 × 0.12 × 0.08
Radiation	MoKα (λ = 0.71073)
2Θ range for data collection/°	5.21 to 50.084
Index ranges	$-14 \le h \le 14$, $-16 \le k \le 15$, $-23 \le l \le 24$
Reflections collected	39257
Independent reflections	11547 [R_{int} = 0.0776, R_{sigma} = 0.0943]
Data/restraints/parameters	11547/0/797
Goodness-of-fit on F^2	1.024
Final R indexes [I>=2σ (I)]	R_1 = 0.0594, wR_2 = 0.1400
Final R indexes [all data]	R_1 = 0.1179, wR_2 = 0.1675
Largest diff. peak/hole / e Å^{-3}	1.34/-1.23
CCDC	1985140

*Crystal data and structure refinement for **5a***

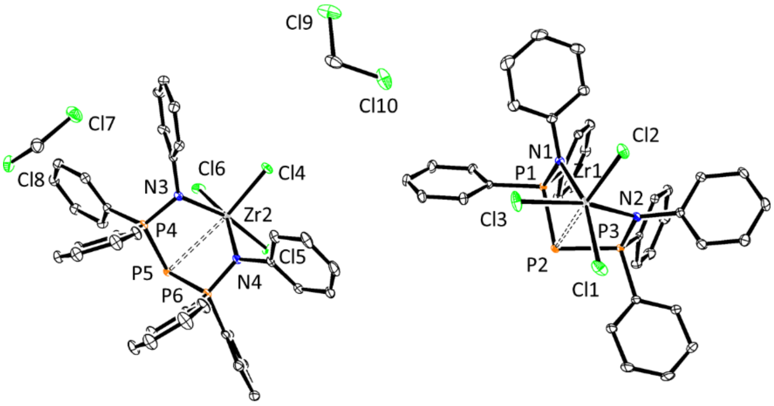

Fig S124: Crystal structure of 5a

Table S5: Crystal data and structure refinement for 5a

Identification code	5a
Empirical formula	$C_{147}H_{126}Cl_{18}N_8P_{12}Zr_4$
Formula weight	3379.17
Temperature/K	100
Crystal system	triclinic
Space group	P-1
a/Å	11.8938(12)
b/Å	12.0699(11)
c/Å	27.548(3)
α/°	82.319(4)
β/°	80.357(5)
γ/°	70.217(4)
Volume/Å^3	3656.1(6)
Z	1
ρ_{calc}g/cm^3	1.535
μ/mm^{-1}	0.791
F(000)	1710.0
Crystal size/mm^3	0.4 × 0.32 × 0.19
Radiation	MoKα (λ = 0.71073)
2Θ range for data collection/°	5.916 to 55.078
Index ranges	$-15 \leq h \leq 15, -15 \leq k \leq 15, -35 \leq l \leq 35$
Reflections collected	106171
Independent reflections	16785 [R_{int} = 0.0270, R_{sigma} = 0.0177]
Data/restraints/parameters	16785/22/865
Goodness-of-fit on F^2	1.037
Final R indexes [I>=2σ (I)]	R_1 = 0.0277, wR_2 = 0.0653
Final R indexes [all data]	R_1 = 0.0335, wR_2 = 0.0681
Largest diff. peak/hole / e Å^{-3}	1.05/-0.76
CCDC	1985141

*Crystal data and structure refinement for **5b***

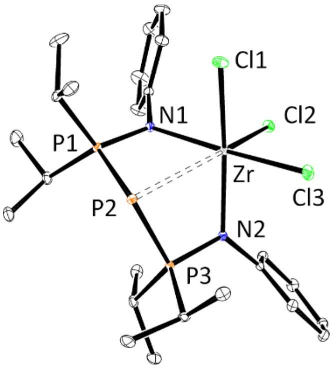

Fig S125: Crystal structure of 5b

Table S6: Crystal data and structure refinement for 5b

Identification code	5b
Empirical formula	$C_{24}H_{38}Cl_3N_2P_3Zr$
Formula weight	645.04
Temperature/K	100
Crystal system	orthorhombic
Space group	Pbca
a/Å	16.4550(9)
b/Å	16.2910(8)
c/Å	22.0025(12)
α/°	90
β/°	90
γ/°	90
Volume/Å^3	5898.2(5)
Z	8
ρ_{calc}g/cm^3	1.453
μ/mm^{-1}	0.824
F(000)	2656.0
Crystal size/mm^3	0.26 × 0.156 × 0.124
Radiation	MoKα (λ = 0.71073)
2Θ range for data collection/°	5.548 to 55.068
Index ranges	$-21 \le h \le 21, -21 \le k \le 21, -28 \le l \le 28$
Reflections collected	103469
Independent reflections	6784 [R_{int} = 0.0452, R_{sigma} = 0.0180]
Data/restraints/parameters	6784/0/306
Goodness-of-fit on F^2	1.050
Final R indexes [I>=2σ (I)]	R_1 = 0.0220, wR_2 = 0.0503
Final R indexes [all data]	R_1 = 0.0307, wR_2 = 0.0540
Largest diff. peak/hole / e Å^{-3}	0.39/-0.27
CCDC	1985135

*Crystal data and structure refinement for **6a-Py***

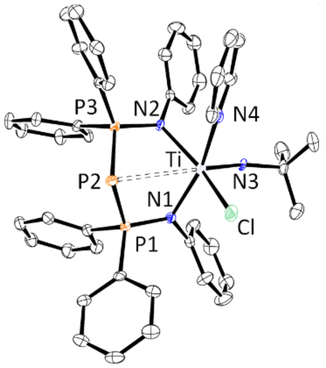

Fig S126: Crystal structure of 6a-py

Table S7 Crystal data and structure refinement for 6a-py

Identification code	6a-py
Internal reference	ad301017_0m_a
Empirical formula	$C_{45}H_{44}ClN_4P_3Ti$
Formula weight	817.10
Temperature/K	115.0
Crystal system	triclinic
Space group	P-1
a/Å	12.209(3)
b/Å	12.264(3)
c/Å	15.876(4)
α/°	97.041(6)
β/°	99.249(6)
γ/°	98.343(6)
Volume/Å^3	2295.2(9)
Z	2
ρ_{calc}g/cm^3	1.182
μ/mm^{-1}	0.383
F(000)	852.0
Crystal size/mm^3	0.25 × 0.075 × 0.025
Radiation	MoKα (λ = 0.71073)
2Θ range for data collection/°	5.818 to 50.11
Index ranges	$-14 \le h \le 14, -14 \le k \le 13, -18 \le l \le 18$
Reflections collected	25340
Independent reflections	8072 [R_{int} = 0.1718, R_{sigma} = 0.2524]
Data/restraints/parameters	8072/421/490
Goodness-of-fit on F^2	0.920
Final R indexes [I>=2σ (I)]	R_1 = 0.0693, wR_2 = 0.1415
Final R indexes [all data]	R_1 = 0.1959, wR_2 = 0.1892
Largest diff. peak/hole / e Å^{-3}	0.59/-0.73
CCDC	1985137

Special refinement details for **6a-py**

The crystal was very poorly diffracting (crystal volume < 50 10^{-6} mm^3). Due to the low <I/σ> of 3.9, the measured data set was not of good quality. Nevertheless, the geometrical parameters of the molecule as well as the thermal ellipsoids seem correctly determined. At the end of the refinement, a region of approximately 400 $Å^3$ presented a diffuse electronic density. But without being able to identify with certainty any solvent (several were used during the synthesis), we decided to apply a solvent mask in order to subtract from our data the contribution of this residual density (Spek, A.L., *Acta Cryst.* **2015**, *C71*, 9-18), 146 e^- were then subtracted.

*Crystal data and structure refinement for **6a***

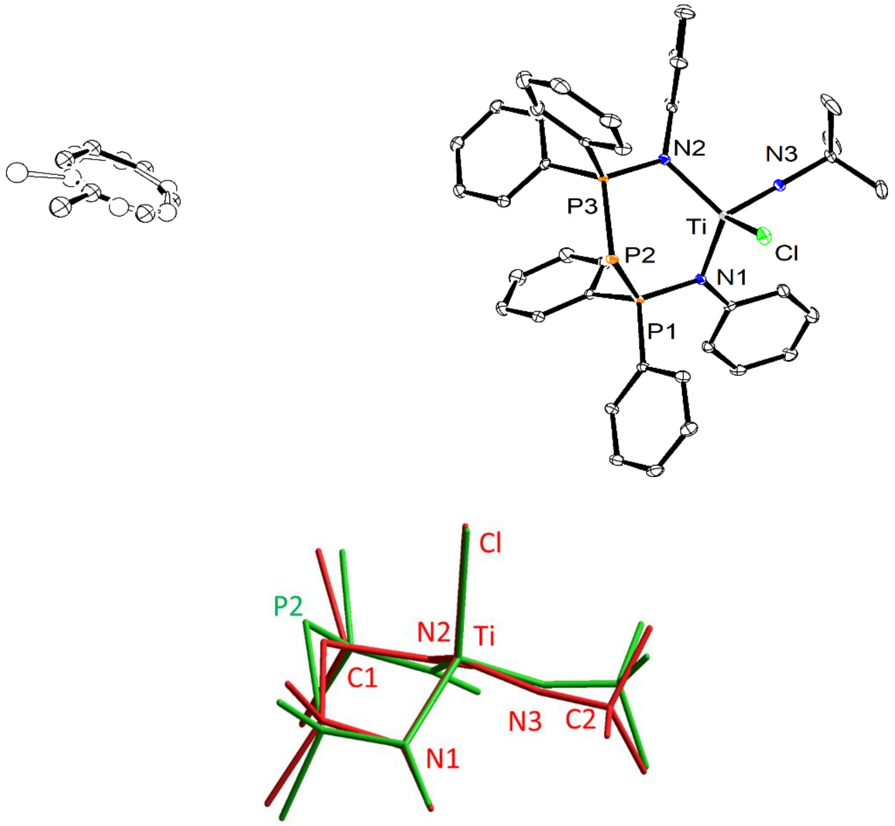

Fig S127: Crystal structure of 6a and superposition with compound C

Table S8: Crystal data and structure refinement for 6a

Identification code	6a
Internal reference	ad021117_0m
Empirical formula	$C_{47}H_{47}ClN_3P_3Ti$
Formula weight	830.13
Temperature/K	115
Crystal system	monoclinic
Space group	$P2_1/c$
a/Å	12.4622(7)
b/Å	22.1019(12)
c/Å	15.1862(5)

α/°	90
β/°	94.5670(10)
γ/°	90
Volume/Å^3	4169.6(4)
Z	4
ρ_{calc}g/cm^3	1.322
μ/mm^{-1}	0.422
F(000)	1736.0
Crystal size/mm^3	0.25 × 0.1 × 0.1
Radiation	MoKα (λ = 0.71073)
2Θ range for data collection/°	5.494 to 55
Index ranges	$-13 \le h \le 16, -28 \le k \le 28, -19 \le l \le 19$
Reflections collected	41349
Independent reflections	9558 [R_{int} = 0.0440, R_{sigma} = 0.0425]
Data/restraints/parameters	9558/0/452
Goodness-of-fit on F^2	1.028
Final R indexes [I>=2σ (I)]	R_1 = 0.0458, wR_2 = 0.1056
Final R indexes [all data]	R_1 = 0.0651, wR_2 = 0.1157
Largest diff. peak/hole / e Å^{-3}	1.20/-0.80
CCDC	1985145

Special refinement details for **6a**

A two components disordered toluene solvent molecule is present in the asymmetric unit. The disorder consists in a rotation of ca 30 deg between the two components. Two rigid groups, whose occupancy factors converged towards 0.64/0.36, where use for the modelling with the use of a global isotropic temperature factor.

*Crystal data and structure refinement for **6b***

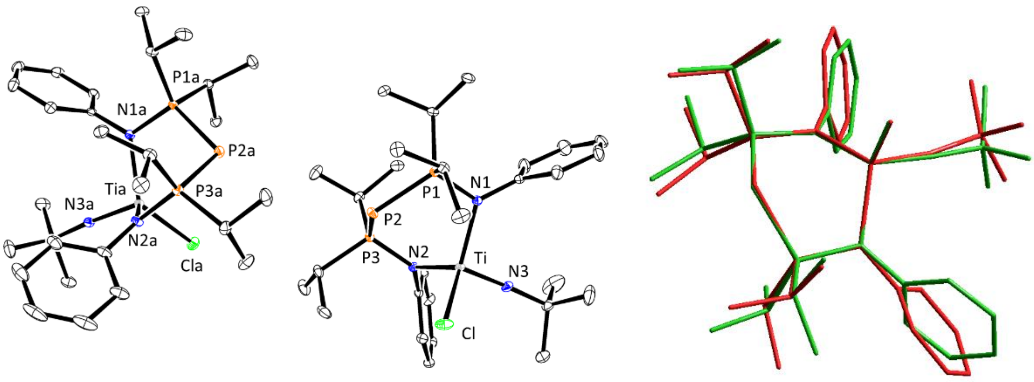

Fig S128: Crystal structure of 6b-1/2 and superposition of both independent molecules (Ph rings truncated)

Table S9: Crystal data and structure refinement for 6b

Identification code	6b
Internal reference	ad290118_0m

Empirical formula	$C_{28}H_{47}ClN_3P_3T_i$
Formula weight	601.94
Temperature/K	115
Crystal system	monoclinic
Space group	P21/n
a/Å	19.7139(8)
b/Å	17.7743(9)
c/Å	20.2496(9)
α/°	90
β/°	112.4110(10)
γ/°	90
Volume/Å3	6559.6(5)
Z	8
ρcalcg/cm3	1.219
μ/mm-1	0.510
F(000)	2560.0
Crystal size/mm3	0.5 × 0.5 × 0.12
Radiation	MoKα (λ = 0.71073)
2Θ range for data collection/°	5.418 to 54.964
Index ranges	-25 ≤ h ≤ 22, -23 ≤ k ≤ 23, -26 ≤ l ≤ 26
Reflections collected	82653
Independent reflections	14979 [R_{int} = 0.0283, R_{sigma} = 0.0230]
Data/restraints/parameters	14979/0/671
Goodness-of-fit on F2	1.059
Final R indexes [I>=2σ (I)]	R1 = 0.0300, wR2 = 0.0675
Final R indexes [all data]	R_1 = 0.0437, wR_2 = 0.0759
Largest diff. peak/hole / e Å^{-3}	0.43/-0.33
CCDC	1985136

Crystal data and structure refinement for ***7b***

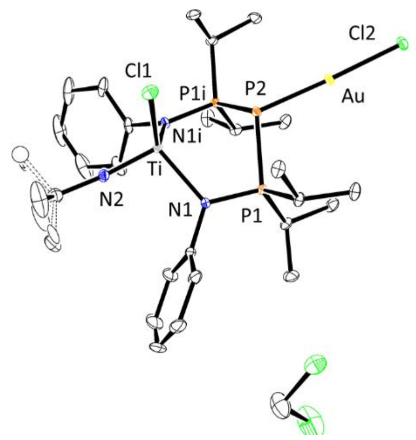

Fig S129: Crystal structure of 7b

Table S10: Crystal data and structure refinement for 7b

Identification code	7b

Empirical formula	$C_{29}H_{49}AuCl_4N_3P_3Ti$
Formula weight	919.29
Temperature/K	100.0
Crystal system	orthorhombic
Space group	Pnma
a/Å	14.2921(8)
b/Å	13.7871(7)
c/Å	18.9179(10)
α/°	90
β/°	90
γ/°	90
Volume/Å^3	3727.7(3)
Z	4
ρ_{calc}g/cm^3	1.638
μ/mm^{-1}	4.585
F(000)	1832.0
Crystal size/mm^3	0.4 × 0.33 × 0.11
Radiation	MoKα (λ = 0.71073)
2Θ range for data collection/°	5.7 to 55.166
Index ranges	$-18 \le h \le 18$, $-17 \le k \le 17$, $-24 \le l \le 24$
Reflections collected	65977
Independent reflections	4478 [R_{int} = 0.0268, R_{sigma} = 0.0114]
Data/restraints/parameters	4478/24/224
Goodness-of-fit on F^2	1.235
Final R indexes [I>=2σ (I)]	R_1 = 0.0249, wR_2 = 0.0497
Final R indexes [all data]	R_1 = 0.0293, wR_2 = 0.0528
Largest diff. peak/hole / e Å^{-3}	1.21/-1.33
CCDC	1985144

Special refinement details for 7b

While the *tert*-butyl group is located on a symmetry plane and hence refined with a carbon multiplicity equal to 0.5, a set of restraints was applied: ISOR for the temperature factors and DFIX for the carbon-carbon distances.

*Crystal data and structure refinement for **8b***

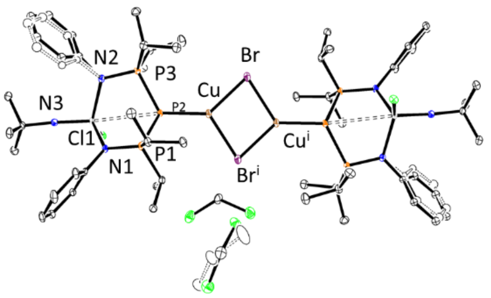

Fig S130: Crystal structure of 8b

Table S11: Crystal data and structure refinement for 8b

Identification code	8b
Empirical formula	$C_{58.28}H_{98.56}Br_2Cl_{6.56}Cu_2N_6P_6Ti_2$
Formula weight	1684.42
Temperature/K	100.0
Crystal system	monoclinic
Space group	$P2_1/c$
a/Å	11.6149(6)
b/Å	16.6838(8)
c/Å	20.0416(9)
α/°	90
β/°	90.810(2)
γ/°	90
Volume/Å^3	3883.3(3)
Z	2
ρ_{calc}g/cm^3	1.441
μ/mm^{-1}	2.155
F(000)	1728.0
Crystal size/mm^3	0.36 × 0.243 × 0.193
Radiation	MoKα (λ = 0.71073)
2Θ range for data collection/°	5.864 to 55.17
Index ranges	$-15 \le h \le 15$, $-21 \le k \le 21$, $-26 \le l \le 26$
Reflections collected	51118
Independent reflections	8943 [R_{int} = 0.0391, R_{sigma} = 0.0324]
Data/restraints/parameters	8943/0/432
Goodness-of-fit on F^2	1.062
Final R indexes [I>=2σ (I)]	R_1 = 0.0428, wR_2 = 0.0939
Final R indexes [all data]	R_1 = 0.0672, wR_2 = 0.1094
Largest diff. peak/hole / e Å^{-3}	1.23/-1.06
CCDC	1985142

Special refinement details for **8b**

One phenyl group was found disordered with occupations factors equal to 0.52:0.48 and was isotropically refined. One dichloromethane solvent molecule was also found disordered with occupation factor converged to 0.5 and one other dichloromethane molecule was refined with an occupation factor converged to 0.14.

Crystal data and structure refinement for ***9b***

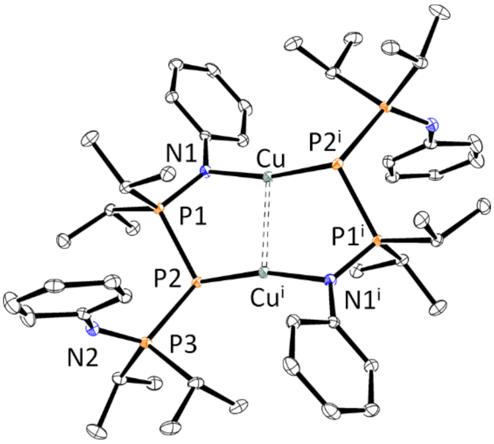

Fig S131: Crystal structure of 9b

Table S12: Crystal data and structure refinement for 9b

Identification code	9b
Empirical formula	$C_{48}H_{76}Cu_2N_4P_6$
Formula weight	1022.02
Temperature/K	99.99
Crystal system	monoclinic
Space group	C2/c
a/Å	31.2123(12)
b/Å	11.3573(4)
c/Å	16.6578(7)
α/°	90
β/°	111.6900(10)
γ/°	90
Volume/Å^3	5486.9(4)
Z	4
ρ_{calc}g/cm^3	1.237
μ/mm^{-1}	0.984
F(000)	2160.0
Crystal size/mm^3	0.427 × 0.197 × 0.134
Radiation	MoKα (λ = 0.71073)
2Θ range for data collection/°	6.09 to 55.18
Index ranges	$-40 \leq h \leq 40$, $-14 \leq k \leq 14$, $-21 \leq l \leq 21$
Reflections collected	31836
Independent reflections	6346 [R_{int} = 0.0358, R_{sigma} = 0.0308]
Data/restraints/parameters	6346/0/279
Goodness-of-fit on F^2	1.021
Final R indexes [I>=2σ (I)]	R_1 = 0.0302, wR_2 = 0.0654
Final R indexes [all data]	R_1 = 0.0448, wR_2 = 0.0711
Largest diff. peak/hole / e Å^{-3}	0.42/-0.30
CCDC	1985139

Special refinement details for **9b**

During the refinement, atoms of solvent were observed (recrystallisation solvents were pentane and tetrahydrofuran), but any attempt to modelize these disordered molecules were unsatisfactory and we decided to use the bypass procedure (Spek, A.L., *Acta Cryst.* **2015**, *C71*, 9-18).

Structural Trans Effect in octahedral BIPP complexes

Table S13. Structural *trans* effect in octahedral BIPP complexes.

Complex	**3a**	**5a-1**	**5a-2**	**5b**
Δ_{N1P2}	-	0.0850(7)	0.0843(7)	0.0439(6)
Δ_{N2P2}	0.0304(8)	0.0633(8)	0.0741(7)	0.0746(6)

values are expressed in Å.

This table compiles the values of Δ_{N1P2} and Δ_{N2P2} in **3a**, **5a** and **5b**. These parameters represent the difference between the M-Cl bond length of the Cl ligands *trans* to N1 (or N2) and that of the Cl ligand *trans* to P2. The positive value of Δ_{N1P2} and Δ_{N2P2} indicate that the iminophosphoranyl side arms exert a greater STE than the central P atom, which is especially visible in **5a** and **5b**.